N° d'Ordre : 42433

THESE DE DOCTORAT

Présentée devant
L'UNIVERSITE DES SCIENCES ET TECHNOLOGIES DE LILLE
UFR CHIMIE

DOCTEUR DE L'UNIVERSITE DE LILLE
Mention « Molécules et Matière Condensée »

Par

Sami FADLALLAH

Ecole Doctorale Sciences de la Matière, du Rayonnement et de L'Environnement
Unité de Catalyse et de Chimie du Solide, UMR CNRS 8181
Equipe Méthodologie Organométallique en Catalyse Homogène

Green Chemistry in Polymerisation: Elaboration and Development of Novel Organometallic Complexes of the Rare-Earth Metals for their Application in (Co)-polymerisation Catalysis

Soutenue le 29 Septembre 2017 à Villeneuve d'Ascq

Thèse Dirigée par
Marc VISSEAUX, Professeur des Universités, Université de Lille 1, directeur de thèse.
Fanny BONNET, Chargée de Recherche CNRS, Université de Lille 1, co-directeur de thèse.

Rapporteurs :
Jun OKUDA, Professeur des Universités, RWTH Aachen University, Allemagne.
Audrey AUFFRANT, Chargée de Recherche CNRS, Ecole Polytechnique, Palaiseau.

Examinateurs :
Laurent MARON, Professeur des Universités, Université Paul Sabatier, Toulouse.
Bernard MARTEL, Professeur des Universités, Université de Lille 1.

ACKNOWLEDGEMENTS

First, I would like to express my gratitude to the directors of my Ph. D.

Prof. Dr. Marc Visseaux and *Dr. Fanny Bonnet*

for accepting me to join their research group in Lille 1.

Prof. Dr. Marc Visseaux "Mon Prof", thank you for your great availability for the many discussions we got, I have found you as a teacher, advisor and friend. Your SMILE, guidance, kindly support and constant encouragement helped me to get through this Ph. D. and gave me the answer to the big question "how to be a real researcher?".

Dr. Fanny Bonnet, thank you for the guidance and support during my three years of research, you taught me everything you could, my deepest thanks for you.

I am grateful to Prof. Dr. Jun Okuda and Dr. Audrey Auffrant, for accepting to read this work and to be the rapporteurs. Special thanks for Dr. Audrey Auffrant for the collaboration in the field of phosphasalen rare-earth complexes.

I equally thank the other members of the jury, Prof. Dr. Laurent Maron and Prof. Dr. Bernard Martel for accepting to be the examiners of the Ph. D. work.

I express my deepest thanks to all the members of the UCCS, especially Prof. Dr. Lionel Montagne, Dr. Francine Agbossou, Prof. Dr. André Mortreux and the CCM axis for the excellent work conditions they maintained within the laboratory. Big thanks are dedicated to Elodie, Jashvini "the ERASMUS student who shared me part of this work", Kader, Julie, Nicholas, Tom, Emma, Dr. Yohan Morin, Dr. Yohan Champouret, Dr. Audrey Favrelle, … it has been a pleasure to share you some moments and to work in the lab with you all.

Special thanks are given to Dr. Christophe Michon, for the energy he always invests in the lab, and for the advices he gave me during the past three years.

Many thanks for Dr. Pascal Roussel and Dr. Frédéric Capet for their expertise in X-ray crystal structure determination, Dr. François Stoffelbach for the MALDI-ToF analyses and Marc Bria for the NMR analyses.

I would like to acknowledge the French Ministry of high education and University of Lille 1 for funding our work.

Finally, although, I will never come close to thanking my parents enough, thank you for encouraging me always, providing support and faith you have shown me in my scientific career. To my brothers, I thank you for the ways you have found to be always there. It is never too late, do not worry, we will achieve our aims. To Hiba, although you are a biologist, you are also a good chemist now. Thanks for the time you spent listening patiently to the problems I got in chemistry. Thanks for your constant patience, faithfulness, trust in me "if your mind can conceive it, and your heart can believe it, then you can achieve it". I would never have succeeded without you, I love you.

Chimie verte en polymérisation: Elaboration et développement de nouveaux complexes organométalliques à base de terres rares pour leur application en catalyse de polymérisation.

Résumé: De nouveaux complexes allyl-borohydrure de terres rares trivalents, $RE(BH_4)_2(C_3H_5)(THF)_x$ (RE = Sc, x = 2; Y, La, Nd, Sm, x = 3) ont été synthétisés. Les complexes ont été caractérisés, y compris par diffraction des rayons X, et leur réactivité vis-à-vis de l'insertion de petites molécules organiques est décrite, qui met en jeu de façon comparative les liaisons métal-borohydrure et métal-allyle. Dans ce travail de thèse, il a été montré que le complexe de néodyme est capable d'amorcer la polymérisation de l'isoprène, seul ou combiné avec un co-catalyseur de type magnésium, conduisant à du *trans*-1,4-polyisoprène avec une bonne activité. Cette famille de complexes est également très active en polymérisation par ouverture de cycle des esters cycliques tels que l'ε-caprolactone et le L-lactide, avec amorçage de la réaction via le ligand borohydrure plutôt que l'allyle. La copolymérisation statistique L-lactide/ε-caprolactone a été réalisée, conduisant à la formation de copolymères avec une large gamme de microstructures, de statistique à alternée. Une autre approche organométallique a été abordée avec la synthèse de nouveaux complexes borohydrures de terres rares (Sc, Y, Nd) à base de ligands Phosphasalen. Certains de ces complexes ont été isolés et caractérisés.

Mots Clés: Terres Rares, Catalyse Homogène, Polymerisation, Isoprène, Lactide, ε-Caprolactone, Copolymères, Borohydrure, Allyl, Ligands Phosphasalen.

Green chemistry in polymerisation: Elaboration and development of novel organometallic complexes of the rare-earth metals for the application in (Co)-polymerisation catalysis.

Abstract: A series of new trivalent rare earth allyl-borohydride complexes with the formula $RE(BH_4)_2(C_3H_5)(THF)_x$ (RE = Sc, x = 2; Y, La, Nd, Sm, x = 3) was synthesized. The complexes were fully characterized including by X-ray and their reactivity toward small organic molecules insertion is described, which involves comparatively metal-borohydride and metal-allyl bonds. In this dissertation, it was shown that the neodymium congener could initiate isoprene polymerisation, as single component or combined with a magnesium co-catalyst, to afford *trans*-1,4-polyisoprene with good activity. All the complexes were also found extremely active toward the Ring-Opening Polymerisation of ε-caprolactone and L-lactide with initiation through the borohydride rather than the allyl moiety. The statistical copolymerisation of L-lactide and ε-caprolactone was successfully performed with all complexes affording copolymers with a wide range of microstructure, from random to fairly alternating. Another organometallic approach has been studied with the synthesis of novel rare earth (Sc, Y, Nd) borohydride complexes based on Phosphasalen ligands. Some of these complexes have been isolated and characterized.

Keywords: Rare Earth, Homogenous Catalysis, Polymerisation, Isoprene, Lactide, ε-Caprolactone, Copolymers, Borohydride, Allyl, Phosphasalen ligands.

TABLE OF CONTENTS

GLOSSARY OF ABBREVIATIONS

B

BD	butadiene
BEM	*n*-butylethylmagnesium, (^{n}Bu)(Et)Mg
BHT	butylated hydroxytoluene
Bn	benzyl
br	broad

C

COSY	correlated spectroscopy
Cp	η^5-cyclopentadienyl
Cp^R	η^5-tetramethylcyclopentadienyl
CTA	chain transfer agent

D

D	deuterated
d	doublet
dd	doublet of doublets
diox	1,4-dioxane, $C_4H_8O_2$
DSC	differential scanning calorimetry
Đ	polydispersity index
Δ	chemical shift

E

Et	ethyl
Et_2O	diethylether
EtOH	ethanol
***ε*-CL**	*ε*-caprolactone

I

^{i}Pr	isopropyl

IP isoprene

K

KHMDS potassium bis(trimethylsilyl)amide

L

Lactide LA

$[LA]_o$ initial concentration of lactide

l_i number-average sequence length

$(l_i)_{random}$ bernoullian random number-average sequence length

M

M metal

m meta

m multiplet

MAO methylaluminoxane, $[AlMeO]_n$

MALDI-ToF matrix assisted laser desorption ionisation-time of flight

Me methyl

MeOH methanol

M_n number-average molecular weight

$M_{n\ (theo)}$ theoretical number average molecular weight

M_w weight-average molecular weight

N

N abundance

N_3 1,4,7-Trimethyl-1,4,7-triazacyclononane

NMR nuclear magnetic resonance

O

o ortho

ORTEP oak ridge thermal ellipsoid program

P

p	penta
p	para
PBD	polybutadiene
PCL	poly(ε-caprolactone)
PIP	polyisoprene
PLA	poly(L-lactide)
Ph	phenyl, -C_6H_5
ppm	part(s) per million
PS	polystyrene

Q

q	quartet

R

R	alkyl or aryl
R	randomness character
r	reactivity ratios
rac-	racemic mixture
RE	rare-earth
ROP	ring opening polymerisation
RT	room-temperature

S

s	singlet
SEC	size exclusion chromatography

T

T	temperature
t	triplet
T_m	melting temperature
T_g	glass transition temperature

T_{II}	second mode transesterification degree
TMS	trimethylsilyl, -$SiMe_3$
TOF	turn over frequency
TON	turn over number

X

XRD	x-ray diffraction

GENERAL INTRODUCTION

Organometallic chemistry of the rare-earths (RE) was first developed in 1954 by Wilkinson and Birmingham, who reported the synthesis of tricyclopentadienyl metal compounds, $RE(C_5H_5)_3$ (RE = Sc, Y, La, Ce, Pr, Nd, Sm, Gd).[1,2] Since then, the chemistry of RE metals started to advance, especially, when modern analytical techniques, such as X-ray diffraction, started to be intended as a research tool in the late 1970s. Several families of precursors have been developed for the synthesis of rare-earth compounds, such as chlorides (halides),[3] triflates,[4] amides,[5] aluminates,[6] alkyls,[7] borohydrides[8-10] and alkoxides[11] (Scheme 1).

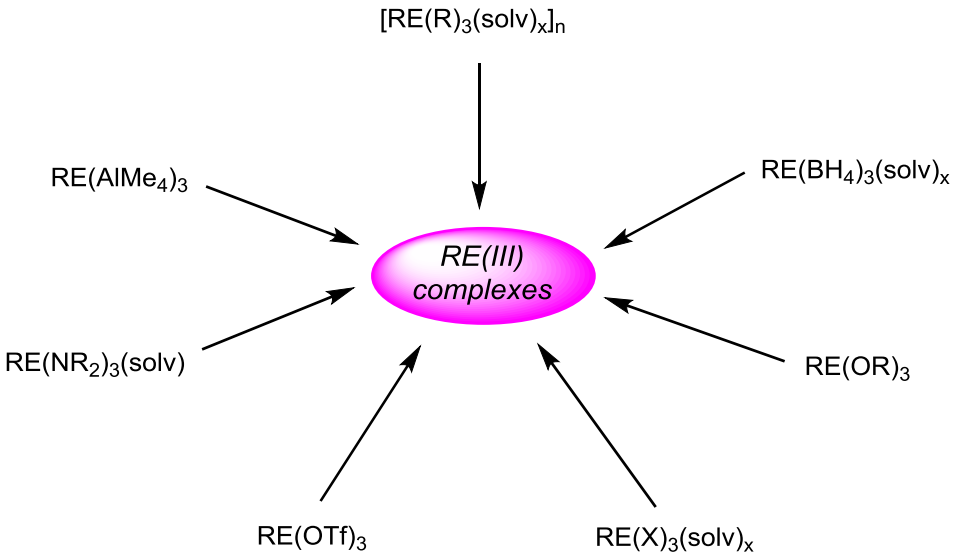

Scheme 1 The common precursors used for the synthesis of RE(III) complexes.
R = alkyl or aryl, X = halogen, OTf = O_3SCF_3, solv = solvent.

The rare-earth halide precursors are largely used, as they are stable precursors which make them easy to synthesize and store. As a comparison, they are much easier to handle than the alkyl-RE precursors, which are particularly sensitive to air and moisture. However, rare-earth halide display low solubility in common non-polar solvent, and to overcome this problem, rare-earth tris(borohydride) precursors, $RE(BH_4)_3(THF)_x$, are good candidates, due to the following reasons:[12]

- They have higher solubility than the halide analogs.
- They are stable under heating (the same for halides).
- The BH_4 ligand can be easily characterized by ^1H or ^{11}B NMR spectroscopy, allowing NMR monitoring of the reactions.

- The borohydride is considered as more electron donating than the halide ion (e.g. chloride), allowing the isolation of a monomeric compounds rather than forming clusters or "ate" complexes.

Associated with the high progression in the field of rare-earth metal complexes, a wide range of catalytic applications involving these compounds have been reported in the literature records.[40] Those include, C—C[13-15] and C—X (X = H, B, Si, N, P)[16-19] bond forming reactions and polymerisation catalysis of a large variety of non-polar (ethylene,[20] α-olefins,[21] butadiene,[22] isoprene,[23] styrene,[24] etc.) and polar monomers (methyl methacrylate,[25] lactides,[26] lactones,[27] alkyl acrylate,[28] etc.).

Among these reactions, the development and synthesis of new initiators for the production of polymers - especially the biodegradable ones - from renewable resources is a hot topic in chemical research. One example is the ring-opening polymerisation (ROP) of cyclic esters, and in particular lactides (LA) and ε-caprolactone (ε-CL), to afford polylactide (PLA) and poly(ε-caprolactone) (PCL) respectively.[29]

Nowadays, these polymeric materials find numerous applications in various fields such as biomedical, agricultural and electronics. However, the use of such polymers for some specific applications requires some precise physical properties which can be reached by introducing some groups to the polymeric structure or by forming (co)polymers. For example, PLA has been known to display low elongation break value due to its high glass transition temperature and crystallinity.[30] The latter properties can be improved by insertion into its polymer chain a monomer of which the corresponding polymer displays a low glass transition temperature such as PCL.[30] Thus, the copolymerisation of LA and ε-CL can be a promising way to give rise to copolymers with controlled mechanical properties. Noteworthy, the properties of the obtained copolymers depend essentially on the sequence distribution of the two monomers in the copolymer chain which can be incorporated in random, alternating, block or tapered fashions (Figure 1).

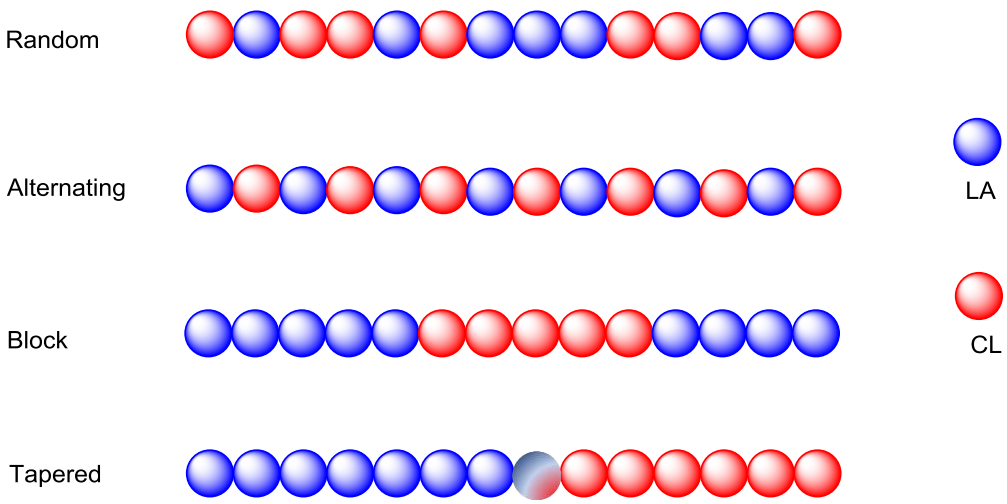

Figure 1 Types of poly(LA-*co*-CL) copolymers.

It is well known that the nature of the initiating group of the polymerisation catalyst greatly affects the activity and the stereoselectivity of the catalyst, which can be directed toward specific kind of monomers. Rare-earth complexes carrying allyl ligand are very relevant in dienes polymerisation.[31,32] Moreover, further progresses in this field has been broadly proclaimed, showing that allylic compounds could be interestingly designed to mediate the polymerisation of olefins.[21] On the other hand, borohydride initiators are very efficient for the polymerisation of polar monomers, such as LA[26,33,34] and ε-CL[35], in addition to the non-polar monomers ethylene,[20] styrene[36,37] and conjugated diene,[38] upon combination with metal alkylating agents (MgR_2, AlR_3, R = alkyl).

Recently, Okuda *et al.* reported the first mixed alkyl/borohydride complex $[Y(BH_4)(Me)(THF)_5][BPh_4]$, which was further shown to be an efficient initiator for the ROP of ε-CL. DFT studies have shown that the polymerisation was found to be kinetically more facile *via* the BH_4 group than through the allyl one, even if both groups are able to initiate such a reaction.[39]

Such organometallic compounds having two distinctive reactive ligands have been scarcely described. Their study is of particular interest due to their potential dual activity while also questioning the influence of one ligand toward the other.

In this context, the aim of this thesis work was to develop a new family of catalysts that bear two different reactive groups, borohydride and allyl, which allows a wide range of application especially in the synthesis of new (co)-polymers with controlled microstructures.

Chapter 1 presents an introduction to the allyl rare-earth metal complexes, and in particular towards the most recent advances in that field. Those include homoleptic neutral, "ate" and cationic rare-earth allyl complexes, in addition to the cyclopentadienyl and non-cyclopentadienyl-supported species. The use of these compounds in homogeneous catalysis is also described.

Chapter 2 describes the synthesis and characterization of a new family of rare-earth complexes bearing two different types of ligands, borohydride and allyl, $RE(BH_4)_2(C_3H_5)(THF)_x$ (RE = Sc , x = 2; Y, La, Nd, Sm, x = 3), as well as, their reactivity toward small organic molecules such as benzophenone, cyclopentadienes (Cp^RH, where Cp = C_5Me_4, R = H or ethyl), silane derivatives (phenyl- and triethyl-silane) and 1,4,7-Trimethyl-1,4,7-triazacyclononane (N_3).

Chapter 3 investigates the catalytic activity of these new mixed allyl-borohydride complexes for the polymerisation of the non-polar monomer isoprene and the polar monomers *L*-LA and *ε*-CL. In addition, the chain-end group analysis of the isolated PLAs and PCLs is reported, which allows the determination of the nature of the initiating group, *ie.* the borohydride or the allyl one.

Chapter 4 illustrates the statistical "one-pot" copolymerisation of *L*-LA and *ε*-CL using the rare-earth allyl-borohydride initiators. Deep microstructure analysis of the obtained copolymers was conducted by ^1H and ^{13}C NMR spectroscopy.

Finally, *chapter 5* deals with attempts of synthesis and characterization of new phosphasalen-based rare-earth complexes.

References

[1] G. Wilkinson, J. M. Birmingham, *J. Am. Chem. Soc*. **1954**, *76*, 6210.

[2] J. M.Birmimghan, G. Wilkinson, *J. Am. Chem. Soc.* **1956**, *78*, 42.

[3] D. Belli Dell'Amico, F. Calderazzo, C. della Porta, A. Merigo, P. Biagini, G. Lugli, T. Wagner, *Inorg. Chim. Acta* **1995**, *240*, 1.

[4] S. *Kobayashi, I. Hachiya, J. Org. Chem.1994, 59, 3590.* R. W. Marshmann, *Aldrichim. Acta* **1995**, *28*, 77.

[5] D. C. Bradley, J. S. Ghotra, F. Alan Hart, *J. Chem. Soc., Dalton Trans.* **1973**, 1021.

[6] H. M. Dietrich, G. Raudaschl-Sieber, R. Anwander, *Angew. Chem., Int. Ed.* **2005**, *44*, 5303.

[7] P. B. Hitchcock, M. F. Lappert, R. G. Smith, R. A. Bartlett, P. P. Power, *J. Chem. Soc., Chem. Commun.* **1988**, 1007.

[8] E. Zange, *Chem. Ber*. **1960**, *93*, 652.

[9] J. H. Morris, W. E. Smith. *Chem Commun*. **1970**, *4*, 245.

[10] U. Mirsaidov, T. G. Rotenberg, T. N. Dymova, *Dokl. Akad. Nauk. Tadzh. SSR* **1976**, *19*, 30.

[11] P. S. Gradeff, K. Yunlu, T. J. Deming, J. M. Olofson, R. J. Doedens, W. J. Evans, *Inorg. Chem.* **1990**, 420.

[12] M. Ephritikhine, *Chem. Rev*. **1997**, *97*, 2193.

[13] F. Xu, L. L. Zhang, Y. M. Yao, Y. C. Ding, Z. M. Bai, Q. Shen, *Chin. Chem. Lett.* **1995**, *6*, 617.

[14] A. A. Trifonov, P. Van de Weghe, J. Collin, A. Domingos, I. Santos, *J. Organomet. Chem.* **1997**, *527*, 225.

[15] M. N. Bochkarev, A. V. Protchenko, L. N. Zakharov, G. K. Fukin, Y. T. Struchkov, *J. Organomet. Chem.* **1995**, *501*, 123.

[16] P. M. Gatti, W. J. de Oliveira, *Alloys Compd.* **1998**, 894.

[17] Z. Hou, Y. Zhang, Y. Wakatsuki, *Kidorui* **1997**, *30*, 40; *Chem. Abstr.* **1997**, *127*, 95656.

[18] V. M. Arredondo, S. Tian, F. E. McDonald, T. J. Marks, *J. Am. Chem. Soc.* **1999**, *121*, 3633.

[19] M. R. Douglass, T. J. Marks, *J. Am. Chem. Soc.* **2000**, *122*, 1824.

[20] M. Visseaux, T. Chenal, P. Roussel, A. Mortreux, *J. Organomet. Chem.* **2006**, *691*, 86.

[21] W. J. Evans, D. M. DeCoster, J. Greaves, *Organometallics* **1996**, *15*, 3210.

[22] R. Taube, H. Windisch, *J. Organomet. Chem.* **1994**, *472*, 71.

[23] F. Bonnet, M. Visseaux, A. Pereira, D. Barbier-Baudry, *Macromolecules* **2005**, *38*, 3162.

[24] Y. Zhang, Z. Hou, Y. Wakatsuki, *Macromolecules* **1999**, *32*, 939.

[25] N. Barros, M. Schappacher, P. Dessuge, L. Maron, S. M. Guillaume, *Chemistry* **2008**, *14(6)*, 1881.

[26] F. Bonnet, A. R. Cowley, P. Mountford, *Inorg. Chem.* **2005**, *44*, 9046.

[27] J. Okuda, F. Amor, T. Eberle, K. C. Hultzsch, T. P. Spaniol, *Polym. Prepr.* **1999**, *40*, 371.

[28] M. Nishiura, Z. Hou, T. Koizumi, T. Imamoto, Y. Wakatsuki, *Macromolecules* **1999**, *32*, 8245.

[29] C. M. Thomas, *Chem. Soc. Rev*. **2010**, *39*, 165.

[30] J. Fernandez, E. Meaurio, A. Chaos, A. Etxeberria, A. Alonso-Varona, J. R. Sarasua, *Polymer* **2013**, *54*, 2621.

[31] D. Barbier-Baudry, N. Andre, A. Dormond, C. Pardes, P. Richard, M. Visseaux, C. J. Zhu, *Eur. J. Inorg. Chem.* **1998**, 1721.

[32] D. Barbier-Baudry, F. Bonnet, B. Domenichini, A. Dormond, M. Visseaux, *J. Organomet. Chem.* **1998**, *647*, 167.

[33] Y. Nakayama, S. Okuda, H. Yasuda, T. Shiono, *React. Funct. Polym*. **2007**, *67*, 798.

[34] Y. Nakayama, K. Sasaki, N. Watanabe, Z. Cai, T. Shiono, *Polymer* **2009**, *50*, 4788.

[35] I. Palard, A. Soum, S. Guillaume, *Macromolecules*, **2005**, *38*, 6888.

[36] D. Barbier-Baudry, O. Blacque, A. Hafid, A. Nyassi, H. Sitzmann, M. Visseaux, *Eur. J. Inorg. Chem.* **2000**, *11*, 2333.

[37] P. Zinck, M. Visseaux, A. Mortreux, *Z. Anorg. Allg. Chem.* **2006**, *632*, 1943.

[38] M. Terrier, M. Visseaux, T. Chenal, A. Mortreux, *J. Polym.Sci.: Part A: Polym. Chem.* **2007**, *45*, 2400.

[39] N. Susperregui, M. U. Kramer, J. Okuda, L. Maron, *Organometallics* **2011**, *30*, 1326.

[40] M. Visseaux, F. Bonnet, *Coord. Chem. Rev*. **2011**, *255*, 374.

CHAPTER 1
BIBLIOGRAPHY

1.1 Context

Rare-earth (RE) allyl complexes are of both fundamental and applied interest due to their high performances in the stereospecific polymerisation of dienes and olefins.[1-6] For example, the neutral tris(allyl) complexes, $RE(\eta^3\text{-}C_3H_5)_3(diox)_x$ (RE = La, x = 1.5; Nd, x = 1) and $Nd(\eta^3\text{-}C_3H_5)_3$ were found to catalyze the *trans*-selective polymerisation of butadiene, while combining the former with aluminum co-catalysts shifted to *cis*-selective polymerisation.[7] Notably, numerous molecular allyl-based complexes have been recorded in the literature since Tsutsui synthesized the first organo-RE complexes containing an allyl moiety $(C_5H_5)_2RE(\eta^3\text{-}C_3H_5)$ (RE = Sm, Ho, Er) (Figure 1.1).[8]

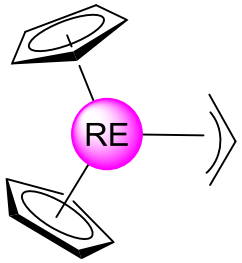

Figure 1.1 The first allyl rare-earth complex, $(C_5H_5)_2RE(\eta^3\text{-}C_3H_5)$ (RE = Sm, Ho, Er).[8]

Furthermore, allylic RE complexes have been shown to initiate effectively the polymerisation of polar monomers, such as cyclic esters or methyl methacrylate.[9-12] For instance, the synthesis of high molecular weight poly(*L*-lactide) was reported by using $(\eta^3\text{-}C_3H_5)_2Sm(\mu^2\text{-}Cl)_2(\mu^3\text{-}Cl)_2Mg(tmed)(\mu^2\text{-}Cl)Mg(tmed)$, and the initiation postulated to occur via the allyl group.[13]

In 2010, Carpentier *et al*. reviewed allyl rare earth complexes that have been studied over the past 50 years along with their reactivity.[14] In this chapter we describe the recent development dealing with this class of compounds including the early remarkable ones and their performances in polymerisation catalysis and fine chemicals synthesis.

1.2 Homoleptic neutral, "ate" and cationic rare-earth allyl complexes

1.2.1 Synthesis, reactivity and structural features

1.2.1.1 Neutral

Following the discoveries of the homoleptic allyl "ate" complexes (section 1.2.1.2), Taube *et al.* did a significant breakthrough in this chemistry, notably by reporting the neutral tris(allyl) complexes $[RE(\eta^3\text{-}C_3H_5)_3(diox)_x]_n$ (RE = La, x = 1.5; Nd, x = 1), obtained *via* allyllithium abstraction of $[Li(diox)_x][RE(C_3H_5)_4]$ with BEt_3 as Lewis acid acceptor in dioxane (Scheme 1.1).[7]

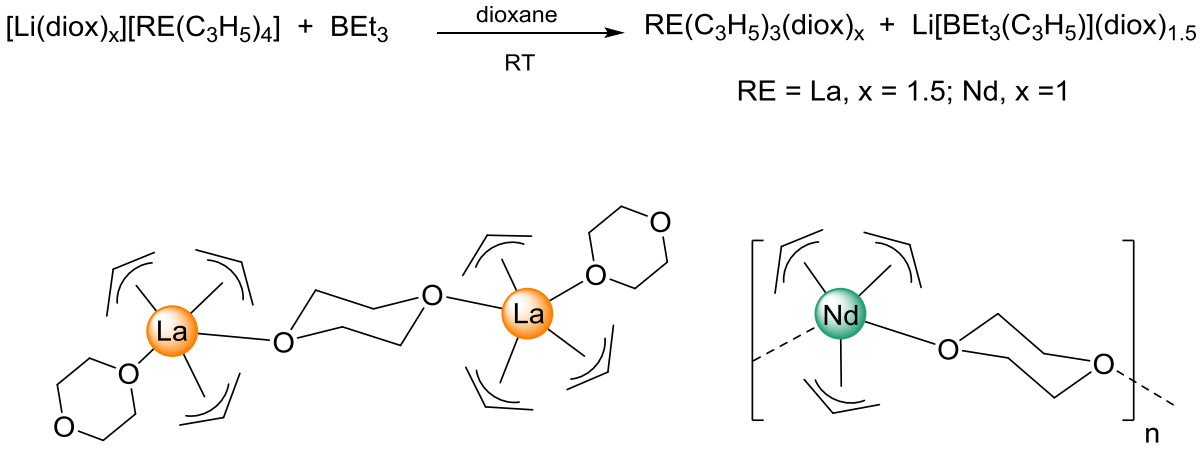

Scheme 1.1 Synthesis and structure of the homoleptic complex $[RE(\eta^3\text{-}C_3H_5)_3(diox)_x]_n$ (RE = La, Nd).[14]

Bochmann and co-workers then synthesized the neutral tris(allyl) complex, $RE(\eta^3\text{-}C_3H_5)_3(diox)$ (RE = Y, La, Ce, Pr, Nd) by reacting $RECl_3$ with 3 equiv. of $(C_3H_5)MgCl$ (Scheme 1.2).[15]

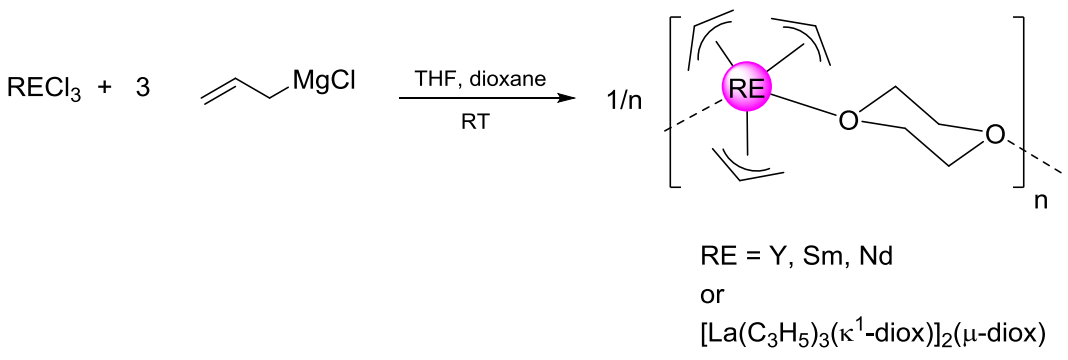

Scheme 1.2 Synthesis of $RE(\eta^3\text{-}C_3H_5)_3(diox)$ (RE = Y, Sm, Nd) using $(C_3H_5)MgCl$.[15]

Recently, Okuda *et al.* conducted further studies on these tris(allyl) complexes.[16] The X-ray structures of cerium and praseodymium monomeric tris(allyl) complexes were obtained by recrystallization of RE(η^3-C_3H_5)$_3$(diox) (RE = Ce, Pr) from a THF/pentane mixture, both displaying a monomeric structure in agreement with the formula RE(η^3-C_3H_5)$_3$(THF)$_2$ (RE = Ce, Pr). Both complexes showed a similar distorted trigonal-bipyramidal geometry, where two of the allyl groups were bonded in the equatorial position while the third one was bonded in the axial position. The dimeric cerium complex [Ce(η^3-C_3H_5)$_3$(κ^1-diox)]$_2$(μ-diox) could be isolated by recrystallization of Ce(η^3-C_3H_5)$_3$(diox) in dioxane and was shown to be isostructural to the previously mentioned lanthanum analogue reported by Taube.[14]

The same research group also synthesized the homoleptic tris(allyl) scandium complex by reacting anhydrous $ScCl_3$ with either K(C_3H_5) or Ca(η^3-C_3H_5) in THF at 0 °C (Scheme 1.3).[17] The X-ray structure revealed a monomeric structure corresponding to Sc(η^3-C_3H_5)$_2$(η^1-C_3H_5)(THF)$_2$ where the scandium atom was coordinated to two η^3-allyl ligands and one η^1-allyl ligand, the two THF ligands being in the axial position. The solvent-free complex Sc(C_3H_5)$_3$ could be obtained by treating the former THF-solvated compound under vacuum at 25 °C for 1h.

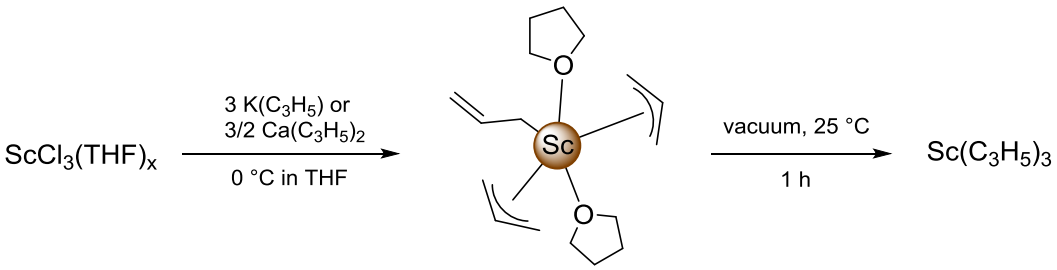

Scheme 1.3 Synthesis of Sc(η^3- C_3H_5)$_2$(η^1-C_3H_5)(THF)$_2$.[17]

1.2.1.2 “Ate”

The first assay toward the synthesis of homoleptic allyl “ate” complexes arose in the 1980s. Mazzei and Lugli prepared the anionic tetra-allyl complexes [Li(diox)$_x$][RE(η^3-C_3H_5)$_4$] (RE = Ce, Nd, Sm, Gd, Dy, x = 2; diox = dioxane) by reacting $RECl_3$ and Sn(C_3H_5)$_4$ with 4 equiv.

of *n*-butyllithium at room temperature (RT), followed by precipitation using dioxane (Scheme 1.4).[18,19]

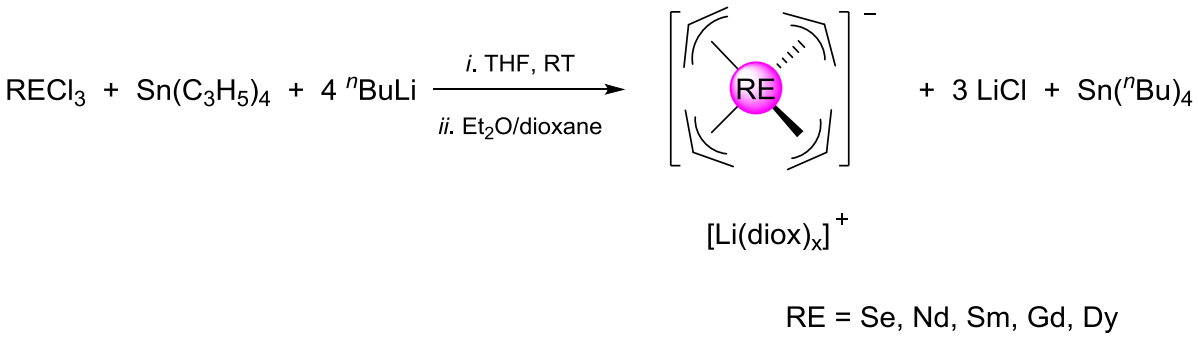

Scheme 1.4 Preparation of "ate" complex $[Li(diox)_x][RE(\eta^3\text{-}C_3H_5)_4]$.[18,19]

At the same time Wu *et al.* reported the first structurally characterized anionic allyl-cerium complex of formula $[Li_2(\mu\text{-}C_3H_5)(diox)_3][Ce(\eta^3\text{-}C_3H_5)_4]$ using 5 equiv. of allyllithium.[20-22]

Following similar synthetic procedure, involving the *in situ* preparation of the allyllithium reagent from tetra-allyltin and *n*-butyllithium, Taube and Schumann prepared the tetra-allyl lanthanum complex $[Li(diox)_{1.5}][La(\eta^3\text{-}C_3H_5)_4]$, which was also characterized at the solid state by X-ray diffraction studies (Figure 1.2).[23]

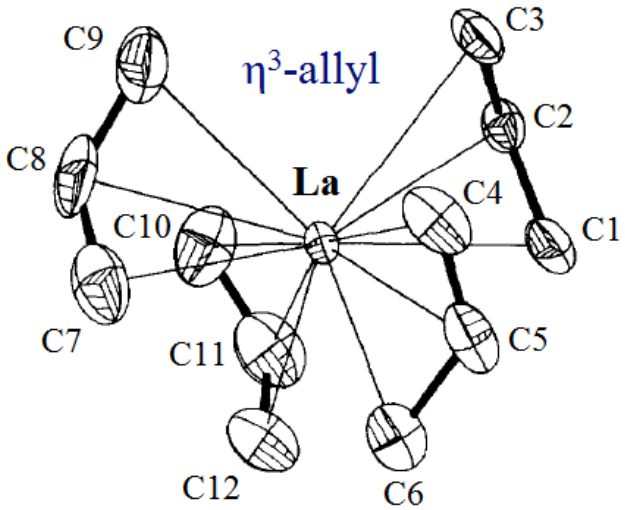

Figure 1.2 ORTEO drawing of the anionic part of $[Li(diox)_{1.5}][La(\eta^3\text{-}C_3H_5)_4]$. Hydrogen atoms are omitted for clarity.[23]

$K[Sc(C_3H_5)_4]$ was synthesized by reacting $ScCl_3$ with 4 equiv. of $[K(C_3H_5)]$. It was also possible to isolate this complex by reacting $Sc(\eta^3\text{-}C_3H_5)_2(\eta^1\text{-}C_3H_5)(THF)_2$ with 1 equiv. of $[K(C_3H_5)]$ in THF (Scheme 1.5). Scandium anionic compound $[Ca(THF)_6][Sc(C_3H_5)_4]_2$ was obtained by reacting $ScCl_3$ with $Ca(\eta^3\text{-}C_3H_5)_2$ in THF at 0 °C. $ScCl_3$ was also reacted with $(C_3H_5)MgCl$ in THF to afford $[Mg(THF)_6][Sc(C_3H_5)_4]_2$ (Scheme 1.5), which was further analysed by X-ray crystallography showing that two of the allyl ligands were η^1-coordinated, the other two being in the η^3-mode (Figure 1.3).[17]

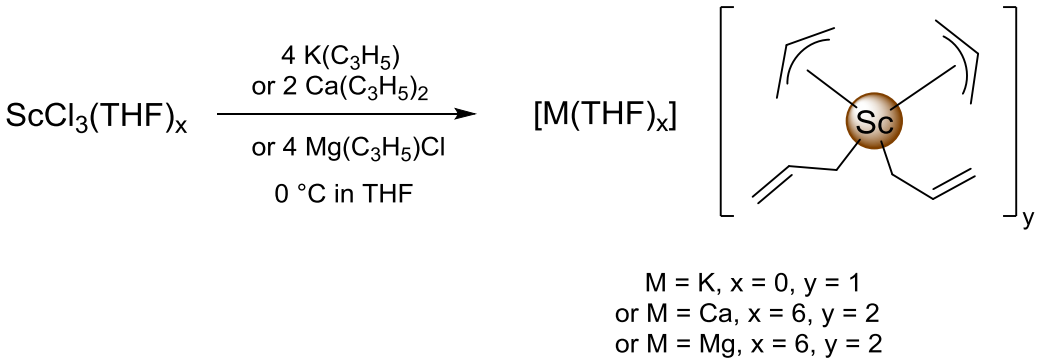

Scheme 1.5 Synthesis of $K[Sc(C_3H_5)_4]$, $[Ca(THF)_6][Sc(C_3H_5)_4]_2$ and $[Mg(THF)_6][Sc(C_3H_5)_4]_2$.[17]

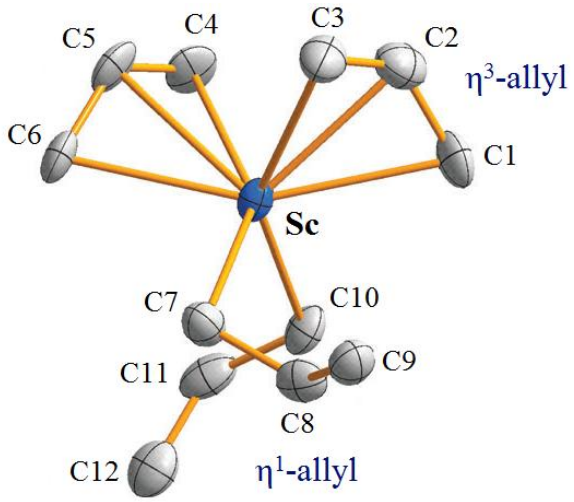

Figure 1.3 ORTEP drawing of the anionic part of $[Mg(THF)_6][Sc(\eta^1\text{-}C_3H_5)_2(\eta^3\text{-}C_3H_5)_2]_2$. Hydrogen atoms are omitted for clarity.[17]

1.2.1.3 Cationic

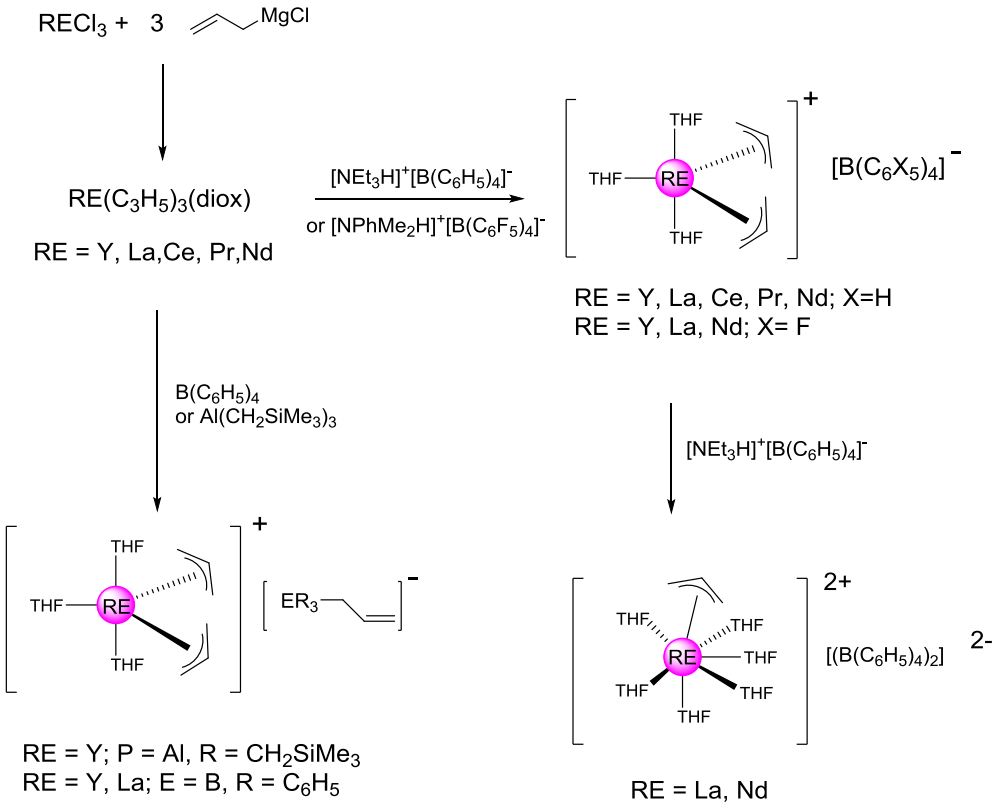

Scheme 1.6 Reactivity of RE(η^3-C_3H_5)$_3$(diox) (RE = Y, La, Ce, Pr, Nd).[16]

Okuda's group also reported the synthesis and comprehensive structural characterization of a series of mono- and dicationic allylic complexes (Scheme 1.6).[16] The neutral tris(allyl) complexes RE(η^3-C_3H_5)$_3$(diox) were further reacted with 1 equiv. of borate reagents [NPhMe$_2$H][B(C_6F_5)$_4$] or [NEt$_3$H][BPh$_4$] in THF, affording the monocationic bis(allyl) complexes [RE(η^3-C_3H_5)$_2$(THF)$_3$][B(C_6X_5)$_4$] (RE = Y, La, Ce, Pr, Nd, X = H; RE = Y, La, Nd, X = F).

The yttrium complex Y(η^3-C_3H_5)$_3$(diox) was reacted with Al(CH_2SiMe_3)$_3$ to give the ion pair, [Y(η^3-C_3H_5)$_2$(THF)$_3$][Al(η^1-$CH_2CH{=}CH_2$)(CH_2SiMe_3)$_3$], whereas RE(η^3-C_3H_5)$_3$(diox) (RE = Y, La) when reacted with B(C_6H_5)$_3$, gave rise to the corresponding cationic complexes [RE(η^3-C_3H_5)$_2$(THF)$_3$][B(η^1-$CH_2CH{=}CH_2$)Ph$_3$] (Scheme 1.6).[16] ^{1}H-NMR of [Y(η^3-C_3H_5)$_2$(THF)$_3$][Al(η^1-$CH_2CH{=}CH_2$)(CH_2SiMe_3)$_3$] and [RE(η^3-C_3H_5)$_2$(THF)$_3$][B(η^1-$CH_2CH{=}CH_2$)Ph$_3$] (RE = Y, La) showed that the coordination between

the allyl moiety and the Group 13 element was η^1.

Benzophenone was shown to clearly insert into the La—C_{allyl} bond of $[La(\eta^3\text{-}C_3H_5)_2(THF)_3][BPh_4]$ to form the alkoxy complex $[La\{OCPh_2(CH_2\text{-}CH{=}CH_2\}_2(THF)_3][BPh_4]$. However, no reaction occurred between $[Y(\eta^3\text{-}C_3H_5)_2(THF)_3][BPh_4]$ and benzophenone even after two days. These reactions were monitored by ^1H NMR.[16]

The RE dications, $[RE(\eta^3\text{-}C_3H_5)(THF)_6][B(C_6H_5)_4]_2$ (RE = La, Nd) were produced by reacting $RE(\eta^3\text{-}C_3H_5)_3(diox)$ with 2 equiv. of $[NEt_3H][B(C_6H_5)_4]$ in THF (Scheme 1.6).[16] The X-ray structures of both resulting complexes showed the presence of six THF molecules to complete the coordination sphere of the under coordinated species along with one allyl moiety in the axial position.

The scandium bis(allyl) monocationic complex $[Sc(\eta^3\text{-}C_3H_5)_2(THF)_3][B(C_6F_5)_4]$ was synthesized starting from $Sc(\eta^3\text{-}C_3H_5)_2(\eta^1\text{-}C_3H_5)(THF)_2$ which was protonated with the bronsted acids $[NPhMe_2H][B(C_6F_5)_4]$, $[NEt_3H][B(C_6H_5)_4]$ or $[NMe_3H][B(C_6H_3Cl_2)_4]$ in THF (Scheme 1.7).[17] The X-ray structure of the cationic scandium compound $[Sc(\eta^3\text{-}C_3H_5)_2(THF)_3][B(C_6H_5)_4]$, revealed that the allyl ligands are both η^3-coordinated and in equatorial position. The ^1H NMR of $[Sc(\eta^3\text{-}C_3H_5)_2(THF)_3][B(C_6H_5)_4]$ showed a doublet at 3.10 ppm for the four methylene protons and a quintet at 5.99 ppm for the methine one, which is typical of fluxional behavior of the allyl moiety. The signal for the methylene allyl protons was at lower field in comparison to $Sc(\eta^3\text{-}C_3H_5)_2(\eta^1\text{-}C_3H_5)(THF)_2$, in agreement with the more pronounced cationic character of the ion pair.

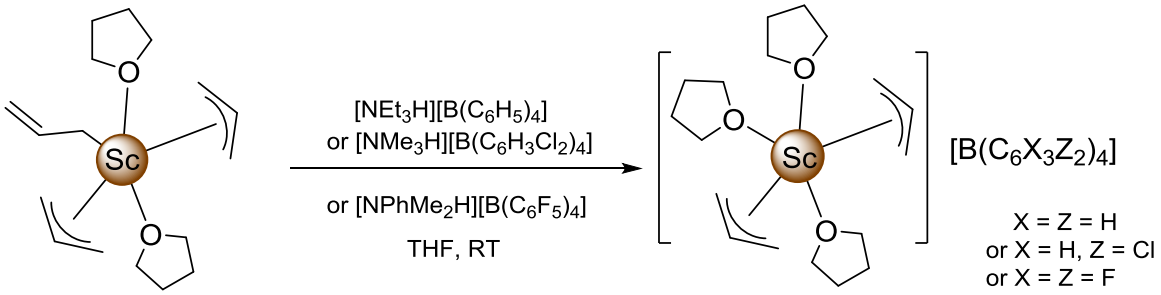

Scheme 1.7 Synthesis of $[Sc(\eta^3\text{-}C_3H_5)_2(THF)_3][B(C_6X_3Z_2)_4]$.[17]

1.2.2 Polymerisation of butadiene mediated by homoleptic rare earth allyl-based complexes

Polybutadiene (PBD), arising from the polymerisation of butadiene; a petro-sourced monomer, was first synthesized in the 20th century by using a sodium-based catalyst.[24] The most notable advance regarding the polymerisation of dienes, since then, was the discovery of the Ziegler-Natta catalysts, which are still being used for industrial scale process for more than half a century producing highly stereoselective polydienes (Scheme 1.8). In the past decade, RE complexes and among them allyl-based catalysts, have shown the ability to produce highly stereoregular polydienes with high activities.[1-6]

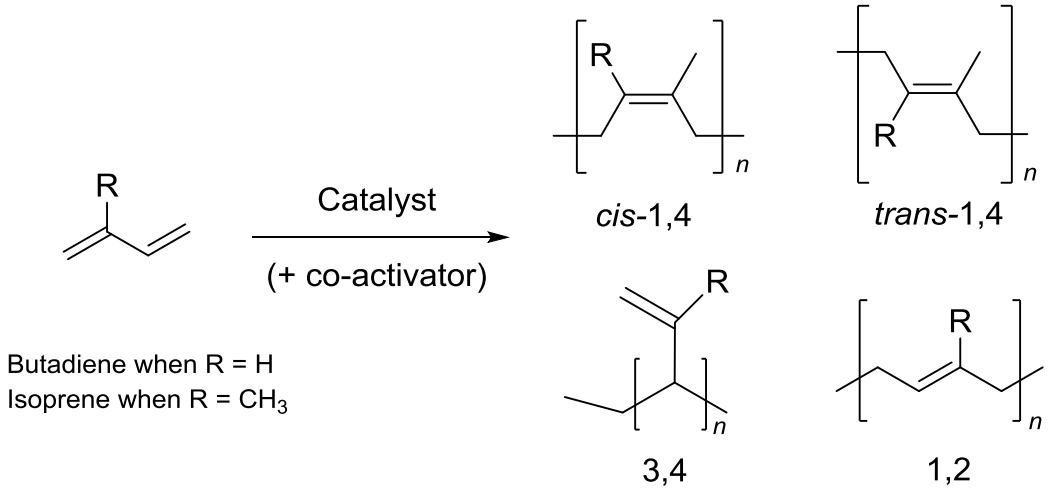

Scheme 1.8 Polymerisation of butadiene and isoprene.

Anionic and neutral allyl-RE complexes were proved to be active for the homogeneous polymerisation of butadiene (BD) (and isoprene). In the absence of co-catalyst, allyl-based catalysts mostly produce *trans*-PBD, while adding aluminum Lewis acidic compounds can switch the selectivity to *cis*-PBD. In most cases, neodymium-based catalysts scored the highest selectivity for ambiguous reasons, as compared to other rare-earths, regardless of the ionic radius. For instance, the neutral tris(allyl) complexes, RE(η^3-$C_3H_5)_3$(diox)$_x$ (RE = La, x = 1.5; Nd, x = 1) and Nd(η^3-$C_3H_5)_3$ polymerise BD in toluene at 50 °C with turnover frequencies (TOFs) of 500, 600 and 1300 mol(BD)/mol(RE)$^{-1}$.h^{-1} and *trans* selectivity of 83, 94 and 89 %, respectively.[7] However the addition of $AlEt_2Cl$ or

MAO (methylaluminoxane) to La(η^3-C_3H_5)$_3$(diox)$_{1.5}$ and Nd(η^3-C_3H_5)$_3$(diox) afforded TOFs of 4700 and 14000 h^{-1} and *cis*-PBD of 65 and 79 %, respectively.[7]

Controlled BD polymerisation was performed by using the cationic complexes [RE(η^3-C_3H_5)$_2$(THF)$_3$][B(C_6F_5)$_4$] (RE = Y, La, Nd) [16] in the presence of Al(^{i}Bu)$_3$, while the latter displayed no activity when tested on their own. Unexpectedly, [Y(η^3-C_3H_5)$_2$(THF)$_3$][B(C_6F_5)$_4$], was found to be the most reactive one (571 kg.mol^{-1}.h^{-1}) leading to the formation of PBD with the highest 1,4-*cis* stereoregularity of 90 % (32.7 % and 75.4 % of 1,4-*cis* units for La and Nd respectively). The *in situ* addition of one additional equiv. of [NPhMe$_2$H][B(C_6F_5)$_4$] to the yttrium monocationic system in the polymerisation mixture led to an increase in both the activity (up to 665 kg.mol^{-1}.h^{-1}) and the selectivity (up to 92.5 % of 1,4-*cis*-PBD). Interestingly, the lanthanum-based catalytic system showed reverse stereoselectivity affording 80.5 % of 1,4-*cis*-PBD when associated with Al(^{i}Bu)$_3$ and 1 equiv. of the borate reagent, whereas 1,4-*trans*-PBD was obtained at 63.3 % when the monocation was associated with Al(^{i}Bu)$_3$ only.

The cationic scandium complex [Sc(η^3-C_3H_5)$_2$(THF)$_3$][B(C_6F_5)$_4$] was also assessed towards the polymerisation of BD.[17] When combined with Al(^{i}Bu)$_3$ as the co-catalyst, a mixture of 1,4-PBD (2:1 ratio of the *cis:trans* isomers), and 1,2-polybutadiene was obtained with fair activity (16 kg.mol^{-1}.h^{-1}) as the reaction was conducted at RT. The activity was improved (64 kg.mol^{-1}.h^{-1}) with the addition of 1 equiv. of [NPhMe$_2$H][B(C_6F_5)$_4$] in the polymerisation mixture but no change in the selectivity was observed.

1.2.3 Ring-opening polymerisation of polar monomers mediated by homoleptic rare-earth allyl-based complexes

1.2.3.1 *ε*-Caprolactone polymerisation

Poly(*ε*-caprolactone) (PCL) is one of the most widely used and studied biopolymer, due to its high biodegradability. It is a saturated aliphatic polyester with hexanoate repeat units (Scheme 1.9) which can be classed as semi-crystalline biopolymer. Its degree of crystallinity

depends on average molar masses and it decreases with increasing the later due to chain folding.[25]

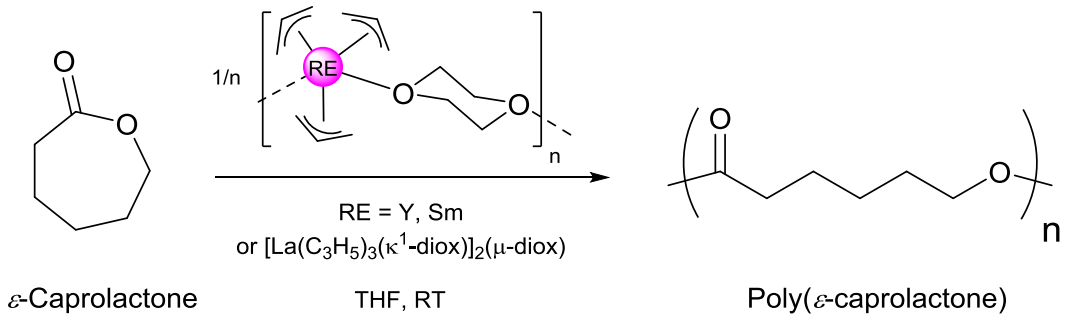

Scheme 1.9 Polymerisation od ε-caprolactone catalyzed by $[RE(\eta^3\text{-}C_3H_5)_3(\mu\text{-diox})]_n$ (RE = Y, Sm) and $[La(\eta^3\text{-}C_3H_5)_3(\kappa^1\text{-diox})]_2(\mu\text{-diox})$.[15]

The group of Bochmann showed that the tris(allyl) complexes $[RE(\eta^3\text{-}C_3H_5)_3(\mu\text{-diox})]_n$ (RE = Y, Sm) act as highly active catalysts for the polymerisation of ε-caprolactone (ε-CL) at RT (Scheme 1.9),[15] as $[Sm(\eta^3\text{-}C_3H_5)_3(\mu\text{-diox})]_n$ gave complete conversion of 200 equiv. of monomers in 1.5 mins. The polymerisation conducted under such conditions was well controlled and gave rise to high molar masses (M_w = 51000 g.mol^{-1}) and narrow dispersities (M_w/M_n = 1.4).

Decreasing the temperature to -20 °C, deactivated $[Y(\eta^3\text{-}C_3H_5)_3(\mu\text{-diox})]_n$ and only traces of polymer were found. However, $[Sm(\eta^3\text{-}C_3H_5)_3(\mu\text{-diox})]_n$ stayed active at -20 °C and reached a ε-CL conversion of 47 % after 3.5 mins.[15]

The same research group showed that the dimeric complex $[La(\eta^3\text{-}C_3H_5)_3(\kappa^1\text{-diox})]_2(\mu\text{-diox})$ was an extremely active catalyst as was able to fully convert 200 equiv. of ε-CL in 0.3 min at 20 °C with M_w = 151000 g.mol^{-1} and M_w/M_n = 1.4. This catalyst was shown to maintain its activity at -20 °C, affording 73 % of conversion along with lower dispersity of the final polymer (M_w/M_n = 1.1).[15]

1.2.3.2 *rac*-lactide polymerisation

Poly-*L*-lactide (PLA) is a very important biodegradable material as it is used as a commodity thermoplastic for the packaging industries and as a biomaterial for pharmaceutical and medical uses.[26,27] It is produced mainly through metal-mediated ROP of *L*-Lactide (the cyclic dimer of lactic acid), a bioresourced monomer derived from fermentation of starch (especially from corn) consisting of two stereoisomers S- and R- lactic acid. Hence, there is noticeable interest in the ring-opening polymerisation of this monomer by well-defined metal initiators where the relief of the ring strain is the driving force of the polymerisation.[28-30]

Lactide has two chiral centers and therefore exists as three stereoisomers: *D*-Lactide (two *R*-lactic acids combined) and *L*-lactide (two *S*-lactic acids combined) and meso-lactide (*R*- and *S*-lactic acids combined) knowing that the racemic equimolar mixture of *D*- and *L*-lactide is called the *rac*-lactide (*rac*-LA) (Figure 1.4).

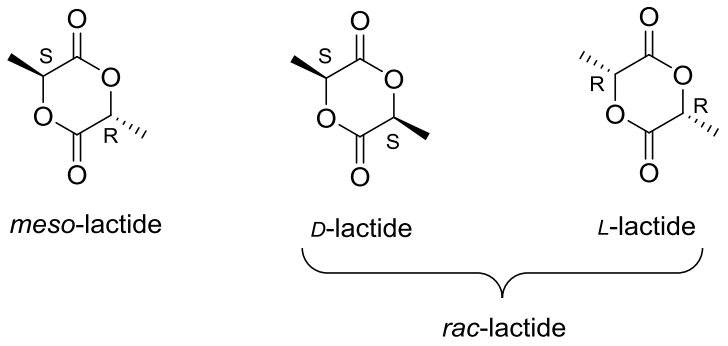

Figure 1.4 Stereoisomers of lactide.

Bochmann *et al*. showed that allylic rare-earth complexes are high active catalysts for the polymerisation of *rac*-LA (Scheme 1.10). $[RE(\eta^3\text{-}C_3H_5)_3(\mu\text{-diox})]_n$ (RE = Y, Sm) was shown to effectively initiate the polymerisations of *rac*-LA at 40 °C.[15] For instance, The Y complex reached 76 % conversion of 100 equiv. of *rac*-LA after 4.7 h at 40 °C, affording polylactide displaying moderate molar mass along with narrow dispersity (20000 $g.mol^{-1}$ and 1.2 respectively).

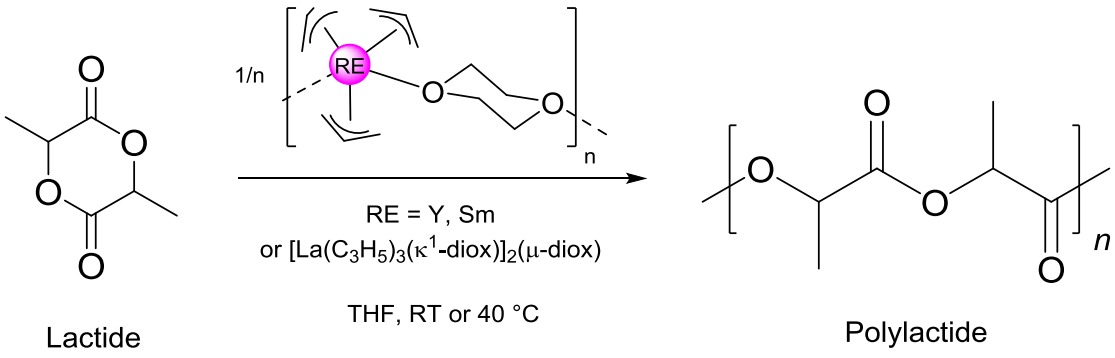

Scheme 1.10 Polymerisation of lactide catalyzed by $[RE(\eta^3\text{-}C_3H_5)_3(\mu\text{-diox})]_n$ (RE = Y, Sm) and $[La(\eta^3\text{-}C_3H_5)_3(\kappa^1\text{-diox})]_2(\mu\text{-diox})$.[15]

When, the same reaction was conducted at RT, both Y and Sm catalysts led to the formation of traces of polymer only. However, increasing the reaction time to several hours did result in significant polymer formation. For example, $[Sm(\eta^3\text{-}C_3H_5)_3(\mu\text{-diox})]_n$ converted 86 % of 100 equiv. of *rac*-LA at RT in 7.5 h, and a polylactide of molar mass of 30000 $g.mol^{-1}$ and dispersity of 1.4 was obtained. The lanthanum complex $[La(\eta^3\text{-}C_3H_5)_3(\kappa^1\text{-dioxane})]_2(\mu\text{-diox})$ showed to be more active than the Y and Sm analogs at RT and 40 °C.[15]

1.3 Cyclopentadienyl containing rare-earth allylic complexes

1.3.1 Lanthanidocenes mono(allyl) complexes

1.3.1.1 Synthesis and characterization

A variety of cyclopentadienyl (Cp = $C_5H_5^-$) containing RE allylic complexes have been synthesized including mono-Cp and bis-Cp complexes. Changing substituents size on Cp ring, introducing nitrogen or oxygen to Cp ring, using ansa, indenyl or fluorenyl bis-Cp related ligands made the synthesis and stabilization of these types of Cp containing complexes available.

The first allyl RE compounds recorded were the complexes supported by Cp rings. The field was pioneered by Tsutsui and Ely in 1975 who reported the mono(allyl) lanthanidocene $Cp_2RE(\eta^3\text{-}C_3H_5)$ (RE = Sm, Ho, Er).[8] It was synthesized by the reaction of

Cp_2RECl compounds (RE = Sm, Ho, Er) with allylmagnesium bromide in THF/ether solution at –78 °C, followed by the addition of dioxane to precipitate the magnesium dichloride salt (Scheme 1.11).

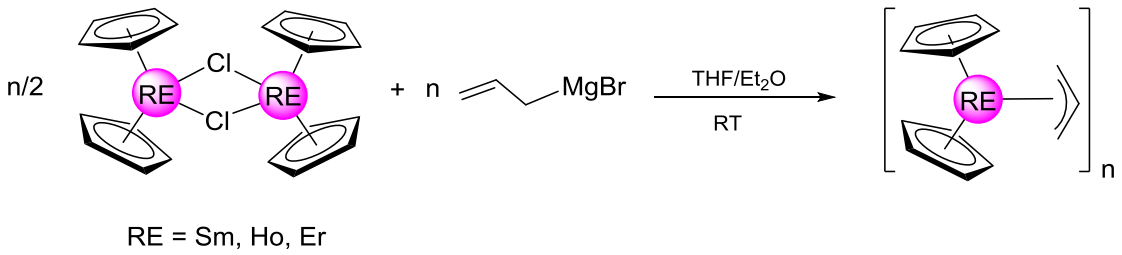

Scheme 1.11 Synthesis of allyl-lanthanidocene $Cp_2RE(\eta^3\text{-}C_3H_5)$ (RE = Sm, Ho, Er).[8]

This methodology proved to be quite general and a variety of allyl-lanthanidocenes and related complexes supported by cyclopentadienyl ancillaries were prepared successfully following similar transmetallation methods.[31]

Regarding very recent advances in the field, Carpentier and colleagues synthesized the well-defined *ansa*-bis(indenyl) mono(allyl) RE complexes, *rac*-$\{CMe_2(Ind)_2\}RE(\eta^3\text{-}C_3H_5)(THF)$ (RE = Y, Nd; Ind = 2-indenyl) (Scheme 1.12), by first reacting bis(ind) ligand with *n*-butyllithium with $RECl_3$ and then with the Grignard reagent, $(C_3H_5)MgCl$.[32] These complexes were proved to be very efficient for the polymerisation of styrene, as discussed in the next section.[32-34]

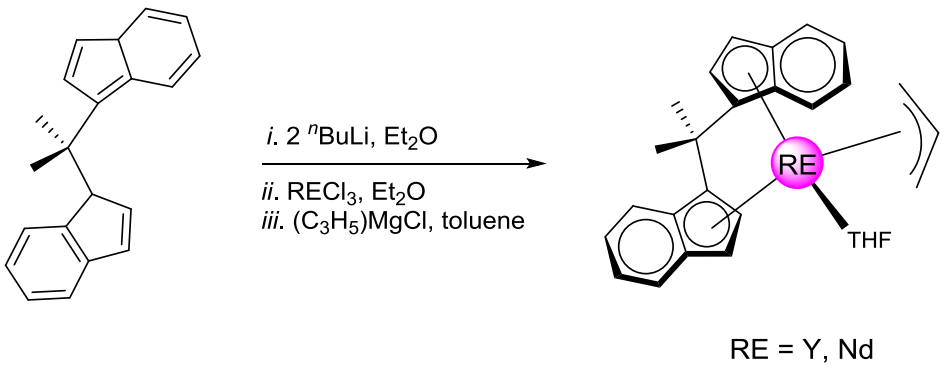

Scheme 1.12 Synthesis of *rac*-$\{CMe_2(Indenyl)_2\}RE(\eta^3\text{-}C_3H_5)(THF)$ (RE = Y, Nd; Ind = 2-indenyl).[32]

The neutral mono(allyl) *ansa*-neodymocene, $\{Me_2C(Cp)(Flu)\}Nd[1,3\text{-}(SiMe_3)_2C_3H_3]$ (Flu = 9-fluorenyl) was synthesized through the reaction of $\{Me_2C(Cp)(Flu)\}Nd(\mu\text{-}Cl)]$ and 1 equiv. of $K[1,3\text{-}(SiMe_3)_2C_3H_3]$ and characterized by ^1H NMR and elemental analysis, as no

single crystals suitable for X-Ray analysis could be isolated (Scheme 1.13).[34]

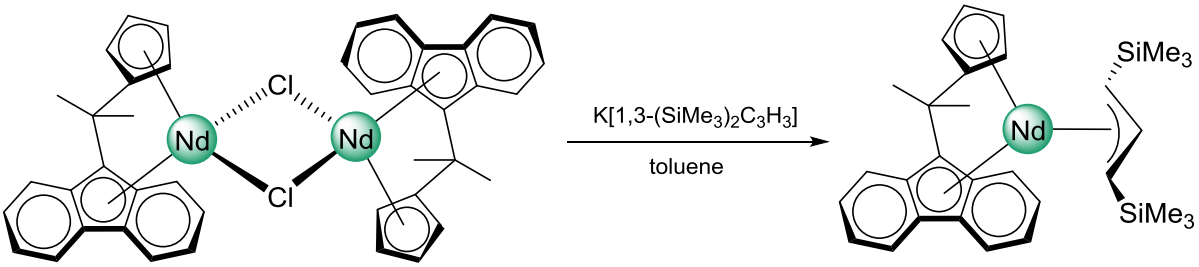

Scheme 1.13 Synthesis of {$Me_2C(Cp)(Flu)$}Nd[1,3-$(SiMe_3)_2C_3H_3$].[34]

[$(\eta^5$-$C_5H_4SiMe_3)_2Lu(\mu$-η^1:η^1-$C_3H_5)]_4$ was synthesised from the reaction between [$(\eta^5$-$C_5H_4SiMe_3)Lu(\mu$-Cl)]$_2$ and $(C_3H_5)MgCl$ in toluene (Scheme 1.14).[35] The X-ray analysis shows that two lutetium atom centres are bridged through the allyl ligands in a *trans* bis-η^1 mode. When this complex was reacted with a suspension of $[HNEt_3][B(C_6H_5)_4]$ in toluene or THF, it afforded the corresponding cation $[(C_5H_4SiMe_3)_2Lu(THF)_2][B(C_6H_5)_4]$.

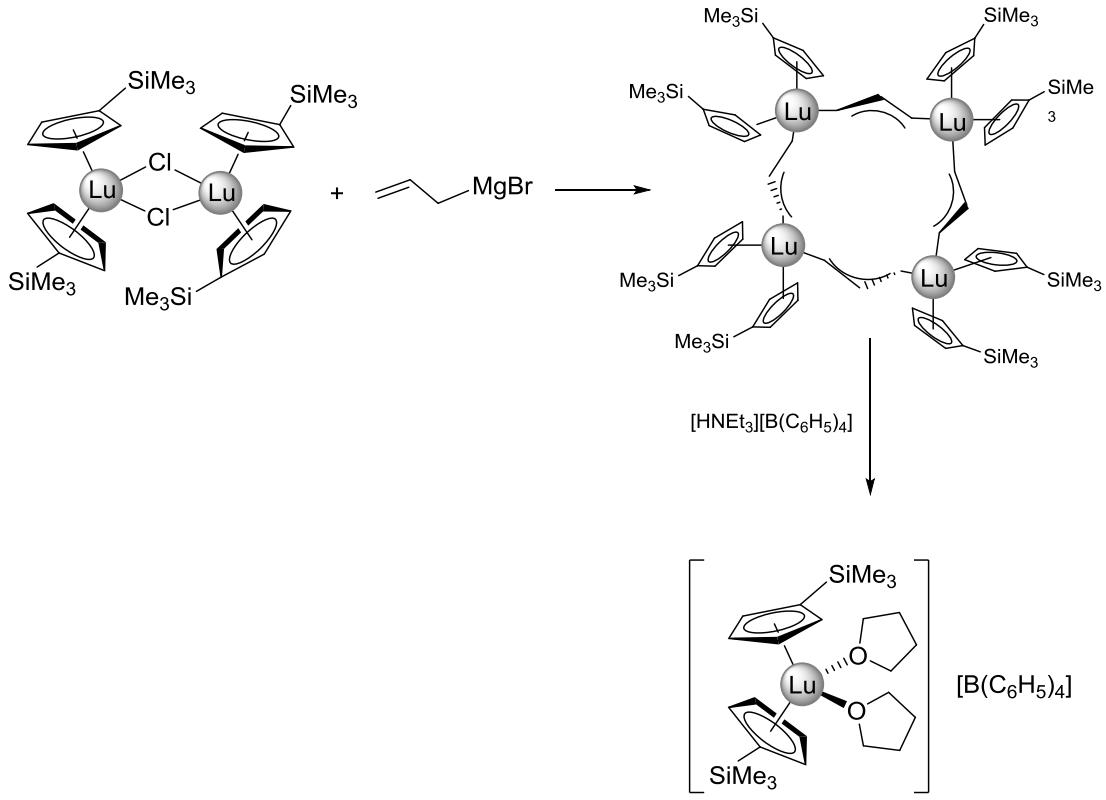

Scheme 1.14 Synthesis of $[(C_5H_4SiMe_3)_2Lu(\mu$-η^1:η^1-$C_3H_5)]_4$.[35]

1.3.1.2 Catalytic application in styrene polymerisation

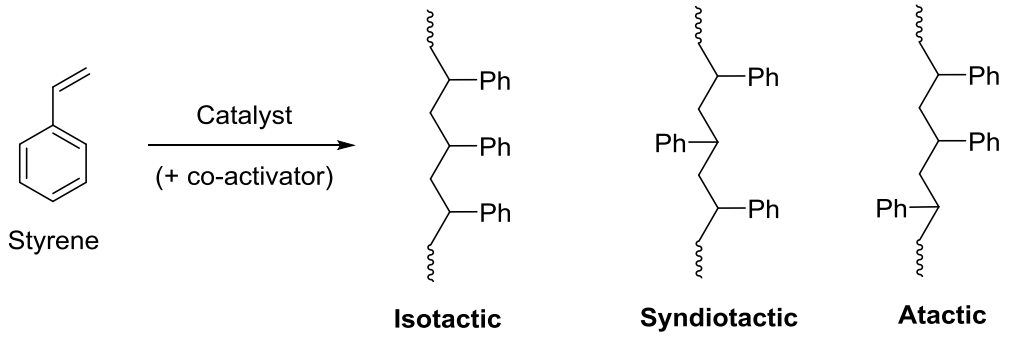

Scheme 1.15 Different microstructures of polystyrene

Polystyrene is a thermoplastic polymer mostly known for its applications in long lasting packaging. Styrene when polymerised can give rise to polystyrene under three different forms: isotactic, syndiotactic or atactic (Scheme 1.15). The term isotactic is used when all of the phenyl rings are situated on the same side of the main polymer chain. Syndiotactic relates to the phenyl groups being distributed in an alternate fashion along the backbone of the polymer chain leading to highly crystalline material with high melting temperature. Finally, the atactic structure is related to the phenyl ring being on random sides.[36-37]

Carpentier, Okuda *et al* assessed the ansa-bis(ind) allyl rare-earth complexes *rac*-{$CMe_2(Ind)_2$}RE(C_3H_5)(THF) (RE = Y, Nd) towards styrene polymerisation.[33] They were found to be active in bulk conditions between 60 and 120 °C, affording isotatic polystyrene with relatively narrow dispersities (1.5 – 2.0). The yttrium complex displayed an activity up to 527 $kg.mol^{-1}.h^{-1}$ at 100 °C, whereas the neodymium analogue afforded 307 $kg.mol^{-1}.h^{-1}$ in the same experimental conditions. The activities were found to increase along with the temperature (from 26 to 94 $kg.mol^{-1}.h^{-1}$ for Y, from 52 to 158 $kg.mol^{-1}.h^{-1}$ for Nd, when the T = 60 and 100 °C respectively) thus inducing a decrease of the molar masses. When the polymerisation was carried out in solution instead of bulk, in solvents such as cyclohexane or heptane, a decrease of the activity was observed (27.5 $kg.mol^{-1}.h^{-1}$ for Y, 16 $kg.mol^{-1}.h^{-1}$ for Nd, in both solvents).[33]

The activity of *rac*-{$Me_2C(Ind)_2$}Y[1,3-$(SiMe_3)_2C_3H_3$] was also tested towards the polymerisation of styrene in combination with di(*n*-butyl)magnesium.[34] The yttrium complex showed high activity in the presence of up to 100 equiv. of $Mg(^nBu)_2$ and up to 10000 equiv. of styrene was converted. The resulting polymer displays narrower dispersities of 1.4-1.6 along with quite low molar masses of 2.6 to 16.2 x 10^3 $g.mol^{-1}$.[34]

The neodymium complex $Me_2C(Cp)(Flu)$}Nd[1,3-$(SiMe_3)_2C_3H_3$] on its own produced highly syndiospecific polystyrene but at a slower rate [20-60 $mol_{st}(mol_{Nd}h)^{-1}$ at 60-80 °C] than the THF-adducts {$Me_2C(Cp)(Flu)$}RE(C_3H_5)(THF) [RE = Y, La, Nd, 1,000–17,000 of polymer $(mol\ of\ RE)^{-1}\ h^{-1}$].[34] Adding excess of $Mg(^nBu)_2$ to the reaction mixture generated a fast binary catalytic system for the highly syndioselective polymerisation of styrene in toluene, heptane or bulk monomer at 80 – 100 °C. The molar masses obtained ranged between 2300 (for 500 equiv. of styrene) to 15000 $g.mol^{-1}$ (1000 equiv. of styrene) with narrow dispersities (1.6-1.7) and faster rates than the single component system. When the loading of monomer was increased to 5000 - 25000 equiv., the catalytic system showed high catalytic activity [400-2500 $mol_{st}(mol_{Nd}h)^{-1}$] and narrow dispersities (1.7-2.1) with increase of molar mass up to 35000 $g.mol^{-1}$ (10000 equiv. of styrene). However, at even higher loadings as high as 50000 equivalent of styrene the control was lost. When the reaction was conducted in bulk conditions between 110-120 °C, it was difficult to obtain reproducible data as the reaction was not well-controlled.[34]

1.3.2 Half sandwich rare-earth bis(allyl) complexes

1.3.2.1 Synthesis and characterization

The Cp containing bis(allylic) complexes, (η^5-$C_5Me_4SiMe_3$)RE(η^3-$C_3H_5)_2$(THF) (RE = Y, La) was isolated from the reaction of $(C_5Me_4H)SiMe_3$ with the neutral tris(allyl) complex, RE(η^3-$C_3H_5)_3$(diox) in THF (Scheme 1.16).[16]

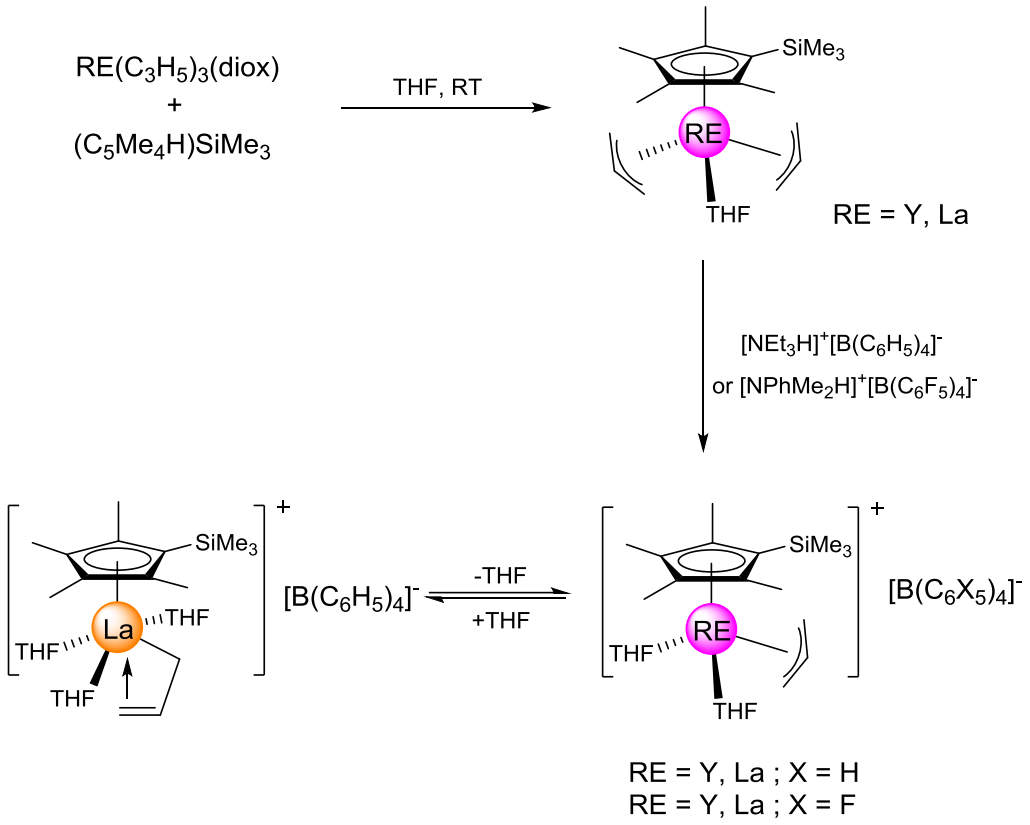

Scheme 1.16 Reactivity of RE(η^3-C_3H_5)$_3$(diox) (RE = Y, La).[16]

Monoallylic cationic species [(η^5-$C_5Me_4SiMe_3$)RE(η^3-C_3H_5)(THF)$_2$][B(C_6X_5)$_4$] (RE = Y, La; X = H or F) could be further isolated by reaction of the previous Cp-based complexes with 1 equiv. of [NEt_3H][BPh_4] or [$NPhMe_2H$][B(C_6F_5)$_4$] in THF (Scheme 1.16). The ^{1}H NMR spectrum of (η^5-$C_5Me_4SiMe_3$)Y(η^3-C_3H_5)$_2$(THF) showed no coupling between the allylic protons and the yttrium center. Hence, there was a faster exchange in the *syn* and *anti* positions, than in the allylic groups in the lanthanum complexes, resulting in two broad signals at RT with 1:4 ratio.[16]

The X-ray structure of the monocation lanthanum complex was determined after recrystallization in THF leading to the formula [(η^5-$C_5Me_4SiMe_3$)La(η^3-C_3H_5)(THF)$_3$][B(C_6H_5)$_4$] where three THF molecules were coordinated instead of two in the crude product. The carbon-carbon bond in the allyl moiety was of unequal lengths due to the *trans* influence of the ring moiety.[16]

Cui *et al*. synthesized the pyridyl-functionalized half-sandwich bis(allyl) compound (C_5Me_4-C_5H_4N)Lu(η^3-C_3H_5)$_2$ by protonolysis reaction of Lu(η^3-C_3H_5)$_3$(diox) and C_5Me_4H-

C_5H_4N in THF (Scheme 1.17).[38] ^1H NMR displayed the typical 1 (pentet)/4 (doublet) set of signals for allyl groups in dynamic equilibrium. The X-ray analysis showed that both the allyl groups coordinate to the lutetium in a η^3 mode. Due to the coordination of the pyridyl moiety, the complex was isolated as solvent free (Figure 1.5).

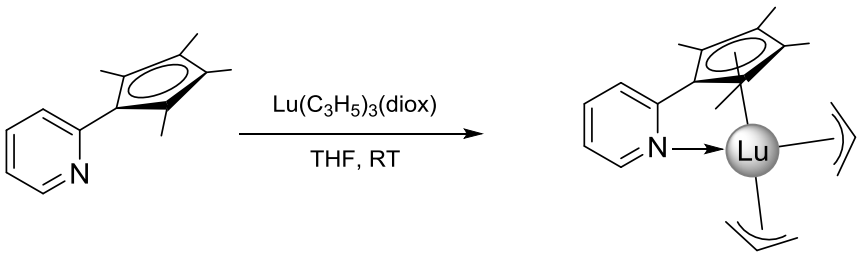

Scheme 1.17 Synthesis of $(C_5Me_4\text{-}C_5H_4N)Lu(\eta^3\text{-}C_3H_5)_2$.[38]

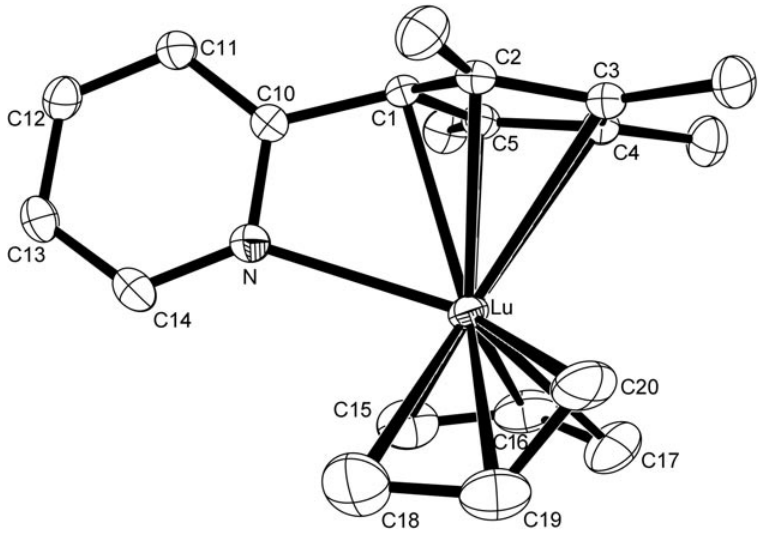

Figure 1.5 X-ray structure of solvent free $(C_5Me_4\text{-}C_5H_4N)Lu(\eta^3\text{-}C_3H_5)_2$. Hydrogen atoms are omitted for clarity.[38]

In combination with trityl borate activator, $(C_5Me_4\text{-}C_5H_4N)Lu(\eta^3\text{-}C_3H_5)_2$ exhibited very effective and rare dual catalysis ability for both syndiotactic styrene polymerisation (activity 6240 $kg.mol^{-1}.h^{-1}$) and *cis*-1,4-selective butadiene polymerisation (activity 6480 $kg.mol^{-1}.h^{-1}$).[38]

The bis(allyl) yttrium and scandium analogues $(C_5Me_4\text{-}C_5H_4N)RE(\eta^3\text{-}C_3H_5)_2$ (RE = Y, Sc) were further synthesized by reacting $(C_5Me_4\text{-}C_5H_4N)Li$ with 1 equiv. of $RECl_3$, followed by addition of 2 equiv. of the Grignard reagent, $(C_3H_5)MgCl$ in THF at RT (Scheme 1.18).[39]

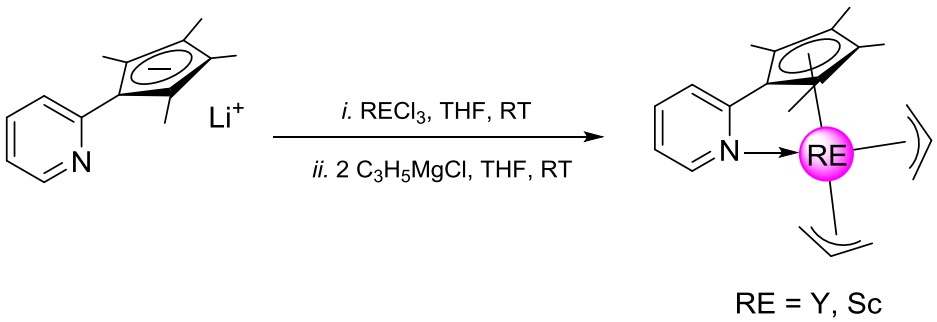

Scheme 1.18 Synthesis of bis(allyl) complexes $(C_5Me_4\text{-}C_5H_4N)RE(\eta^3\text{-}C_3H_5)_2$ (RE = Y, Sc).[39]

Hou, Cui and co-workers synthesized the aminophenyl-cyclopentadienyl bis(allyl) complexes $(C_5Me_4\text{–}C_6H_4\text{-}o\text{-}NMe_2)RE(\eta^3\text{-}C_3H_5)_2$ (RE = Y, Nd, Gd, Dy, Lu) from first reacting $(C_5Me_4\text{–}C_6H_4\text{-}o\text{-}NMe_2)Li$ with $RECl_3$ and then with the Grignard reagent, $(C_3H_5)MgCl$ (Scheme 1.19). The yttrium, gadolinium and dysprosium complexes were characterized by X-ray crystallography as solvent-free - even though the reaction was performed in THF - isostructural complexes showing that both allyl moieties coordinate in η^3-mode.[39,40]

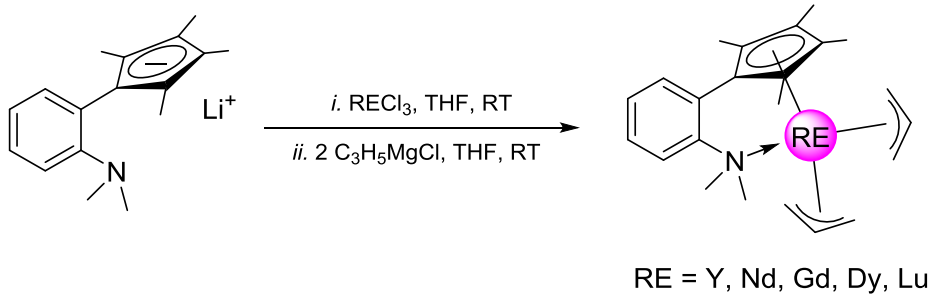

Scheme 1.19 Synthesis of $(C_5Me_4\text{–}C_6H_4\text{-}o\text{-}NMe_2)RE(\eta^3\text{-}C_3H_5)_2$ (RE = Y, Nd, Gd, Dy, Lu).[39,40]

Luo, Chen *et al.* synthesized the pyrrolidinyl-functionalized bis(allyl) half-sandwich complexes $(C_5Me_4\text{-}SiMe_2NC_4H_8)RE(\eta^3\text{-}C_3H_5)_2$ (RE = Y, Sc, Lu) by first reacting $RECl_3$ with 1 equiv. of $C_5Me_4SiMe_2\text{-}NC_4H_8Li$ and then with 2 equiv. of $(C_3H_5)MgCl$ in THF at RT (Scheme 1.20).[41] The ^1H NMR spectra of the three complexes indicated a fluxional allyl ligand in solution, with one sharp doublet signal for the terminal allylic protons and one

multiplet for the central allylic protons. X-ray analysis shows that for the scandium complex, the pendant pyrrolidinyl ligand does not coordinate to the metal center through the nitrogen (Figure 1.6, left), however, this coordination was present in the yttrium (Figure 1.6, right) and lutetium complexes. This could be due to the Sc^{3+} being small in size in comparison to the Lu^{3+} and Y^{3+}.[41]

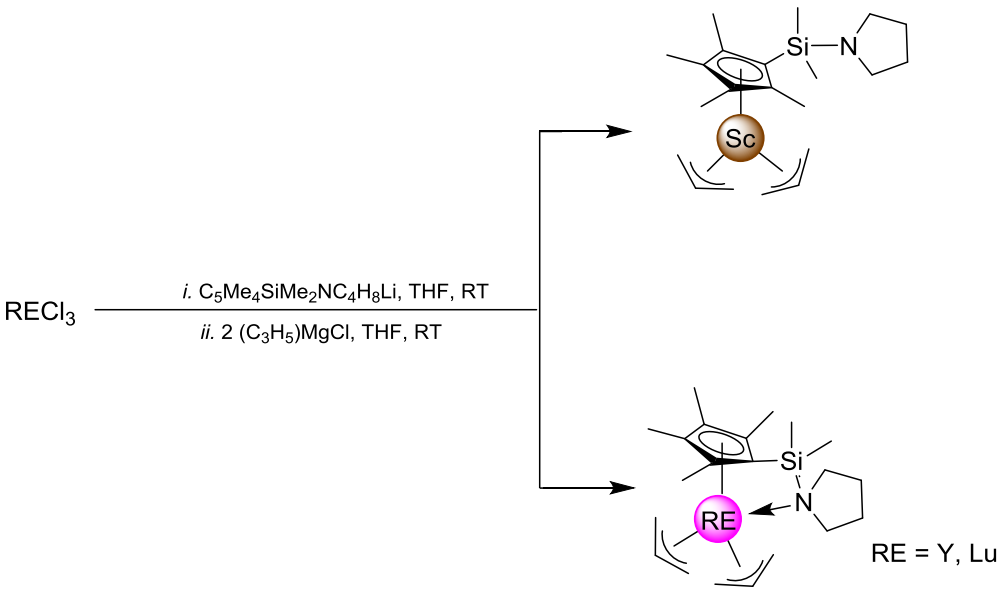

Scheme 1.20 Synthesis of the half-sandwich complexes $(C_5Me_4\text{-}SiMe_2NC_4H_8)RE(\eta^3\text{-}C_3H_5)_2$ (RE = Sc, Y, Lu).[41]

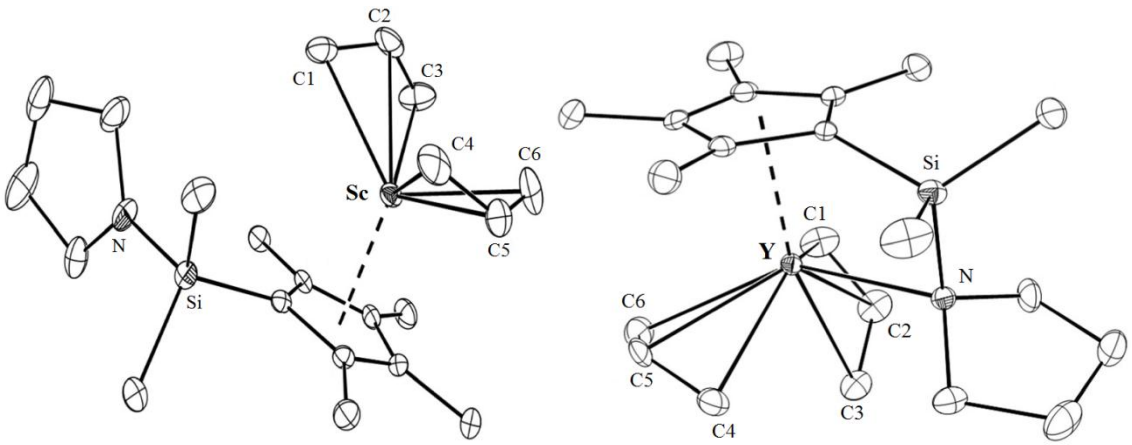

Figure 1.6 X-ray structures of $(C_5Me_4\text{-}SiMe_2NC_4H_8)RE(\eta^3\text{-}C_3H_5)_2$ (RE = Sc (left), Y (right)). Hydrogen atoms are omitted for clarity.[41]

Anwander *et al.* synthesized the half-sandwich bis(allyl) complexes, $Cp^{NMe2}RE(\eta^3\text{-}C_3H_5)_2$ (Cp^{NMe2} = $C_5Me_4CH_2CH_2NMe_2$; RE = Y, Ho, Lu) having a more flexible (*N*,*N*-dimethylamino)ethyl-functionalized cyclopentadienyl ligand (Scheme 1.21).[42] The reaction was conducted in two steps by first reacting $RECl_3$ with $Cp^{NMe2}Li$ at RT and then adding 2 equiv. of the Grignard reagent $(C_3H_5)MgCl$ to give the expected products. When the same procedure was conducted with the neodymium complex, a mono(allyl) chloro derivative $[Cp^{NMe2}Nd(\eta^3\text{-}C_3H_5)(\mu\text{-}Cl)]_2$ was isolated as depicted by X-ray data, instead of the expected bis(allyl) half-sandwich complex as isolated for RE = Y, Ho, Lu. Some attempts to synthesize the lanthanum analogue dis not succeed. X-ray analysis of the monomeric bis(allyl) half-sandwich complexes showed that all the complexes were isostructural.

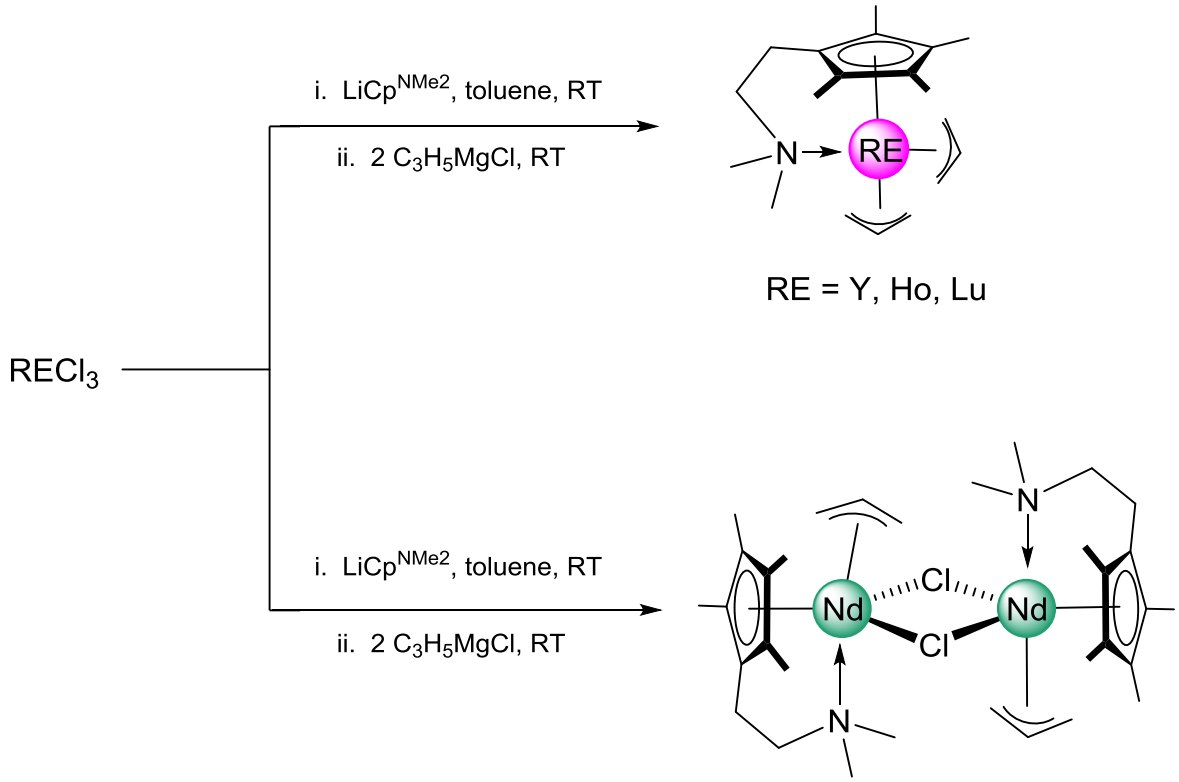

Scheme 1.21 Synthesis of $Cp^{NMe2}RE(\eta^3\text{-}C_3H_5)_2$ (RE = Y, Ho, Lu) and $[Cp^{NMe2}Nd(\eta^3\text{-}C_3H_5)_2(\mu\text{-}Cl)]$.[42]

When 2 equiv. of Et_2AlCl was added to the yttrium and holmium complexes $Cp^{NMe2}RE(\eta^3\text{-}C_3H_5)_2$ in deuterated benzene, a complete exchange of the allyl ligands by the chlorido one was observed giving rise to the complexes $[\{(Cp^{NMe2}AlEt_3)_2(Cp^{NMe2})RE_3(\mu_2\text{-}Cl)_3(\mu_3\text{-}Cl)_2\}(\mu_2\text{-}Cl)]_2$ (RE = Y, Ho) (Scheme 1.22 A).[42] The reaction of $Cp^{NMe2}Y(\eta^3\text{-}C_3H_5)_2$ with a ten-fold excess of trimethylaluminum was monitored by ^1H NMR. The allyl signals

disappeared to afford the corresponding bis(tetramethylaluminate) complex $Cp^{NMe2}AlMe_3Y(AlMe_4)_2$ (Scheme 1.22 B), prefiguring a possible pre-catalytic species for dienes polymerisation.[42]

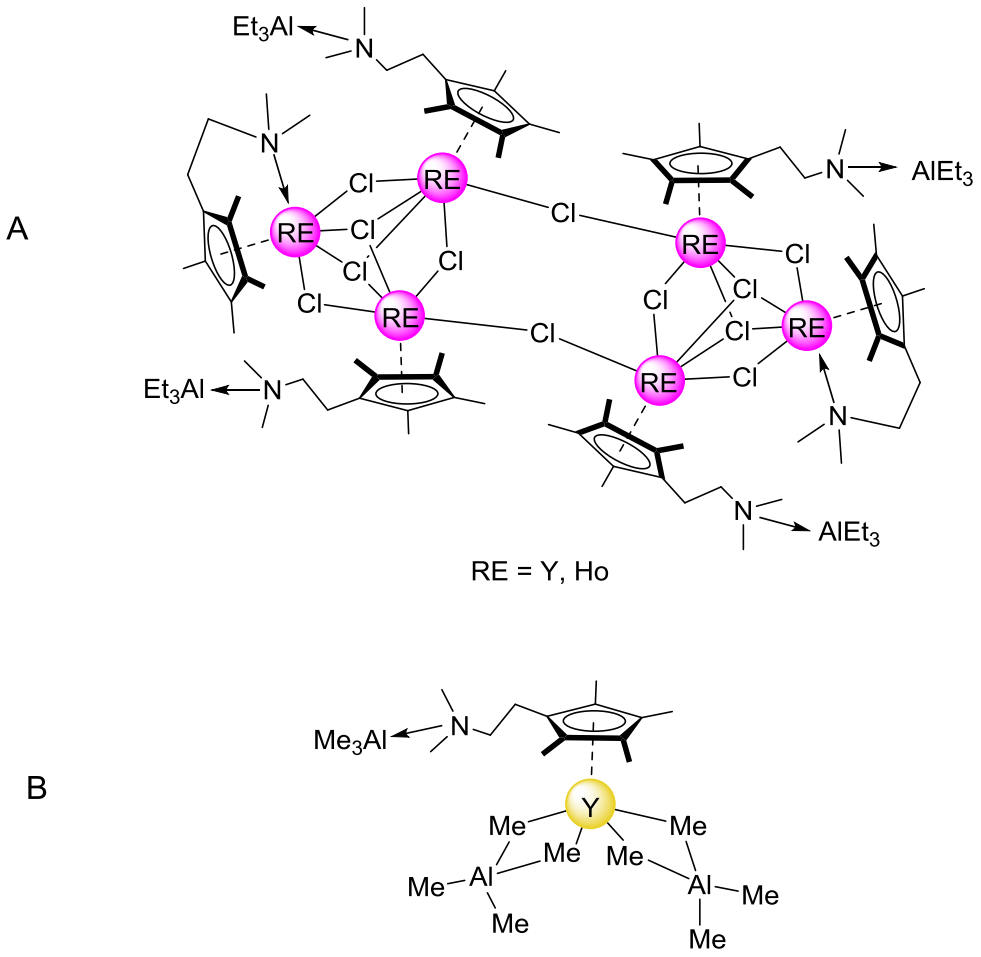

Scheme 1.22 Synthesis of $[\{(Cp^{NMe2}AlEt_3)_2(Cp^{NMe2}RE(\mu_2\text{-}Cl)_3(\mu_3\text{-}Cl)_2\}(\mu_2\text{-}Cl)]_2$ (RE = Y, Ho) (A) and $Cp^{NMe2}AlMe_3Y(AlMe_4)_2$ (B).[42]

1.3.2.2 Isoprene polymerisation

Polyisoprene (PIP) can be extracted from tree sap (known as natural rubber) or manufactured synthetically by polymerisation of isoprene (IP), a petro-sourced monomer. It is used in rubber compounds for numerous applications in the fields of adhesive, sport equipment and tires industry.[43,44] The polymerisation of IP can lead to the formation of PIP containing four different isomers; 1,2-, *cis*-1,4, *trans*-1,4 and 3,4- (Scheme 1.8). Stereoselective PIP can be

produced by the use of specific metal-based catalytic systems. In particular, rare earth-based catalysts are known to be highly active and stereoselective for the polymerisation of dienes.

The activity of the bis(allyl) complexes [(C_5Me_4–C_6H_4-*o*-NMe_2)RE(η^3- C_3H_5)$_2$] RE = Y, Nd, Gd, Dy) was assessed towards the polymerisation of IP in the presence of Al^{i}Bu$_3$ and [$PhMe_2NH$][$B(C_6F_5)_4$] in toluene at RT.[40] The neodymium complex had the highest activity, followed by gadolinium and then the dysprosium analogue, whereas the yttrium complex was almost inert towards this reaction. The gadolinium analogue afforded the highest *cis*-regular PIP at 99.2% when the reaction was conducted at 0°C, along with a living character of the polymerisation.

The activity of the neodymium complex [$Cp^{NMe2}Nd(\eta^3$-$C_3H_5)(\mu$-Cl)]$_2$ was tested towards the polymerisation of IP with the use of either [Ph_3C][$B(C_6F_5)_4$] or [$PhNMe_2H$][$B(C_6F_5)_4$] as the co-catalysts.[42] No activity was observed when the neodymium over co-catalyst ratio was 1:1 hence it can be concluded that both allyl groups were displaced. However, when half an equiv. of the co-catalyst was added to the neodymium complex, (Nd to co-catalyst was 2:1), PIP with mainly 3,4-sturcture of up to 66 % was isolated along with narrow dispersities (1.10 - 1.11) and high molar masses of up to 47 kg.mol^{-1}. When $AlMe_3$ was added to the system along with [$PhNMe_2H$][$B(C_6F_5)_4$], a switch in the stereo-selectivity was observed as *trans*-1,4-PIP (85 %) was obtained while the addition of Al(^{i}Bu)$_3$ gave rise to 3,4-PIP (85 %).

The half-sandwich complexes [Cp^{NMe2}RE(η^3-C_3H_5)$_2$] (RE = Y, Ho, Lu) were assessed towards the polymerisation of IP with the use of either [Ph_3C][$B(C_6F_5)_4$] or [$PhNMe_2H$][$B(C_6F_5)_4$] (1 equiv.) as co-catalysts.[42] The yttrium and holmium complexes afforded predominantly 3,4-PIP with both co-catalysts showing low activity (7 kg.mol^{-1}.h^{-1}). The lutetium complex afforded polymers with equal amounts of each isomer (*cis*-1,4, *trans*-1,4 and 3,4-PIP) but was found to be more active (33 kg.mol^{-1}.h^{-1}). The dispersities were very narrow (1.04 - 1.17) for all complexes tested, speaking in favor of the formation of a unique active species. The complexes were also associated with [$PhNMe_2H$][$B(C_6F_5)_4$] and $AlMe_3$ or Al(^{i}Bu)$_3$, to further investigate their activity and selectivity. For the yttrium and holmium systems, when $AlMe_3$ was used, it afforded a much more active catalyst (up to 660 kg.mol^{-1}.h^{-1}) with a switch in selectivity towards *trans*-1,4-PIP (71 % Y, 72 % Ho). In contrast when

$Al(^{i}Bu)_3$ was added to the yttrium and holmium systems, it afforded moderate selectivity towards *cis*-1,4-PIP (74% Y, 74% Ho) however the activity was largely improved (330 $kg.mol^{-1}.h^{-1}$). For the lutetium complex, the main effect was a similar gain of activity (up to 660 $kg.mol^{-1}.h^{-1}$) when $AlMe_3$ or $Al(^{i}Bu)_3$ were added into the system, along with a small change in the stereo control.[42]

1.3.2.3 (Co)-polymerisation of styrene and butadiene

The catalyst system composed of $(C_5Me_4\text{-}C_5H_4N)Lu(\eta^3\text{-}C_3H_5)_2$ and trityl borate activator $[Ph_3C][B(C_6F_5)_4]$ (1 equiv.) showed high activity (up to 400 $kg.mol^{-1}.h^{-1}$) for both the statistical and sequenced copolymerisation of butadiene and styrene (Scheme 1.23).[38] The addition of both the monomers, with the styrene feeding molar fractions ranging from 10 – 90 %, afforded copolymers containing highly *cis*-1,4-regulated polybutadiene and syndiotactic polystyrene segments, along with high molar masses (M_n = 8.8-12.1 x 10^4 $g.mol^{-1}$) and narrow dispersities (1.29 - 1.68) across the styrene feeding ratio range.

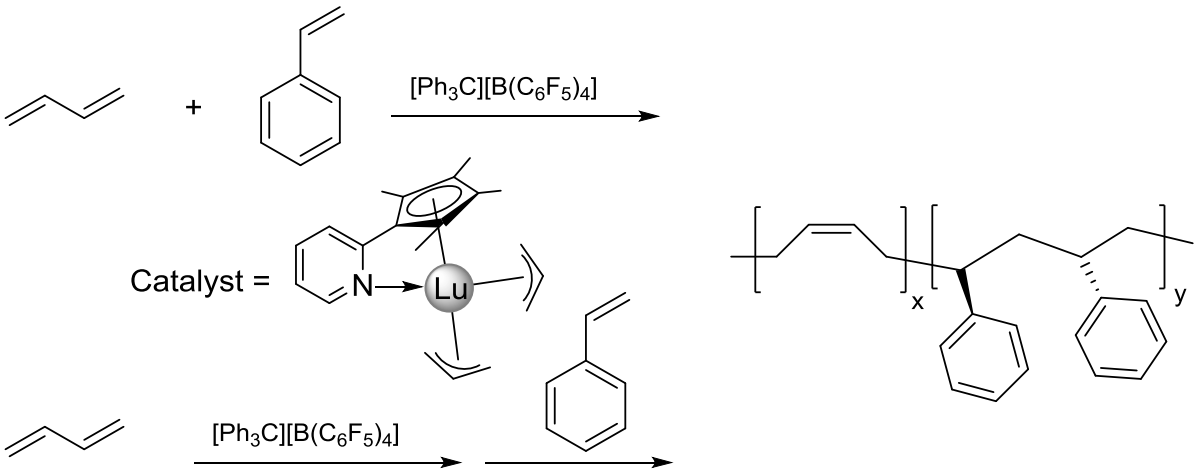

Scheme 1.23 Statistical and sequenced copolymerisation of butadiene and styrene catalyzed by $[(C_5Me_4\text{-}C_5H_4N)Lu(\eta^3\text{-}C_3H_5)_2]$ and $[Ph_3C][B(C_6F_5)_4]$.[38]

1.4 Synthesis, characterization and reactivity of non-Cp containing allyl rare-earth complexes

From 1990's, allyl RE complexes with ancillary ligands other than Cp ones started to be explored. Non-Cp ligands, such as amido(diphosphino),[45,46] β-diketiminates,[12,47,48] biphenolates or crown aza have been introduced into this chemistry.

1.4.1 Crown-Aza supported complexes

1.4.1.1 Neutral and "ate" complexes

Okuda *et al.* showed that the tris(allyl) RE complexes $RE(\eta^3\text{-}C_3H_5)_3(diox)$ reacts with the ligand $(Me_3TACD)H$ (Me_3TACD = 1,4,7-trimethyl-1,4,7,10-tetraazacyclododecane) in THF with elimination of one allyl group to form $(Me_3TACD)RE(\eta^3\text{-}C_3H_5)_2$ (RE = Y, La, Ce, Pr, Nd, Sm) (Scheme 1.24).[49]

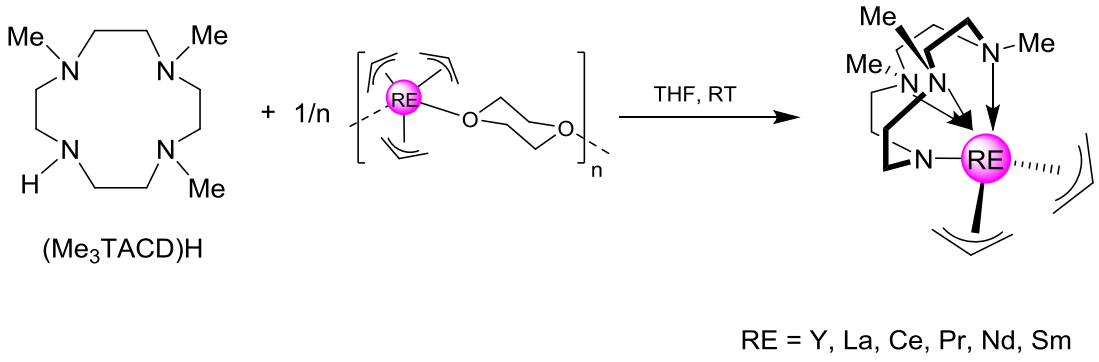

Scheme 1.24 Synthesis of $(Me_3TACD)RE(\eta^3\text{-}C_3H_5)_2$.[49]

The X-ray diffraction of the yttrium, lanthanum, praseodymium and samarium complexes revealed non-solvated hexa-coordinated complexes in which the distance between the amido nitrogen and the metal was found to be shorter than the distance between the three amino nitrogen atoms and the metal. It also showed an increase bend of the ring and migration of the metal towards the cavity of the ligand when the ionic radius decreased when going from the lanthanum complex to the yttrium complex (Figure 1.7).[49]

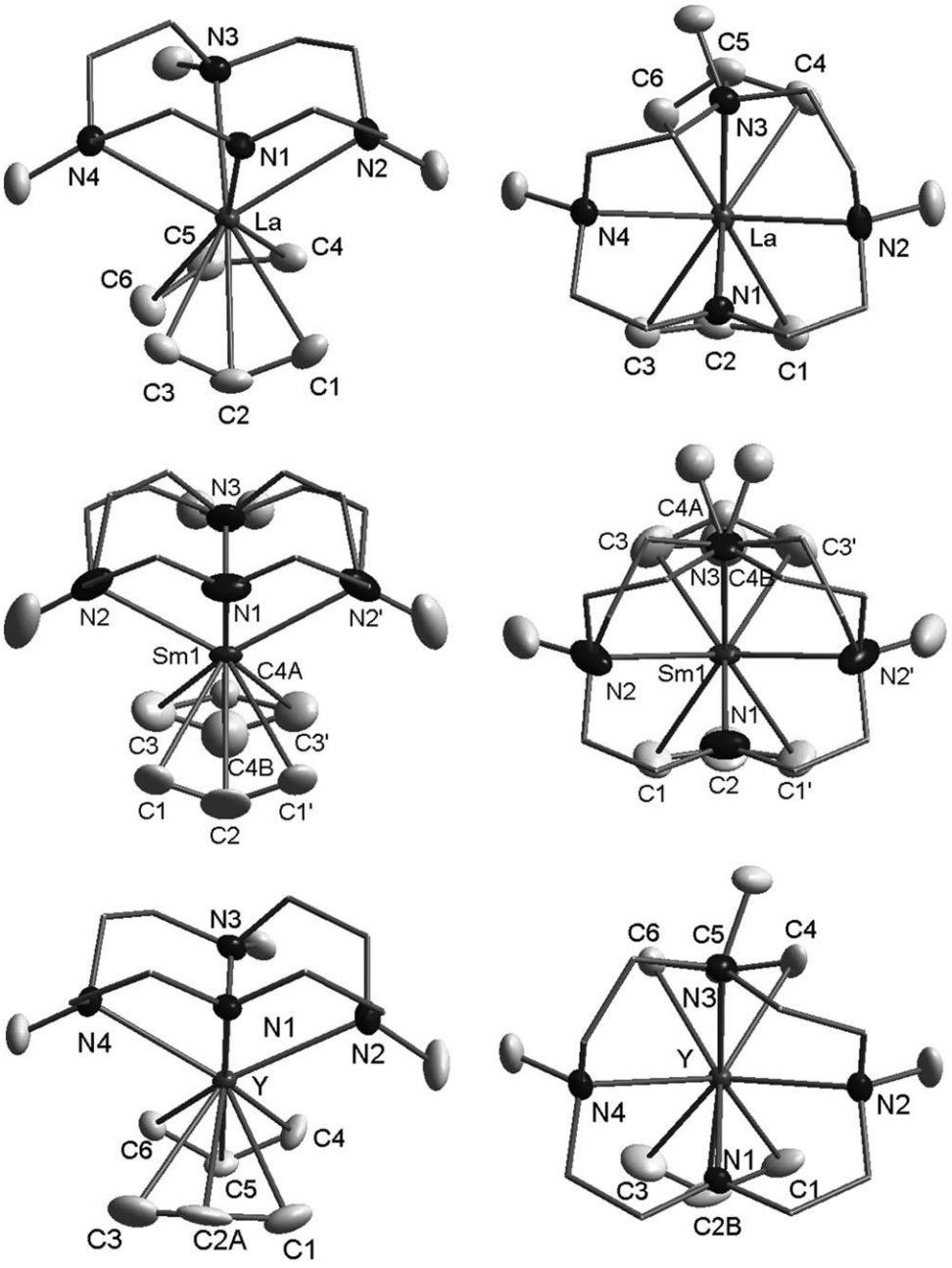

Figure 1.7 X-ray structures of $(Me_3TACD)RE(\eta^3\text{-}C_3H_5)_2$ (RE = Y, La, Sm). Hydrogen atoms are omitted for clarity.[49]

The neutral mono(allyl) complexes $[(1,7\text{-}Me_2TACD)RE(\eta^3\text{-}C_3H_5)]_2$ (RE = Y, La) were synthesized starting from $RE(\eta^3\text{-}C_3H_5)_3(diox)$ with 1 equiv. of $(1,7\text{-}Me_2TACD)H_2$ in THF at RT (Scheme 1.25).[50] X-ray analysis of the lanthanum complex showed that the structure was a centrosymmetric dimer.

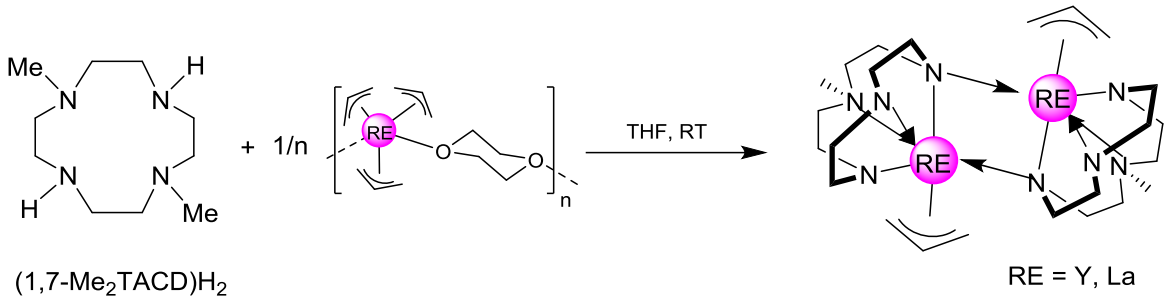

Scheme 1.25 Synthesis of $[(1,7\text{-}Me_2TACD)RE(\eta^3\text{-}C_3H_5)]_2$.[50]

The same research group synthesized the bis(allyl) "ate" complexes $[(1,7\text{-}Me_2TACD)RE(\eta^3\text{-}C_3H_5)_2K(THF)]_n$ (RE = Y, La), which were isolated under a polymeric form, by the reaction of $K(C_3H_5)$ with the monoallyl $[(1,7\text{-}Me_2TACD)RE(\eta^3\text{-}C_3H_5)]_2$ in THF at RT (Scheme 1.26).[50] The average Y−C(allyl) bond length is significantly longer than that in $(Me_3TACD)Y(\eta^3\text{-}C_3H_5)_2$ (2.77 vs. 2.69 Å) possibly as a consequence of potassium coordination on the opposite side of the allyl ligand. Both yttrium and lanthanum complexes were reacted with H_2 in THF to give the dimer $[(1,7\text{-}Me_2TACD)_2Y_2H_3K(THF)_2]_2$ and the complex $[(1,7\text{-}Me_2TACD)_3La_3H_7K_4(THF)_7]$.

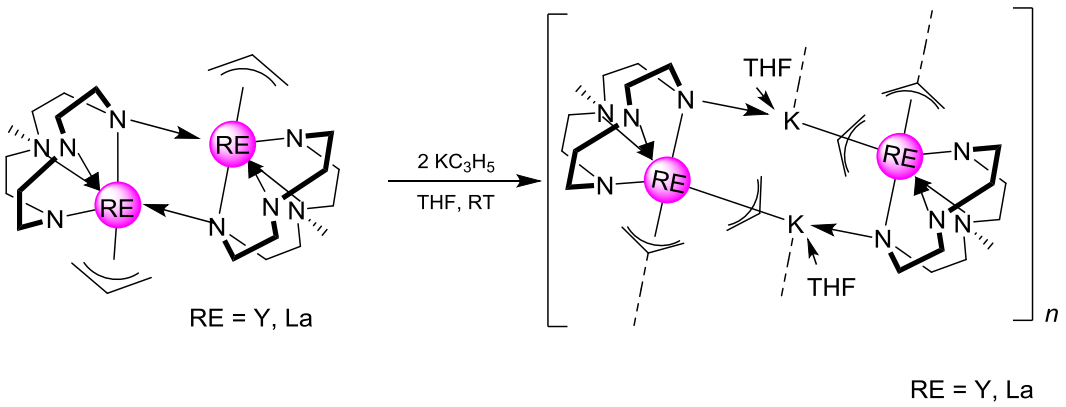

Scheme 1.26 Synthesis of $[(1,7\text{-}Me_2TACD)RE(\eta^3\text{-}C_3H_5)_2K(THF)]_n$ (Ln = Y, La).[50]

The mono(allyl) scandium complex $(1,7\text{-}Me_2TACD)Sc(\eta^3\text{-}C_3H_5)$ was synthesized by reacting $Sc(C_3H_5)_3(THF)_2$ with 1 equiv. of $(1,7\text{-}Me_2TACD)H_2$ in THF (Scheme 1.27).[51] The structure was confirmed to be monomeric from VT-NMR analysis. The scandium mono(allyl) was treated with H_2 in THF and gave the ion pair $[(1,7\text{-}Me_2TACD)_3Sc_3H_2][(1,7\text{-}Me_2TACD)_3Sc_3H_4]$ (Scheme 1.27).

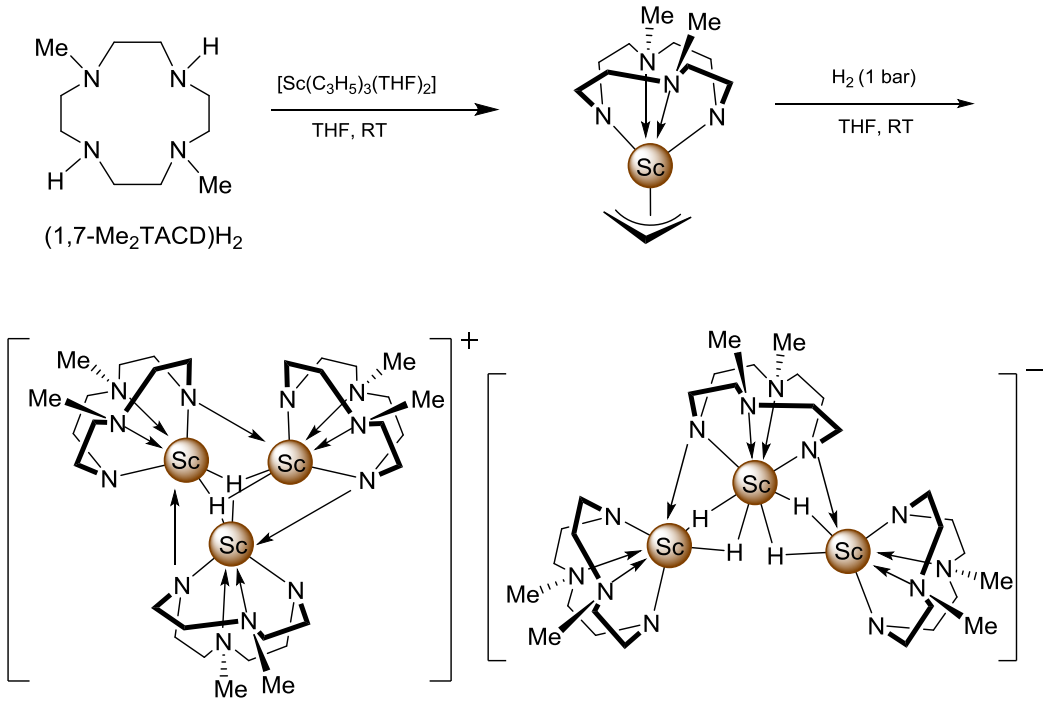

Scheme 1.27 Synthesis of $[(1,7\text{-}Me_2TACD)_3Sc_3H_2][(1,7\text{-}Me_2TACD)_3Sc_3H_4]$.[51]

1.4.1.2 Monocationic and hydride complexes

The crown aza bis(allylic) complex $(Me_3TACD)RE(\eta^3\text{-}C_3H_5)_2$ (RE = La, Ce, Nd) were reacted with $[NEt_3H][B(C_6H_5)_4]$, affording the monocationic allyl species $[(Me_3TACD)RE(\eta^3\text{-}C_3H_5)(THF)_2][(C_6H_5)_4]$ (Scheme 1.28).[49] In order to increase the solubility of the cation, $[NEt_3H][B(C_6F_5)_4]$ was used instead of $[NEt_3H][B(C_6H_5)_4]$ giving rise to $[(Me_3TACD)La(\eta^3\text{-}C_3H_5)(THF)_2][(C_6F_5)_4]$.

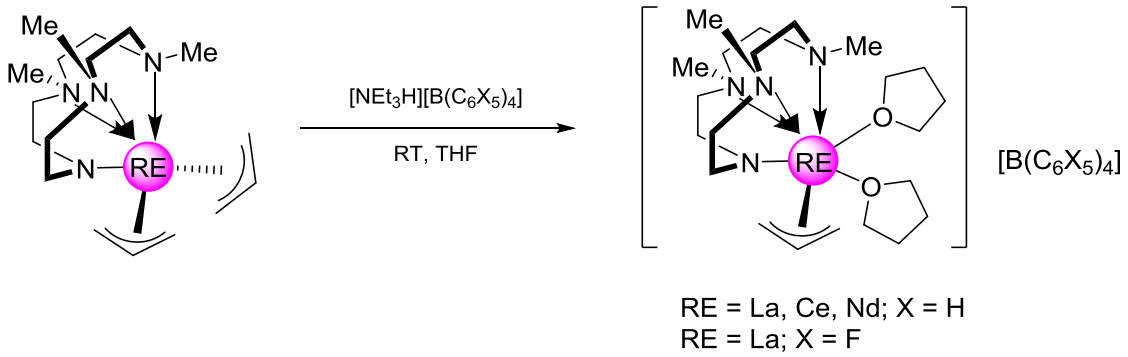

Scheme 1.28 Synthesis of $[(Me_3TACD)RE(\eta^3\text{-}C_3H_5)(THF)_2][(C_6H_5)_4]$ and $[(Me_3TACD)La(\eta^3\text{-}C_3H_5)(THF)_2][(C_6F_5)_4]$.[49]

Mono(allylic) [RE(Me_3TACD)(η^3-C_3H_5)(μ-H)]$_2$ (RE = Nd, Sm) were synthesized by reacting (Me_3TACD)RE(η^3-C_3H_5)$_2$ with 2 equiv. of phenysilane (Scheme 1.29).[52] X-ray analysis showed that both complexes were isostructural dimers with hydrogen bridges.

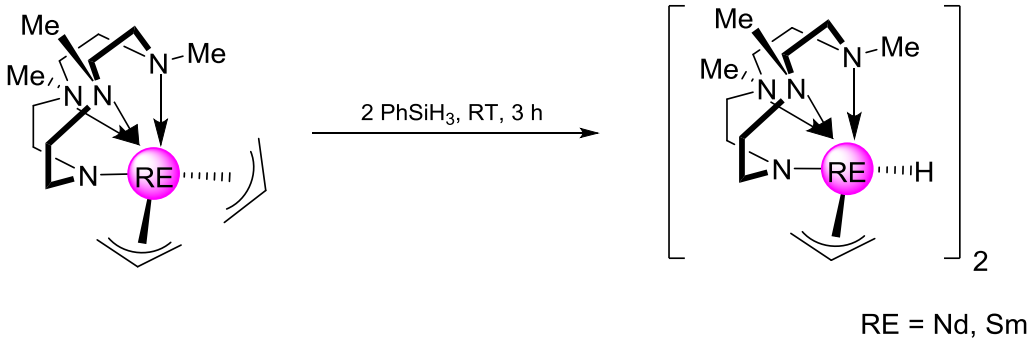

Scheme 1.29 Synthesis of [(Me_3TACD)RE(η^3-C_3H_5)(μ-H)]$_2$.[52]

The activity of the former hydride complexes were assessed towards the copolymerisation of cyclohexene oxide and carbon dioxide with a pressure of 12 bars at 110 °C (Scheme 1.30).[52] The samarium complex had higher activity (129 mol of CHO consumed (mol of Sm)$^{-1}$) than the neodymium complex (119 mol of CHO consumed (mol of Nd)$^{-1}$). The copolymers was found to be atactic with high carbonate linkage (98 %) and with broad dispersities (10.6 and 8.9 for Nd and Sm respectively) which is normal for such copolymerisation at high temperatures and using RE based catalytic systems.[53]

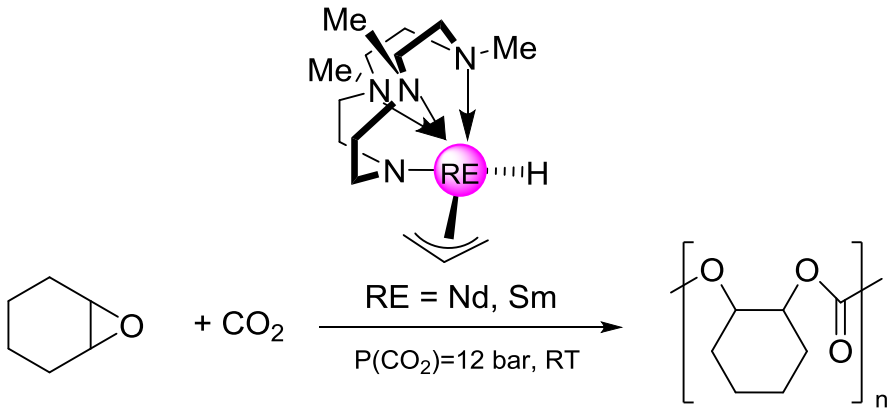

Scheme 1.30 Copolymerisation of cyclohexane oxide with CO_2.[52]

1.4.2 Bis(phenolato) supported complexes

The reaction of RE(η^3-C_3H_5)$_3$(diox) with bis(phenol) in THF afforded the allyl bis(phenolato) complexes, (tbbp)RE(η^3-C_3H_5)(THF)$_x$ (RE = Y, La; x = 3-4; tbbp = tetra(3-benzimidazolyl)-4,4'-bipyridine tetra- anion) and (etbbp)RE(η^3-C_3H_5)(THF)$_x$ (RE = La, Ce, Nd, Sm, x = 1-2; etbbp = 1,4-dithiabutanediylbis(4,6-di-*tert*-butylphenolato)) (Scheme 1.31).[54] They were able to get crystals of (tbbp)Y(η^3-C_3H_5)(THF)$_3$ and (etbbp)RE(η^3-C_3H_5)(THF)$_2$ (RE = La, Ce). X-ray analysis showed that the geometry is pentagonal bipyramidal and the allyl group is coordinated in the axial position in the three complexes. ^{1}H NMR of (etbbp)La(η^3-C_3H_5)(THF)$_x$ showed that the *syn* and *anti* protons on the allyl group were distinguishable at -30 °C.

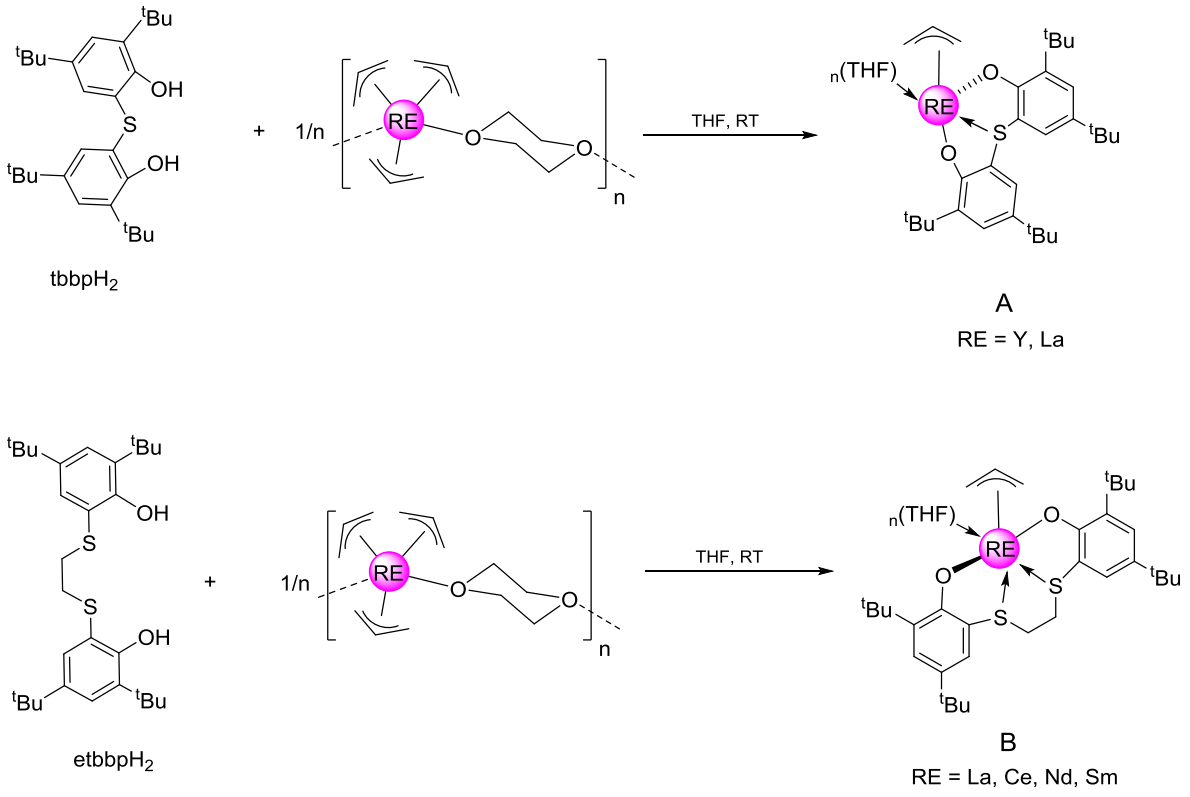

Scheme 1.31 Structure of A: (tbbp)RE(η^3- C_3H_5)(THF)$_x$ (RE = Y, La) and B: (etbbp)RE(η^3-C_3H_5)(THF)$_x$ (RE = La, Ce, Nd, Sm).[54]

(etbbp)RE(η^3-C_3H_5)(THF)$_x$ (RE = La, Ce, Nd, Sm, x = 1-2) was involved in the hydrosilation of 1-hexene with phenylsilane to produce the *anti*-Markovnikov product at high conversions (93-95%), the neodymium complex being the most active (Scheme 1.32).[54] 1,5-hexadiene was also hydrasilated with phenylsilane by using the same lanthanum, cerium and neodymium bis(phenolato) complexes. Full conversion was reached in 10-14 h at 50 °C and the formation of the linear disilylated product was found to be high (91 % Ce, 95 % La). When *n*-butylsilane was used for the hydrosilation of 1,5-hexadiene, the formation of the resulting linear product was much lower (38 % in 20 h for Ce, 67 % in 17 h for Nd) than with phenylsilane (91% in 14 h for Ce, 93 % in 10 h for Nd).

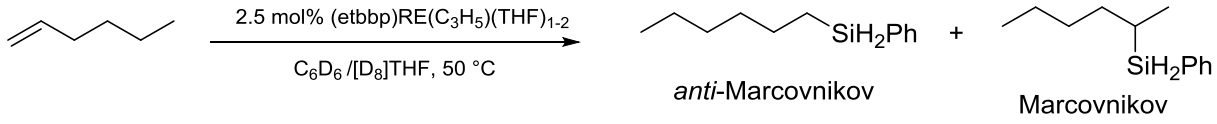

Scheme 1.32 Hydrosilation of 1-hexene with phenylsilane.[54]

The hydrosilation of styrene with phenylsilane was catalyzed by these bis(phenolato) complexes (Scheme 1.33).[54] The regioselectivity was the highest (97 % of the Markovnikov product) with the lanthanum and cerium complexes and full conversion was observed in less than 30 minutes at RT. The neodymium complex afforded full conversion in 3 h while the samarium needed 7 h and higher temperature in order to reach full conversion.

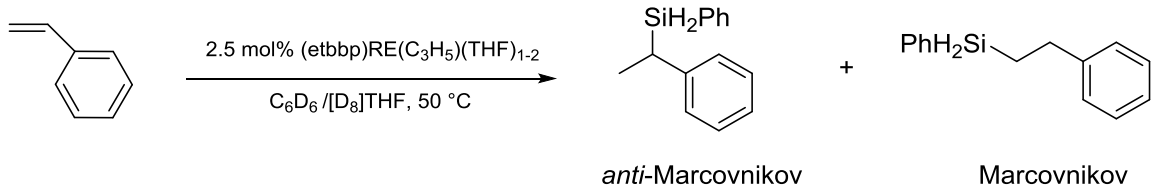

Scheme 1.33 Hydrosilylation of styrene with phenylsilane.[54]

1.5 References

[1] W. J. Evans, D. M. DeCoster, J. Greaves, *Organometallics* **1996**, *15*, 3210.

[2] R. Taube, *in Metalorganic Catalysts for Synthesis and Polymerisation*, (Ed: W. Kaminsky,), Springer, Berlin, **1999**, pp. 531

[3] L. Porri, G. Ricci, A. Giarrusso, N. Shubin, Z. Lu, *Recent Developments in Lanthanide Catalysts for 1,3-Diene Polymerisation, in Olefin Polymerisation, Vol. 749* (Eds: P. Arjunan, J. E. McGrath, T. L. Hanlon), ACS Symposium Series, Washington, DC, **1999**, pp. 15.

[4] A. Fischbach, R. Anwander, *Adv. Polym. Sci*. **2006**, *204*, 155.

[5] Z. C. Zhang, D. M. Cui, B. L. Wang, B. Liu, Y. Yang, *Struct. Bonding* (Berlin) **2010**, *137*, 49.

[6] D. Takeuchi, *Stereoselective Polymerisation of Conjugated Dienes*, in Encyclopedia of Polymer Science and Technology, John Wiley & Sons, New York, **2013**, pp. 1

[7] R. Taube, H. Windisch, S. Maiwald, H. Hemling, H. Schumann, *J. Organomet. Chem*. **1996**, *513*, 49.

[8] M. Tsutsui, N. Ely, *J. Am. Chem. Soc*. **1975**, *97*, 3551.

[9] T. J. Woodman, M. Schormann, D. L. Hughes, M. Bochmann, *Organometallics* **2003**, *22*, 3028.

[10] T. J. Woodman, M. Schormann, M. Bochmann, *Organometallics* **2003**, *22*, 2938.

[11] T. J. Woodman, M. Schormann, D. L. Hughes, M. Bochmann, *Organometallics* **2004**, *23*, 2972.

[12] L. F. Sanchez-Barba, D. L. Hughes, S. M. Humphrey, M. Bochmann, *Organometallics* **2005**, *24*, 3792.

[13] M. Yuan, C. Xiong, X. Li, X. Deng, *J. of App. Polym. Sci.* **1999**, *73*, 2857.

[14] J.-F. Carpentier, S. M. Guillaume, E. Kirillov, Y. Sarazin, *C. R. Chimie* **2010**, *13*, 608.

[15] L. F. Sanchez-Barba, D. L. Hughes, S. M. Humphrey, M. Bochmann, *Organometallics* **2005**, *24*, 3792.

[16] D. Robert, E. Abinet, T. P. Spaniol, J. Okuda, *Chem. Eur. J.* **2009**, *15*, 11937.

[17] S. Standfuss, E. Abinet, T. P. Spaniol, J. Okuda, *Chem. Commun*. **2011**, *47*, 11441.

[18] A. Mazzei, *Makromol. Chem. Suppl.***1981**, *4*, 61.

[19] M. Brunelli, S. Pogcio, U. Pederetti, G. Lugli, *Inorganica Chimica Acta.* **1987**, *131*, 281.

[20] Z. Huang, M. Chen, W. Qiu, W. Wu, *Inorganica Chimica Acta*. **1987**, *139*, 203.

[21] Z. Huang, W. Qiu, R. Cai, S. Zhuang, S. He, F. Li, J. Wei, Y. Sheng, W. Wu, *Acta Chim. Sin*. **1986**, *44*, 817.

[22] W. Qiu, Z. Huang, S. Zhuang, W. Wu, J. *Inorg. Chem. (China)* **1985**, *I*, 173.

[23] R. Taube, H. Windisch, F. H. Gorlitz, H. Schumann, *J. Organomet. Chem*. **1993**, *445*, 85.

[24] J. A. Brydson, *Plastics Materials*, Butterworth-Heinemann, Oxford, **1999**, pp. 920.

[25] T. Hayashi, *Progr. Polym. Sci*. **1994**, *19*, 663.

[26] C. M. Thomas, *Chem. Soc. Rev*. **2010**, *39*, 165.

[27] O. Dechy-Cabaret, B. Martin-Vaca, D. Bourissou, *Chem. Rev.* **2004**, *104*, 6.

[28] R. E. Drumright, P. R. Gruber, D. E. Henton, *Adv. Mater*. **2000**, *12*, 1841.

[29] M. H. Chisholm, Z. Zhou, *J. Mater. Chem*. **2004**, *14*, 3081.

[30] C. K. Ha, Jr J. A. Gardella, *Chem. Rev*. **2005**, *105*, 4205.

[31] C. Changtao, W. Chunhong, C. Yaofeng, *Acta Chim. Sinica.* **2014**, *72*, 883.

[32] A. S. Rodrigues, E. Kirillov, T. Roisnel, A. Razavi, B. Vuillemin, J.-F.Carpentier, *Angew. Chem. Int. Ed*. **2007**, *46*, 7240 .

[33] L. Annunziata, A. S. Rodrigues, E. Kirillov, Y. Sarazin, J. Okuda, L. Perrin, L. Maron, J.-F. Carpentier, *Macromol*. **2011**, *44*, 3312.

[34] Y. Sarazin, P. de Frmont, L. Annunziata, M. Duc, J.-F.Carpentier, *Adv. Synth. Catal*. **2011**, *353*, 1367.

[35] J. K. Peterson, M. R. MacDonald, J. W. Ziller, W. J. Evans, *Organometallics* **2013**, *32*, 2625.

[36] J. L. Gurman, L. Baier, B. C. Levin, *Fire and Materials* **1987**, *11*, 109.

[37] J. Maul,B. G. FrushourJ. R. Kontoff, H. Eichenauer, K. H. Ott, C. Schade, C. "Polystyrene and Styrene Copolymers" in *Ullmann's Encyclopedia of Industrial Chemistry* Wiley-VCH, Weinheim, **2007**, pp. 475.

[38] Z. Jian, S. Tang, D. Cui, *Chem. Eur. J.* **2010**, *16*, 14007.

[39] Z. Jian, D. Cui, Z. Hou, *Chem. Eur. J.* **2012**, *18*, 2674.

[40] Z. Jian, D. Cui, Z. Hou, X. Li, *Chem. Commun.* **2010**, 46, 3022.

[41] Y. Luo, S. Chi, J. Chen, *New. J. Chem*. **2013**, *37*, 2675.

[42] L. N. Jende, C. O. Hollfelder, C. Maichle-Mossmer, R. Anwander, *Organometallics* **2015**, *34*, 32.

[43] D. J. Kind, T. R. Hulla, *Polym. Degrad. Stabil.* **2012**, *97*, 201.

[44] R. F.Yan, *Chin .Chem. Bull.* **1991**, *1*, 1.

[45] M.D. Fryzuk, T.S. Haddad, S.J. Rettig, *Organometallics* **1991**, 10, 2026.

[46] M.D. Fryzuk, T.S. Haddad, S.J. Rettig, *Organometallics* **1992**, *11*, 2967.

[47] L.F. Sanchez-Barba, D.L. Hughes, S.M. Humphrey, M. Bochmann, *Organometallics* **2005**, *24*, 5329.

[48] L.F. Sanchez-Barba, D.L. Hughes, S.M. Humphrey, M. Bochmann, *Organometallics* **2006**, *25*, 1012.

[49] E. Abinet, D. Martin, S. Standfuss, H. Kulinna, T. P. Spaniol, J. Okuda, *Chem. Eur. J.* **2011**, *17*, 15014.

[50] P. Cui, T. P. Spaniol, J, Okuda, *Organometallics* **2013**, *32*, 1176.

[51] P. Cui, T. P. Spaniol, L. Maron, J, Okuda, *Chem. Commun.***2014**, *50*, 424.

[52] D. Martin, J. Kleemann, E. Abinet, T. P. Spaniol, L. Maron, J. Okuda, *Eur. J. Inorg. Chem.* **2013**, 3987.

[53] D. Cui, M. Nishiura, O. Tardif, Z. Hou, *Organometallics* **2008**, *27*, 2428.

[54] E. Abinet, T. P. Spaniol, J. Okuda, *Chem. Asian J.* **2011**, *6*, 389.

CHAPTER 2

MIXED ALLYL-BOROHYDRIDE RARE-EARTH COMPLEXES

2.1 Introduction

2.1.1 Borohydride rare-earth complexes

The chemistry of borohydride rare-earth (RE) complexes has received significant attention during the past three decades. The preparation, structure and chemical reactivity of these complexes have been described in some reviews.[1,4]

Generally, borohydride complexes of RE contain at least one BH_4 anionic ligand. One of the advantages of BH_4 ligand is its versatility regarding the coordination mode and reactivity. Borohydride can adapt their hapticity to satisfy the size of the coordination sphere around a metal, adopting di-hapto κ^2 and tri-hapto κ^3 binding modes through the RE(μ-H)B bonds. In addition, a borohydride group may be connected to one single metal (terminal), or up to three metal atoms (bridging) (Figure 2.1). To determine the mode of coordination, X-ray is widely used nowadays, and is considered the best method where it can locates the hydride atoms of the BH_4 or at least calculates the RE···B distance from which one can conclude the coordination type.[5]

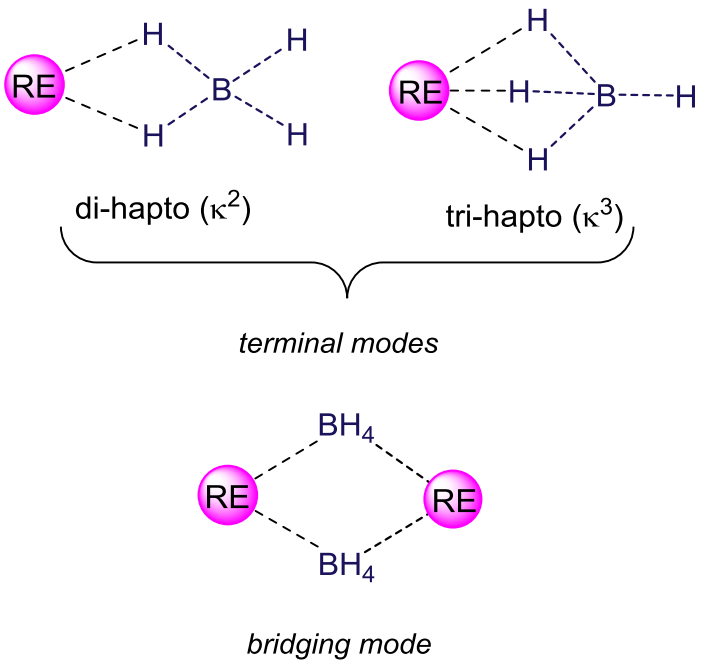

Figure 2.1 Coordination modes of borohydride ligand in RE complexes.

From a chemical point of view, on one hand, borohydride can be considered as *pseudo*-halide and thus its reactivity must be compared with that of halide compounds knowing that the former is considered as more electron donating and the bond formed is more covalent than the latter, in addition to its higher solubility in common organic solvents, which allows NMR spectroscopy analysis, in contrary to the halide analogues. On the other hand, the BH_4 ligand can also be considered as an hydride supported by borane molecule, showing reactivity associated with a hydridic moiety and wide range of reactions especially in polymerisation of a range of cyclic esters where they found to be very active initiating groups on their own.[6-8] Surprisingly, apart from polymerisation, very little records were reported regarding the use of RE-borohydride compounds in the organic catalysis.[9-11]

$RE(BH_4)_3(THF)_x$ (RE = Y, Sm, Eu, Gd, Tb, Dy, Ho, Er, Tm, Yb, Lu) were originally prepared in 1959 by the reaction of rare-earth alkoxides $RE(OCH_3)_3$ and diborane $(BH_3)_2$ (Scheme 2.1), the low solubility of $RE(OCH_3)_3$ along with the very good solubility of the resulting $RE(BH_4)_3(THF)_x$ allowed the isolation of the reaction solution in which only the latter is not volatile.[12,13] The number of THF coordinated to the RE metal center depends on its size and of the drying conditions.

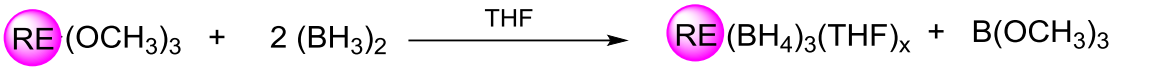

Scheme 2.1 Preparation of $RE(BH_4)_3(THF)_x$ from rare-earth alkoxides and diborane.[13]

A more convenient approach for the synthesis of such compounds is the reaction of $RECl_3$ with $LiBH_4$ (RE = Sc) [14] or $NaBH_4$ (RE = Y, La, Ce, Pr, Nd, Sm, Lu) [15-19] (Scheme 2.2).

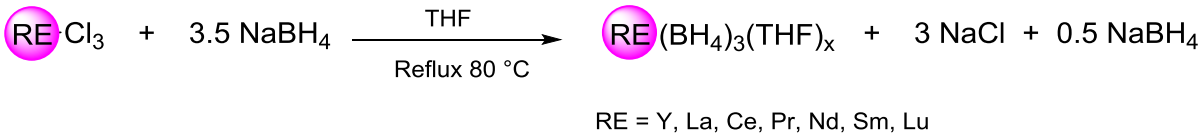

Scheme 2.2 Preparation of $RE(BH_4)_3(THF)_x$ from rare-earth chloride and sodium borohydride.[15-19]

In terms of reactivity the borohydride group of $RE(BH_4)_3(THF)_x$ can be easily substituted by anionic reagent, hence this class of compounds can be considered as starting material to access different coordination and organometallic RE complexes.

In this context, heteroleptic $(L)RE(BH_4)$ (L = active or/and stabilizing ligand) compounds have been widely described. Two main methods are known for the preparation of such complexes starting from the RE borohydride precursors $RE(BH_4)_3(THF)_x$, the ionic metathesis and the comproportionation reaction (Scheme 2.3).

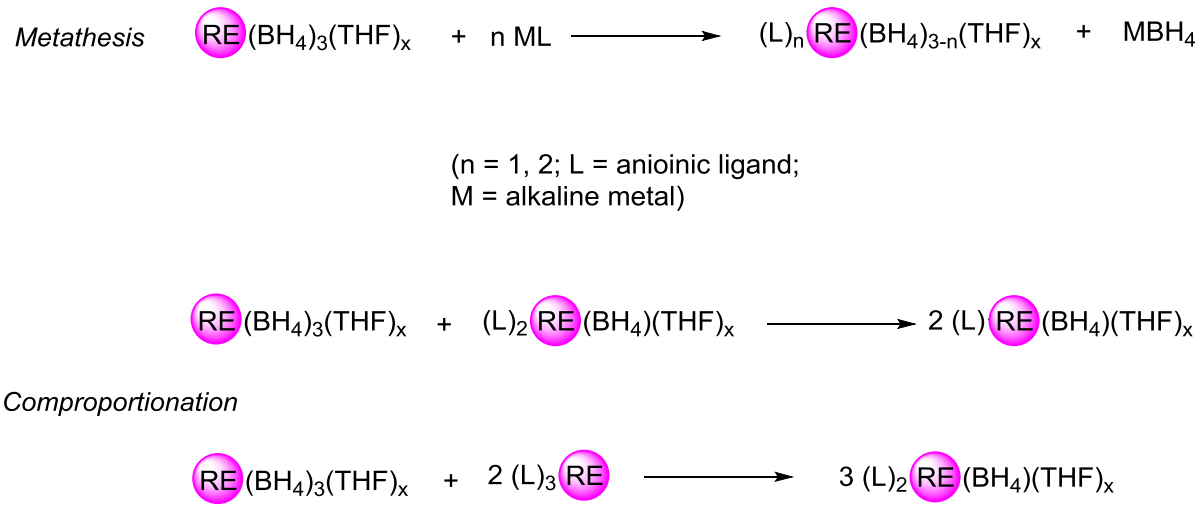

Scheme 2.3 Two different ways of synthesis of heteroleptic RE complexes.

2.1.2 Allyl and borohydride as two active ligands

Rare-earth complexes carrying allyl ligand are of recurring interest due to their high performance in stereospecific diene polymerisation, as presented in the bibliographic part of this manuscript (see chapter 1).[20] For instance, the homoleptic tris- and tetra- anionic allyl complexes (Nd, La) disclosed by Taube were found to catalyze the *trans*-selective polymerisation of butadiene [21-23]. Further progresses in this field has been broadly proclaimed, showing that allylic compounds could be interestingly designed to mediate the polymerisation of olefins.[24]

On the other hand, the borohydride complexes of RE are nowadays considered as being very efficient initiators for polymerisation toward polar monomers such as ε-

caprolatone, *L*- and *rac*-lactide.[1,6-8] Although inactive towards non polar monomers when used on their own, it was found that when combined with alkyl reagents (MgR_2 or AlR_3) , they are able to initiate the polymerisation of ethylene,[25] styrene[26,27] and conjugated diene.[28,29]

Recently, Okuda *et al.* showed that when the mixed alkyl/borohydride complex $[Y(BH_4)(Me)(THF)_5][BPh_4]$ is used as the initiator, the ROP of ε-caprolactone can be promoted by either the borohydride or the methyl ligand, but was found to be kinetically more facile *via* the BH_4 group, as shown by DFT calculations. Interestingly, the initiation through the methyl group was favored with $[Y(Me)(NMe_2)(THF)_5]$, in which the *trans* (BH_4) ligand was substituted with the more electron-donating group NMe_2.[30]

Such organometallic compounds having two distinctive reactive ligands have been scarcely described. Their study is of particular interest due to their potential dual activity while also questioning the influence of one ligand toward the other. Thus, we became interested in the design of a new family of RE complexes that contain both borohydride and allyl group active ligands. Herein, we report the synthesis of mixed allyl-borohydride complexes $RE(BH_4)_2(C_3H_5)(THF)_x$ (RE = Sc, x = 2; Y, La, Nd, Sm, x = 3). The comparison of the spectroscopic and geometric data of their molecular structure is described as long as their reactivity toward various molecules. In addition, trials to form the bis(allyl) mono(borohydride) rare-earth complexes $RE(BH_4)_2(C_3H_5)(THF)_x$ using different sources of allyl group and various conditions is also reported.

2.2 Mono(allyl) bis(borohydride) rare-earth complexes

2.2.1 Synthesis of magnesium bis(allyl) reagent

Allyl magnesium complexes are commonly used as allyl transfer agents in organic and organometallic chemistry. Among these allylic complexes is the bis(allyl)magnesium; $Mg(C_3H_5)_2(dioxane)_y(THF)_z$, that we chose to use as the source of the allyl ion.

The origin of $Mg(C_3H_5)_2(dioxane)_y(THF)_z$, is the Grignard reagent invented by Victor Grignard.[31] After serious attempts to explain the composition of Grignard reagent in

solution,[32-37] Shlenck and Shlenck suggested the two equilibriums shown in Scheme 2.4 to show the unsymmetrical dimeric structure ($R_2Mg.MgX_2$) of Grignard compound in ether solution and found that the addition of dioxane to such solutions leads to selective precipitation of dihalide MgX_2(diox) (X = Cl, Br and I), driving the equilibrium completely to the right side of the equation (Scheme 2.4).[38]

$$2RMgX \rightleftharpoons R_2Mg + MgX_2$$

$$R_2Mg + MgX_2 \rightleftharpoons R_2Mg.MgX_2$$

Scheme 2.4 Schlenk equilibria.[38]

Remarkably, Noller and White showed that the amount of MgX_2, precipitated as the bis-dioxane complex, is a function of time.[39] In 1950, Kullman confirmed the original findings of Noller and White, and he showed that upon treating ethylmagnesium bromide with dioxane, 55 to 93 % of the total $MgBr_2$ precipitates depending on the mode of addition and the duration of stirring.[40]

Although the synthesis of bis(allyl) magnesium is based on the Schlenk equilibrium, we recognized that the way the compound is extracted from the resulting mixture after adding the dioxane, has a strong effect on the final structure of that compound, in which dioxane, THF or even both ended to be coordinated to the magnesium metal center. Okuda reported the dioxane adduct of this compound where the solvent molecules occupy axial positions, and their bridging coordination mode leads to a one-dimensional coordination polymer of [Mg(η^1-C_3H_5)$_2$(THF)(μ^2-1,4-dioxane)] in the solid state (Figure 2.2).[41]

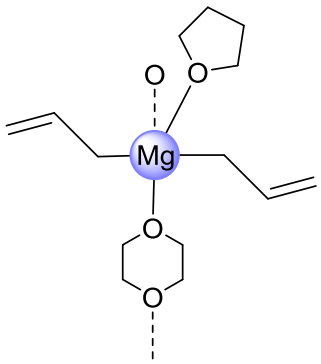

Figure 2.2 Structure of Mg(η^1- C_3H_5)$_2$(THF)(μ^2-1,4-dioxane).[41]

Hill *et al.* proved the fact that bis(allyl) magnesium is sparingly soluble in ether, and proposed a more convenient way to access the final product in better yield in which the ether evaporated and the magnesium bis(allyl) extracted using THF instead of ether.[42]

However, when this experiment was conducted in our laboratory, we realized that when extracted the magnesium bis(allyl) product using diethyl ether only, the final texture; after thoroughly drying the product, is well solid pale-yellow colored powder (yield 20%) which could be characterized by ^{1}H NMR in [D_6]benzene and showed to be coordinated with 0.06 of dioxane molecule. However, when extracted with THF, no dioxane was found to be coordinated to the magnesium center and the aspect is white pasty product (30% yield), not soluble in [D_6]benzene as showed by Hill *et al.*, so difficult to be characterized.

2.2.2 Synthesis of mono(allyl) bis(borohydride) rare-earth complexes

The mixed allyl-borohydride complexes $RE(BH_4)_2(C_3H_5)(THF)_x$ (RE = Sc (**1**), x = 2; Y (**2**), La (**3**), Nd (**4**), Sm (**5**), x = 3)[43] were prepared in good yields *via* the straightforward reaction of $RE(BH_4)_3(THF)_x$ (RE = Sc (**6**), x =2; Y (**7**), La (**8**), Nd (**9**), Sm(**10**), x = 3)[45] with half an equiv. of $Mg(C_3H_5)_2(THF)_y(diox)_z$ (y = 1.5 and 3, z = 0, depending on the crop of reagent used, for RE = Nd, Sm, respectively; y = 0, z = 0.06 for RE = Sc, Y, La)[42] (Scheme 2.5).
The reactions were conducted in THF at room temperature for 2 hours (Scheme 2.5). The reactions seemed to be instantaneous showing an instant color change upon mixing the reagents, affording brown-green, green and violet, solutions for scandium (**1**), neodymium (**4**) and samarium (**5**) respectively and pale-yellow solutions in the case of yttrium (**2**) and lanthanum (**3**). The ^{1}H NMR spectra of the same reaction conducted at the NMR scale and recorded straight after mixing of the reagents, showed their total consumption and revealed the immediacy of that reaction.

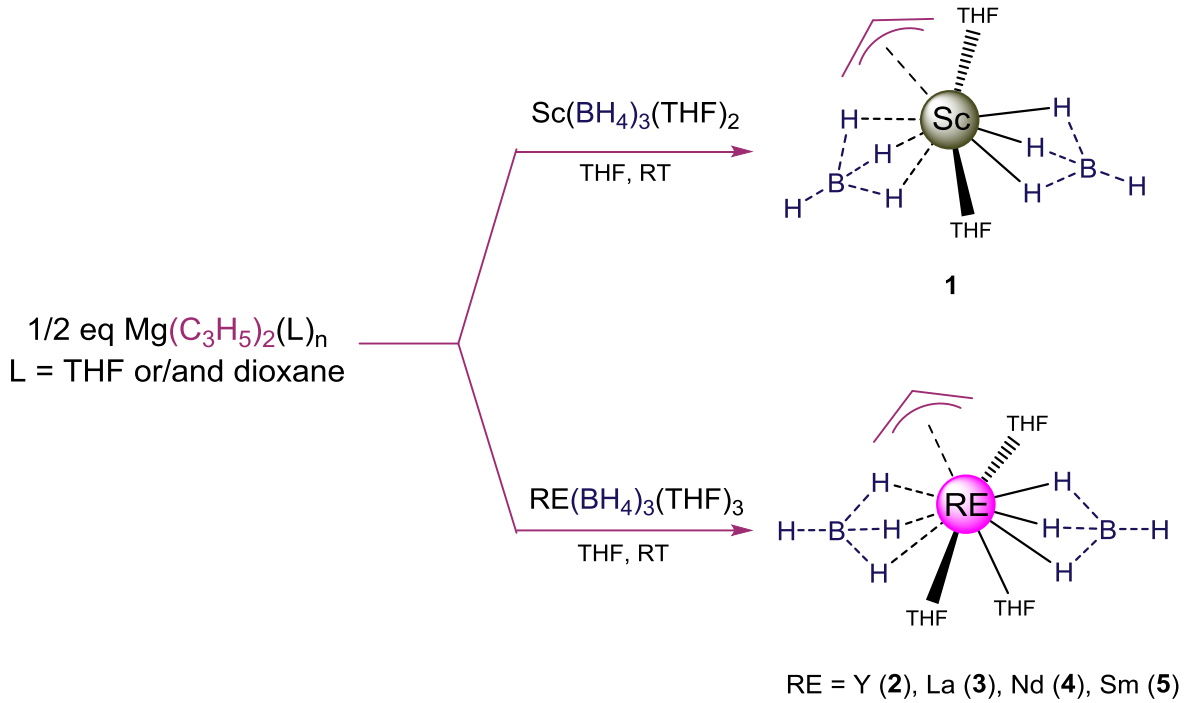

Scheme 2.5 Synthesis of mixed allyl-borohydride complexes **1**-**5**.

In the case of complexes **1**, **3**, **4,** the filtration of the resulting solution, evaporation of the THF and several recrystallization in THF afforded the corresponding mono(allyl) bis(borohydride) complexes in good yields, $Sc(BH_4)_2(C_3H_5)(THF)_{2.5}$ (60 %), $La(BH_4)_2(C_3H_5)(THF)_3$ (89 %) and $Nd(BH_4)_2(C_3H_5)(THF)_4$ (89 %) according to ^{1}H NMR analysis (see the following discussion).

An additional step was in turn necessary to get **2** and **5** as a pure compound: extraction with toluene then re-dissolution in THF and removal of the volatiles followed by several re-crystallization from THF/pentane mixtures to yield $Y(BH_4)_2(C_3H_5)(THF)_{3.6}$ (65 %) and $Sm(BH_4)_2(C_3H_5)(THF)_{3.5}$ (83 %) according to ^{1}H NMR analysis.

The ^{1}H NMR spectra of the diamagnetic yttrium complex **2** recorded in [D_6]benzene showed the expected resonances for mixed allyl-borohydride derivative (Figures 2.3). The spectrum showed a typical BH_4 quadruplet at δ = 1.32 ppm and two signals for the allyl moiety at δ = 3.16 and 6.07 ppm, in a relative 4:1 ratio. Such uncommon fluxionally of the RE-allyl moiety, also observed in the case of complexes **1**, **3** and **5**, has been previously reported. It is noteworthy that according to ^{1}H NMR analysis complex **2** was found to contain

a slight excess of THF, 3.6 THF per metal at δ = 1.15 and 3.60 ppm, as compared to its molecular formula deduced from the X-ray studies (see further).

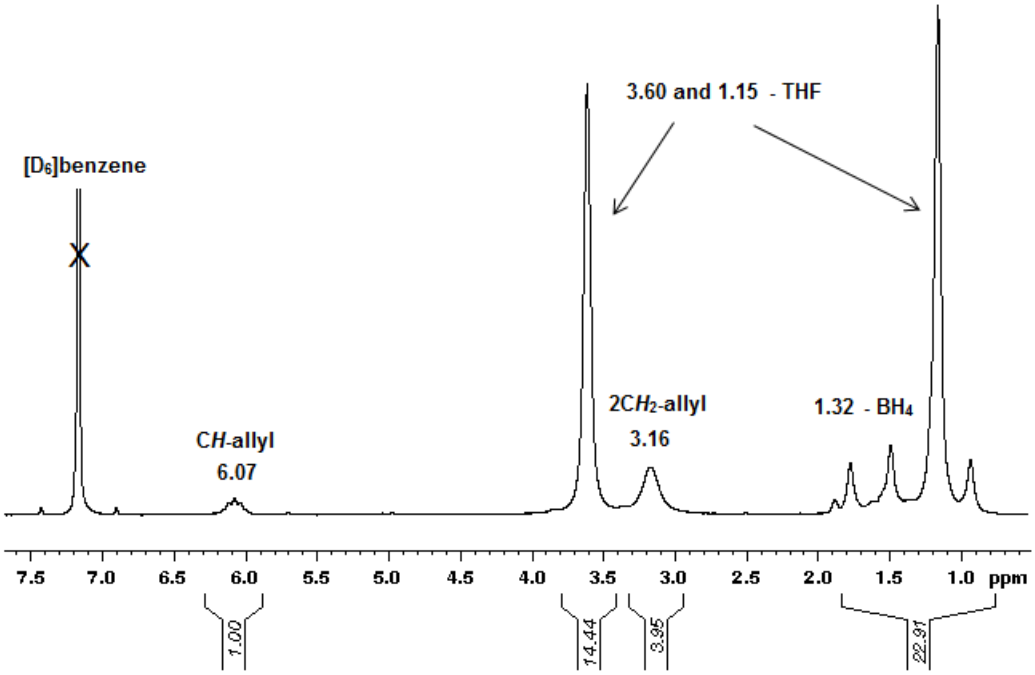

Figure 2.3 ^{1}H NMR spectrum of $Y(BH_4)_2(C_3H_5)(THF)_{3.6}$ in $[D_6]$benzene.

Complexes **1** and **3** were found to be sparingly soluble in $[D_6]$benzene, so, their ^{1}H NMR spectra were recorded in $[D_8]$THF. For the scandium complex **1**, the BH_4 groups displayed a broad quadruplet singlet at δ = –0.17 ppm, the allyl group was identified by two signals at δ = 2.90 ppm and 6.13 ppm within a 4:1 relative ratio, revealing a dynamic *syn-anti* interconversion of the allyl group (Figure 2.4). In the case of lanthanum complex **3**, it revealed one broad BH_4 quadruplet at δ = 0.65 ppm and three allyl signals at δ = 2.81, 3.09 and 6.20 ppm with 2:2:1 pattern, indicating a less fluxional allyl group in this latter case (Figure 2.5).

Elemental analysis for the scandium complex **1** led to the same formula as determined by ^{1}H NMR, with two THF per scandium atom. Regarding yttrium and lanthanum derivatives, analyses performed after one week of storage in the glove box, were both indicative of partially desolvated compounds containing 1.5 THF molecule per metal. After three days only, the lanthanum complex was found to contain 2 THF per metal. Such a loss of THF is not rare in the chemistry of monosubstituted bis(borohydride) derivatives of the rare earths. It has already been observed for the family of complexes $(C_5Me_4{}^{n}Pr)RE(BH_4)_2$ (RE = Nd, Sm) the existence of several molecular forms : bis-THF solvate or non-solvated hexamer

cluster.[44] In the present case, it is likely that a similar clustering process is occurring, which is also correlated to the well-known bridging ability of the BH_4 group.[1,3] Furthermore, the quantity of THF molecules coordinated in the tris(borohydride) of the rare earths is known to strongly depend on the nature of the metal and the duration of storage, for instance, we clearly realized that complexes **1-5**, started being less soluble with time as a result of losing part of THF molecules coordinated, which is another prove of desolvation process.

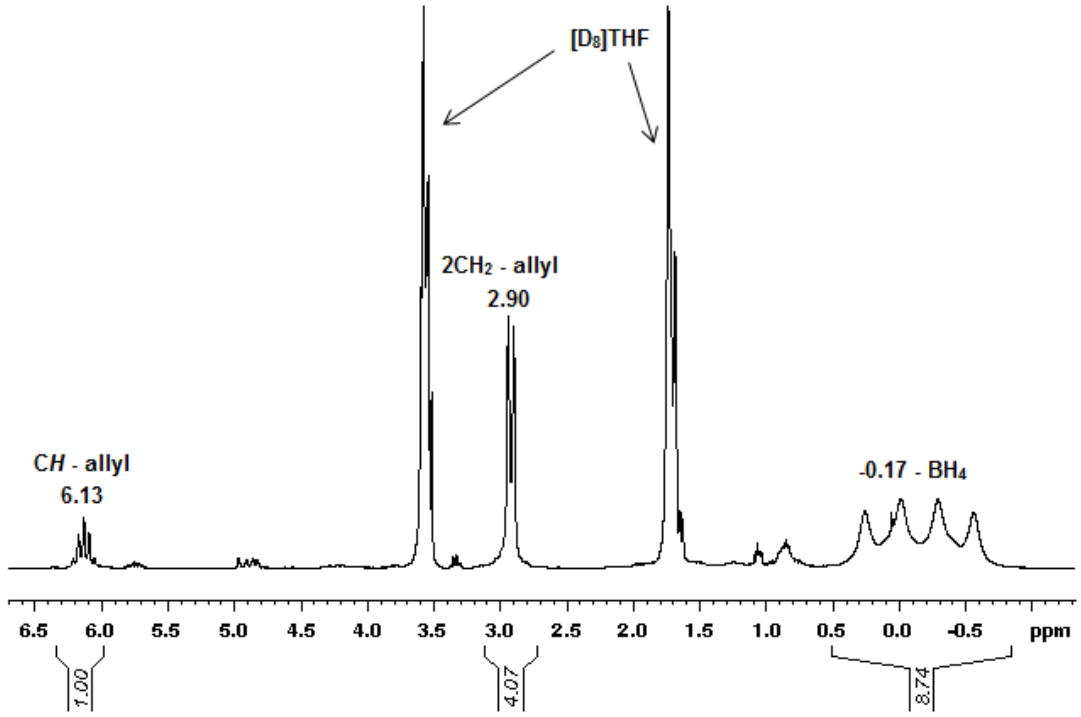

Figure 2.4 ^{1}H NMR spectrum of $Sc(BH_4)_2(C_3H_5)(THF)_2$ in $[D_8]THF$.

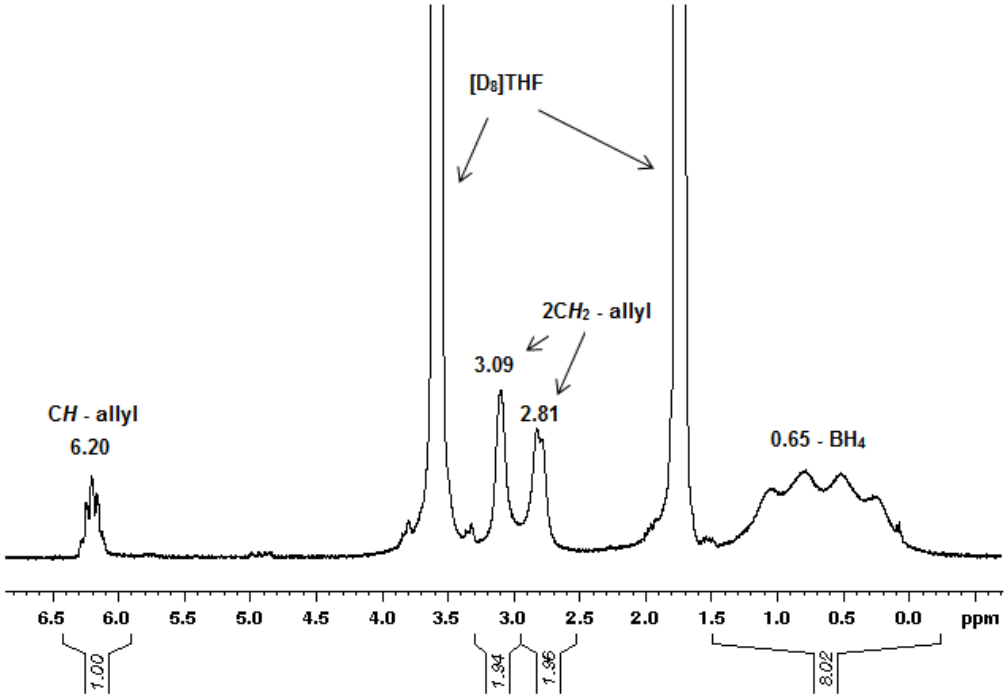

Figure 2.5 ^{1}H NMR spectrum of $La(BH_4)_2(C_3H_5)(THF)_3$ in $[D_8]THF$.

Although paramagnetic, both ^{1}H NMR spectra of neodymium **4** and samarium **5** complexes could be interpreted (Figures 2.6 and 2.7). ^{1}H NMR spectrum of **4** in $[D_6]$benzene displays a broad BH_4 signal at δ = 91.90 ppm, three allyl signals at δ = 22.60, 13.10 and 1.28 ppm with a typical 1/2/2 allyl pattern, and the THF resonances at –2.47 and –5.69 ppm. Note that in $[D_8]$THF the spectrum is very similar. Complex **5** behaves differently: in $[D_6]$benzene, the two BH_4 groups display a broad singlet at –11.8 ppm, allyl signals are at 15.79, 11.14 and 9.62 ppm (relative intensities 1:2:2), and the THF resonances appear at 2.00 ppm and 0.40 ppm. In $[D_8]$THF in turn, two signals standing for the allyl group within a 4:1 ratio (11.40 and 8.97 ppm, respectively) are this time observed, revealing a dynamic *syn-anti* interconversion of the allyl group in this solvent. Such uncommon fluxionality of the RE—allyl moiety has been noticed recently by Okuda.[46]

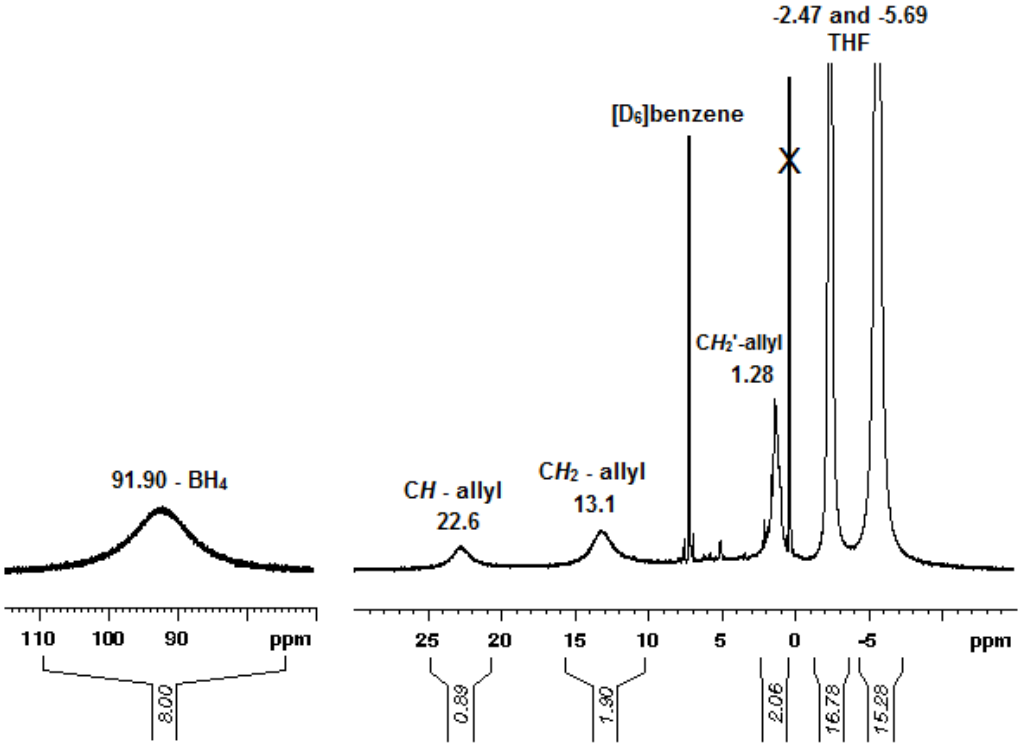

Figure 2.6 ^{1}H NMR spectrum of $Nd(BH_4)_2(C_3H_5)(THF)_4$ in [D_6]benzene.

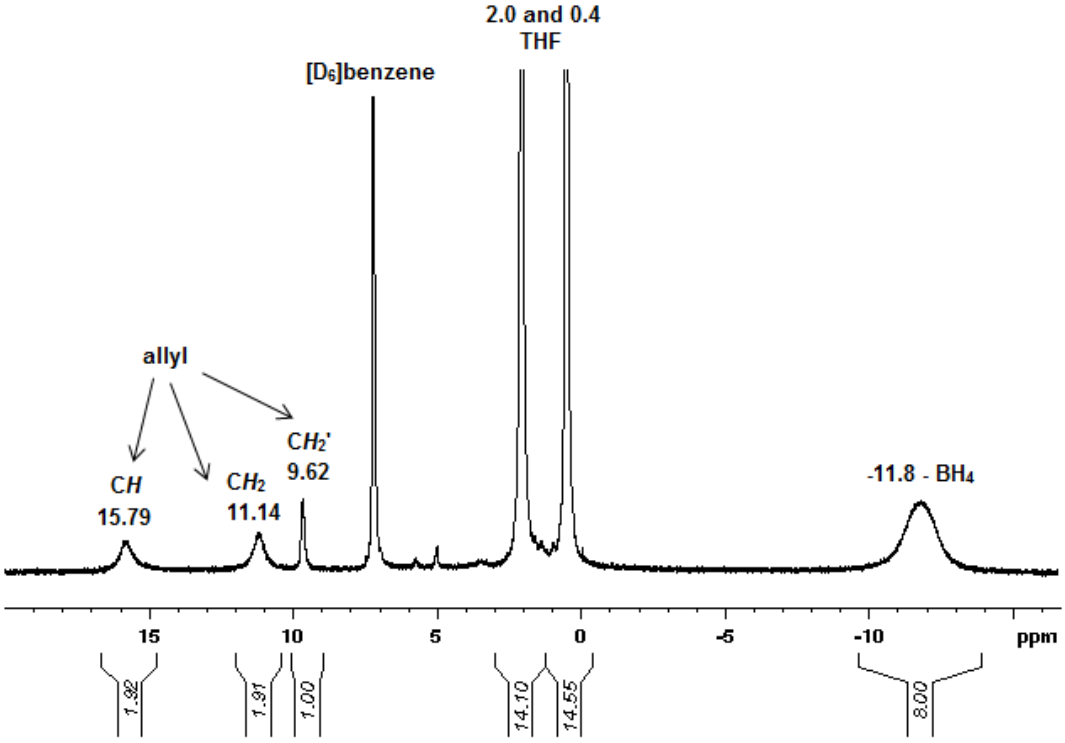

Figure 2.7 ^{1}H NMR spectrum of $Sm(BH_4)_2(C_3H_5)(THF)_{3.6}$ in [D_6]benzene.

Single crystals of the five complexes **1-5** were obtained, from a concentrated THF solution at –20 °C for **1-4** and in a THF-pentane mixture for **5**. Their molecular solid-state structures were established using X-ray diffraction methods (Figures 2.8-2.12). The complexes were all found to be monomeric in the solid state and in agreement with the formula $RE(BH_4)_2(C_3H_5)(THF)_x$ (RE = Sc (**1**), x = 2; Y (**2**), La (**3**), Nd (**4**), Sm (**5**), x = 3). Noteworthy, the scandium **1** complex displayed only two coordinated THF molecules, instead of three for complexes **2-5**, due to its smaller ionic radius.

Complex **1** crystallizes in the monoclinic space group C 2/c with two THF molecules in the unit cell and forms a 5-fold coordination sphere with distorted trigonal bipyramidal molecular geometry (Figure 2.8). Two borohydride groups and one allyl are in the equatorial plane while two THF molecules occupy the apical position. The 2 BH_4 groups coordinate the Sc center in κ^3 (H) mode. In contrast to **2-5** the two borohydride groups are not in *trans* position, forming an angle B1···Sc···B2 equal to 104.1°. Similar to complex **3**, the two boron atoms are exactly at the same distance from the Sc center (Sc···B = 2.47 Å). In addition, the two borohydride groups are totally symmetrical by a plane of symmetry passing through the Sc atom. Concerning the allyl group, Sc—C_{allyl} bonds are not equidistant and smaller compared to RE—C_{allyl} in this family, the central carbon atom is at 2.46 Å and the other two carbons are located at 2.50 and 2.49 Å, which fall in the range of the Sc—C_{allyl} recorded for the complexes $(C_5Me_4SiMe_3)Sc(C_3H_5)_2$ and $(C_5Me_5)Sc(C_3H_5)_2$.[47] The allyl ligand binds the Sc center in η^3 mode with 2-fold symmetry disorder. Again it is not vertical with Sc center showing a degree of formed by its carbon skeletal being of 126.9°.

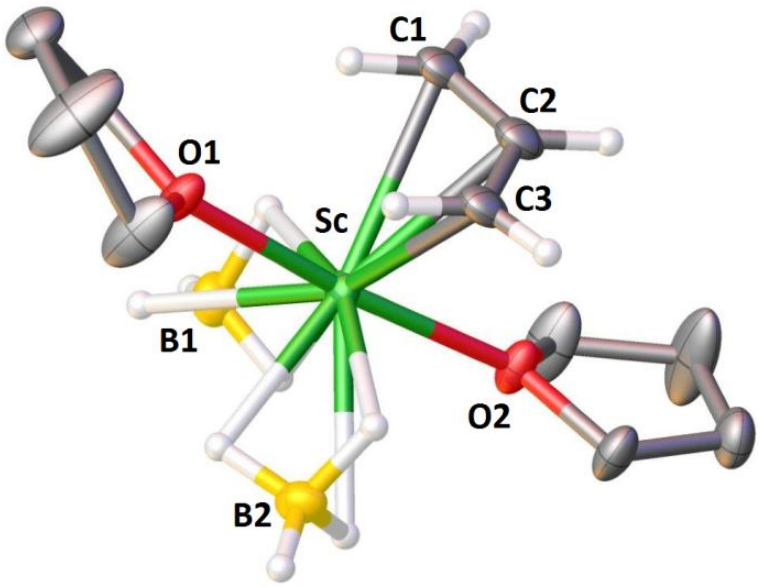

Figure 2.8 X-Ray structure of $Sc(BH_4)_2(C_3H_5)(THF)_3$ **1**. Hydrogen atoms partially omitted for the aid of clarity. Selected bond lengths (Å) and angles (°): Sc—C1 = 2.50, Sc—C2 = 2.46, Sc—C3 = 2.49, Sc···B1 = Sc···B2 = 2.47, Sc—O1 = Sc—O2 =2.55, B1···Sc···B2 = 104.1.

Complex **2** (Figure 2.9) crystallizes in the orthorhombic Pbcn, while **3-5** (Figures 2.10-2.12, respectively) in the monoclinic P 2_1/n space groups. **2-5** are isostructural, with little variations of angles and distances due to the lanthanide contraction; i.e. decrease in ionic radii from lanthanum to yttrium metal centers. In all complexes, the 6-fold coordination sphere (formal coordination number seven if allyl counts for two) around the metal center is formed by the η^3-allylic ligand, two tridentate BH_4 ligands, and three THF molecules, showing an octahedral geometry. By comparing with $RE(BH_4)_3(THF)_3$ complexes, which are known to be monomeric and display one bidentate and two tridentate borohydride ligands,[42] one bidentate BH_4 in each herein reported structure is replaced by an allyl group.

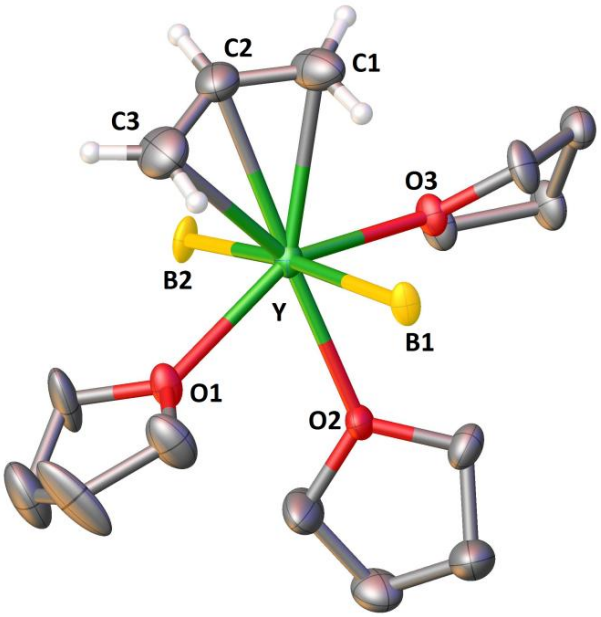

Figure 2.9 X-Ray structure of $Y(BH_4)_2(C_3H_5)(THF)_3$ **2**. Hydrogen atoms partially omitted for the aid of clarity. Selected bond lengths (Å) and angles (°): Y—C1 = 2.62, Y—C2 = 2.63, Y—C3 = 2.61, Y···B1 = 2.74, Y···B2 = 2.55, Y—O1 = 2.38, Y—O2 = 2.43, Y—O3 = 2.43, B1···Y···B2 = 173.2.

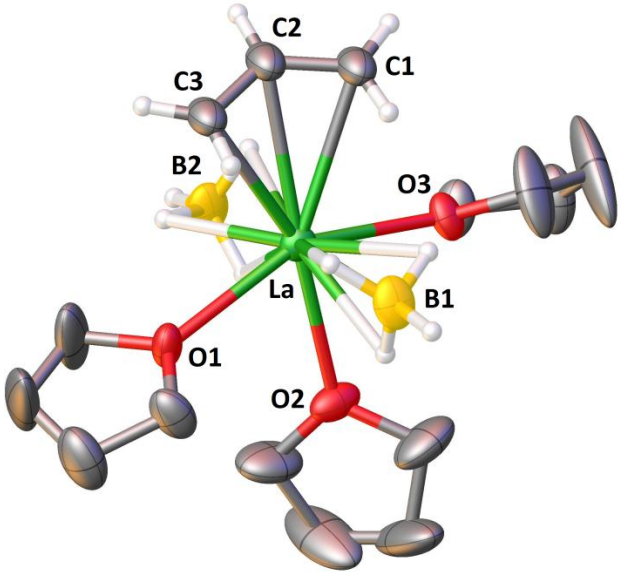

Figure 2.10 X-Ray structure of $La(BH_4)_2(C_3H_5)(THF)_3$ **3**. Hydrogen atoms partially omitted for the aid of clarity. Selected bond lengths (Å) and angles (°): La—C1 = 2.71, La—C2 = 2.81, La—C3 = 2.81, La···B1 = La···B2 = 2.75, La—O1 = 2.55, La—O2 = 2.589, La—O3 = 2.55, B1···La···B2 = 172.4.

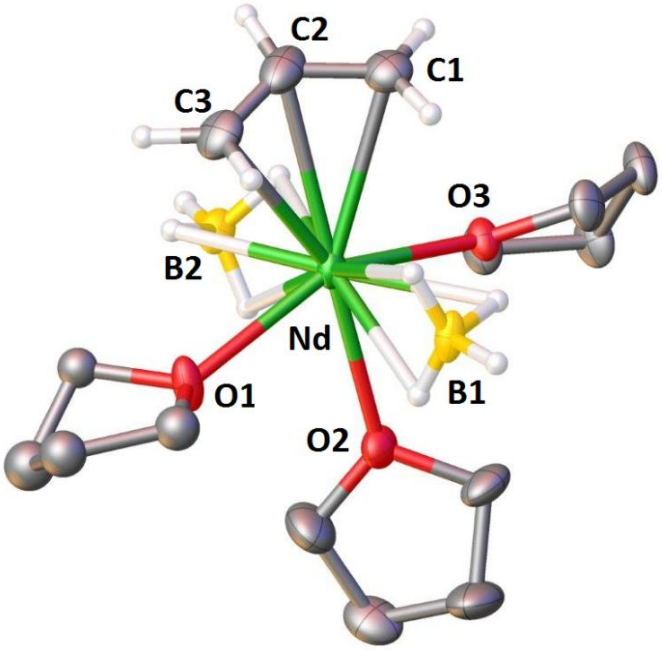

Figure 2.11 X-Ray structure of $Nd(BH_4)_2(C_3H_5)(THF)_3$ **4**. Hydrogen atoms partially omitted for the aid of clarity. Selected bond lengths (Å) and angles (°): Nd—C1 = 2.71, Nd—C2 = 2.74, Nd—C3 = 2.69, Nd···B1 = 2.72, Nd···B2 = 2.67, Nd—O1 = 2.52, Nd—O2 = 2.49, Nd—O3 = 2.55. B1···Nd···B2 = 171.6.

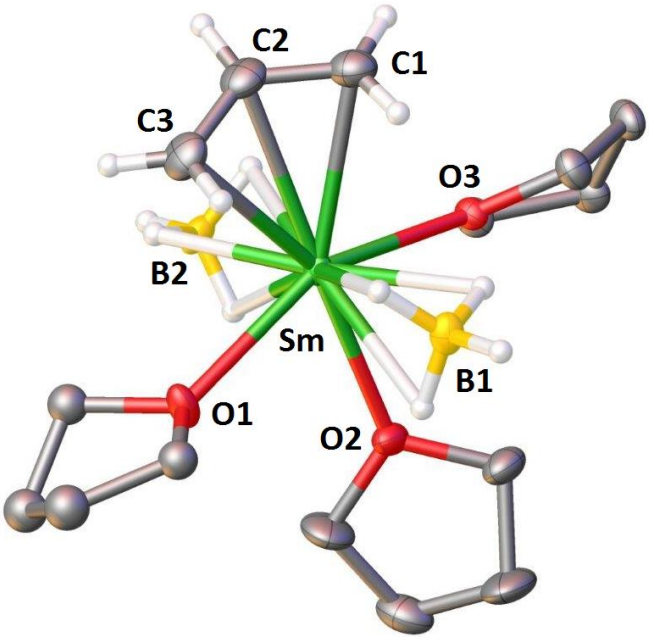

Figure 2.12 X-Ray structure of $Sm(BH_4)_2(C_3H_5)(THF)_3$ **5**. Hydrogen atoms partially omitted for the aid of clarity. Selected bond lengths (Å) and angles (°): Sm—C1 =2.66, Sm—C2 =2.69, Sm—C3 =2.68, Sm···B1 = 2.73, Sm···B2 = 2.63, Sm—O1 = 2.48, Sm—O2 =2.47, Sm—O3 =2.51. B1···Sm···B2 = 171.8.

The two BH_4 groups in lanthanum complex **3** feature a tri-hapto κ^3 (H) coordination mode to the metal center and are equidistant (La···B1 = La···B2 = 2.75 Å), which was not the case for Nd(**4**)···B and Sm(**5**)···B, The Nd(**4**)···B distances are 2.67 and 2.72 Å and the Sm(**5**)···B ones are 2.63 and 2.73 Å. The hydrogen atoms were not located for the yttrium complex **2** and a notable disparity is observed (Y···B1 = 2.74 Å and Y···B2 = 2.55 Å) for the Y···B lengths values. The shorter one is in full agreement with a tri-hapto terminal coordination mode of the BH_4 ligand, *i.e.* in the 2.50-2.60 Å range.[37] The longer Y···B distance is in contrast revealing a likely di-hapto terminal mode, as encountered in $Y(BH_4)_3(THF)_3$,[1,48,49] which marks a clear difference between yttrium and other complexes in this family. For complexes **2-5**, the borohydride groups are almost in *trans* position to each other, showing a nearly linear setup (B1···Y···B2 = 173.2°, B1···La···B2 = 172.4°, B1···Nd···B2 = 171.6° and B1···Sm···B2 = 171.8°), as same as in homoleptic $Y(BH_4)_3$,[50] $Y(BH_4)_3(THF)_3$,[49] $[Y(BH_4)_2(THF)_5]^+$ [51] whereas much tighter B1···RE···B2 angles were found in bulky (NPCN),[52] (NCCCN)[53] and (NCN) [54] mono(substituted) bis(borohydride) RE complexes.

The allyl moieties bind the RE metals of **2-5** in η^3 modes. In the case of La complex **3** it shows 2-fold symmetry disorder, whereas no such disorder was found in complexes **2**, **4** and **5**. The carbon atoms of the allyl groups in **2-5** are not equidistant from the metal center, the central carbon atom being at 2.63 Å from the Y center and the other two being located at 2.62 and 2.61 Å (2.81, 2.71 and 2.81 Å from the La center; 2.74 Å, 2.69 and 2.71 Å from the Nd center; 2.69, 2.68, 2.66, respectively, from the Sm center) similar to the Y—C_{allyl} bonds observed in the dimeric mono(amido-diphosphine) compound $\{Y(C_3H_5)[N(SiMe_2CH_2PMe_2)_2]\}_2(\mu\text{-}Cl)_2$,[55] and the bis(allyl) monocationic $[Y(C_3H_5)_2(THF)_3][BPh_4]$.[56] La—$C_{allyl}$ in **3** is the longest among the other RE—C_{allyl} of this complex family (**1-5**), and is similar to the RE—C_{allyl} bonds obtained by Taube for the $La(allyl)_3(diox)_x$ complex,[21] this related to the fact that La is the largest metal along the RE series. In **2**, the allyl group is not vertical with Y center showing a degree of inclination close to Nd (**4**) and Sm (**5**) (see further discussion), the same kind of inclination is observed for **3**.

Moreover, Nd—C(allyl) distance is in the range observed in complexes: $Nd(C_3H_5)_3(diox)$,[21] $(C_5Me_5)Nd(C_3H_5)_2(diox)$,[57] $[Nd(C_3H_5)_2Cl(THF)_2]_2$[58] and $[Mg(THF)_6][Sm(C_3H_5)_4]_2\text{-}(THF)_2$[59] (2.74 , 2.72, 2.71 and 2.72 Å, respectively). In **4**, the

allyl group is not vertical with the Nd atom but it shows a degree of inclination (Figure 2.13) close to that found for the complexes already described by Taube,[60,61] with Nd—C1—H10 and Nd—C3—H13 angles of 78.1 and 76.9°, respectively, while Nd—C1—H9, Nd—C3—H12 and Nd—C2—H11 angle are 116.2, 117.0° and 128.5°, respectively (Figure 2.13). Nd—O distances between the metal center and the THF molecules in **4** (2.49, 2.55 and 2.52 Å) are slightly shorter than those observed for Nd—O in 1,4-diox complexes of Taube: 2.60 Å in $Nd(C_3H_5)_3(diox)$ and 2.58 Å in $Nd(C_5Me_5)(C_3H_5)_2(diox)$.[21,62]

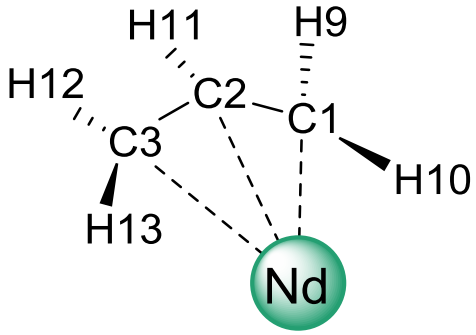

Figure 2.13 Schematic view showing the inclination of the allyl group in **4**.

In fact, complex **4** is the borohydride parent of the chloro $NdCl_2(C_3H_5)(THF)_2$ derivative. But this latter complex, which was not structurally characterized, is supposed to be strongly associated,[48] similarly as the hexameric dimethylpentadienyl $[Nd_6(2,4\text{-}(CH_3)_2C_5H_5)_6Cl_{12}(THF)_2]$.[62] This is another evidence that the borohydride group brings a steric/electronic compromise that allows different structural/chemical behavior *vs.* the chloride one.[1]

2.3 Bis(allyl) mono(borohydride) rare-earth complexes

Following our previous studies on mixed mono(allyl) bis(borohydride) rare-earth complexes, extending the synthesis of these compounds to bis(allyl) analogues is of high interest, as this would extend the general reactivity of this family.

2.3.1 Attempts of synthesis of $RE(C_3H_5)_2(BH_4)(THF)_x$ using $Mg(C_3H_5)_2(L)_n$ (L= THF/dioxane)

As previously mentioned, the synthesis of the mono(allyl) bis(borohydride) RE complexes, utilizes the reagent $Mg(C_3H_5)_2(L)_n$ (L= THF/dioxane) in 0.5 equivalence to the tris(borohydride) complex $RE(BH_4)_3(THF)_x$. We thus attempted to synthesize the bis(allyl) mono(borohydride) complexes $RE(C_3H_5)_2(BH_4)(THF)_x$, at scale up, using 1 equiv. (or 1.2 equiv.) of the same bis(allyl) magnesium reagent with 1 equiv. $RE(BH_4)_3(THF)_{2-3}$ (RE = Sc, Y, La and Sm).

The ^1H NMR spectra in $[D_8]THF$ of successive additions of 0.5 equiv. of $Mg(C_3H_5)_2(diox)_{0.06}$ to $Y(BH_4)_3(THF)_3$ was monitored by NMR tube equipped with Young valve, and showed that the bis(allyl) mono(borohydride) complex could be formed, but after the addition of huge excess of the allyl source (3.5 equiv.) (Figure 2.14, Table 2.1). This can be confirmed by the shift of allyl signals at 6.09 ppm corresponding to the C*H* hydrogen (Figure 2.14, A) to a higher resonance of 6.18 ppm (Figure 2.14, F), while the signal at 3.21 ppm corresponding to the terminal CH_2 hydrogens in the allyl ligand (Figure 2.14, A), shifted to a lower chemical shift at 3.02 ppm (Figure 2.14, F). Moreover, the integrals of the allyl signals and the borohydride ones reached 2:1 ratio (Figure 2.14, F). The shifts in the allyl signals and the relative integrals indicate the presence of a second allyl ligand coordinated to the scandium metal, and thus the formation of $Y(C_3H_5)_2(BH_4)(THF)_x$.

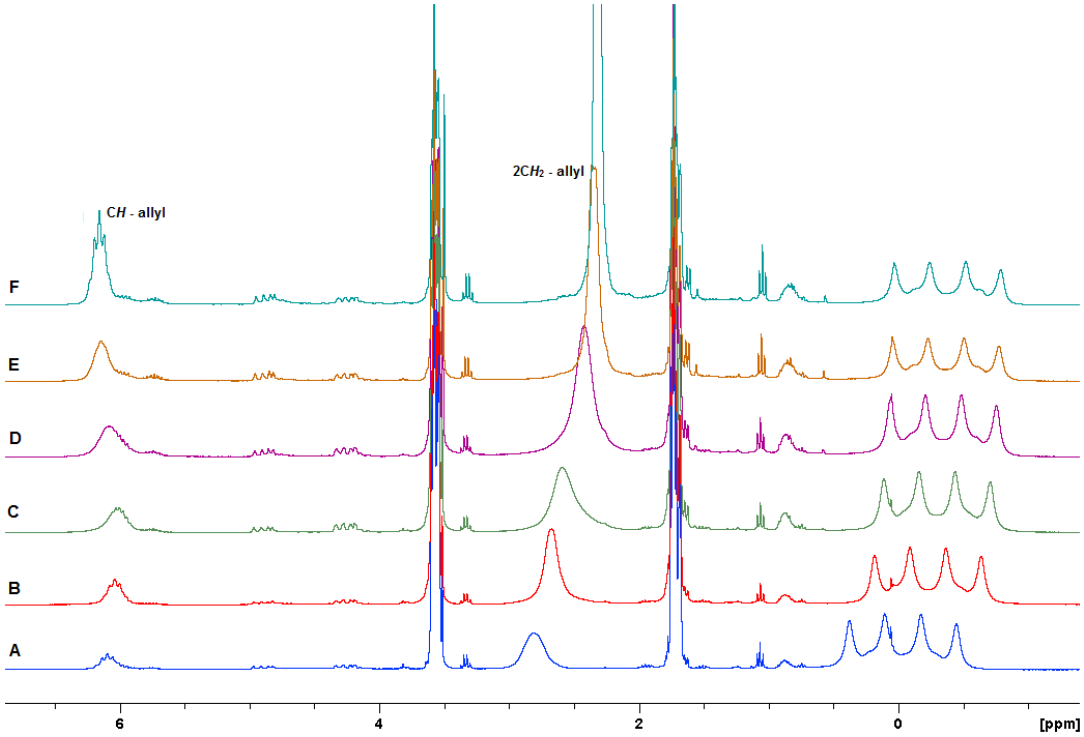

Figure 2.14 ^{1}H NMR spectra showing the effect of adding successive 0.5 equiv. of $Mg(C_3H_5)_2(diox)_{0.06}$ to $Y(BH_4)_3(THF)_3$ in [D_8] THF. A: $Y(BH_4)_3(THF)_3$ + 0.5 $Mg(C_3H_5)_2(diox)_{0.06}$, F: $Y(BH_4)_3(THF)_3$ + 3 $Mg(C_3H_5)_2(diox)_{0.06}$

Table 2.1 Summary of the NMR peaks of the allyl group signals in [D_8] THF related to Figure 2.14.

Spectrum	CH signal (ppm)	CH_2 signal (ppm)
A	6.09	2.81
B	6.09	2.68
C	6.09	2.60
D	6.11	2.43
E	6.15	2.35
F	6.18	2.32

Bulk scale reactions were then attempted, the reaction of $Mg(C_3H_5)_2(diox)_{0.06}$ (1.2 equiv.) and $Y(BH_4)_3(THF)_3$ (1 equiv.) yielded yellow pasty product (81%) with formula $Y(C_3H_5)(BH_4)_2(THF)_x$ in accordance with ^{1}H NMR of the isolated product in [D_8]THF (Appendix I). The same kind of reactivity was observed when reacted the $RE(BH_4)_3(THF)_x$

(RE = Sc, La and Sm) with 1 equiv. of $Mg(allyl)_2(diox)_{0.06}$, where only the mono(allyl) bis(borohydride) complexes were obtained.

2.3.2 Attempts of synthesis of $RE(C_3H_5)_2(BH_4)(THF)_x$ using the Grignard reagents

Attempts of synthesis of mono(allyl) bis(borohydride) complexes via alternative synthetic routes

It was reported that Grignard reagents like $(C_3H_5)MgBr$, $(C_3H_5)MgCl$ and $(C_3H_5)MgI$ could be used to synthesize allyl complexes of RE metals. For instance Bochmann *et al*. reported the easy synthesis of tris(allyl) RE complexes, $[RE(\eta^3\text{-}C_3H_5)_3(\mu\text{-diox})]_\infty$ (RE = Y, Sm, Nd), by reacting $RECl_3(THF)_x$ with 3 equiv. of $(C_3H_5)MgCl$.

Alternative routes for the synthesis of the mono(allyl) bis(borohydride) complex using $(C_3H_5)MgBr$ and $(C_3H_5)MgCl$ were explored. In his thesis,[63] M. Terrier reacted 1 equiv. of $(C_3H_5)MgCl$ with $Nd(BH_4)_3(THF)_3$, that resulted in the formation of a mixed chloride-allyl bimetallic compound, $Nd(C_3H_5)_2Cl_5Mg_2(THF)_4$ (Figure 2.15) which was previously reported by Zhou and co-workers.[64]

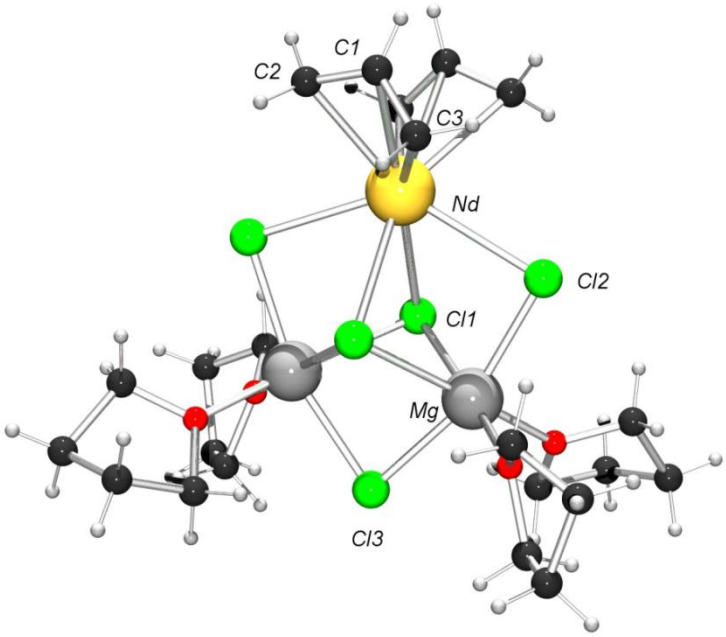

Figure 2.15 X-ray structure of $Nd(C_3H_5)_2Cl_5Mg_2(THF)_4$.[63]

This study was extended to see if another Grignard reagent, such as $(C_3H_5)MgBr$, could produce the mono allyl complex. When one equivalent of $(C_3H_5)MgBr$ was allowed to react with $Nd(BH_4)_3(THF)_3$ in $[D_6]$benzene, it resulted in the formation of a compound in which no signals relative to BH_4 coordinated to the neodymium center could be detected in its ^1H NMR spectrum. It can be hypothesized that a brominated complex similar to $Nd(C_3H_5)_2Cl_5Mg_2(THF)_4$ (e.g. $Nd(C_3H_5)_2Br_5Mg_2(THF)$) could have been synthesized, which cannot be confirmed through ^1H NMR. This could be attributed to the borohydride complexes having a high affinity to form mixed X/BH_4 (X= halide) species in the presence of halide ions.[57]

The formation of mono(allyl) bis(borohydride) complex with smaller rare earth metals, such as scandium and yttrium, with the Grignard reagent had not been explored yet. Their small coordination sphere due to their small ionic radii could potentially allow them to form more stable mononuclear mono(allyl) complexes without forming bimetallic structures. the NMR scale reaction of 1 equiv. of $(C_3H_5)MgCl$ and $Sc(BH_4)(THF)_2$ in $[D_6]$benzene resulted in a brown solution with the formation brown precipitate, which could correspond to an unstable Sc—allyl or Sc—alkyl or Sc—H that decomposed through reduction, to afford a colloidal metal. The ^1H NMR spectrum of the resulting solution displayed signals relative to the allyl group at 6.40 ppm and 3.22 ppm in the ratio of 1:4. This corresponds to the formation of the mono(allyl) bis(borohydride) scandium complex, $Sc(C_3H_5)(BH_4)_2(THF)_x$, previously reported by the group by using $Mg(C_3H_5)_2(L)_x$ (L = THF or diaoxane). The same was observed when $(C_3H_5)MgBr$ was used in scale up (Appendix II) instead of $(C_3H_5)MgCl$. Hence, a new alternative route to synthesize the mono(allyl) bis(borohydride) was developed for the smaller rare earth metal scandium. This removes a reaction step from the current synthesis by using directly the commercially available Grignard reagent, instead of $Mg(C_3H_5)_2(L)_n$.

Attempts of synthesis of bis(allyl) mono(borohydride) complexes

When an additional equivalent of $(C_3H_5)MgCl$ was added to the Young's tube, containing the mono(allyl) scandium complex formed *in situ*, the solution maintained its dark brown color. ^1H NMR shows the same ratio of the allyl signals in a 1:4 ratio, however they had shifted. The signal at 6.40 ppm corresponding to the C*H* hydrogen in the allyl ligand, shifted to a

higher chemical shift of 6.83 ppm while the signal at 3.21 ppm corresponding to the terminal C*H*$_2$ hydrogens in the allyl ligand, shifted to a lower chemical shift at 3.02 ppm (Figure 2.16). Despite the integrals of the allyl signals and the borohydride ones not corresponding to a 2:1 ratio, the integrals of the BH_4 signal decreased when the second equivalent of the $(C_3H_5)MgCl$ was added. The shifts in the allyl signals and the relative integrals seem to indicate the presence of a second allyl ligand coordinated to the scandium metal, and thus the formation of the expected bis-allyl complex $Sc(C_3H_5)_2(BH_4)(THF)_x$. The same was observed with Yttrium metal when reacted the $Y(BH_4)(THF)_3$ with two successive equiv. of $(C_3H_5)MgX$ (X = Cl or Br).

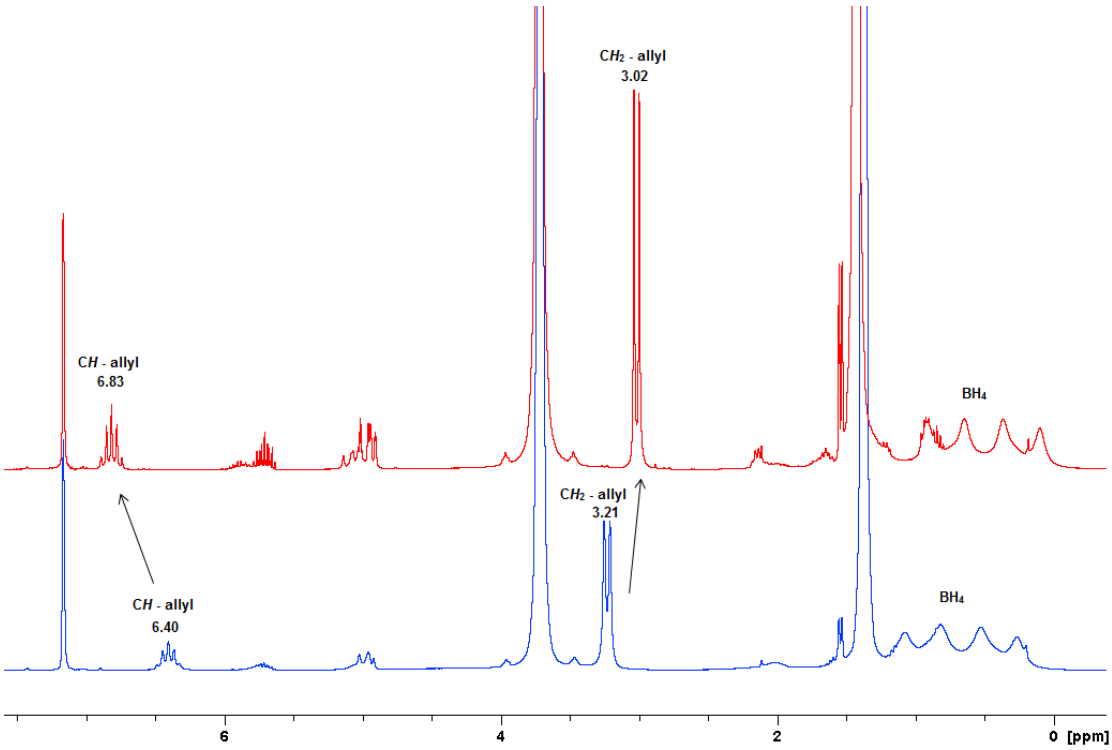

Figure 2.16 ^{1}H NMR spectra of showing the effect of adding two successive equiv. of $(C_3H_5)MgCl$ to $Sc(BH_4)_3(THF)_2$ in [D_8] THF (down: blue, corresponds to 1 equiv. of $(C_3H_5)MgCl$, up: red, 2 equiv. $(C_3H_5)MgCl$).

Unfortunately, a series of attempts to synthesize the $RE(C_3H_5)_2(BH_4)(THF)_x$ (RE = Sc, Y) in scale up, using 2 equiv. (or slight excess) of $(C_3H_5)MgX$ (X = Cl or Br) were unsuccessful and led to incurable mixture of allyl groups with minor and major fractions next to each other. For example when $Y(BH_4)_3(THF)_3$ reacted with 2 equiv. of $(C_3H_5)MgCl$ in scale up, a product obtained with minor signals of 13% at 6.42 and 2.93 ppm, and major signals of 87% at 6.18 and 2.39 ppm (Figure 2.17). Trials to separate the products by adding

Tetramethylethylenediamine (TMEDA) or dioxane to the solution mixture at different stages, failed and the mixture remained unchanged.

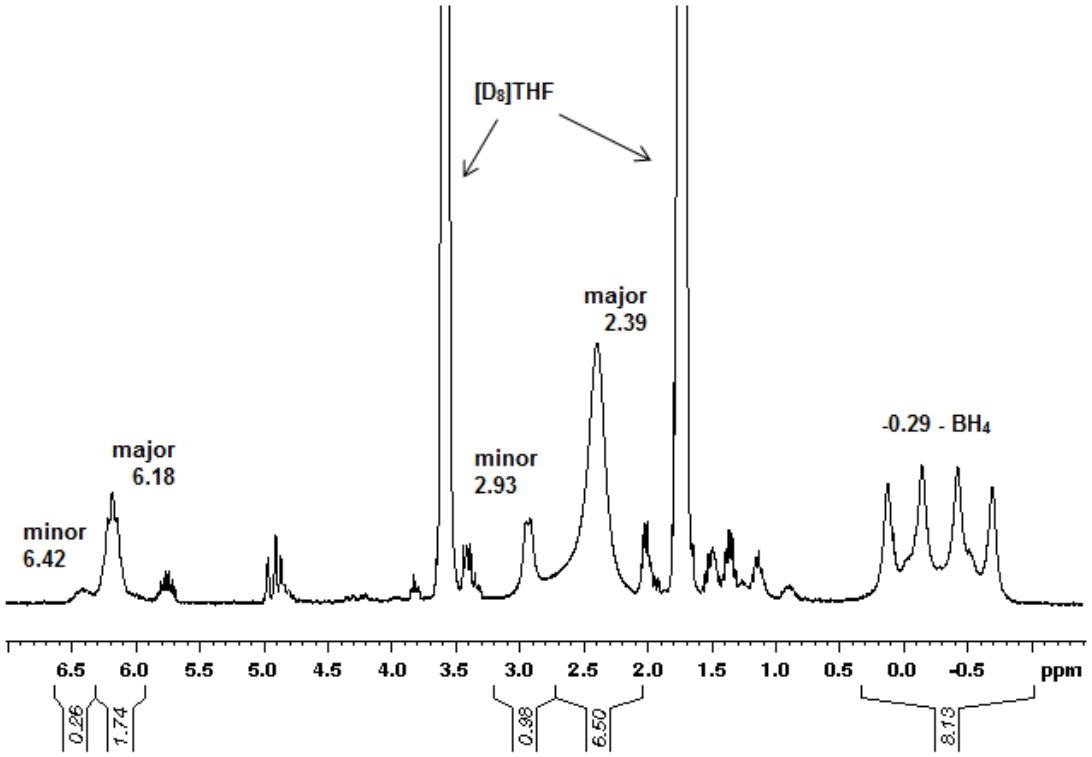

Figure 2.17 ^{1}H NMR of the product obtained by the reaction of $Y(BH_4)_3(THF)_2$ and 2 equiv. $(C_3H_5)MgCl$ in $[D_8]THF$.

2.3.3 Attempts of synthesis of $Y(C_3H_5)_2(BH_4)(THF)_x$ using comproportionation reaction

In 1998, Taube *et al.* took advantage of the comproportionation reaction to reach the neodymium-allyl complexes, $Nd(\eta^3\text{-}C_3H_5)Cl_2(THF)_2$ and $Nd(\eta^3\text{-}C_3H_5)_2Cl(THF)_{1.5}$ by reacting $Nd(\eta^3\text{-}C_3H_5)_3(diox)$ and $NdCl_3(THF)_2$ in THF in the corresponding molar ratio. Using the same concept, attempts to synthesize the expected bis(allyl) complex by using this method were conducted (Scheme 2.6).

$$YCl_3 + 3\,(C_3H_5)MgBr \xrightarrow[3\text{ days, RT}]{[D_8]THF} Y(C_3H_5)_3(THF)_x + MgBrCl$$

$$2\,Y(C_3H_5)_3(THF)_x + Y(BH_4)_3(THF)_x \longrightarrow 3\,Y(C_3H_5)_2(BH_4)(THF)_x$$

Scheme 2.6 Attempt of synthesis of $RE(C_3H_5)_2(BH_4)(THF)_x$ using the comproportionation reaction.

$Y(C_3H_5)_3$ was first prepared at the NMR scale as reported in the literature.[59] YCl_3 was reacted with 3 equiv. of $(C_3H_5)MgBr$ in $[D_8]THF$, An immediate change in the color of the solution from colorless to a yellow solution was observed and after three days, the solution turned to orange. The appearance of the allyl signals at 6.21 ppm and 2.34 ppm on the ^1H NMR spectrum are consistent with the formation of the tris(allyl) yttrium complex. Then half equiv. of $Y(BH_4)_3(THF)_3$ added to the former prepared solution, but there were no changes in the allyl signals and there was the appearance of a BH_4 signal which had the same chemical shift as $Y(BH_4)_3(THF)_3$, suggesting that the $Y(BH_4)_3(THF)_3$ did not react. When another half equivalent of $Y(BH_4)_3(THF)_3$ was added, the BH_4 signal increased but there were no changes in the shifts of the allyl signals even after heating at 50 °C for 1 hour. Only small hydrolysis the allyl ligand resulting in the formation of propene could be observed, which could be due to the instability of the allyl ligand under heating. The bis(allyl) mono(borohydride) yttrium complex seems to be not accessible using the comproportionation reaction under our conditions.

Moreover, the addition of 1 equiv. of $NaBH_4$ to $Y(C_3H_5)_3$ prepared *in situ* in $[D_8]THF$ failed to afford the targeted complex, even after leaving the mixture for 3 days and heating at 50 °C. The sole result was the increase of the ratio of the propene signal, corresponding to the hydrolysis of the allyl group belongs to the tris(allyl) yttrium (Appendix III).

2.4 Reactivity of mono(allyl) bis(borohydride) rare-earth complexes with various reagents

An efficient way to test the reactivity of the $RE(BH_4)_2(C_3H_5)(THF)_x$ (RE = Sc (**1**), x = 2; Y (**2**), La (**3**), Nd (**4**), Sm (**5**), x = 3) and thus to compare the reactivity of the allyl moieties towards the borohydride one, is to conduct NMR scale reactions using NMR tubes equipped with Young valves and monitor the changes by ^1H NMR analysis. This is of a special interest for these complexes as they bear two distinct potentially active ligands, which is rare in this field.

The reactivity of the complexes **1-5** was assessed towards benzophenone, cyclopentadienes (Cp^RH, where Cp = C_5Me_4, R = H or ethyl), phenylsilane, triethylsilane,

and 1,4,7-Trimethyl-1,4,7-triazacyclononane (N_3, this symbol corresponds to only 1 equiv. of the ligand) either in [D_6]benzene or [D_8]THF, depending on their solubility. Due to the neodymium effect (see chapter 3) The neodymium complex **4** was the primary complex used against all the reagents in [D_6]benzene.

2.4.1 Benzophenone

Rare earth complexes bearing an alkyl bond are known to react with a range of carbonyls such as carbon dioxide (CO_2) and benzophenone (Ph_2CO) by the insertion of the molecule into the metal—carbon bond.[65,66-68] Similar reactions were carried out at the NMR scale using equimolar amounts of the mono(allyl) bis(borohydride) RE complexes **1-5** and benzophenone. This could result to insertion of benzophenone into either the RE—allyl or the RE—BH_4 bond (Scheme 2.7).

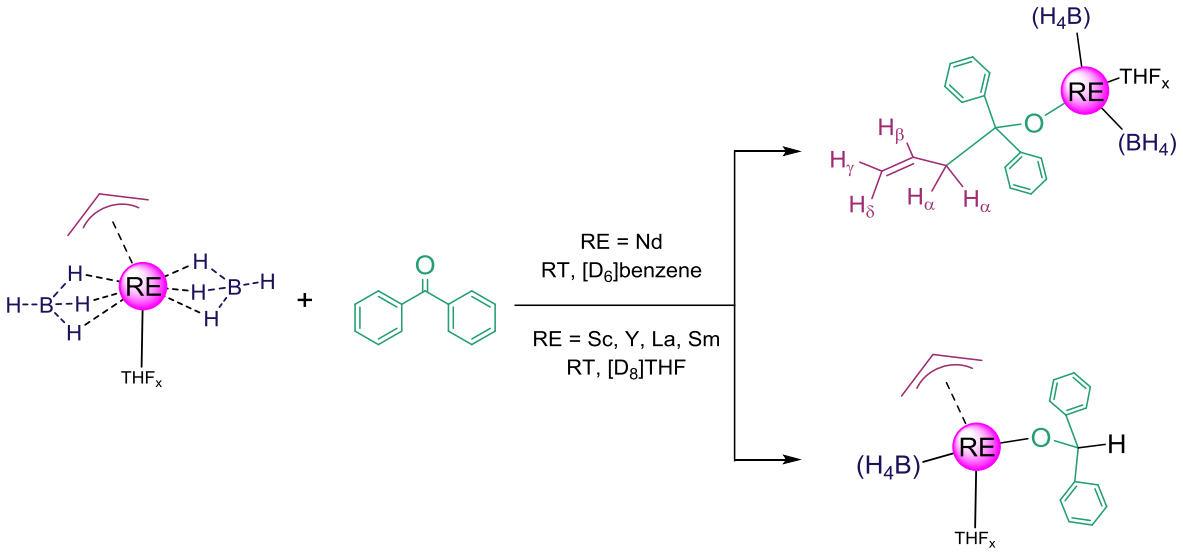

Scheme 2.7 Possible reaction pathways for the insertion of benzophenone into $RE(BH_4)_2(C_3H_5)(THF)_x$ (RE = Sc, Y, La, Nd, Sm).

For the diamagnetic complexes **1-3**, the C=O bond of benzophenone inserted successfully into the RE—allyl bond, yielded the alkoxy compound $RE(OC(allyl)Ph_2)(BH_4)_2(THF)_x$ as seen in the ^{1}H NMR in [D_6]benzene. The signals of phenyl rings appeared in the region 7.45-7.00 ppm for the three complexes, CH_α, CH_β, CH_γ

and CH_δ of the allyl group (represented in Scheme 2.7) were at 3.08, 4.92, 5.05, 5.91 ppm (complex **1**), 3.13, 4.75, 4.88, 5.88 ppm (complex **2**), 3.07, 4.79, 4.91 and 5.84 ppm (complex **3**, Figure 2.18). These signals are consistent with that of the previously synthesized alkoxy complex, [La{$OCPh_2(CH_2CH=CH_2)$}$_2(THF)_3$][BPh_4] by Okuda *et al.* (Table 2.2).[51]

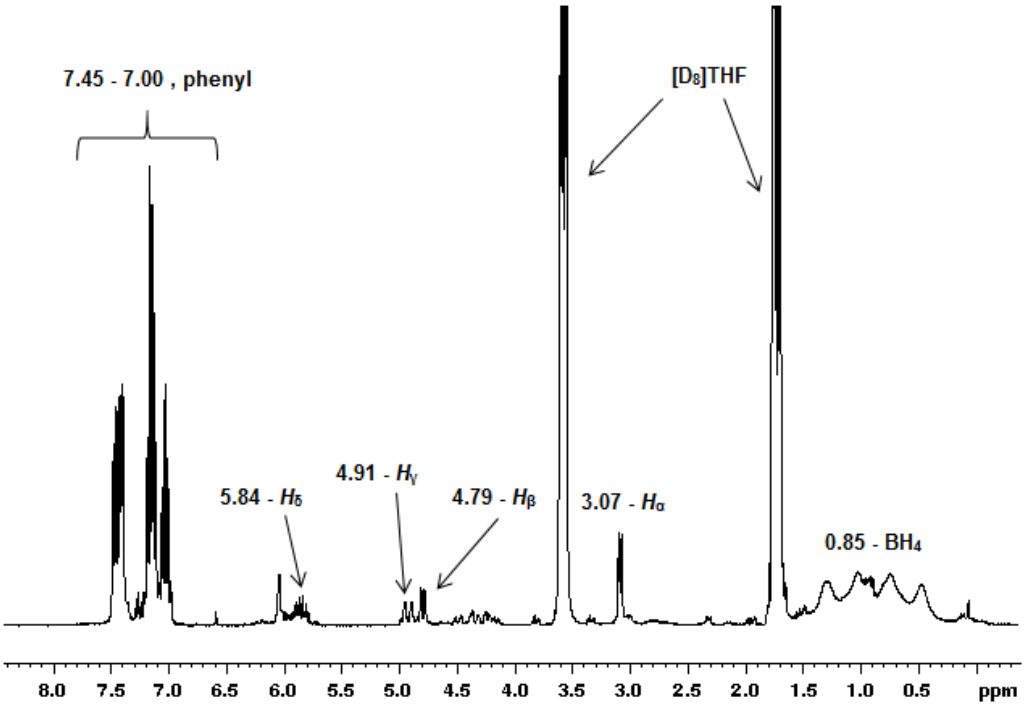

Figure 2.18 ^{1}H NMR in [D_8]THF of the reaction of benzophenone and $La(BH_4)_2(C_3H_5)(THF)_3$.

Table 2.2 ^{1}H NMR assignment of CH_α, CH_β, CH_γ and CH_δ of the allyl group connected to benzophenone in [D_8]THF according to the literature.[51]

Hydrogen	Chemical shift (ppm)
H_α	3.08
H_β	4.93
H_γ	4.87
H_δ	5.74
Phenyl rings	7.13- 7.36

In the case of paramagnetic complexes (RE = Nd (**4**), Sm (**5**)), many high- and low-field signals were observed in the ^{1}H NMR spectra, of which no unambiguous assignment could be carried out. Thus no clear evidence for the conversion of the **4** and **5** into the alkoxy-

complex with inserted benzophenone could thus be drawn from spectroscopic data. However, it can be noted that there was a disappearance in the allyl signals and formation of new broad signal at lower chemical shif while the BH_4 signal remained unchanged but with lower intensity.

For the aid of better understanding of the ^1H NMR recorded in the latter cases, one equiv. of benzophenone was added to the tris(borohydride) complex, $Nd(BH_4)_3(THF)_3$ in $[D_6]$benzene, ^1H NMR showed a new small but broad signal at –3.42 ppm. When another equiv. of benzophenone was added, this signal increased while the original BH_4 signal decreased (Appendix IV). This shows that benzophenone also has the potential to insert into the BH_4 moiety at 98 ppm (Scheme 2.7). In case of excess addition of benzophenone, the electron rich oxygen on the benzophenone bonds to the electron deficient boron to give borate (Scheme 2.8).

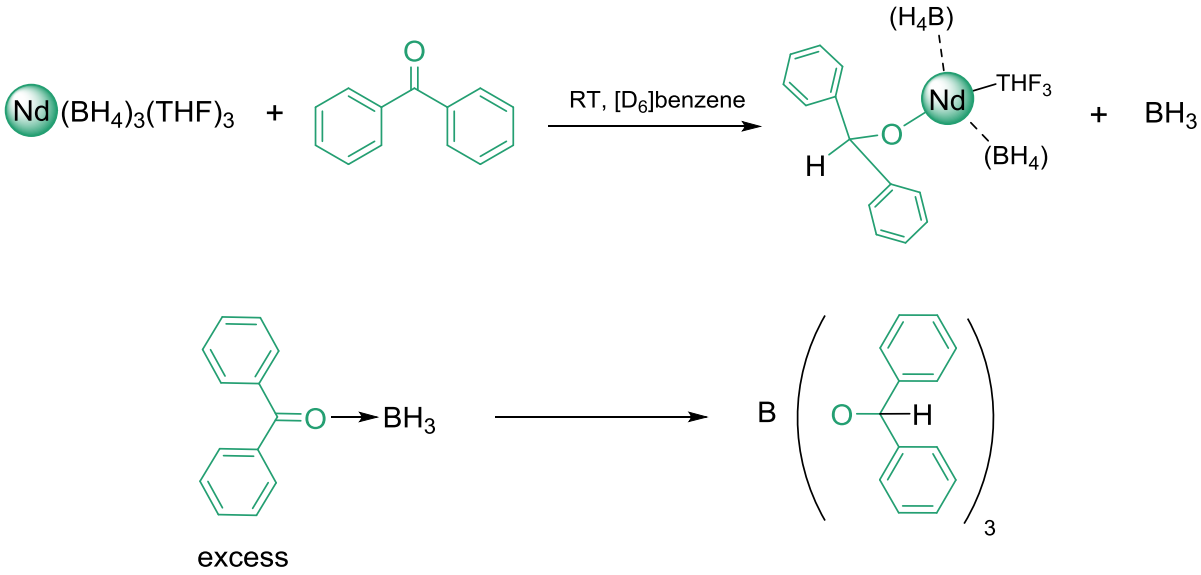

Scheme 2.8 Reaction between benzophenone and $Nd(BH_4)_3(THF)_3$.

Therefore, it can be seen that benzophenone has a higher affinity to insert into the RE—allyl bond in comparison to the RE—(BH_4) one, even if both reactions are possible. Furthermore, unlike in the case of the previous mentioned monocationic complex, $[La\{OCPh_2(CH_2CH{=}CH_2)\}_2(THF)_3][BPh_4]$, where the benzophenone was not inserted into the yttrium analogue, the reactivity of the benzophenone was not limited by the rare earth it was reacted with complexes **1-5**.

2.4.2 Cyclopentadienes (Cp^RH, Cp = C_5Me_4, R = H or ethyl)

Half-lanthanidocenes, or more generally known as half-sandwich RE, have been explored extensively over the past three decades. The introduction of new substituted Cp-ligands (namely Cp^R) into the metal sphere is of interest as it could improve the ability of the catalyst or completely change its stereoselectivity towards various reactions.[69] However, the synthesis of half-lanthanidocenes have shown to be difficult[70] due to comproportionation reactions.

Ephritikhine and co-workers first synthesized the half-sandwich complex, $Cp^*Nd(BH_4)_2(THF)_2$ ($Cp^* = C_5Me_5$) [71] by the ionic metathesis reaction of $Nd(BH_4)_3(THF)_3$ and KCp*. Our group extended this study by reacting $Nd(BH_4)_3(THF)_3$ and Cp*H.[58] However, the ^1H NMR reaction showed no reaction between the tris(borohydride) complex, and Cp*H. While when half an equivalence of BEM was added to a solution with $Nd(BH_4)_3(THF)_3$ and Cp*H, so called borohydride/alkyl route, it resulted in a bimetalic complex, $[Cp^*Nd(BH_4)_3][Mg(THF)_6]$ (Scheme 2.9).[72]

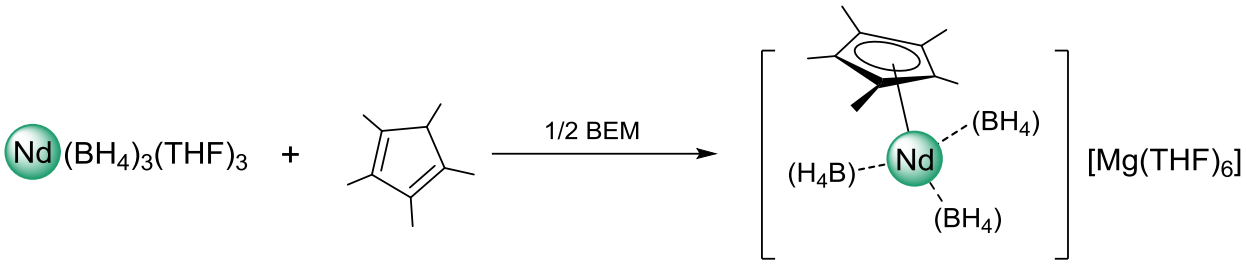

Scheme 2.9 Synthesis of hemi-lanthanocene by borohydride/alkyl route.[72]

On the other hand, allylic rare earth complexes have shown to react with cyclopentadiene ligands in an acid-base type reaction to form the half sandwiches without the production of salts, for instance Taube showed that the allyl group of $Nd(C_3H_5)_3(diox)$ can react with Cp*H to form the bis(allyl) cyclopentadiene containing complex $Cp^*Nd(C_3H_5)_2(diox)$ (Scheme 2.10).[57]

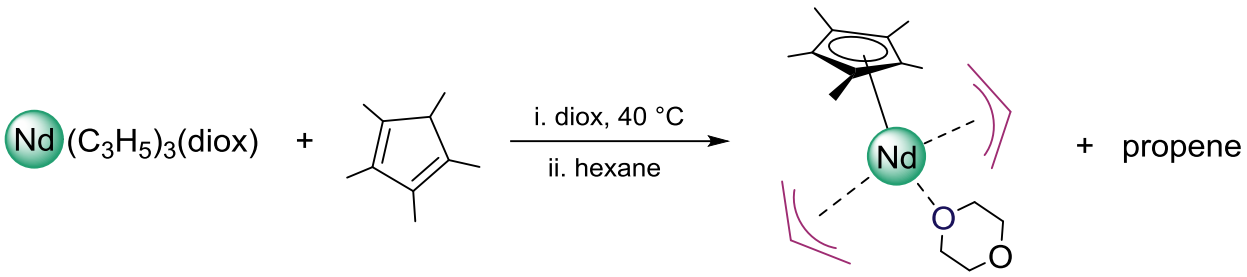

Scheme 2.10 Synthesis of Cp*Nd(C_3H_5)$_2$(diox).[57]

When we reacted Cp^HH (1,2,3,4-tetramethyl-1,3-cyclopentadiene, Cp^H = C_5Me_4H) with one equiv. of Nd(BH_4)$_2$(C_3H_5)(THF)$_3$ complex, there was a shift in the signals on the Cp^H ligand from 2.57, 1.84 and 1.74 ppm to 7.56 and 9.36 ppm. This shows that the cyclopentadiene ligand has coordinated to the paramagnetic neodymium metal through σ-bond metathesis, hence resulting in the shift of these signals. The disappearance of the allyl signals and the formation of the side product, propene can be seen at the signals 1.54, 4.97 and 5.71 ppm showed that the Cp^H reacted with allyl ligand rather than the borohydride one, knowing that the broad singlet of the BH_4 signal remains unreacted at 92.77 ppm (Figure 2.19) thus revealing the formation of (Cp^H)Nd(BH_4)$_2$(THF)$_x$ (Scheme 2.11).

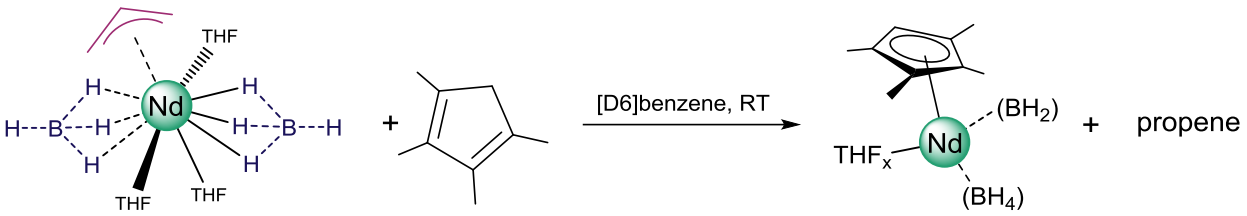

Scheme 2.11 Synthesis of (Cp^H)Nd(BH_4)$_2$(THF)$_3$.

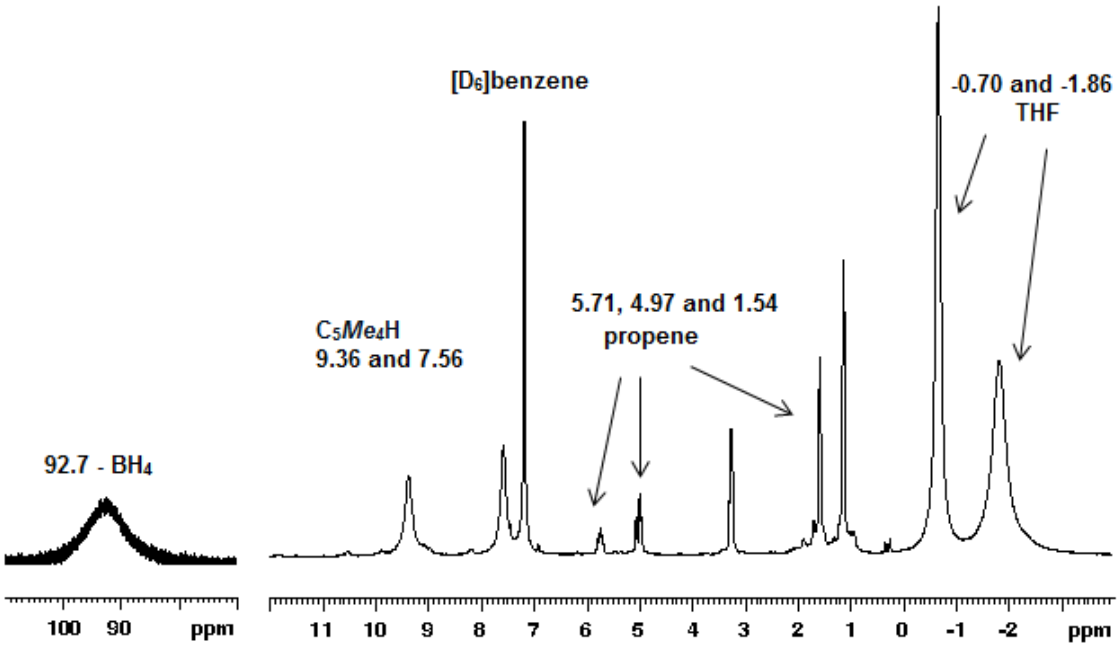

Figure 2.19 ^{1}H NMR of reaction of $Cp^{H}H$ and $Nd(BH_4)_2(C_3H_5)(THF)_3$ in [D_6]benzene.

The same was observed when $Cp^{Et}H$ (Ethyl-tetramethylcyclopentadiene, Cp^{Et} = $C_5Me_4(CH_2CH_3)$) was reacted with $Nd(BH_4)_2(C_3H_5)(THF)_3$ where the Cp^{Et} ligand was coordinated to the complex resulting in $(Cp^{Et})Nd(BH_4)_2(THF)_x$ (Scheme 2.12, Figure 2.20).

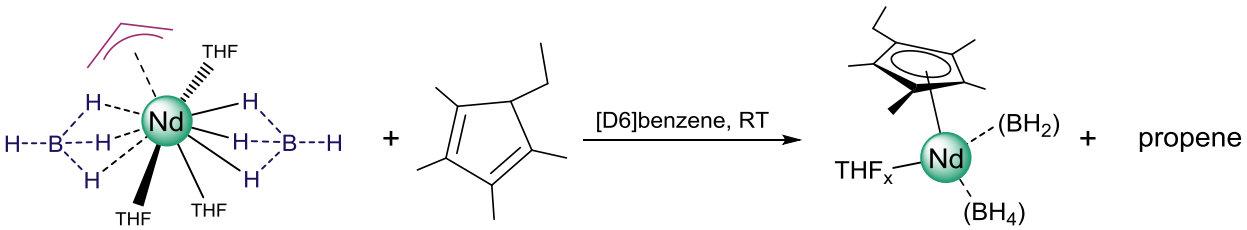

Scheme 2.12 Synthesis of $(Cp^{Et})Nd(BH_4)_2(THF)_x$.

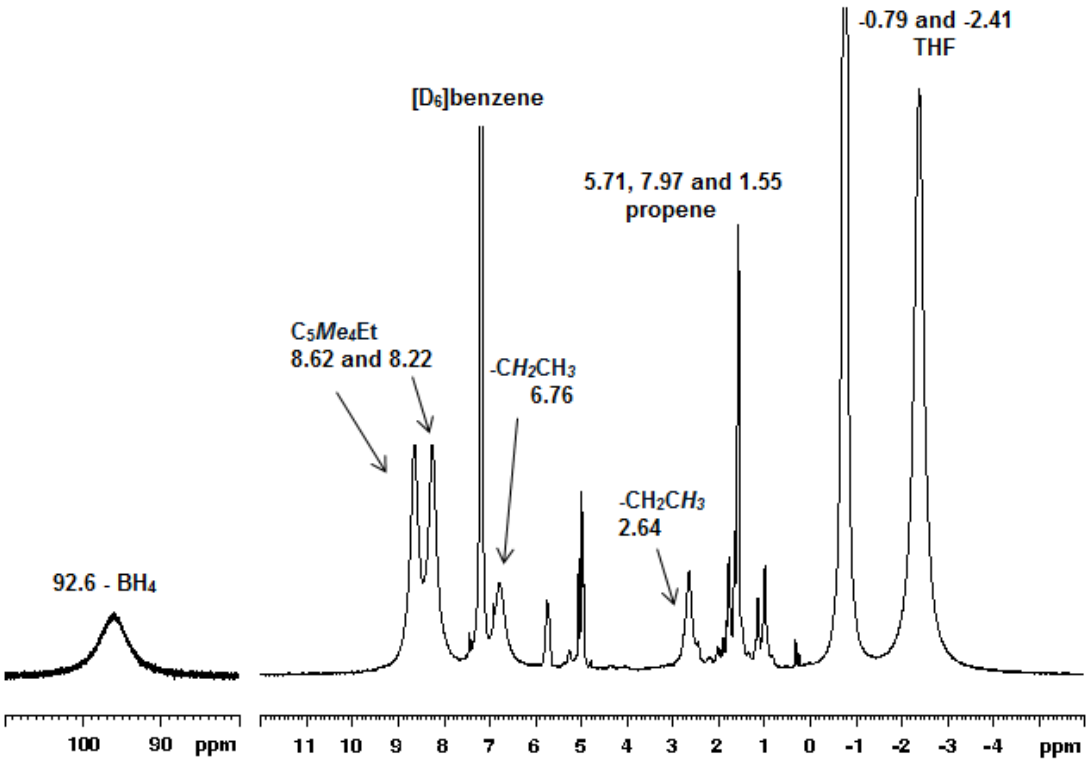

Figure 2.20 ^{1}H NMR of reaction of $Cp^{Et}H$ and $Nd(BH_4)_2(C_3H_5)(THF)_3$ in $[D_6]$benzene.

This NMR study showed that when $Nd(BH_4)_2(C_3H_5)(THF)_3$ was reacted with the organic cyclopentadiene derivatives, HCp^{H} and HCp^{Et}, it cleanly produced a similar half sandwich complex of $(Cp^{H}H)Nd(BH_4)_2(THF)_x$ and $(Cp^{Et})Nd(BH_4)_2(THF)_x$ respectively and has the potential to be a new synthetic route to obtain the half-sandwich RE borohydride complexes. This method has the disadvantage of having to use the highly water and air sensitive complex containing an allyl ligand. Scale up synthesis of these half-sandwich complexes using this method would require extra precaution in terms of using inert environments for its synthesis. However, the benefit of using this method would be a cleaner work-up as there would be no formation of salts, and the use of toluene rather than the polar solvent THF, that promotes comproportionation reactions.

2.4.3 Silane derivatives (Phenylsilane and triethylsilane)

Previously, Okuda's group synthesized the hydrido rare earth complexes, $[RE(Me_3TACD)(\eta^3\text{-}C_3H_5)(\mu\text{-}H)]_2$ (RE = Nd, Sm) and $[RE(Me_3TACD)(\mu\text{-}H)_2]_{3\text{-}4}$ (RE = Y, La, Ce, Pr, Sm) from the crown-aza adducts bis(allyl) rare earth complexes, $RE(Me_3TACD)(\eta^3\text{-}C_3H_5)_2$ using either H_2 or $PhSiH_3$ (Figure 2.21) (see chapter 1). [73,74]

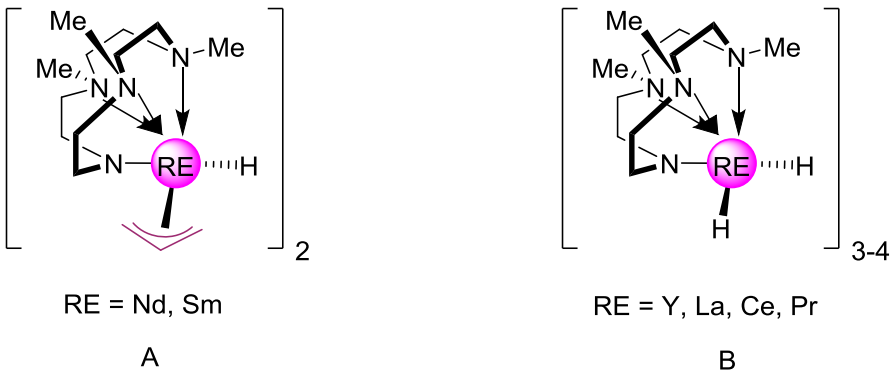

Figure 2.21 Structural presentation of $[RE(Me_3TACD)(\eta^3\text{-}C_3H_5)(\mu\text{-}H)]_2$ (RE = Nd, Sm) and $[RE(Me_3TACD)(\mu\text{-}H)_2]_{3\text{-}4}$ (RE = Y, La, Ce, Pr, Sm).[73,74]

Likewise, we investigated the reaction between the neodymium mono(allyl) bis(borohydride) complex and $PhSiH_3$ to tentatively perform the hydrogenolysis of the complex to produce a hydrido complex, consequentially resulting in the hydrosilylation of the allyl group as postulated in Scheme 2.13.

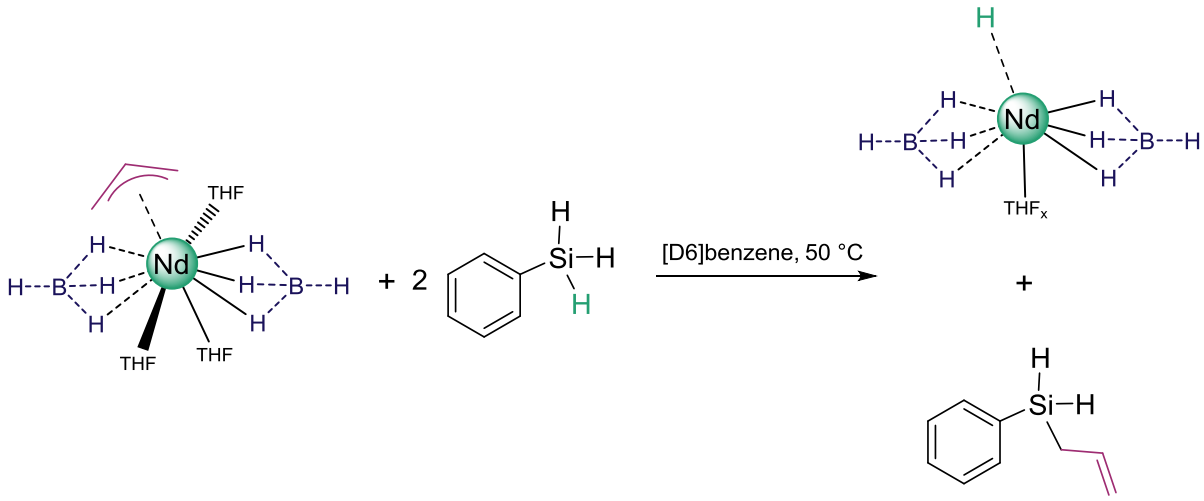

Scheme 2.13 Hydrogenolysis of $Nd(BH_4)_2(C_3H_5)(THF)_3$.

When an equiv. of phenylsilane was added to the neodymium complex **4**, both the allyl and borohydride signals remained on the same position. Moreover, additional equiv. of phenylsilane to the same mixture did not lead to change in the NMR signals of the two groups. This was not the case for the formation of $[Nd(Me_3TACD)(\eta^3\text{-}C_3H_5)(\mu\text{-}H)]_2$ as after addition of 2 equivalents of $PhSiH_3$ and 48 hours later at 25°C, the hydride complex formed.[74]

However, upon prolonged heating (6 days) at 50°C, the presence of the allyl signal slowly decreased and eventually, completely disappeared (Figure 2.22). However, the new signals at 5.74 and 4.97 ppm corresponds more to the formation of propene rather than an alkene group bonded to silicon. The formation of propene could be due to the hydrogenolysis of the allyl group by the $PhSiH_3$. The paramagnetism of the neodymium ion can cause the hydride signal to broaden and move away from the typical signal (2-9 ppm), an example being that the BH_4 signal appears at 90 ppm. Unfortunately, there was also no hydride signals formed even at higher chemical shifts (up to 300 ppm).

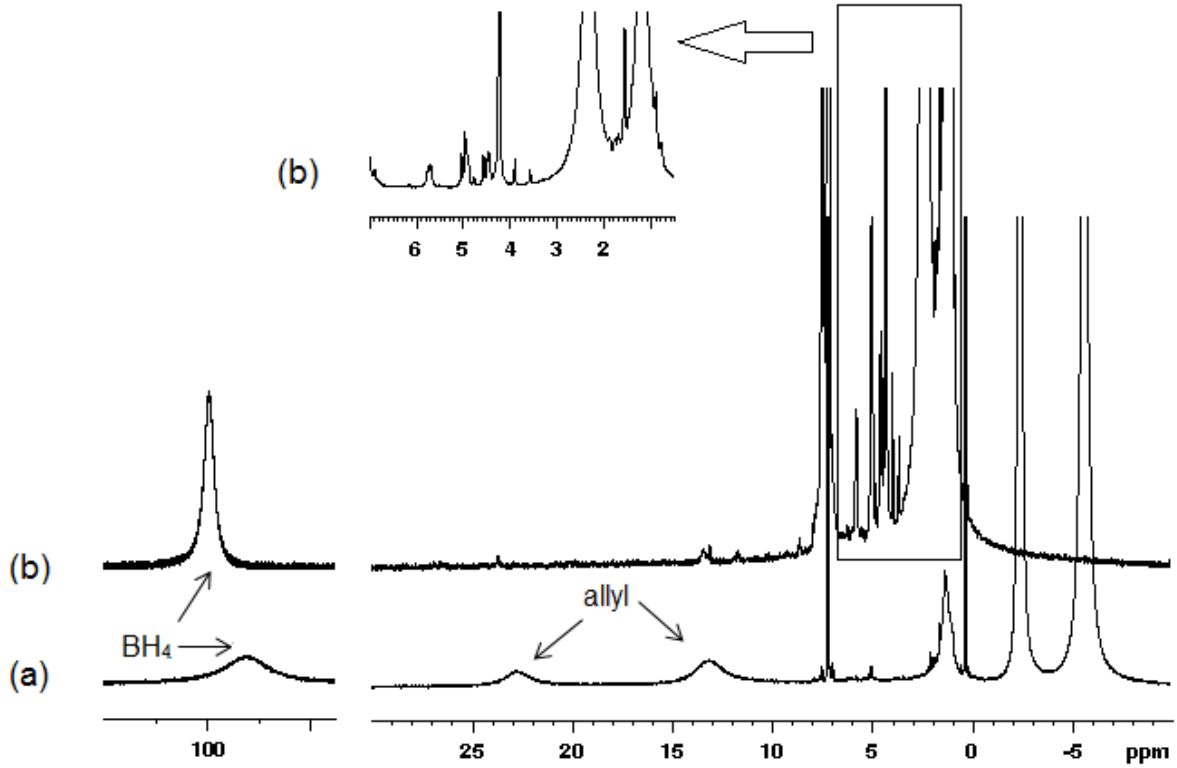

Figure 2.22 ^{1}H NMR spectra in [D_6]benzene of: (a) $Nd(BH_4)_2(C_3H_5)(THF)_3$ and (b) the reaction of $Nd(BH_4)_2(C_3H_5)(THF)_3$ with $PhSiH_3$.

Another silane derivative, triethylsilane Et_3SiH, was reacted with the neodymium complex. However, despite adding up to two equivalence of Et_3SiH and heating the reaction tube for up to 4 days at 50 ^oC, there were no signals indicating the formation of Si-$CH_2CH{=}CH_2$. The allyl ligands did diminish but formed propene instead (Appendix V). This could be due to the same reason as above with the reaction using $PhSiH_3$. The allyl group

underwent hydrogenolysis, rather than hydrosilylation, by the Et_3SiH and hence forming the propene.

Trifonov *et al.*[75] hydrogenolysed the lutetium alkly complex, $[Lu\{(Me_3Si)_2NC(NiPr)_2\}_2(CH_2SiMe_3)]$ using phenylsilane, $PhSiH_3$, to form the hydrido rare-earth complex, $[Lu\{(Me_3Si)_2NC(N^iPr)_2\}_2(\mu\text{-}H)]_2$. It was discussed in the literature that the stability was attributed to the bulky nature of the bis(guanidinate) ligand, $(Me_3Si)_2NC(N^iPr)_2$.

Hence, for the reaction between $Nd(BH_4)_2(C_3H_5)(THF)_3$ and silane derivatives, the hydride may have formed, but it could be unstable and then transform into low valent species to finally afford zero valent metal, as indicated by the appearance of darkness in the mixture. This can be due to the supporting ligands not being stable enough to sustain a hydride coordinating to the complex (Scheme 2.13).[76]

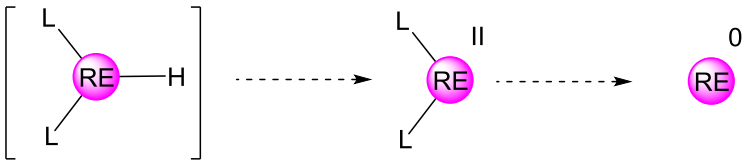

Scheme 2.13 Reduction of the rare-earth compounds.

2.4.4 1,4,7-Trimethyl-1,4,7-triazacyclononane (N_3)

After in-depth studies of lanthanidocenes and half-lanthanidocenes, some non-Cp supported rare-earth complexes were developed more recently.[77] Among them, rare-earth complexes bearing triazacyclononane ligands were explored. The first of these complexes, N_3RECl_3 and $N_3RE(CH_3)_3$ (RE = Sc, Y, N_3 = 1,4,7-trimethyl-1,4,7-triazacylononane), were only reported two decades ago (Figure 2.23).[78]

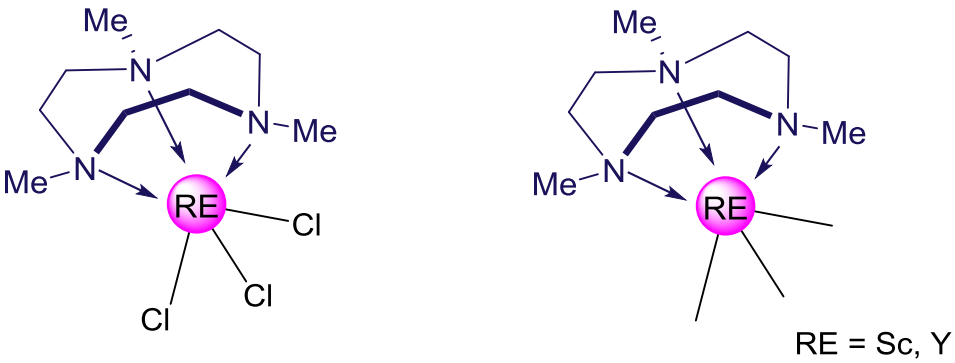

Figure 2.23 Structural presentation of N_3RECl_3 and $N_3RE(CH_3)_3$.[78]

The group previously successfully synthesized the N_3 coordinated tris(borohydride) rare earth complexes, $RE(BH_4)_3(N_3)$ (RE = Nd, Sm) (Scheme 2.14).[63] We proved the cease of the reaction by ^{1}H NMR but we were unable to crystallize the complex. This complex was used in the polymerisation of polyisoprene in the presence of (^{n}butyl)(ethyl)Mg (BEM) and it showed good stereoselectivity and better efficiency than when the tris(borohydride) RE complex with the THF coordinated was used.[63]

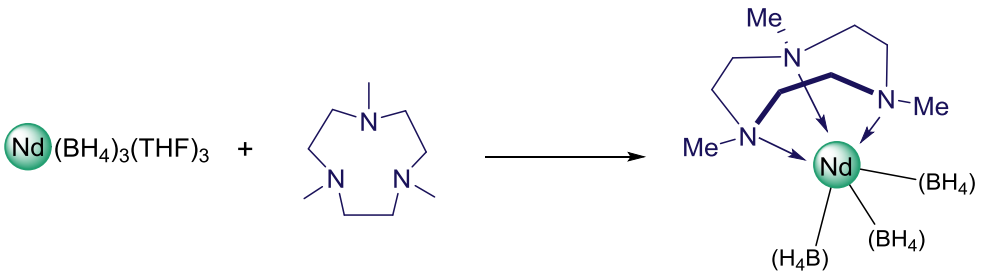

Scheme 2.14. Reaction of $Nd(BH_4)_3(THF)_3$ and N_3 ligand.[63]

The NMR scale reaction of N_3 and $Nd(BH_4)_2(C_3H_5)(THF)_3$ was carried out in [D_6]benzene which resulted in a green solution with green precipitate which could contain the desired product. The signals of free THF of the solution suggest that THF was liberated from the complex. When the green precipitate was dissolved in [D_8]THF, signals at δ = 12.80 (CH_2), 5.38 (CH_2') and 2.83 ppm (CH_3) correspond to the N_3 ligand coordinating directly on the neodymium metal. Hence, the tridentate ligand N_3 successfully substituted the monodentate THF molecules (Scheme 2.15).

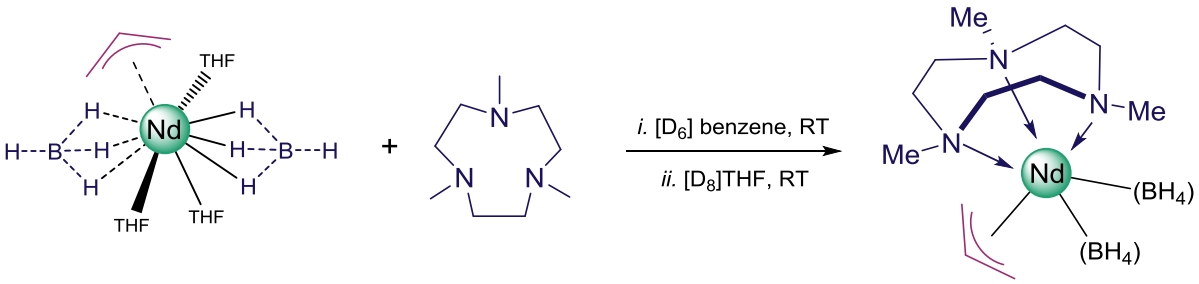

Scheme 2.15 Reaction of $Nd(BH_4)_2(C_3H_5)(THF)_3$ and N_3 ligand.

The NMR scale reaction of N_3 and the other mono(ally) bis(borohydride) complexes **1**-**3** and **5** were also conducted directly in $[D_8]$THF. In the case of the diamagnetic complexes **1**-**3**, a poor solubility was observed prior to use, as a result, the allyl signals could not be clearly detected. There was also an excess of N_3 based on the free N_3 signals at 2.30 and 2.64 ppm. Furthermore, it can be seen that the N_3 ligand was coordinated to the complex at 2.84 and 3.11 ppm indicating that the N_3 ligand was coordinated to the RE metals.

Regarding the samarium metal, in an attempt to rectify the issue of solubility, $Sm(BH_4)_2(C_3H_5)(THF)_3$ was dissolved in $[D_6]$benzene and pressurized with THF followed by which N_3 was added resulting in a pink solution with purple precipitate. The precipitate was found to be partially soluble in $[D_8]$THF. The ^{1}H NMR of the precipitate in $[D_8]$THF showed the N_3 ligand coordinated at 1.42, 3.09 and 4.34 ppm and that the BH_4 signal shifted down –22 ppm. These are all evidence that the N_3 has coordinated to the Sm metal.

Further study on the polymerisation ability of these complexes towards isoprene could be carried out to see the effect of the N_3 coordination on the stereoregularity of the polymer as well as other aspects such as activity and control of the reaction.

2.5 Conclusion

A series of trivalent rare-earth allyl-borohydride complexes of formula $RE(BH_4)_2(C_3H_5)(THF)_x$ (RE = Sc (**1**), x = 2; Y (**2**), La (**3**), Nd(**4**), Sm (**5**), x = 3) were synthesized by reaction of the corresponding rare-earth trisborohydrides $RE(BH_4)_3(THF)_x$ with half an equivalent of bis(allyl)magnesium $Mg(C_3H_5)_2(L)_n$ (L =THF or dioxane). The complexes were fully characterized including by X-ray diffraction methods. All display a

monomeric structure with two BH_4 groups, one allyl ligand, three THF molecules for **2-5**, and two THF molecules for **1**. In all complexes, the BH_4 groups coordinate in a κ^3 (H) mode and the allyl group in η^3 (C) mode.

An alternative route to synthesize the mono(allyl) bis(borohydride) RE complexes using $(C_3H_5)MgX$ (X = Cl or Br) was developed for the smaller rare earth metal scandium. This removes a reaction step from the synthesis by using directly the commercially available Grignard reagent, instead of $Mg(C_3H_5)_2(L)_n$ (L =THF or dioxane).

Attempts to synthesize $RE(C_3H_5)_2(BH_4)(THF)_x$ (RE = Sc, Y, La, Nd, Sm) mostly failed. A series of scale up reactions were done in this purpose. Trials to substitute two borohydride groups of $RE(BH_4)_3(THF)_x$ (RE = Sc, Y, La, Nd, Sm) by two allyl ligands using $Mg(C_3H_5)_2(L)_n$ (L =THF or dioxane) or Grignard reagent like $(C_3H_5)MgX$ (X = Cl or Br) led to the formation of the mono(allyl) bis(borohydride) derivatives, substitution of the three borohydride groups and production of the tris(allyl)RE complexes or incurable mixtures with minor and major products. This is probably due to the high sensitivity of such complexes towards moisture, along with possible instability towards concentration. Indeed, the bis(allyl) mono(borohydride) complexes were observed to be formed at the NMR scale, but could not be isolated. The most promising result was the formation of the bis(allyl) complex via the reaction between $(C_3H_5)MgX$ (X = Cl or Br) and $RE(BH_4)_3(THF)_x$ (RE = Sc, Y). These complexes could potentially be synthesized *in situ* and then be used towards polymerisation.

For the aid of studying and comparing the reactivity of the two active groups; borohydride and allyl, of the mixed allyl-borohydride complexes **1**-**5**, several reaction were conducted using NMR tubes equipped with Young valves. It was concluded that the allyl moiety was in general found to be more reactive than the borohydride. The reactivity was tested toward benzophenone, Cp^RH (Cp = C_5Me_4, R = H or ethyl), phenylsilane, triethylsilane, and 1,4,7-Trimethyl-1,4,7-triazacyclononane (N_3) at room temperature in either [D_6]benzene or [D_8]THF depending of the solubility of complexes **1**-**5**. In case of the diamagnetic complexes **1**-**3**, the analysis of the ^1H NMR spectra of the reactivity reactions was easy to achieve while for the paramagnetic complexes **4** and **5** and apart from few reactions, many high- and low-field signals were observed in the ^1H NMR spectra, of which no unambiguous assignment could be carried out. The reactivity of the benzophenone was not

limited by the rare-earth metal used and it was reacted with complexes **1-5**, where the C=O bond of benzophenone inserted successfully into the RE—allyl bond, yielded the alkoxy compound $RE(OC(allyl)Ph_2)(BH_4)_2(THF)_x$ (RE = Sc, Y and La). The NMR study showed that when complex **4** was reacted with Cp^HH and $Cp^{Et}H$, it cleanly produced the half sandwich complexes of $(Cp^H)Nd(BH_4)_2(THF)_x$ and $(Cp^{Et})Nd(BH_4)_2(THF)_x$ respectively and has the potential to be a new synthetic route to obtain the half-sandwich RE borohydride complexes, although it uses the highly water and air sensitive complex containing an allyl ligand. Concerning the reactivity of complex **4** toward the silane derivatives (Phenylsilane and triethylsilane) no clear evidence that a hydrido neodymium complex was formed. In addition the reaction between N_3 and complexes **1-5**, showed that the THF ligands were successfully substituted with the tridentate N_3 ligand, to give a N_3 substituted complex which could potentially be used towards polymerisation studies.

2.6 References

[1] M. Visseaux, F. Bonnet, *Coord. Chem. Rev*. **2011**, *255*, 374.

[2] V. D. Makhaev, *Russ. Chem. Rev*. **2000**, *69(9)*, 727.

[3] M. Ephritikhine, *Chem. Rev*. **1997**, *97*, 2193.

[4] Z. Xhu, Z. Lin, *Coord. Chem. Rev*. **1996**, *156*, 139.

[5] N. Edelstein, *Inorg. Chem*. **1981**, *20*, 297.

[6] S. Guillaume, M. Schappacher, A. Soum, *Macromolecules*, **2003**, *36*, 54.

[7] F. Bonnet, A. R. Cowley, P. Mountford, *Inorg. Chem.* **2005**, *44*, 9046.

[8] Y. Nakayama, S. Okuda, H. Yasuda, T. Shiono, *React. Funct. Polym*. **2007**, *67*, 798.

[9] C. Villiers, M. Ephritikhine, *J. Chem. Soc., Chem. Commun*. **1995**, 979.

[10] T. Imamoto, T. Kusumoto, N. Suzuki, K. Sato, *J. Am. Chem. Soc*. **1985**, *107*, 5301.

[11] S. A. Kulkarni, N. Koga, *J. Mol. Struct.: Theochem*. **1999**, *461*, 297.

[12] O. Klejnot, Dissertation, University of Munich, **1955**.

[13] E. Zange, *Chem. Ber*. **1960**, *93*, 652.

[14] E. Zange, *Chem. Ber*. **1960**, *93*, 652.

[15] J. H. Morris, W. E. Smith. *Chem Commun*. **1970**, *4*, 245.

[16] U. Mirsaidov, T. G. Rotenberg, T. N. Dymova, *Dokl. Akad. Nauk. Tadzh. SSR* **1976**, *19*, 30.

[17] U. Mirsaidov, A. Kurbonbekov, T. G. Rotenberg, K. Dzhuraev, *Izv. Akad. Nauk. SSR* **1978**, *14*, 1722.

[18] U. Mirsaidov, A. Kurbonbekov, *Dokl. Akad. Nauk. Tadzh. SSR* **1979**, *22*, 313.

[19] U. Mirsaidov, I. B. Shaimuradov, M. Khikmatov, *Z. Neorganich. Khim*. **1986**, *31*, 1321.

[20] L. Porri, G. Ricci, A. Giarrusso, N. Shubin, Z. Lu, *Recent Developments in Lanthanide Catalysts for 1,3-Diene Polymerisation, in Olefin Polymerisation, Vol. 749* (Eds: P. Arjunan, J. E. McGrath, T. L. Hanlon), ACS Symposium Series, Washington, DC, **1999**, pp. 15.

[21] R. Taube, H. Windischm S. Maiwald, H. Hemling, H. Schumann, *J. Organomet. Chem.* **1996**, *513*, 49.

[22] R. Taube, H. Windisch, H. Weissenborn, H. Hemling, H. Schumann, *J. Organomet. Chem*. **1997**, *548*, 229.

[23] S. Maiwald, H. Weissenborn, C. Sommer, G. Muller, R. Taube, *J. Organomet.Chem*. **2001**, *640*, 1.

[24] J.-F. Carpentier, S. M. Guillaume, E. Kirillov, Y. Sarazin, *C. R. Chimie* **2010**, *13*, 608.

[25] M. Visseaux, T. Chenal, P. Roussel, A. Mortreux, *J. Organomet. Chem.* **2006**, *691*, 86.

[26] D. Barbier-Baudry, O. Blacque, A. Hafid, A. Nyassi, H. Sitzmann, M. Visseaux, *Eur. J. Inorg. Chem.* **2000**, *11*, 2333.

[27] P. Zinck, M. Visseaux, A. Mortreux, *Z. Anorg. Allg. Chem.* **2006**, *632*, 1943.

[28] F. Bonnet, M. Visseaux, A. Pereira, D. Barbier-Baudry, *Macromolecules* **2005**, *38*, 3162.

[29] M. Terrier, M. Visseaux, T. Chenal, A. Mortreux, *J. Polym.Sci.: Part A: Polym. Chem.* **2007**, *45*, 2400.

[30] N. Susperregui, M. U. Kramer, J. Okuda, L. Maron, *Organometallics* **2011**, *30*, 1326.

[31] V. Grignard, *Compt. Rend.* **1900**, *130*, 1322.

[32] A. Baeyer, V. Villiger *Ber*. **1902**, *35*, 1201.

[33] V. Grignard, *Compt. rend*. **1903**, *136*, 1260.

[34] R. Abegg, *Ber.* **1905**, *38*, 4112.

[35] P. Jolibois, *Compt. rend*. **1912**, *155*, 353.

[36] T. Zerevitinov, *Ber*. **1908**, *41*, 2244.

[37] A. Terentiev, *Z. anorg. Chem*. **1926**, *156* , 73.

[38] W. Schlenk, J. W. Schlenk, *Ber.* **1929**, *62, B*, 920.

[39] C. R. Noller, W. R. White, *Am. Chem. Soc.* **1937**, *59*, 1354.

[40] R. Kullman, *Compt. rend*. **1950**, *231*, 866.

[41] C. Lichtenberg, T. P. Spaniol, I. Peckermann, T. P. Hanusa, J. Okuda, *J. Am. Chem. Soc.* **2013**, *135*, 811.

[42] E. A. Hill, W. A. Boyd, H. Desai, A. Darki, L. Bivens, *J. Organomet. Chem*. **1996**, *514*, 1.

[43] (a) S. Fadlallah, M. Terrier, C. Jones, P. Roussel, F. Bonnet, M. Visseaux, *Organometallics* 2016, *35*, 456; (b) S. Fadlallah, J. Jothieswaran, F. Capet, F. Bonnet, M. Visseaux, *Submitted to Chem. Eur. J.*

[44] F. Bonnet, M. Visseaux, D. Barbier-Baudry, A. Hafid, E. Vigier, M .M. Kubicki, *Inorg. Chem.* **2004**, *43*, 3682.

[45] U. Mirsaidov, I. B. Shaimuradov, M. Khikmatov, *Russ. J. Inorg. Chem.* **1986**, *31*, 753.

[46] P. Cui, T. P. Spaniol, J. Okuda, *Organometallics* **2013**, *32*, 1176.

[47] N. Yu, M. Nishiura, X. Li, Z. Xi, Z. Hou *Chem. Asian J.* **2008**, *3*, 1406.

[48] H. Schumann, *Acta Cryst.* **2000**, *C56*, 48.

[49] B. G. Segal, S. J. Lippard, *Inorg. Chem.* **1978**, *17*, 844.

[50] T. Sato, K. Miwa, Y. Nakamori, K. Ohoyama, H. W. Li, T. Noritake, M. Aoki, S. Towata, S. Orimo, *Phys. Rev. B*, **2008**, *77*, 104114.

[51] D. Robert, M. Kondracka, J. Okuda, *Dalton Trans*. **2008**, 2667.

[52] J. Jenter, P. W. Roesky, N. Ajellal, S. M. Guillaume, N. Susperregui, L. Maron, *Chem. Eur. J.* **2010**, *16*, 4629.

[53] D. Li, S. Li, D. Cui, X. Zhang, *Organometallics* **2010**, *29*, 2186.

[54] J. Kratsch, M. Kuzdrowska, M. Schmid, N. Kazeminejad, C. Kaub, P. Ona-Burgos, S. M. Guillaume, P. W. Roesky, *Organometallics* **2013**, *32*, 1230.

[55] M. D. Fryzuk, T. S. Haddad, S. J. Rettigt, *Organometallics* **1992**, *11*, 9.

[56] D. Robert, E. Abinet, T. P. Spaniol, J. Okuda, *Chem. Eur. J.* **2009**, *15*, 11937.

[57] R. Taube, S. Maiwald, J. Sieler, *J. Organomet. Chem*. **2001**, *621*, 327.

[58] S. Maiwald, R. Taube, H. Hemling, H. Schumann, *J. Organomet. Chem.* **1998**, *552*, 195.

[59] L. F.Sanchez-Barba, D. L. Hughes, S. M. Humphrey, M. Bochmann, *Organometallics* **2005**, *24*, 5329.

[60] R. Taube, H. Windisch, H. Weissenborn, H. Hemling, H. Schumann, *J. Organomet. Chem.* **1997**, *548*, 229.

[61] S. Maiwald, H. Weissenborn, C. Sommer, G. Muller, R. Taube, *J. Organomet. Chem.* **2001**, *640*, 1.

[62] J. Sieler, A. Simon, K. Peters, R. Taube, M. Geitner, *J. Organomet. Chem.* **1989**, *362*, 297.

[63] M. Terrier's thesis: « Borohydrures de lanthanides polymérisation et copolymerisation », University of Lille 1, 2008, Dir M. Visseaux.

[64] W. Wu, M. Chen and P. Zhou, *Organometallics* 1991, **10**, 98.

[65] M. U. Kramer, D. Robert, S. Arndt, P. M. Zeimentz, T. P. Spaniol, A. Yahia, L. Maron, O. Eisenstein, J. Okuda, *Inorg. Chem.* **2008**, *47*, 9265.

[66] W. J. Evans, A. L. Wayda, W. E. Hunter and J. L. Atwood, *J. Chem. Soc. Chem. Commun.*, 1981, 706.

[67] R. Duchateau, E. A. C. Brussee, A. Meetsma and J. H. Teuben, *Organometallics*, 1997, **16**, 5506.

[68] Y. Nakajima and J. Okuda, *Organometallics*, 2007, **26**, 1270.

[69] C. Changtao, W. Chunhong, C. Yaofeng, *Acta Chim. Sinica.* **2014**, *72*, 883.

[70] Anwander, M. G. Klimpel, H. M. Dietrich, D. J. Shorokhov and W. Scherer, *Chem. Commun.*, 2003, **20**, 1008.

[71] S. M. Cendrowski-Guillaume, G. Le Gland, M. Nierlich and M. Ephritikhine, *Organometallics*, 2000, **19**, 5654.

[72] M. Visseaux, M. Terrier, A. Mortreux and P. Roussel, *Comptes Rendus Chim.*, 2007, **10**, 1195.

[73] E. Abinet, D. Martin, S. Standfuss, H. Kulinna, T. P. Spaniol and J. Okuda, *Chem. - A Eur. J.*, 2011, **17**, 15014.

[74] D. Martin, J. Kleemann, V. Abinet, T. P. Spaniol, L. Maron and J. Okuda, *Eur. J. Inorg. Chem.*, 2013, 3987.

[75] A. A. Trifonov, E. A. Fedorova, G. K. Fukin and M. N. Bochkarev, *Eur. J. Inorg. Chem.*, 2004, **2004**, 4396.

[76] D. Barbier-baudry and A. Dormond, in *Recent Advances in Hydride Chemistry*, **2001**, pp. 249.

[77] W. E. Piers and D. J. H. Emslie, *Coord. Chem. Rev.* **2002**, *233*, 131.

[78] S. Hajela, W. P. Schaefer and J. E. Bercaw, *J. Organomet. Chem.*, 1997, **532**, 45.

CHAPTER 3

POLYMERISATION STUDIES

3.1 Isoprene polymerisation

3.1.1 Introduction

Polyisoprene (PIP), also known as natural rubber, is one of the most well-known bio-sourced polymers. Natural rubber which is extracted from the Hevea tree is composed predominantly of *cis*-1,4 units whereas the one extracted from Gutta Percha is mainly *trans*-1,4.[1] Synthetic polyisoprene can be produced from the polymerisation of isoprene (IP) leading to the formation of PIP containing four different isomers; 1,2-, *cis*-1,4-, *trans*-1,4- and 3,4-PIP (Scheme 3.1). Both *cis*- and *trans*-PIP found numerous applications in the fields of adhesives, sport equipment or tires industry.[2-5]

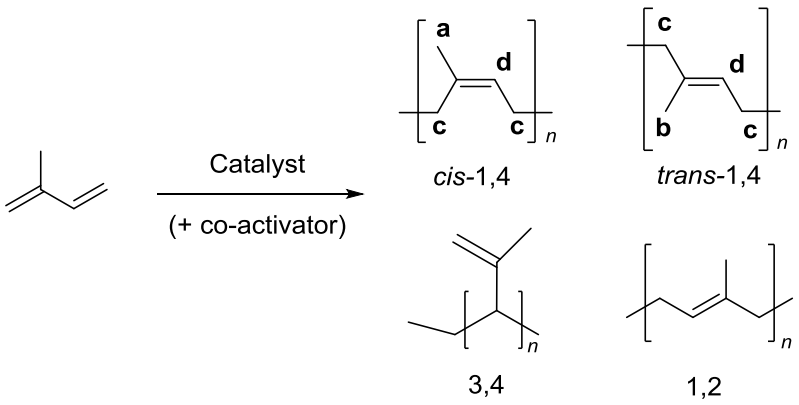

Scheme 3.1 Polymerisation of isoprene.

IP can be polymerised using different kinds of initiators, such as radical,[6] anionic[7] and metal-based complexes.[8] Metal-mediated coordination polymerisation allows the formation of polymers with controlled microstructure. The choice of the pre-catalysts, co-catalysts and the reaction conditions largely influence the final microstructure of the produced polymers. In particular rare-earth (RE) pre-catalysts[9] bearing allyl ligand were found effective and highly selective for the polymerisation of IP as single-component catalyst or in combination with co-catalysts such as aluminum and magnesium alkyl derivatives, affording PIP with highly *cis*-, *trans*- or 3,4- microstructure.[10-15] Figure 3.1 presents selected examples of allyl-RE metal complexes used for the stereoselective polymerisation of IP.

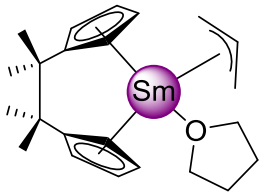

Trans-1,4-polyisoprene > 99% [10]

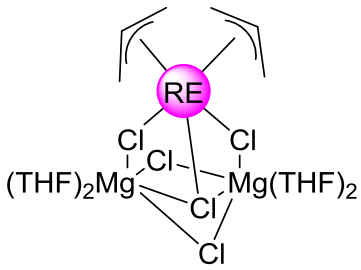

⇒ RE = Nd, co-catalysts MAO
Cis-1,4-polyisoprene 99% [11]
⇒ RE = Y, co-catalysts $AlEt_3$
Trans-1,4-polyisoprene 91% [11]

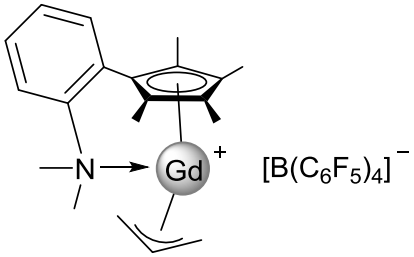

Cis-1,4-polyisoprene 99% [12]

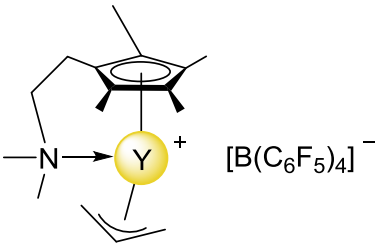

3,4-polyisoprene 79% [13]

Figure 3.1 Representative allyl rare-earth metal complexes for the *cis*-, *trans*- and 3,4-polymerisation of isoprene.

In the present work we investigated the activity of the complexes $RE(BH_4)_2(C_3H_5)(THF)_3$ (RE = Nd (**4**), Sm (**5**)) toward the polymerisation of isoprene, as a single component catalyst or combined with different co-catalysts.[15a] This work was the continuation of studies done previously in our research group.[16]

3.1.2 $Nd(BH_4)_2(C_3H_5)(THF)_3$ as an initiator for the polymerisation of isoprene

For the structural characterization of PIP, ^1H NMR was recorded in $CDCl_3$ to calculate the percentage ratio of stereoregularity produced. This is done by using the integral values of the characteristic signals of each motive (Figure 3.2) and calculated based on the following:

$$\% \, 3{,}4 = \frac{I(\delta = 5.11)}{I\left[\frac{(\delta = 4.69)}{2}\right] + I(\delta = 5.11)} \text{ x } 100\%$$

$$\% \, cis \; 1{,}4 + \% \, trans \; 1{,}4 = 100 \, \% - \% \; 3{,}4$$

$$\% \, trans \; 1{,}4 \text{ x } I \; (\delta = 1.68) = \; \% cis \; 1{,}4 \text{ x } I \; (\delta = 1.59)$$

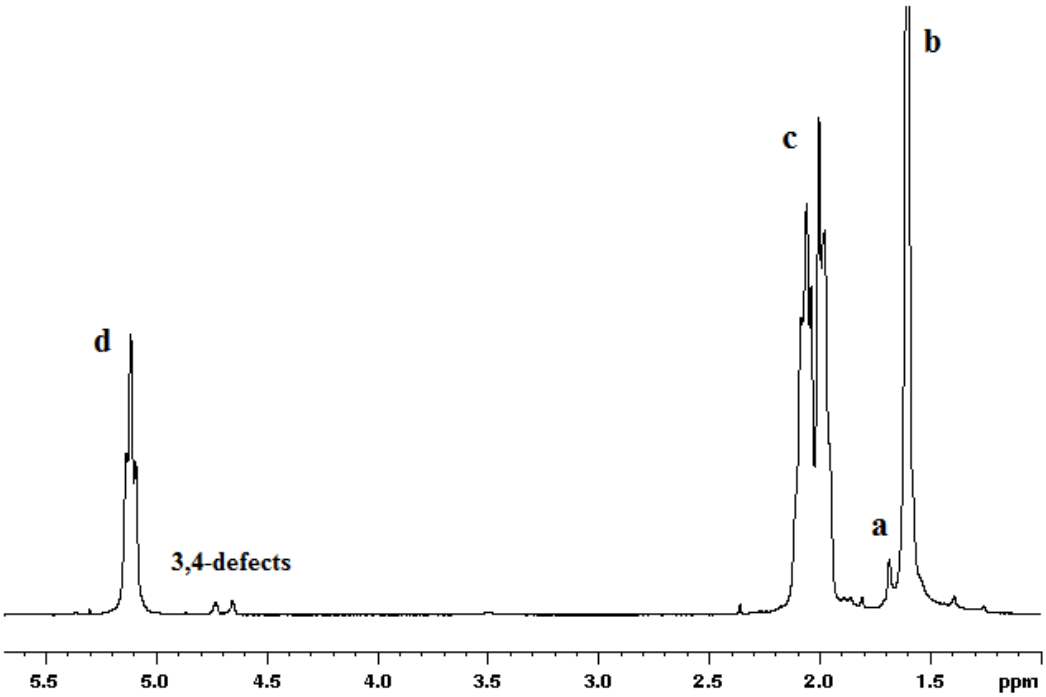

Figure 3.2 ^{1}H NMR of *trans*-polyisoprene in $CDCl_3$ (entry 2, Table 3.1). a: -CH=C(*Me*)-*1,4-trans*, b: -CH=C(*Me*)-*1,4-cis*, c: -CH_2-*cis and* -CH_2- *trans*, d: -C*H*=C(Me)-*cis* + *trans* (Scheme 3.1).

The reactivity of neodymium (**4**) and samarium (**5**) allyl complexes was assessed toward the polymerisation of IP. The neodymium-based complex **4** was found active on its own or in combination with various alkylating agents (MAO, BEM, $Mg(C_3H_5)_2(C_4H_8O_2)_{0.5}$ or TIBA), whereas the same experiments done with its samarium analogue showed no reactivity at all, in line with the well-known "neodymium effect".[9-17] The related results are summarized in Table 3.1.

Table 3.1 Polymerisation of isoprene using $Nd(BH_4)_2(C_2H_5)(THF)_3$ **4**.

Entry [a]	Co-catalyst (equiv. / Nd)	Time (h)	Yield (%)	$M_{n\ SEC}$ (g/mol) / $Đ$ [b]	$M_{n\ theo}$ [c] (g/mol)	*trans*- (*cis*-) [d] (%)
1	-	3	53	29600 / 1.54	35300	92.2 (6.4)
2	BEM (1)	2	58	16900 / 1.54	40900	95.5 (2.7)
3	$Mg(C_3H_5)_2(C_4H_8O_2)_{0.5}$ (1)	2	27	5300 / 1.23	18400	92.7 (1.0)
4	Al^iBu_3 (10)	1	100	20300 / 2.23	67700	78.7 (20.1)
5	MAO (30)	1	97	41600 / 2.23	68700	68.2 (28.6)

[a] Experimental conditions: $V_{toluene}$=1 mL, $V_{(isoprene)}$= 1 mL, [IP]/[Nd] = 1000, T= 50 °C. [b] Determined by SEC in THF at 40 °C with respect to polystyrene standards with the correction $M_{n\ SEC} = M_{n\ PS} \times 0.5$,[66] $Đ = M_w/M_n$. [c] $M_{n\ theo}$ = [IP]/[RE] × 68.12 × conversion. [d] Determined by ^{1}H NMR spectroscopy in $CDCl_3$.

Complex **4** was found to be active as a single-component catalyst, yielding 53 % polyisoprene in 3 h (entry 1). Such reactivity could be expected due to the presence in the complex of a Nd–allyl bond, which is known [10,12,13] to be able to initiate the polymerisation of IP by coordination-insertion mechanism (Scheme 3.2). Typically, the *anti* active species results from s-*cis* coordination insertion of isoprene; it is the kinetic active species (affording *cis*-1,4 PIP), which isomerizes easily into the *syn* thermodynamic one (affording *trans*-1,4 PIP). The *trans*-1,4 polyisoprene may also result from s-*trans* coordination of the monomer.

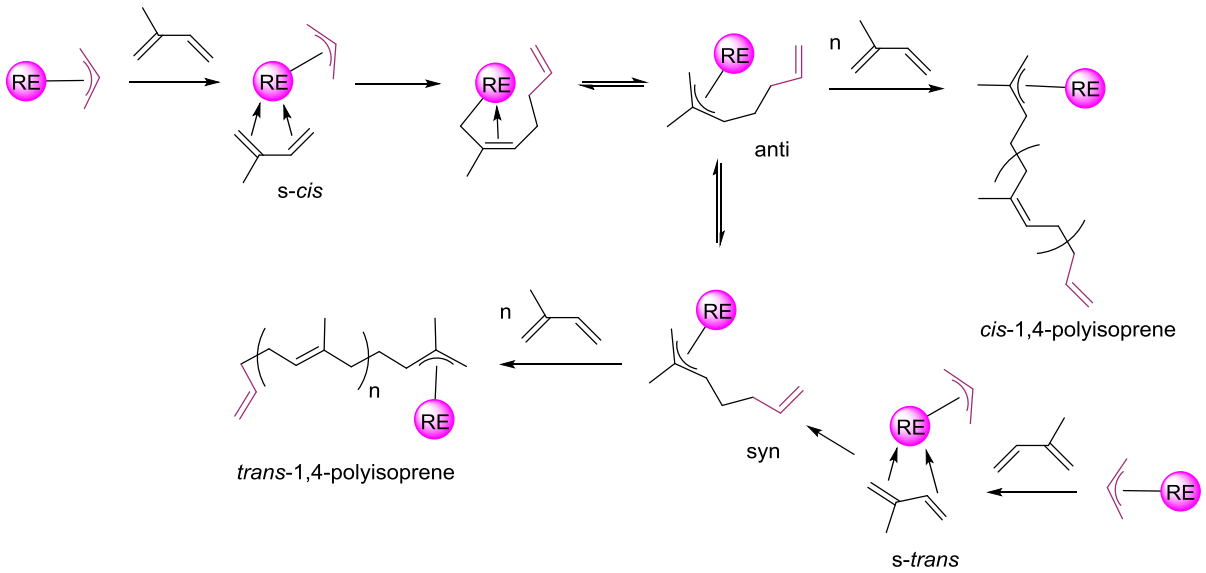

Scheme 3.2 Coordination-insertion mechanism of the polymerisation of isoprene mediated by RE-allyl species.

The M_n value of the isolated polyisoprene (entry 1) determined by SEC (29600 g.mol^{-1}) is in close agreement with the expected molar mass (36000 g.mol^{-1}), along with a rather narrow dispersity ($Đ$ = 1.54), and corresponds to the growth of one polymer chain per metal center through the Nd—allyl bond. Interestingly as well, the polymer displayed a highly *trans*-stereoregular microstructure with 92.2 % of *trans*-units, as already observed with tris- and tetra(allyl)-RE initiators.[18] As a comparison, the activity of catalyst **4** was slightly lower than that previously observed for the dual-component $Nd(BH_4)_3(THF)_3/Mg(C_3H_5)_2$ catalytic system (80 % yield in 3 h at 50 °C), as well as the *trans*-stereoselectivity (95.4 %), with comparable macromolecular data (M_n = 35100 g.mol^{-1}; $Đ$ = 1.34).[19] The rather inferior activity of **4** can be explained by the absence of magnesium element in the catalyst, which can play two roles during the process. First, Mg may coordinate the THF molecules (because of the more oxophilic nature of magnesium as observed in RE/magnesium bimetallic complexes [20-21]), which can compete with the monomer towards the coordination to the RE center. Note that the presence of an excess of THF has an inhibitory effect, reducing the activity without affecting other properties of the catalytic system such as selectivity.[19] Second, the small difference of reactivity observed indicates that the magnesium compound not only acts as an alkylating agent, but probably remains in the RE coordination sphere under the form of a likely bimetallic active species,[22,23] influencing both the activity and the stereo-selectivity of the reaction. In the latter case, two probable Nd-Mg active species could be formed (Figure 3.3).

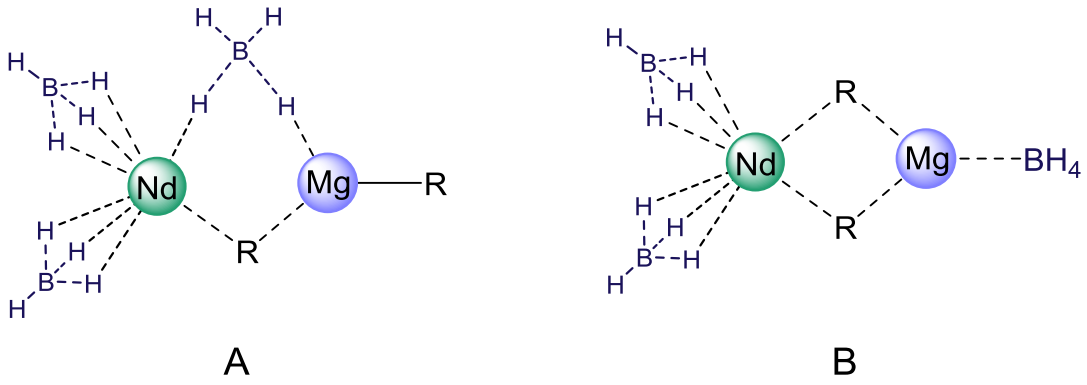

Figure 3.3 Possible Nd/Mg active initiating species, R = $MgBu_2$, $Mg(C_3H_5)_2$ or Mg(Bu)(Et) (THF ligands are omitted).

^{1}H NMR study in [D_6]benzene at the NMR scale (in an NMR tube equipped with Young valve) of the reaction of $Nd(BH_4)_3(THF)_3$ and $Mg(^nBu)_2$ was conducted.[22] The borohydride signal usually appearing at 110 ppm, was significantly shifted at 50 ppm when $Mg(^nBu)_2$was added. A hypothesis could be postulated that the bimetallic compound with bridging BH_4 (Figure 3.3, A) is formed rather than the species displaying terminal Mg—(BH_4) (Figure 3.3, B). Indeed, the two ancillary BH_4 groups and the bridging one are in equilibrium which give rise to one average BH_4 signal in the ^{1}H NMR.

Regarding the IP polymerisation results, the addition of one equiv. of $Mg(^nBu)(Et)$ (BEM for butylethylmagnesium) to $Nd(BH_4)_2(C_3H_5)(THF)_3$ (entry 2, Table 3.1) gave rise to quite identical results to those observed with the previously reported $Nd(BH_4)_3(THF)_3$/BEM catalytic system.[22,23] When compared to entry **1**, both activity and stereospecificity are higher, showing the beneficial role of the magnesium partner in such process. The efficiency ($M_{n\ theo}/M_{n\ SEC}$) in entry 2 is about 2.5, indicating that more than two polymer chains are growing, *i.e.*, at least one chain initiated by the RE—alkyl bond formed by alkylation of RE—(BH_4) with BEM, and one initiated by the genuine RE—allyl group.

When $Mg(C_3H_5)_2(C_4H_8O_2)_{0.5}$ is combined to **4** as the co-catalyst (entry 3) the activity decreases (yield 27 % in 2 h) but the selectivity remains the same (92.7 %) as observed with **4** as a single-component catalyst (92.2 %). With triisobutylaluminum (Al^iBu_3) or methylaluminoxane (MAO) as the co-catalysts, higher activities were obtained (entries **4** and **5**), affording total conversion in only 1 h, but the reactions were less stereo-selective, with more *cis*- proportion, as expected from the previous results reported by Taube *et al.*.[25,26] This change of selectivity is typical of a *syn-anti* isomerization of the metal—allyl active species (Scheme 3.2) as already observed when an aluminum co-catalyst was added to a *trans*-selective (allyl)-RE single component catalyst.[18] It is noteworthy that Al^iBu_3 and MAO are used in large excess to ensure the alkylation of the neodymium catalyst, while stoichiometric amount of $Mg(R)_2$ (R = allyl, butyl or/and ethyl) is enough to activate the catalytic system, thus one can consider that the *cis*-selectivity results from the formation of coordinated RE species (Figure 3.4).

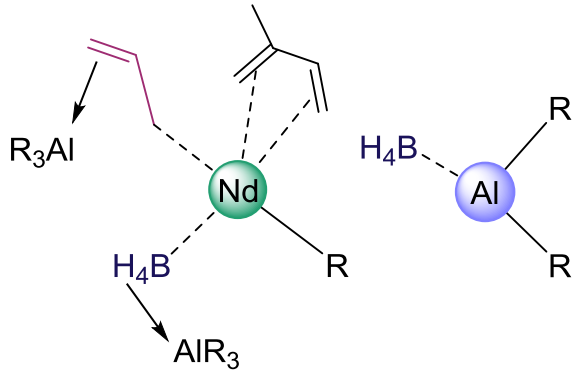

Figure 3.4 Possible Nd/Al active initiating species (THF ligands omitted for clarity).

3.2 Ring-opening polymerisation of cyclic esters

Biodegradable polymers are an environment-friendly alternative to synthetic petrochemical-based polymers which have two major drawbacks, the use of non-renewable sources and the recycling of these large scale commodity polymers. In contrast, most biodegradable polymers use renewable sources for their production and are easily removed by the environment.

Among the different biodegradable polymers, polylactide (PLA) and poly(ε-caprolactone) (PCL) are receiving a significant attention as they found numerous applications and in particular in biomedical fields.[27-29]

The most convenient and efficient method to obtain linear aliphatic polyesters such as PLA and PCL in high yield along with high molar masses, is the ring-opening polymerisation (ROP) of cyclic esters where the thermodynamic driving force is the relief of the ring strain. In contrast to polycondensation,[30] ROP can be conducted under mild conditions, avoiding the formation of small by-products that lower the yield, and allows much higher molar mass and better control of the molecular weight distribution (dispersity).

In practice, the ROP process requires the presence of an appropriate catalyst. Depending on the initiator, the polymerisation proceeds according to four different major reaction mechanisms, i.e. anionic, cationic, “activated monomer” or “coordination insertion” mechanism.

- Anionic ROP starts by the cleavage of the acyl-oxygen bond due to nucleophilic attack at the carbonyl. Another option is the attack on the carbon atom adjacent to the acyl-oxygen. An ion (alkoxide or carboxylate) is formed at the end of the polymer chain which acts as the new initiating species (Scheme 3.3).[31,32]

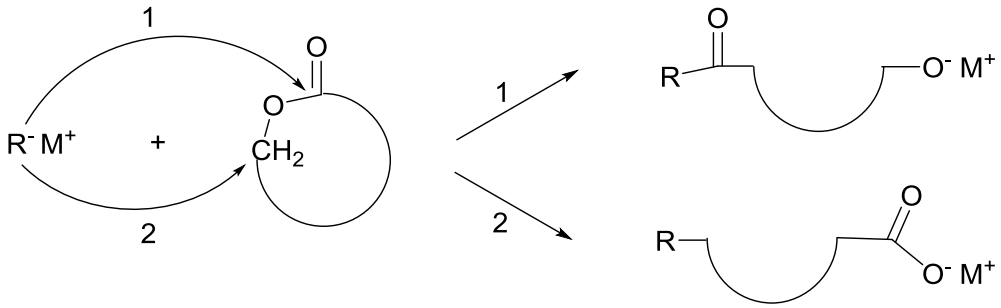

Scheme 3.3 Anionic ROP of cyclic ester.

- In cationic ROP mechanism, the first step involves the protonation of the carbonyl O-atom, followed by a nucleophilic attack of the monomer. This is considered as the least efficient way to polymerise cyclic esters (Scheme 3.4).[33,34]

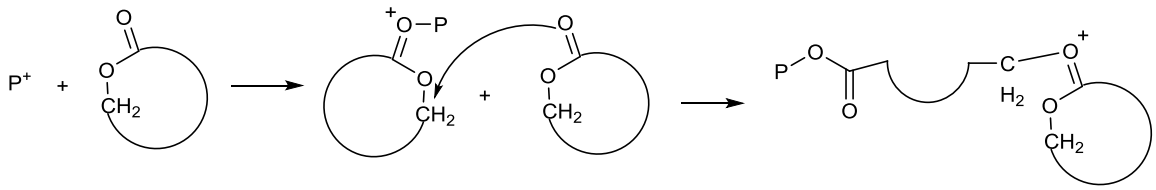

Scheme 3.4 Cationic ROP of cyclic ester.

- In the "activated-monomer" mechanism (Scheme 3.5), the carbonyl of cyclic ester is activated by a protic compound or by a metal-catalyst which is typically a Lewis acid, in addition to the presence of nucleophilic source in the medium which is mostly alcohols. In case the polymerisation is conducted in the presence of Lewis acidic metal center, the metal center activates, upon coordination, the monomer toward the external attack of a neutral nucleophilic initiator. This is in contrast with the coordination mechanism (See next paragraph) where the ROP proceeds via the nucleophilic attack of an inner sphere ligand bonded to the metal.[35,36]

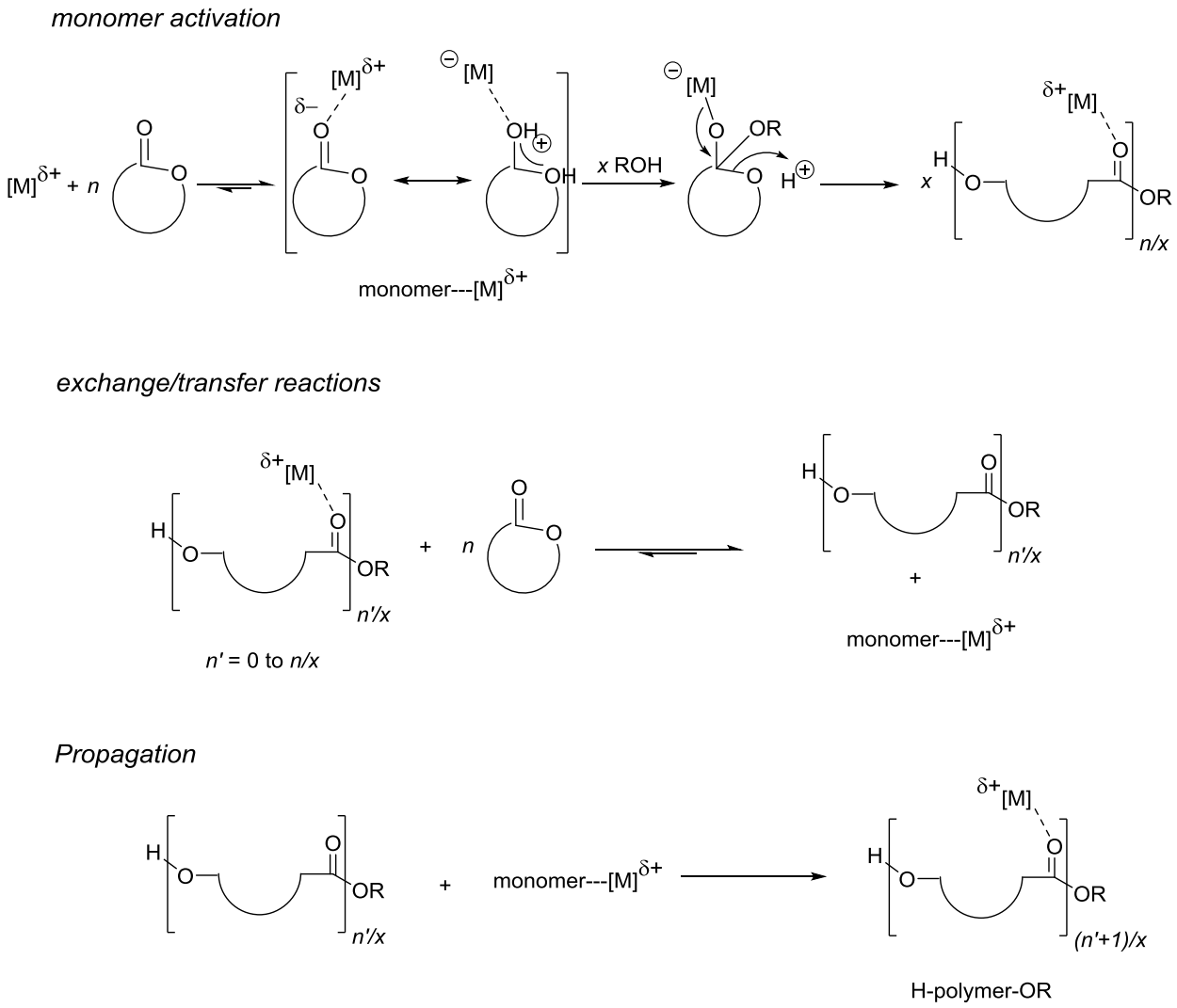

Scheme 3.5 Activated-monomer ROP of cyclic esters.

- Finally, the last method is the coordination-insertion mechanism mediated by a metal-based catalyst, which gained the most attention and now it is accepted as the most efficient method for the production of polyesters. The first step consists in the coordination of the monomer to the Lewis-acidic metallic center, followed by ring-opening via acyl-oxygen cleavage and generation of novel metal-alkoxide species from which the cycle can initiate, and then to terminate the reaction normally a proton source should be added (Scheme 3.6).[37]

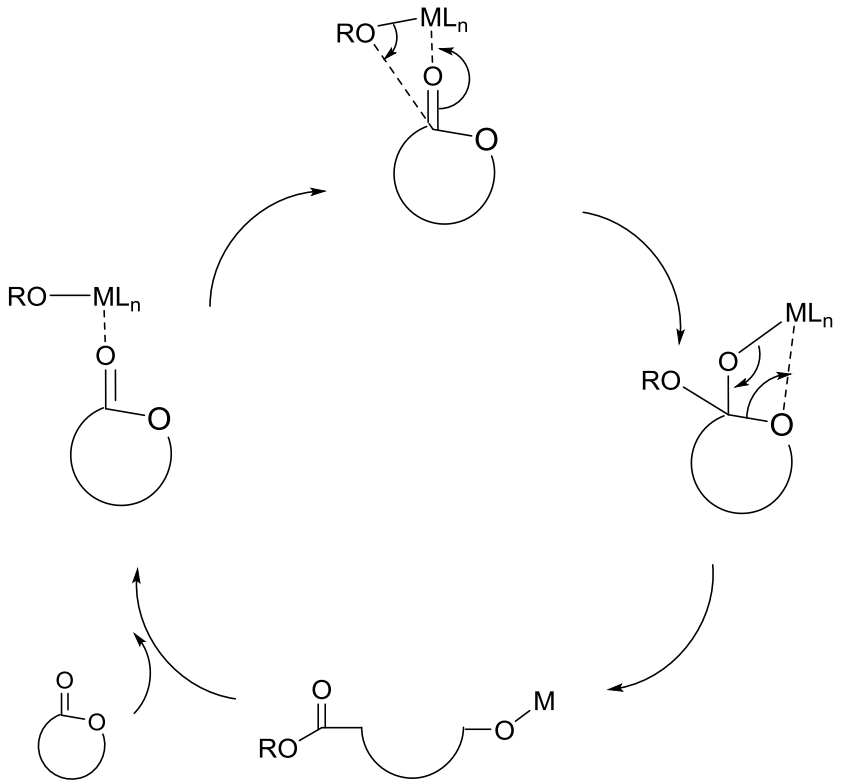

Scheme 3.6 Coordination-insertion mechanism for ROP of cyclic ester.

The coordination-insertion ROP mechanism often proceeds in "classical living controlled" way. As depicted in Figure 3.5, in such "classical living" ROP, there are exactly as many growing polymers as the total number of active sites available from the catalyst *i.e.* one polymer chain per one active site on the metal. But, this way has some limitations: low catalytic productivity and large contamination of the polymer with catalyst residue.[35,36] In order to overcome this problem, the use of a chain transfer agent (CTA) in the reaction course can be considered. The rapid and reversible exchange reaction between the chain transfer agent and the living metal active species allows the formation of more polymer chains from one metal center as compared with the conventional living polymerisation where usually only one chain grows per active species. Moreover, polymerisations conducted under transfer conditions lead to the formation of polymer chain-ends capped with the transfer agent moieties which might contain functional groups. Regarding the polymerisation of cyclic esters, the transfer agents typically used with metal-based catalysts are alcohols, amines, etc., the former being particularly efficient.[38-46]

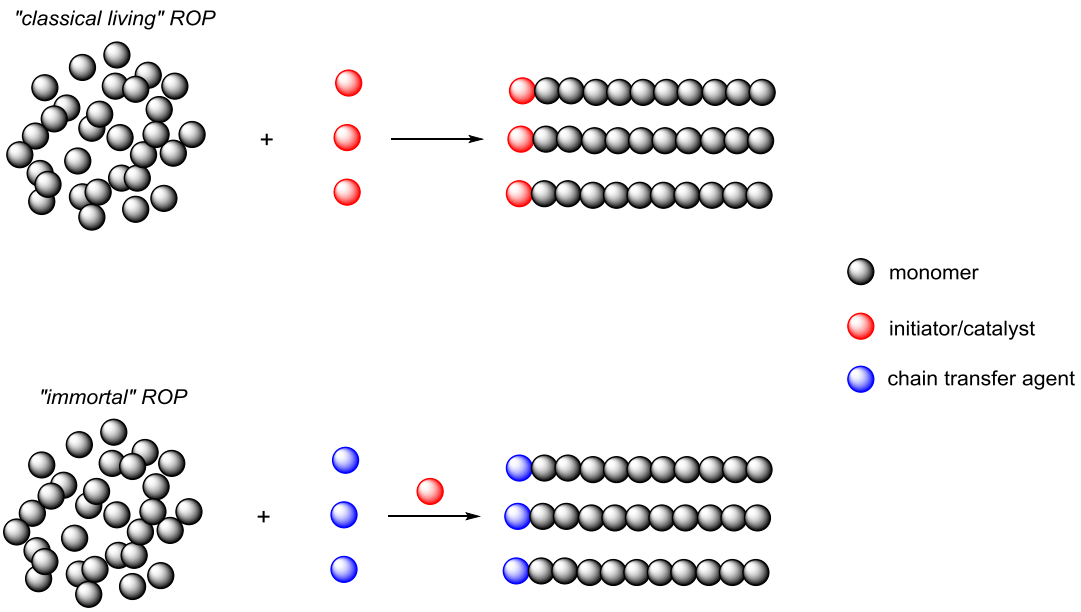

Figure 3.5 Illustration of the distinction between "classical living" and "immortal" ROP processes.[36]

When a CTA is involved in the reaction (Figure 3.5), the external nucleophile associated to the metal-catalyst, can acts simultaneously as the initiator and CTA, in this case, one can talk about "immortal" ROP (iROP). In iROP the mechanism involved is the "activated-monomer" rather than classical coordination-insertion mechanism.[36] Noteworthy, in some cases the CTA is "simply" playing its role in the chain transfer and not as initiator, which indicates no immortal behavior and only the growth of the polymer chain occurs on the metal-catalyst (Scheme 3.7)

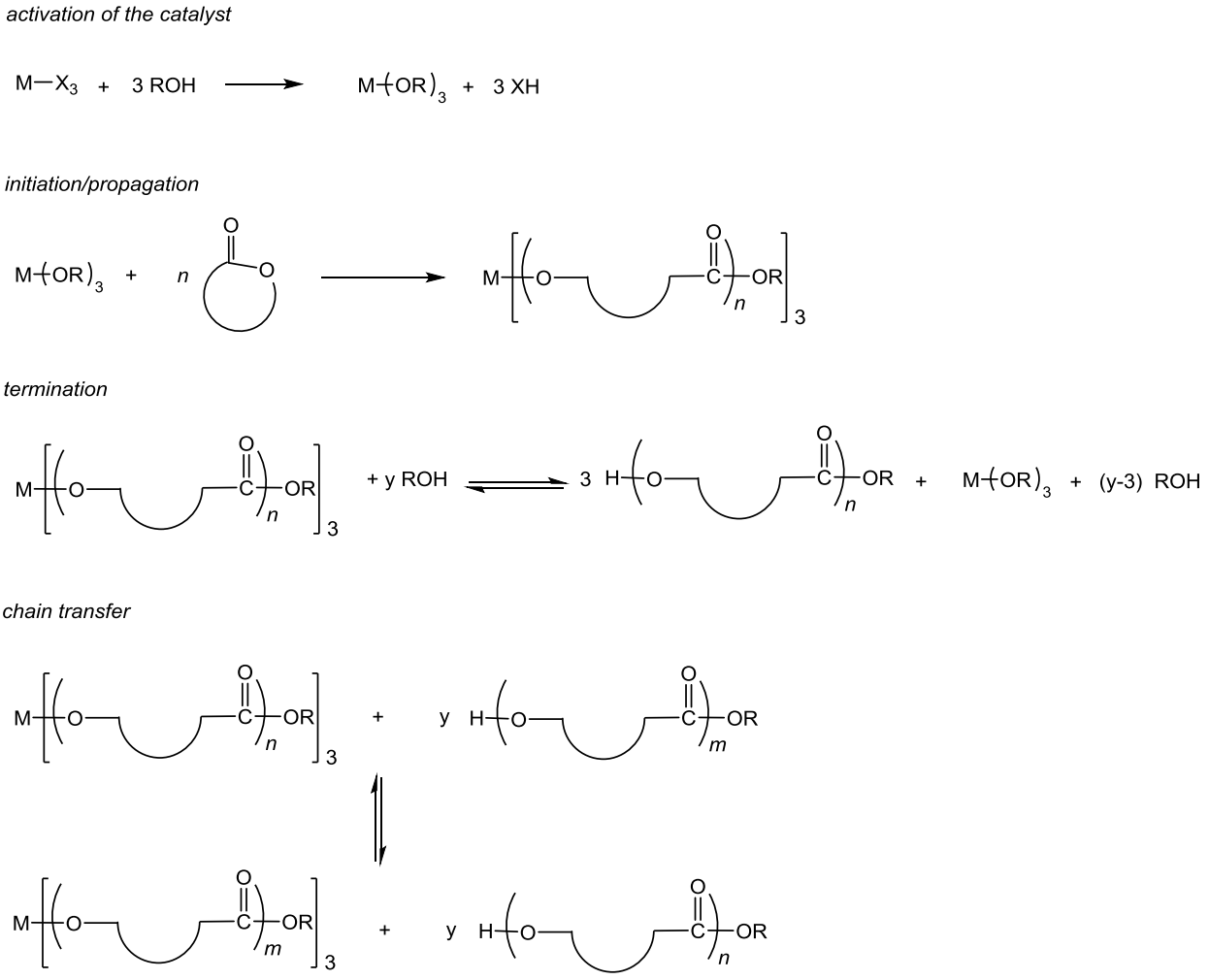

Scheme 3.7 ROP polymerisation of cyclic ester under chain transfer agent condition with in immortal behavior.

Since the pioneering work of Kleine *et. al*,[47] metal-based catalystic systems have been extensively developed, through variation of the metallic center and surrounding ligands, as this allows the formation of polyesters with high molar masses along with controlled microstructure in the case of specific catalysts bearing well-defined ligands[48-50].The metal-based catalysts used for this reaction are, in general, of the type [(L)M—X] where L is the supporting ligand(s), M the metal, X the active function group (hydride, alkyl, aryl, amide, borohydride and alkoxide).[51-55] Notably, the alkoxide initiators are still the most commonly used affording α-hydroxy, ω-alkoxy telechelic polyesters (RO—C(O)—polyester—OH). Moreover, the hydride, alkyl, aryl and amide initiators provide the same nature of polymer. [51-55] Instead, dihydroxy-terminated polyesters can be accessed by using rare-earth complexes (M = RE) bearing the borohydride ligand (X = BH_4) directly producing the corresponding α,ω-dihydroxy telechelic polyesters with two terminal hydroxy groups (HO—polyester—

OH) which are highly desirable as building block toward advanced polymer materials, the first example being reported by Guillaume *et al.*[56,57] who reported the synthesis of dihydroxy telechelic poly(caprolactone). It was then shown that borohydrido complexes of the rare earth could also initiate the polymerisation of L- and *rac*-lactide.[58-60] but in that case the dihydroxy telechelic nature of the polyester is still under debate (see further, section 3.3.3).

3.2.1 ε-Caprolactone polymerisation

3.2.1.1 Introduction

PCL is a very attractive biocompatible polymer. It was studied as early as 1930s by Carruthers group.[61] It is produced by ring-opening polymerisation (ROP) of ε-caprolactone (ε-CL) (Scheme 3.8), a petro-sourced cyclic monomer formed by the Baeyer-Villiger oxidation of cyclohexanone with pancreatic acid.

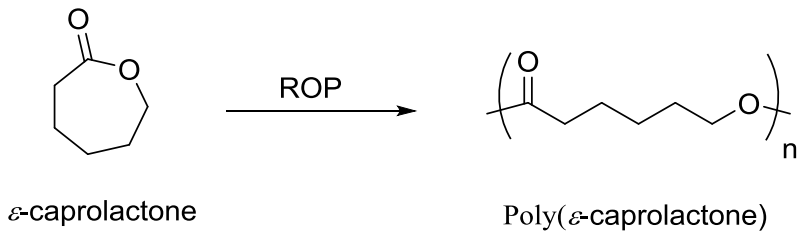

Scheme 3.8 Chemical structure of ε-caprolactone and the resulting polymer produced by ring-opening polymerisation.

PCL is a hydrophobic, semi-crystalline polymer displaying a glass transition temperature (T_g) of −60 °C and a melting point (T_m) ranging between 59 and 64 °C which enables easy formability at relatively low temperature.[62]

PCL is soluble in chloroform, dichloromethane, carbon tetrachloride, benzene, toluene, cyclohexanone and 2-nitropropane at room temperature (RT). It has a low solubility in acetone, 2-butanone, ethyl acetate, dimethylformamide and acetonitrile and is insoluble in alcohol, petroleum ether and diethyl ether.[63]

A wide variety of initiators were reported to initiate the ROP of ε-CL, the most active ones being the metal-based catalysts, due to their activities and the resulting high molar masses PCL they can produce. A wide range of metals are well-known to afford highly active

catalytic systems for this reaction, such as tin, aluminum, zinc and main group metals, group 4 metals, group 3 and rare-earth.[64] Among the latter, borohydrido RE complexes,and in particular trisborohydrides $RE(BH_4)_3(THF)_x$ (RE = La, Nd, Sm), were reported to be efficient for the solution polymerisation of ε-CL at RT to afford α,ω-dihydroxy telechelic polycaprolactone HO—polycaprolactone—OH.[56,57]

Regarding the mechanism of the polymerisation using borohydride initiator (Scheme 3.9), it was postulated that the initiation process consecutively involves (i) monomer coordination to the neodymium center, (ii) insertion into the Nd–hydride(BH_3) bond and (iii) reaction with the (HBH_3) group. The polymerisation subsequently proceeds with an alkoxide initiator to yield α,ω-dihydroxy telechelic polycaprolactone with hydroxy end-groups.[56]

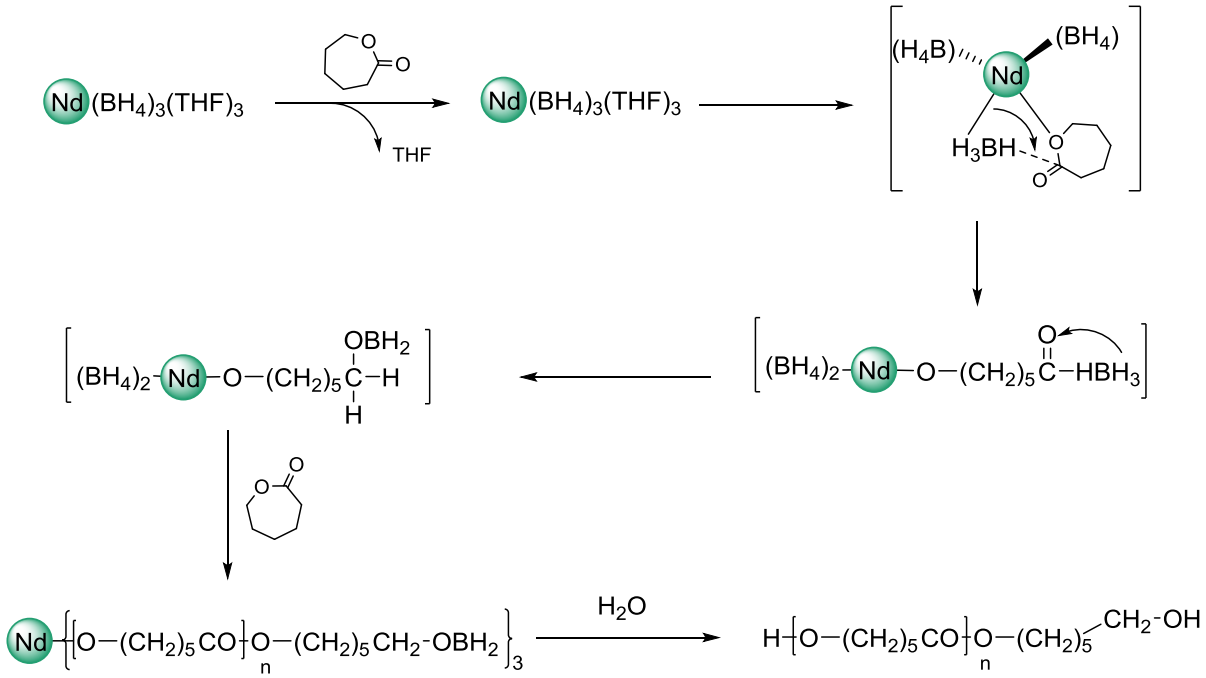

Scheme 3.9 ROP mechanism of ε-caprolactone using $Nd(BH_4)_3(THF)_3$.[56]

3.2.1.2 *ε*-Caprolactone polymerisation mediated by $RE(BH_4)_2(C_3H_5)(THF)_x$

The ability of the complexes $RE(BH_4)_2(C_3H_5)(THF)_x$ (RE = Sc, x = 2; Y, La, Nd, Sm, x = 3), synthesized in the present work, was assessed toward the ROP of *ε*-CL (Table 3.2).[15] In these complexes both $[RE]-(BH_4)$[56-60] and $[RE]-(C_3H_5)$[20] are able to initiate the polymerisation of *ε*-CL and thus to yield PCL (Figure 3.6). The chain-end group analysis of the polycaprolactone isolated is not included in this section (see section 3.3.2)

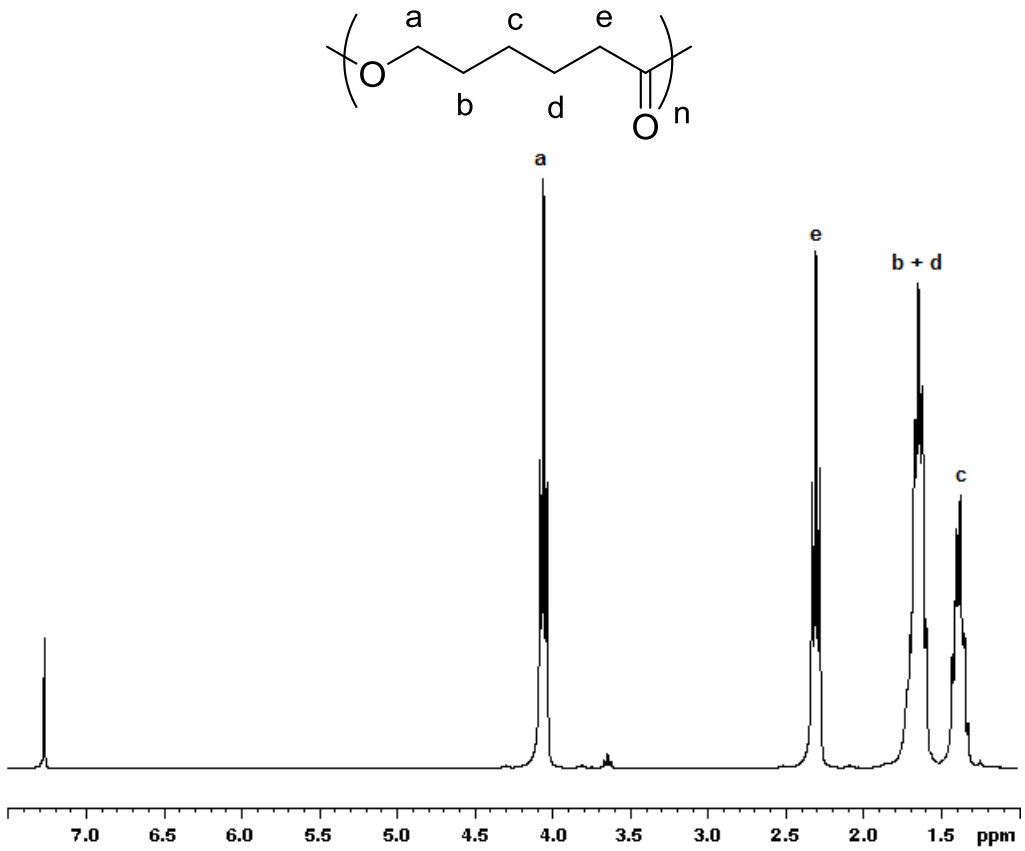

Figure 3.6 ^1H NMR ($CDCl_3$) of an isolated polycaprolactone (entry 9, Table 3.2). Chain-ends of the polycaprolactone are omitted.

Table 3.2 summarizes the results obtained. Upon addition of the monomer to the initiator in THF solution at RT, a very rapid increase of the viscosity was observed, affording 100 % conversion in all cases in less than 1 min (determined by ^1H NMR analysis), the polymer being recovered in a yield of at least 90 %. This corresponds to an activity up to 81 × 10^6 g of polymer (mol of Nd)$^{-1}$ h^{-1} with complex **1** (monomer to catalyst ratio 10000, entry 12), which is to our knowledge, the best ever reported activity for such a reaction using RE

complexes. For the sake of comparison, the activity reaches 3×10^6 g of polymer (mol of La)$^{-1}$ h^{-1} with tris(allyl)-La derivatives[20] and ca. 3×10^5 g of polymer (mol of Sm)$^{-1}$ h^{-1} with samarium tris(borohydrides).[57] A kind of synergy of ligands between allyl and borohydride can be advanced here to account for the outstanding catalytic of catalyst **5**.

Table 3.2 Polymerisation of ε-caprolactone in THF using $Sc(BH_4)_2(C_3H_5)(THF)_2$ **1**; $Y(BH_4)_2(C_3H_5)(THF)_3$ **2;** $La(BH_4)_2(C_3H_5)(THF)_3$ **3**; $Nd(BH_4)_2(C_3H_5)(THF)_3$ **4**; $Sm(BH_4)_2(C_3H_5)(THF)_3$ **5**.[a]

Entry [a]	Initiator	[ε-CL]:[RE]	Time (min)	Yield (%) [b]	$M_{n\,SEC}$ [c] (g/mol)	$Đ$ [c]
6	**1**	1000:1	1	99	25400	1.24
7	**2**	1000:1	0.9	99	30000	1.53
8	**3**	1000:1	0.35	97	32300	1.58
9	**4**	500:1	0.2	90	10600	1.53
10	**4**	1000:1	0.25	98	20000	1.59
11	**4**	5000:1	0.4	97	75000	1.56
12	**4**	10,000:1	0.8	95	120000	1.53
13	**5**	500:1	0.7	86	10900	1.50
14	**5**	1000:1	0.8	98	16000	1.58
15 [d]	**4**	1000:1	0.7	98	19800	1.60
16 [e]	**4**	1000:1	4.5	90	17000	1.44
17 [d]	**5**	1000:1	1.2	96	22000	1.50
18 [e]	**5**	1000:1	6.5	94	22800	1.47

[a] [ε-CL] / [RE] = 1000, n(RE) = 9×10^{-6} mol, T = 25 °C. [b] Determined by gravimmetry (all conversion found to be 100 % by ^{1}H NMR analysis). [c] Determined by SEC in THF at 40 °C against polystyrene standards with the correction $M_{n(exp)} = M_{n\,PS} \times 0.56$, [67] $Đ = M_w/M_n$. [d] $V_{THF} = 5\ V_{CL}$. [d] $V_{THF} = 15\ V_{CL}$.

All the other complexes **1**-**3** and **5** were also found to be extremely active toward the ε-CL. The lowest active initiator was found to be the Sc **1**, which was able to convert 1000 equiv. of the monomer in THF at RT in 1 minute (entry 6). The potency to polymerise ε-CL was observed in the following order: Nd (**4**) > La (**3**) > Sm (**5**) > Y (**2**) > Sc (**1**) which follows the decrease of ionic radii from the six-coordinated lanthanum center to the five-coordinated scandium center, except for Nd (**4**) which already scored high activities with ambiguous reasons.

All the isolated PCL displayed unimodal SEC traces (*e.g.* Figure 3.7). $M_{n\,SEC}$ of the obtained PCLs range from 10600 to 120000 g.mol^{-1} as the ratio [ε-CL]/[RE] increases from 500 to 10000 (entries 6-18), along with relatively narrow dispersities ($Đ$ = 1.24−1.60).

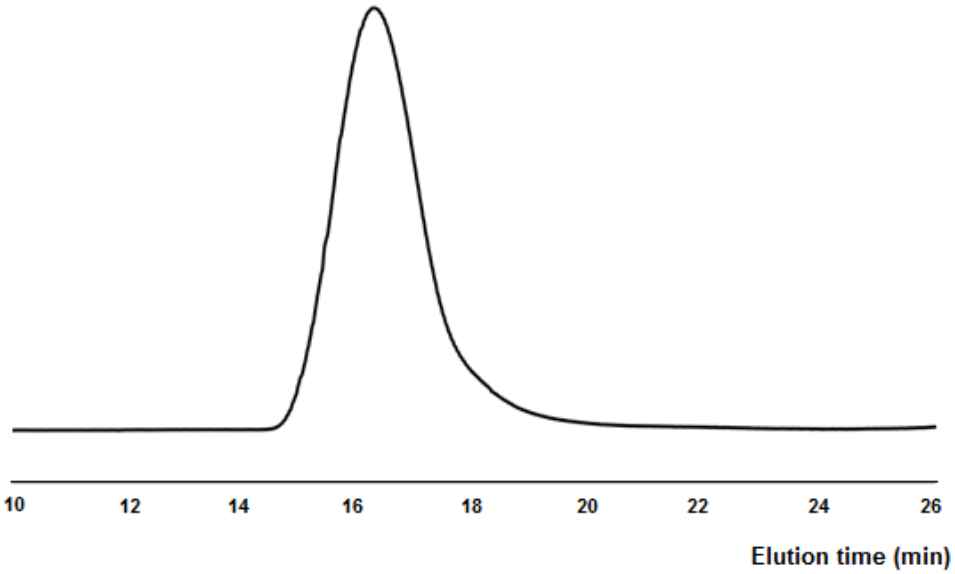

Figure 3.7 SEC trace of polycaprolactone obtained from entry 11, Table 3.2.

The $M_{n\ SEC}$ of the PCLs were limited to 16000 g.mol^{-1} for the experiments done with a monomer to catalyst ratio of 1000 (entry 14), which is clearly different from the theoretical value of 114000 g.mol^{-1} for one growing chain per metal ($M_{n\ th}$ = {[ε-CL]/[RE]} × 114.14 × 100%). Since considering two chains (initiation by the two BH_4) or three chains (initiation by the two BH_4 and the allyl) per metal should lead to theoretical values of 57000 and 38000 g.mol^{-1}, respectively, this limitation in terms of $M_{n\ SEC}$ values could be tentatively ascribed to the occurrence of uncontrolled transesterification reactions, in connection with the exceptional activity of these catalysts. Polymerisations under more diluted conditions (entries 15-18) afforded little improvement in terms of control of the process with slightly narrower dispersities.

3.2.2 Lactide

3.2.2.1 Introduction

Poly-*L*-lactide (PLA) is a very important biodegradable material as it is used as a commodity thermoplastic for the packaging industries and as a biomaterial for pharmaceutical and medical uses.[69] It is produced mainly through metal-mediated ROP of *L*-Lactide (LA, the cyclic dimer of lactic acid), a bioresourced monomer derived from fermentation of starch

(especially from corn) consisting of two stereoisomers S- and R- lactic acid.[70-75] (Scheme 3.10)

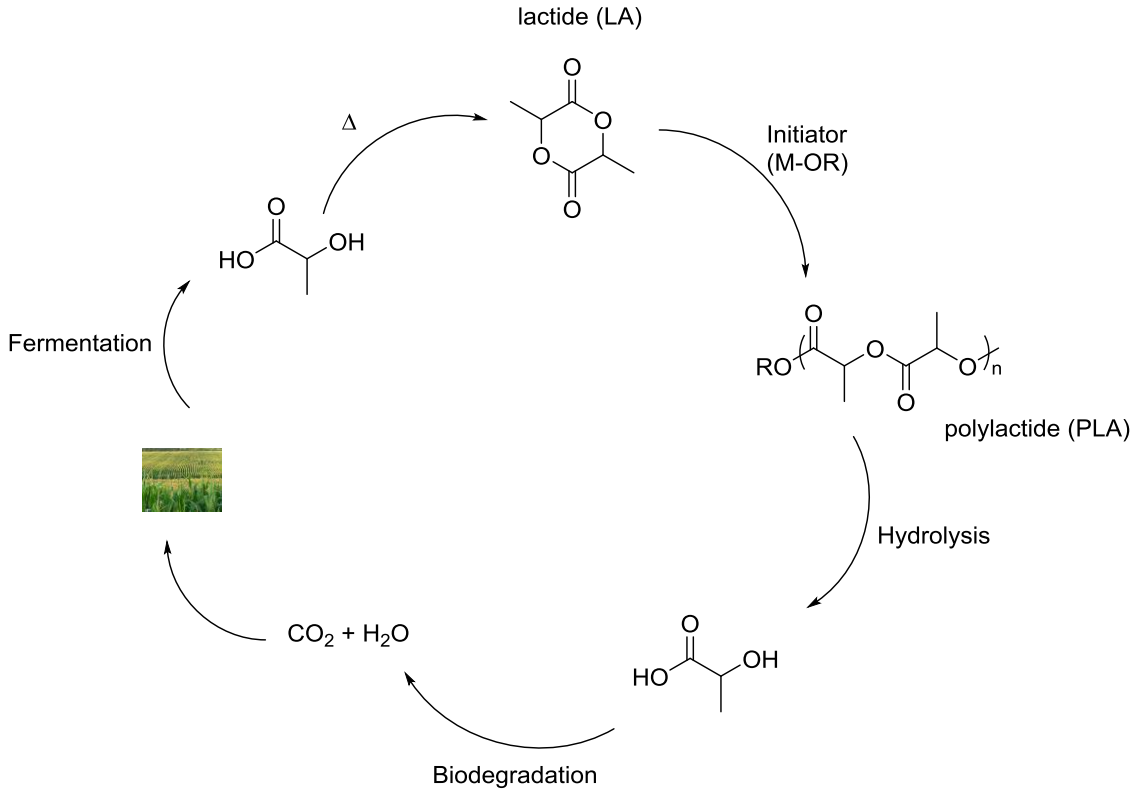

Scheme 3.10 The life cycle of polylactide.

Lactide has two chiral centers and therefore exists as three stereoisomers: *D*-Lactide (two *R*-lactic acids combined) and *L*-lactide (two *S*-lactic acids combined) and meso-lactide (*R*- and *S*-lactic acids combined) knowing that the racemic equimolar mixture of *D*- and *L*-lactide is called the *rac*-lactide (Figure 3.8).

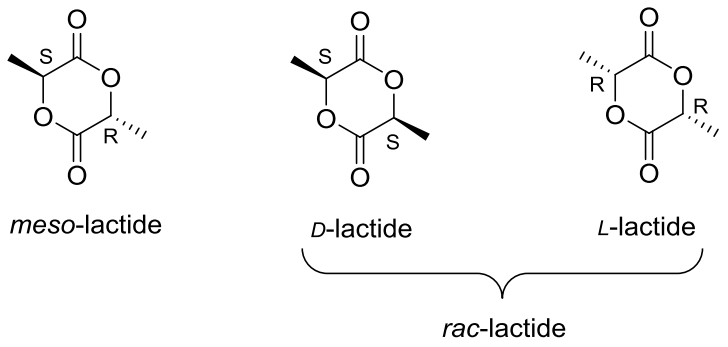

Figure 3.8 Stereoisomers of lactide.

In this section we describe the performances of the allyl-borohydride complexes $RE(BH_4)_2(C_3H_5)(THF)_x$ (RE = Sc, x = 2; Y, La, Nd, Sm, x = 3) as initiators for the ROP of *L*-LA in the presence and absence of benzyl alcohol (BnOH) as a chain transfer agent (Scheme 3.11).[15b] Chain-end analysis of the polylactides obtained is described in section 3.3.3.

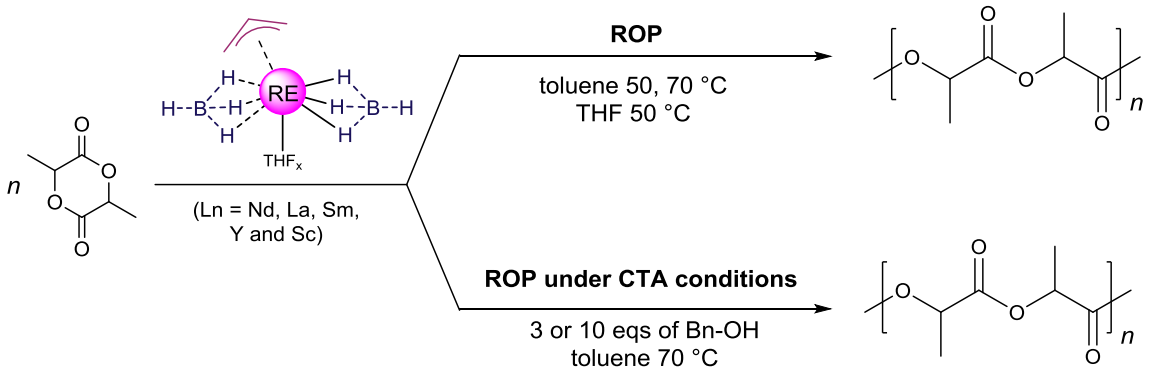

Scheme 3.11 ROP of *L*-lactide initiated by **1**- **5** (Chain-ends of the polylactide are omitted).

3.2.2.2 *L*-lactide polymerisation mediated by $RE(BH_4)_2(C_3H_5)(THF)_x$

The conversion of the *L*-LA monomers was calculated based on ^1H NMR spectroscopy in $CDCl_3$. For polylactide in $CDCl_3$, the quartet resonance due to the methine proton (coupled to the CH_3) undergoes a downfield shift as it is incorporated into the polymer chain. This shift from 5.05 ppm to approximately 5.15 ppm, which allows calculating the conversion by integrating the intensity of the methine protons correspond to *L*-LA and PLA respectively (Figure 3.9).

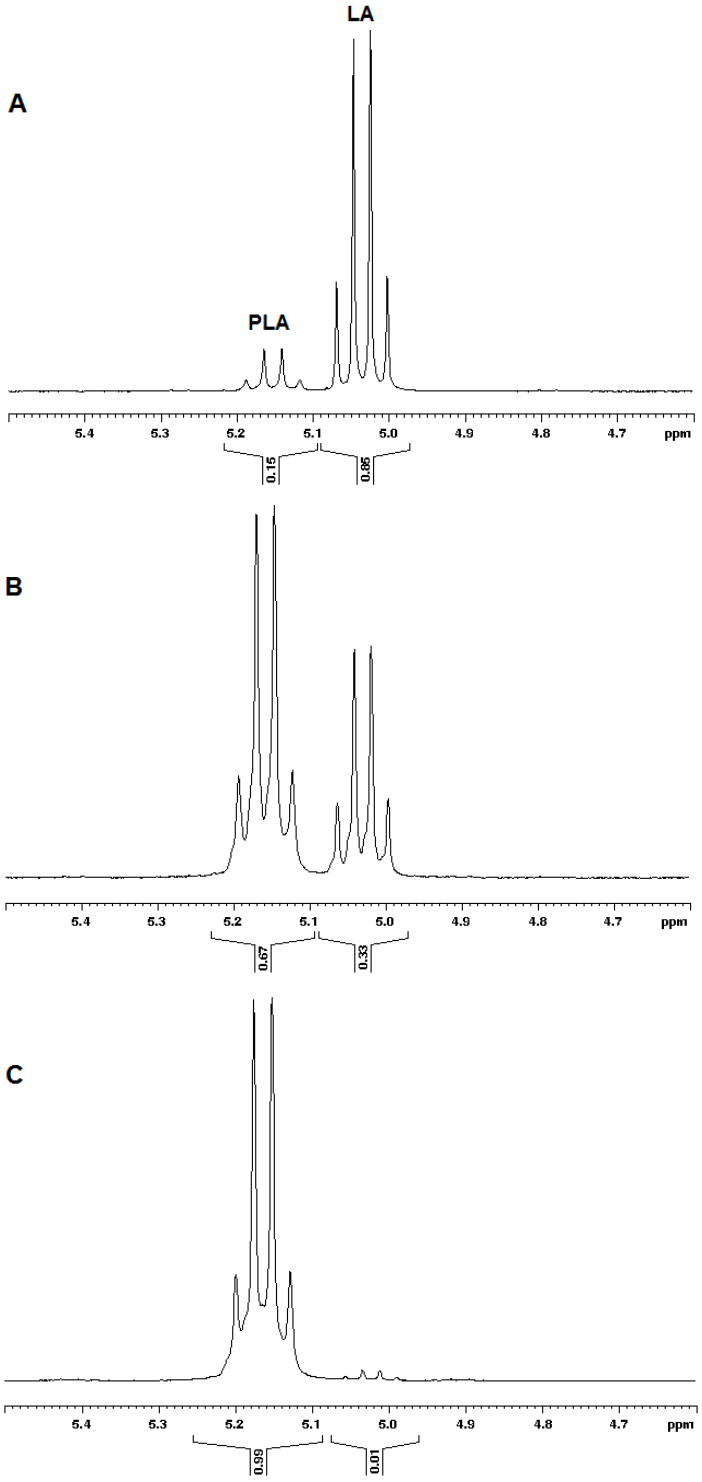

Figure 3.9 Extracts of ^{1}H NMR spectra ($CDCl_3$) for polylactide showing: A- low conversion (15%, entry 11, Table 3.3), B – moderate conversion (67%, entry 15, Table 3.3), C – high conversion (99%, entry 14, Table 3.3).

Table 3.3 Polymerisation of *L*-lactide (*L*-LA) using $Sc(BH_4)_2(C_3H_5)(THF)_2$ **1**; $Y(BH_4)_2(C_3H_5)(THF)_3$ **2**; $La(BH_4)_2(C_3H_5)(THF)_3$ **3**; $Nd(BH_4)_2(C_3H_5)(THF)_3$ **4**; $Sm(BH_4)_2(C_3H_5)(THF)_3$ **5**.

Entry [a]	Initiator	[*L*-LA]:[RE]:[BnOH]	Time (min)	Yield [c] (Conversion [b]) (%)	$M_{n\ SEC}$ [d] (g/mol)	$M_{n(th)}$ [e] (g/mol) (N chains) [f]	$Đ$ [d]
10	**1**	500:1:0	30	31 (40)	14400	28800 (2.0)	1.39
11 [h]	**1**	500:1:0	30	11 (15)	5400	10800 (2.0)	1.42
12	**2**	500:1:0	30	67 (79)	31500	56900 (1.8)	1.87
13	**3**	500:1:0	30	77 (85)	40000	61200 (1.5)	1.63
14	**4**	500:1:0	30	90 (99)	27500	71300 (2.6)	1.70
15 [g]	**4**	500:1:0	60	54 (67)	22000	48200 (2.2)	1.36
16	**5**	500:1:0	30	70 (80)	43000	57600 (1.3)	1.47
17	**1**	100:1:0	30	71 (82)	5600	11800 (2.1)	1.32
18	**2**	100:1:0	30	83 (97)	7300	14000 (1.9)	1.54
19	**4**	100:1:0	30	90 (99)	8600	14300 (1.7)	1.51
20	**4**	1000:1:0	45	93 (98)	49000	141100 (2.9)	1.51
21	**5**	1000:1:0	60	92 (99)	33000	142600 (4.3)	1.59
22	**1**	500:1:3	30	70 (83)	8800	59800 (6.8)	1.27
23	**2**	500:1:3	30	87 (99)	13600	71300 (5.2)	1.20
24	**3**	500:1:3	30	86 (99)	11700	71300 (6.1)	1.24
25	**4**	500:1:3	30	85 (96)	12400	69100 (5.6)	1.28
26	**5**	500:1:3	30	86 (99)	12400	71300 (5.7)	1.23
27	**1**	500:1:10	30	80 (91)	5400	65500 (12.1)	1.19
28	**2**	500:1:10	30	72 (99)	5800	71300 (12.3)	1.17
29	**3**	500:1:10	30	87 (99)	6200	71300 (11.5)	1.18
30	**4**	500:1:10	30	86 (98)	5500	70600 (12.8)	1.19
31	**5**	500:1:10	30	81 (99)	6400	71300 (11.1)	1.16

[a] Experimental conditions: n(RE) = 7 µmol, $[L\text{-LA}]_0$ = 2.0 M, toluene, T = 70°C. [b] Determined by ^{1}H NMR in $CDCl_3$. [c] Determined by gravimetry. [d] Determined by SEC in THF at 40 °C against polystyrene standards with the correction $M_{n\ SEC} = M_{n\ PS} \times 0.58$, [68] $Đ = M_w/M_n$. [e] $M_{n\ th} = \{[L\text{-LA}]/[RE]\} \times 144.13 \times$ conversion. [f] Number of growing chains per metal N = $M_{n\ th}/M_{n\ SEC}$. [g] Performed at 50°C. [h] Performed in THF at 50°C.

The catalytic activities of the allyl-borohydrido RE complexes **1-5** were assessed toward the ring-opening polymerisation of *L*-LA. Typically, the polymerisations were conducted in toluene at 70 °C with an initial monomer concentration of 2.0 M, along with some experiments done in toluene at 50 °C and THF at 50 °C (entries 10-21, Table 3.3). All five complexes display high performances, with up to 1000 equiv. of *L*-LA being fully

converted in 45 min in the case of the Nd catalyst **4**, which corresponds to an activity up to 27 x 10^3 kg (mol Nd)$^{-1}$.h^{-1} (entry 20).

When conducted in toluene, the reaction seemed to be more efficient at 70 °C rather than at 50 °C (entries 14,15) due to the poor solubility of *L*-LA in this solvent. Complex **4** showed high performance, with full conversion of 500 equiv. of *L*-LA monomer in less than 30 mins at 70 °C, whereas, at 50 °C the reaction rate was slower with approximately 67 % conversion in 60 mins only.

Moreover, the ROP of *L*-LA was conducted in THF (polar solvent) at 50 °C in the case of catalyst **1**, leading to much lower activity (11 % *vs.* 30 % conversion, entry 10 *vs.* entry 11). This may be attributed to the competition between the THF molecules and the monomer regarding the coordination to the RE oxophilic center, leading to a slower rate of ROP as compared to toluene. [76]

For various monomer to initiator ratios ranging from 100 to 1000, the neodymium complex **4** invariably displayed the best activities when compared to its congeners **1**-**3** and **5**. The catalytic performances were found to depend on the nature of the metal center and lined in the order Nd (**4**) > La (**3**) > Sm (**5**) > Y (**2**) > Sc (**1**) (99 %, 85 %, 80 %, 79 % and 40 % of conversion of 500 equiv. of *L*-LA after 30 mins, entries 14, 13, 16, 12, 10, respectively). This trend is in good agreement with the decrease of the ionic radii from La^{3+} to Sc^{3+},[77] except for Nd, as observed for *ε*-CL polymerisation (see the previous section).

The molar masses of the isolated PLAs synthesized under these experimental conditions were found in close agreement with the growth of two PLA chains per metal center at monomer to metal ratios of 100 or 500 (entries 10-19). Such a result can be supported by the hypothesis that the PLA chains are initiated by the two RE—(BH_4) moieties in the complexes rather than the RE—allyl group. In addition, the dispersities (*Đ)* were found to be relatively narrow and in the range 1.32-1.87, in accordance with a fairly controlled process. Decreasing the temperature was beneficial to the dispersity, but to the detriment of the activity (entry 15).

However, at higher monomer loading of 1000, the number of polymer chains increases to three or more (entries 20 and 21) and a significant deviation was observed of the experimental molar masses and the expected ones (Figure 3.10). Thus, the ring-opening process appears here to be less controlled, with the possible occurrence of common side reactions (transesterifications) as already observed with a borohydrido-RE complex for the polymerisation of ε-CL.[65] The initiation of a PLA chain by the potentially active RE—allyl moiety may no longer be excluded under such conditions of high monomer loadings.

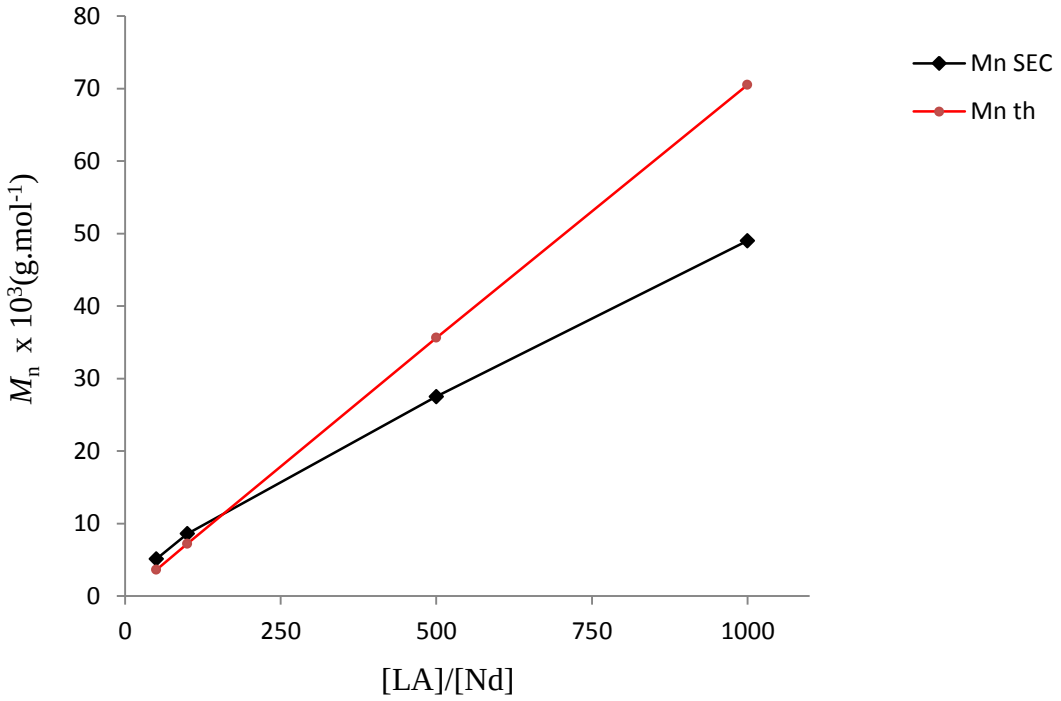

Figure 3.10 Plot of the experimental (SEC) and theoretical molar masses (based on two growing chains of PLA per Nd metal) versus [*L*-LA]/[Nd].

Polymerisation of *L*-lactide under Chain Transfer conditions

The polymerisation of LA was then assessed with complexes **1-5** in the presence of benzyl alcohol (BnOH, 3 or 10 equiv., entries 22-31) as a CTA. Under such conditions, an increase of the activities was observed with all five catalysts, affording quasi quantitative monomer conversion in 30 min, along with narrower dispersities (1.20-1.28 for 3 equiv. BnOH, entries 22-26; 1.16-1.19 for 10 equiv. BnOH, entries 27-31; *vs* 1.39-1.87 without CTA). Notably, the Sc initiator **1** displayed high activity and converted up to 91 % of monomer in 30 mins upon

adding 10 equiv. of BnOH (entry 27), the conversion being only of 40% in the absence of alcohol (entry 10).

Moreover, $M_{n\ SEC}$ values decreased as expected for a ROP process involving reversible chain transfer, with a number of growing chains per metal (calculated with $M_{n(th)}/M_{n\ SEC}$) that was found close to five-six (for 3 equiv. BnOH) and to twelve-thirteen (for 10 equiv. BnOH). For instance, the theoretical mass of 500 equiv. of *L*-LA divided by five (the number of growing chains when 3 equiv. of alcohol added) is equal to 14300 $g.mol^{-1}$ which is quite in accordance with the observed molar masses (13600 $g.mol^{-1}$, entry 23). Moreover, when added 10 equiv. of alcohol the calculated mass is 5900 $g.mol^{-1}$ and in agreement with the experimental mass of 5800 $g.mol^{-1}$ (entry 28).

3.3 Chain-end group Analysis

3.3.1 Introduction

Many papers have described the ROP of lactones and lactide. The major part of these articles reports on the synthesis and standard characterization techniques of the homopolymers obtained. In the specific case where the initiator is a rare-earth borohydride, the polymerisation mechanism of ε-CL and resulting end-groups of PCLs have been clearly established by the work of Guillaume and coworkers as a coordination-insertion process followed by an ultimate reduction step leading to di-hydroxy telechelic polyesters. It is not the same regarding PLAs prepared with the same kind of initiators, which lack in most cases of complete and clear analysis of the chain-end groups, and where some authors initially claimed that the same ROP mechanism as ε-CL was taking place. [20,56,59,60,78-82] According to others, it was stated that: "the nature of the terminus groups in PLAs produced with borohydride complex could not be unambiguously identified".[79]

The determination of the polymer chain-ends is very critical and helps to understand the chemical and physical properties of the polymer obtained and to determine the mechanism of the polymerisation. The most useful tools to determine the structure of the former are NMR spectroscopy and MALDI-ToF mass spectrometry.

NMR spectroscopy can yield significant information about both the polymerisation reaction and the subsequent polymer produced. ^{1}H NMR is commonly used to study the proton environment of the chain-ends. Protons within the end group of a polymer chain have different chemical shifts with respect to those within the repeat units.

MALDI-ToF is one of the most important tools to analyze polymers[83] and biomolecules such as proteins.[84] MALDI-ToF is a soft ionization technique uses a pulsed laser beam to cause adsorption of a matrix from a sample plate that includes ions of the analyte which generates charged ions of various sizes with minimal fragmentation. The choice of the ionizing salt is an important parameter and partially depends on the type of polymer to measure. Generally, alkali metal salts are being used.

This analysis technic can give insight into the composition, the nature of the chain-end groups and the molecular weight of the polymers, but also giving insights on the occurrence or not of intra- or intermolecular transesterification reactions. Intramolecular transesterification, known as back-biting leads to the formation of macrocyclic polylactide and is observed on Maldi spectra by the presence of macrocycles (complete absence of chain-end), whereas intermolecular transesterification consists in transesterification reaction between two different macromolecules and can be advanced in the case of lactide monomer when distributions containing both even-membered and odd-membered oligomers, with peaks separated by 72 Da, corresponding to half a lactide monomer, also called lactyl, are observed (Scheme 3.12).

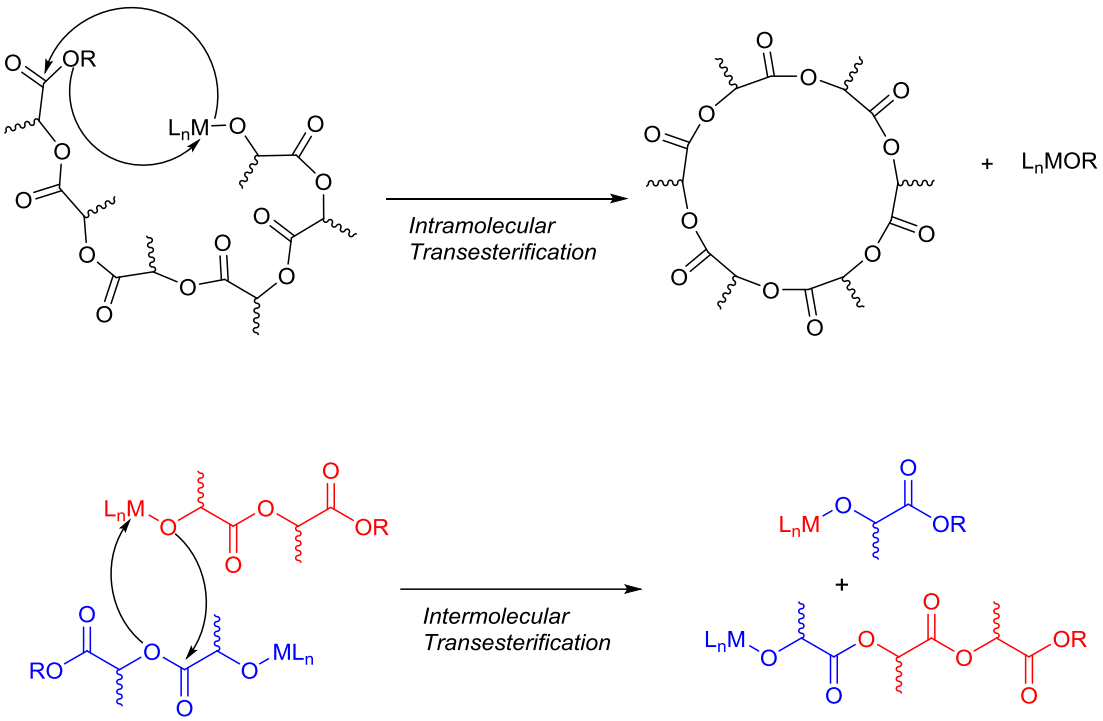

Scheme 3.12 Intramolecular and intermolecular transesterification of PLA, causing macrocyclic rings and chain redistribution.

In the mass spectrum, the difference between consecutive isotope distributions (peaks) is in fact the mass of the repeating unit. While, peak-to-peak distance can directly be used to identify a certain polymeric species, the difference between the experimental (m_{exp}) and calculated masses (m_{cal}) of a proposed polymer structure gives information about the formation of this structure and the end groups (eq. 1 and 2).

$$m_{exp} - m_{cal} \leq 1 \qquad eq.1$$

$$m_{cal} = nM_w + E_I + E_{II} + M^+ \qquad eq.2$$

E_I and E_{II} represent the molar masses of the end groups at opposite sides of the chain, *nMw* represent the number and molar mass of the monomer used, and M^+ the molar mass of the cation.

3.3.2 ε-Caprolactone Polymerisation

3.3.2.1 Initiation by rare-earth (tris)borohydride complexes

Guillaume and coworker[56] proved that when the ROP of ε-CL is initiated by the neodymium borohydride complex, $Nd(BH_4)_3(THF)_3$, the polycaprolactone produced displays a α,ω-dihydroxy telechelic structure (HO-PCL-OH, Scheme 3.13). They supported their study by NMR spectroscopy and MALDI-ToF (the mechanism of initiation is reported in Scheme 3.9).

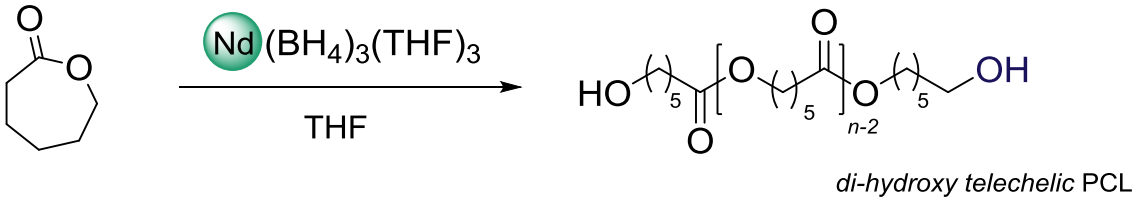

Scheme 3.13 α,ω-dihydroxy telechelic polycaprolactone initiated by $Nd(BH_4)_3(THF)_3$.

3.3.2.2 Initiation by rare-earth allyl complexes

On the other hand, Bochmann *et al.*[20] studied the polymerisation of ε-CL using $[RE(C_3H_5)_3(diox)]_n$ (RE = Y, Nd, Sm, n = ∞; La, n = 1.5). As expected, the end-group analysis by NMR spectroscopy showed that the polymer contained $–CH_2CH=CH_2$ chain-ends, which proves that polymerisation process was initiated by allyl transfer to monomer (Scheme 3.14).

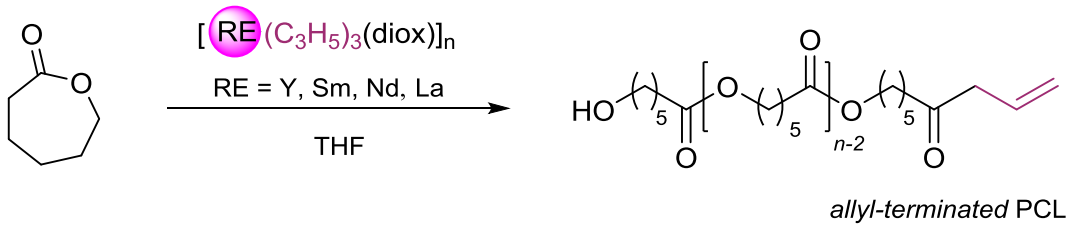

Scheme 3.14 Allyl-terminated polycaprolactone initiated by $[RE(C_3H_5)_3(diox)]_n$ (RE = Y, Nd, Sm, n = ∞; La, n = 1.5).

3.3.2.3 Initiation by allyl-borohydride rare-earth complexes

As previously described in chapter 3, $RE(BH_4)_2(C_3H_5)(THF)_x$ (RE = Sc , x = 2; Y, La, Nd, Sm, x = 3) are extremely active toward the polymerisation of *ε*-CL. Noteworthy, these mixed allyl-borohydride catalysts bear two active ligands; borohydride and allyl, which both have the ability to start the polymerisation of *ε*-CL. The nature of the initiating group could be determined by deep analysis of the chain ends of the polymers formed. In case of the BH_4 initiating the polymerisation, dihydroxy terminals should be formed according to Guillaume's previous work (Scheme 3.13),[56] whereas when the allyl group is the initiating group, one of the terminals should display an allyl moiety (Scheme 3.14).

In order to determine the chain-end structure of the PCLs produced using complexes **1**-**5**, ^1H and ^{13}C NMR of the isolated polymers of small molar masses were recorded in $CDCl_3$. The analyzed polymers are stated in Table 3.4. Keeping in mind that the PCLs produced using catalysts **1**-**5** all display the same structure.

Table 3.4 Polymerisation of *ε*-caprolactone in THF using $Nd(BH_4)_2(C_3H_5)(THF)_3$ **4**, $Mg(allyl)_2(THF)_{1.5}$

Entry [a]	Initiator	$M_{n\ SEC}$ [b] (g/mol)	$Đ$ [b]
32	$Nd(BH_4)_2(C_3H_5)(THF)_3$	5400	1.17
33	$Mg(allyl)_2(THF)_{1.5}$	15200	2.53

[a] [*ε*-CL] / [M] = 100, solvent THF, $V_{THF} = V_{CL}$, T = 25 °C. [b] Determined by SEC in THF at 40 °C against polystyrene standards with the correction $M_{n\ SEC} = M_{n\ PS} \times 0.56$, [67] $Đ = M_w/M_n$.

^1H and ^{13}C NMR spectra of the isolated polymers showed α,ω-dihydroxy telechelic HO—PCL—OH structure. Accordingly, it can be proposed that the ROP process was initiated through the RE—(BH_4) bond rather than by insertion into the allyl group. Confirmation was given by a polymerisation conducted with $Mg(C_3H_5)_2(THF)_{1.5}$ (entry 33), which clearly displayed an allylic group at the chain end at δ = 5.85 and 5.15-5.07 ppm for ^1H NMR (Figure 3.11) and δ = 133.78 and 118.65 ppm for ^{13}C NMR (Figure 3.12) that were totally absent in the PCL prepared with $Nd(BH_4)_2(C_3H_5)(THF)_3$, at low monomer to initiator ratio (entry 32). C*H*$_2$OH resonances was clearly identified at δ = 3.57 ppm and δ = 62.67 ppm in the ^1H NMR and ^{13}C NMR respectively for the polymer initiated by catalyst **4**, this

suggested that both ends groups of the polymer chain are alike and of hydroxy type. This result is in line with the study carried out by Okuda *et al.*[85] with the mixed alkyl-borohydride $[Y(BH_4)(Me)(THF)_5][BPh_4]$, who concluded that ring opening of ε-CL was favored with the borohydride rather than with the methyl moiety. However, initiation through Nd—allyl at high monomer to initiator ratios cannot be excluded, when taking into account the number of growing chains calculated under such conditions.

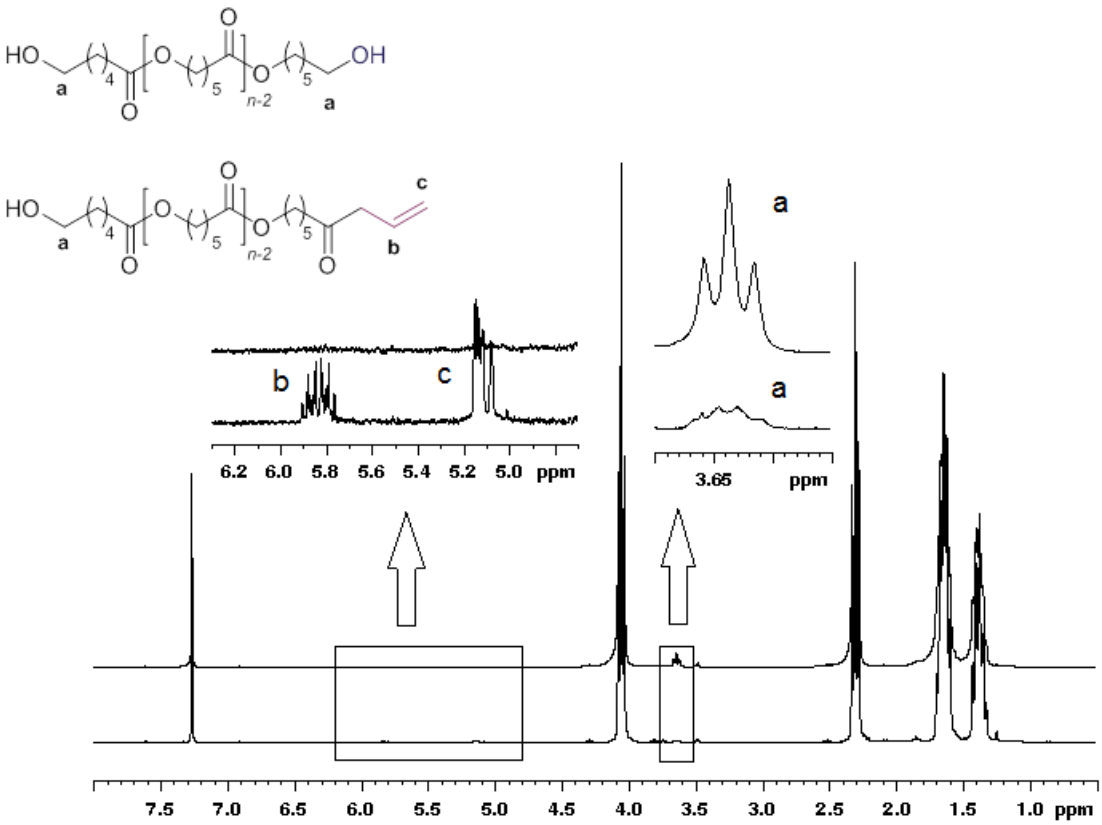

Figure 3.11 ^{1}H NMR spectra of isolated polycaprolactone in $CDCl_3$ initiated with $Nd(BH_4)_2(C_3H_5)(THF)_3$ **4** (top, entry 32) and with $Mg(C_3H_5)_2(THF)_{1.5}$ (bottom, entry 33).

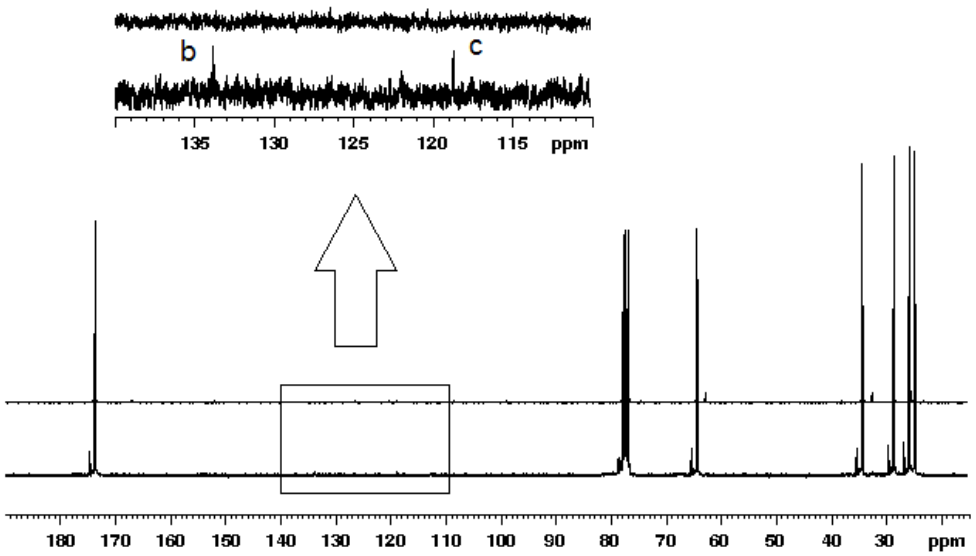

Figure 3.12 ^{13}C {^{1}H} NMR spectra of isolated polycaprolactone in $CDCl_3$ initiated with $Nd(BH_4)_2(C_3H_5)(THF)_3$ **4** (top, entry 32) and with $Mg(C_3H_5)_2(THF)_{1.5}$ (bottom, entry 33).

3.3.3 *L*-lactide Polymerisation

3.3.3.1 Initiation by Rare borohydride compelxes

As mentioned above, the ROP of ε-CL, using RE borohydride compounds can lead to the formation of α,ω-dihydroxy polyesters. However the use of such compounds for the polymerisation of other cyclic esters does not necessarily afford similar di-functional polymers. For example, Guillaume *et al.* showed that the polymerisation of trimethylene carbonate (TMC) conducted by $Sm(BH_4)_3(THF)_3$ yielded poly(TMC) that contains both —CH_2OH and —CHO terminal groups.[86] In the case of lactide, Nakayama and coworkers proposed that *rac*- or *L*-LA polymerises to give α,ω-dihydroxy telechelic polylactide via the neodymium borohydride initiator, $Nd(BH_4)_3(THF)_3$, but no NMR data are available to support this result[59,60] Whereas, Carpentier and Trifonov discussed that a mixture of —$CH(Me)CH_2OH$ and —CH(Me)CHO terminals was produced with RE borohydride complexes with bulky guanidinate ligands.[78,79] Furthermore, Mountford *et al.* proved by means of MALDI-TOF analysis (exclusively, not corroborated by NMR) that, —$CH(Me)CH_2OH$ or —CH(Me)CHO end groups in addition to cyclic polylactides could be formed, depending on the bis(phenolate) RE borohydride catalyst they used.[80]

In a general manner, polymerising the lactide monomer by a borohydride catalyst can lead to three main structures: α,ω-dihydroxy telechelic (H—PLA—CH(Me)CH_2OH, A, named as "HO—PLA—OH" to better show the two hydroxy), α-hydroxy ω-aldehyde termination (H—PLA—H, B) or cyclic (C). The latter can be opened by MeOH or H_2O upon precipitation (in case the solvent used for precipitation is methanol) to yield two more chain-end types, H—PLA—OMe (D) or H—PLA—OH (E), respectively (Scheme 3.15). The value of the molecular peak will vary from 72xn (C) to 72xn+32(D).

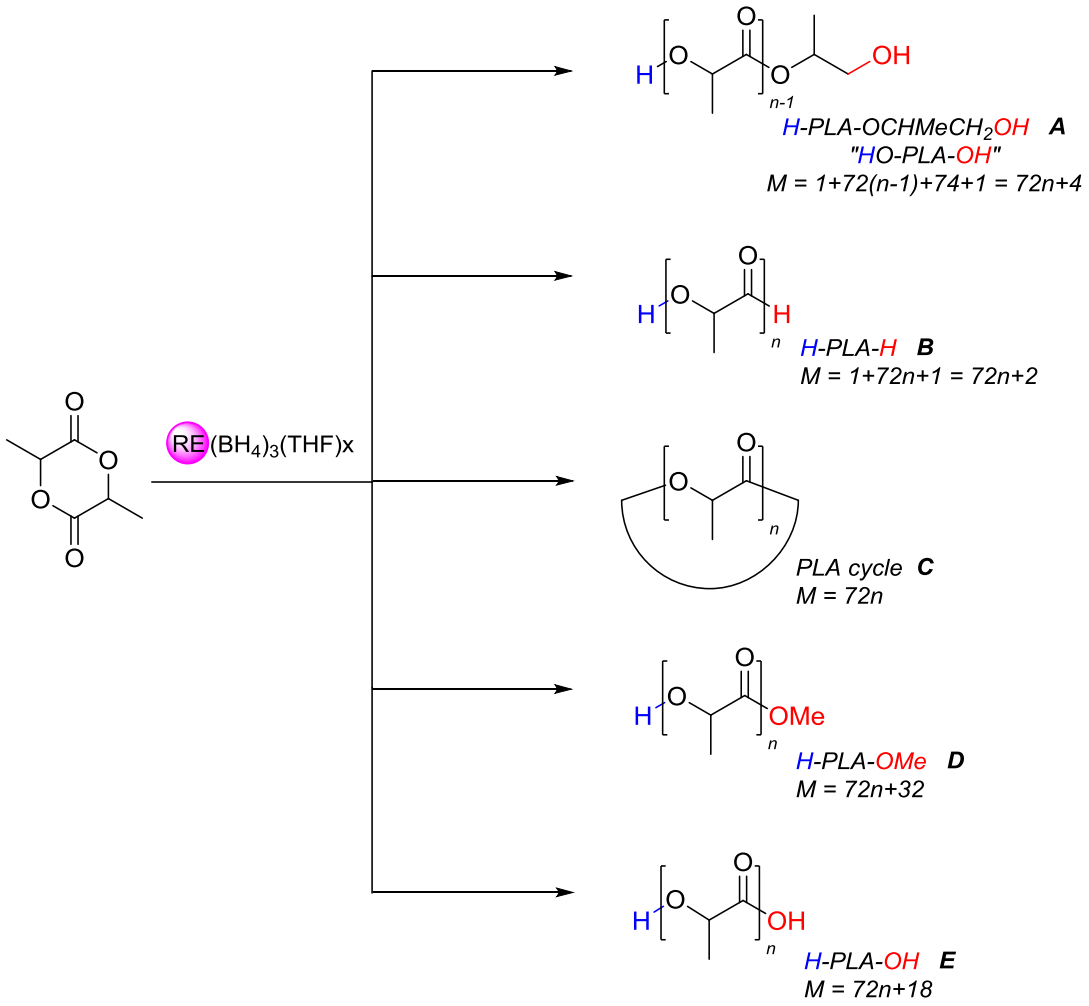

Scheme 3.15 Possible structures of polylactide when synthesized by borohydride rare-earth catalysts.

To identify the exact nature of the chain-ends of PLAs, the authors[59,60,79,80] used MALDI-ToF. Although, they also recorded the ^{1}H NMR spectra of the corresponding PLAs

produced, no clear interpretation or even NMR figures with clear assignment or good resolution were found in the literature records,[78,81,82] as can be seen in Figure 3.13.

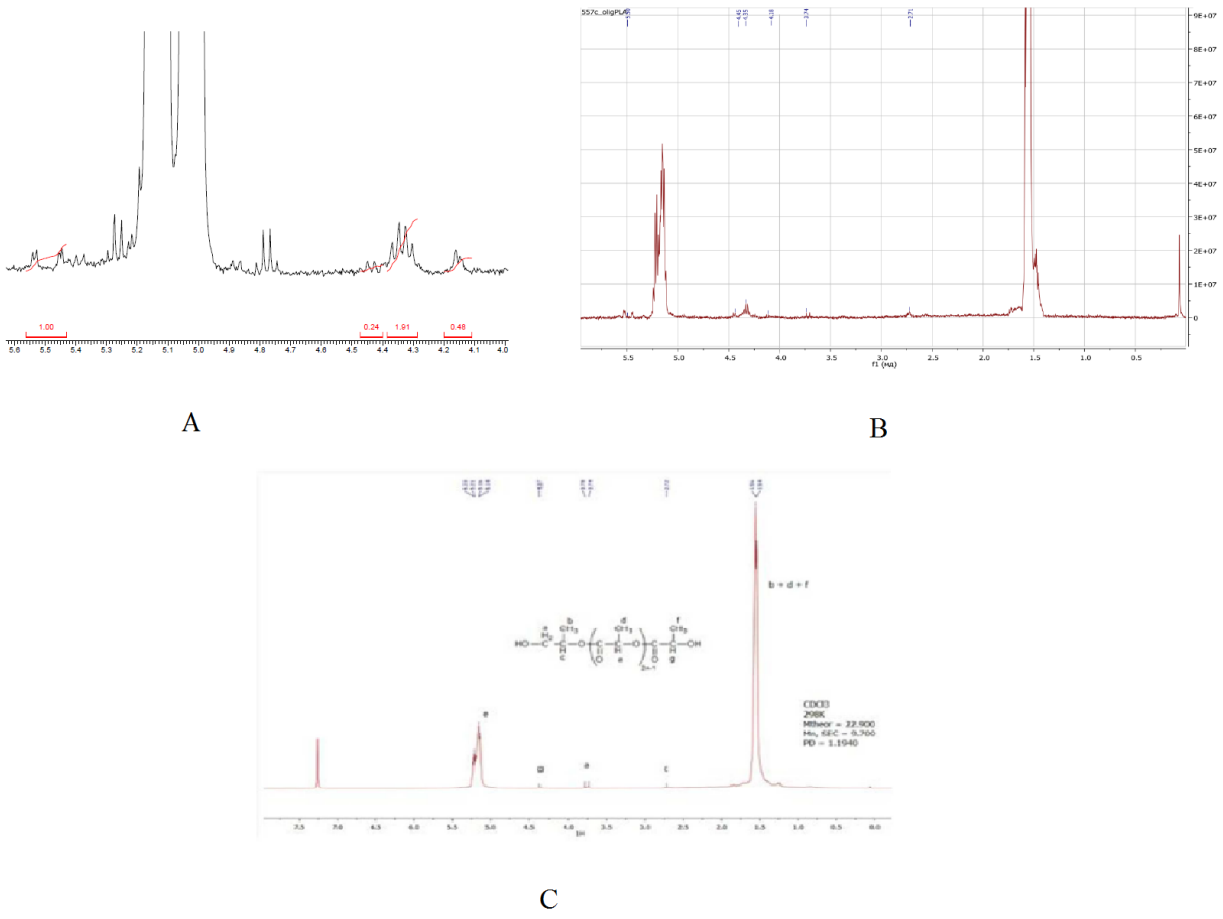

Figure 3.13 ^{1}H NMR spectra (A,[78] B,[82] C[81]) of low molecular weight polylactides in $CDCl_3$ reported in the literature.

3.3.3.2 Initiation by rare-earth allyl complexes

Rare-earth allyl complexes have been used as initiators for the ROP of lactide. Deng *et al.*[87] reported the synthesis of high molecular weight poly(*L*-lactide) by using $(\eta^3\text{-}C_3H_5)_2Sm(\mu^2\text{-}Cl)_2(\mu^3\text{-}Cl)_2Mg(tmed)(\mu^2\text{-}Cl)Mg(tmed)$. Bochmann *et al.*,[20] moreover, showed that $[RE(C_3H_5)_3(diox)]_n$ (RE = Y, Nd, Sm, n = ∞; La, n = 1.5) are effective initiators for the polymerisation of *rac*-LA. In both cases, the initiation was postulated to occur via the allyl group.

In contrast to ROP process by borohydride initiators, after migration of the metal-bound initiating group "allyl" to the carbonyl bond of the lactide, ring-opening occurs which results in polymer with allyl termination of the type H—PLA—allyl (Scheme 3.16).

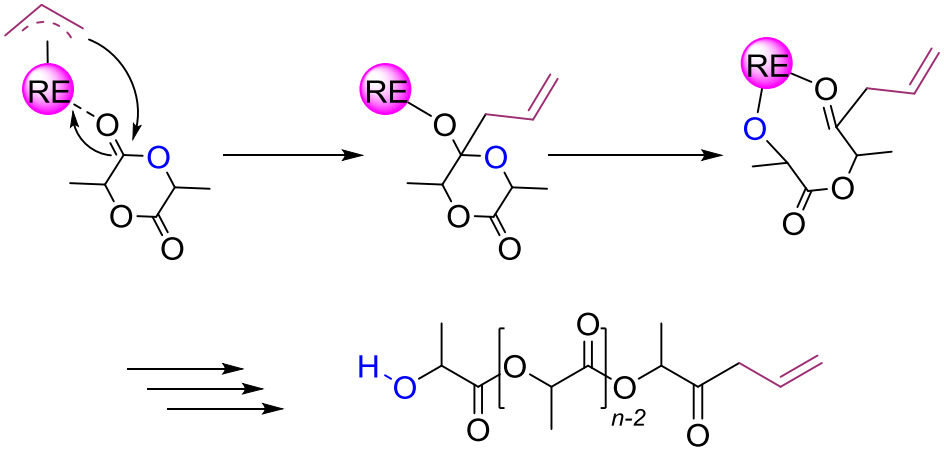

Scheme 3.16 Ring-opening polymerisation of lactide initiated by allyl-RE complex.

3.3.3.3 Initiation by allyl-borohydride rare-earth complexes

To determine the nature of the chain ends of the PLAs synthesized using our RE allyl-borohydride catalysts **1-5** (section 3.2.1), we analyzed low molecular weight polylactides formed using these latter catalysts, with monomer to catalyst ratio: 100:1, in toluene at 70 °C (Table 3.5). The techniques used to analyze the polymers were ^{1}H-NMR spectroscopy and MALDI-ToF.

As described in the previous section, such complexes bear two different possible initiating groups, BH_4 and allyl, in which being able to initiate the polymerisation of *L*-LA. In order to focus on the initiation process, a polymerisation was initiated with magnesium bis(allyl) (entry 39, Table 3.5), revealing by ^{1}H NMR a typical allylic signals of an allyl terminated PLA at 5.79 ppm. In turn, this signal was totally absent in the ^{1}H NMR spectra of all the PLA samples synthesized with Sc (**1**) , Y (**2**), La (**3**), Nd (**4**) and Sm (**5**) (entries 34-38 respectively) (Figure 3.14). This supports a preferential initiation through the RE—(BH_4) bond rather than through the RE—carbon bond of the allyl group, as established in the case of the ROP of ε-CL mediated by the same mixed allyl-borohydride complexes.

Table 3.5 Low molecular weight polylactides prepared using complexes **1-5** and $Mg(C_3H_5)_2(diox)_{0.06}$ and $Nd(BH_4)_3(THF)_3$.

Entry [a]	Initiator	$M_{n\ SEC}$ [b] (g/mol)	$Đ$ [b]
34	**1** (Sc)	5600	1.32
35	**2** (Y)	7300	1.54
36	**3** (La)	11000	1.32
37	**4** (Nd)	8100	1.37
38	**5** (Sm)	9100	1.39
39	$Mg(C_3H_5)_2(diox)_{0.06}$	8100	1.97
40	$Nd(BH_4)_3(THF)_3$	10400	1.65

[a] [*L*-LA] / [M] = 100, [*L*-LA] = 2 M, solvent toluene, T = 70 °C for 30 mins. [b] Determined by SEC in THF at 40 °C against polystyrene standards with the correction $M_{n\ SEC} = M_{n\ PS} \times 0.58$,[68] $Đ = M_w/M_n$.

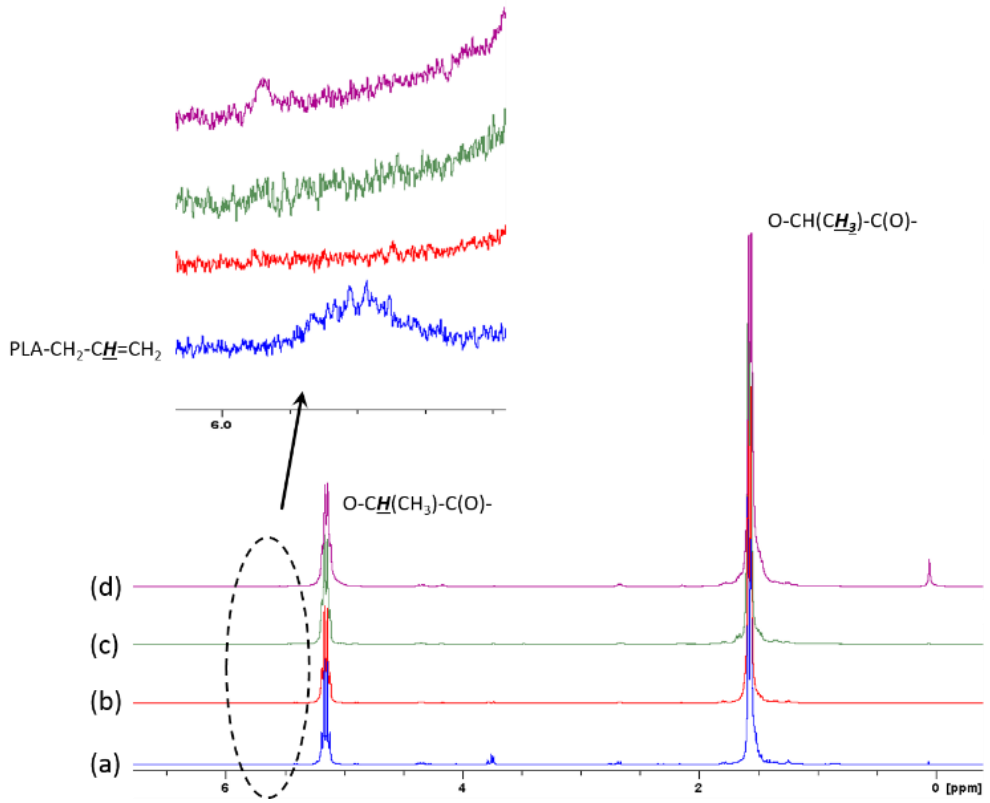

Figure 3.14 ^1H NMR spectra in $CDCl_3$ of isolated polyactides synthesized with $Mg(C_3H_5)_2(diox)_{0.06}$ ((a), entry 39), $Nd(BH_4)_2(C_3H_5)(THF)_3$ (**4**) ((b), entry 37), $Y(BH_4)_2(C_3H_5)(THF)_3$ (**2**) ((c), entry 35) and $Sc(BH_4)_2(C_3H_5)(THF)_2$ (**1**) ((d), entry 34).

Furthermore, careful examination of the ^{1}H NMR spectra of the isolated PLAs of entries 34-38 in the region between 4.35 and 2.66 ppm, shows first the signals at 4.35 at 2.66 ppm, which are known and correspond to H_b and H_a respectively (Figure 3.15). Moreover, there exist two recurrent signals at 4.17 and 3.73 ppm which appear for PLAs initiated by RE borohydride complexes. It is noteworthy that these signals, though not interpretated, were also present in the ^{1}H NMR spectra of PLAs initiated with other RE initators bearing a BH_4 ligand (ref 82 for example). However, no clear, logical and direct assignment of these signals, are present in the literature records, as shown in Figure 3.13. This was confirmed by comparison with the ^{1}H NMR spectra of a PLAs synthesized with $Nd(BH_4)_3(THF)_3$ as the initiator (entry 40), where the same signals appeared to exist.

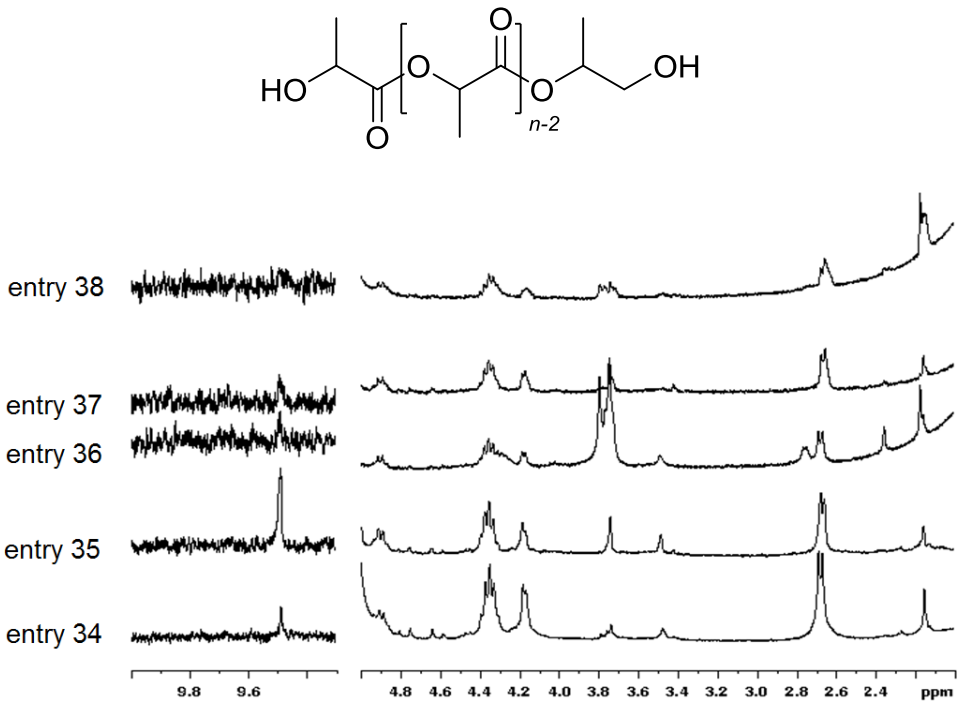

Figure 3.15 ^{1}H NMR spectra of polylactides synthesized with complexes **1-5** (entries 34-38) in $CDCl_3$. The aldehyde signal is shown at 9.49 ppm (left).

Further analysis done by 2D NMR spectroscopy where then conducted to correlate the unknown signals of the ^{1}H NMR spectra related to such kind of polymers. The postulated assignment of proton signals ($H_{a–g}$) of a PLA obtained using $Nd(BH_4)_3(THF)_3$ (entry 40) can be derived from ^{1}H/^{1}H-COSY NMR spectrum (Figure 3.16). For assignment of proton signals of type H_a and H_b, H_b and H_c the respective correlation between the signals at 2.66 and 4.35 ppm, 4.35 and 1.48 ppm is clear. In comparison, the correlation between the signals at 1.26

ppm and 5.17 ppm can be related to H_g and H_f (overlapped with the signal corresponding to H_d of the main chain polymer) respectively.

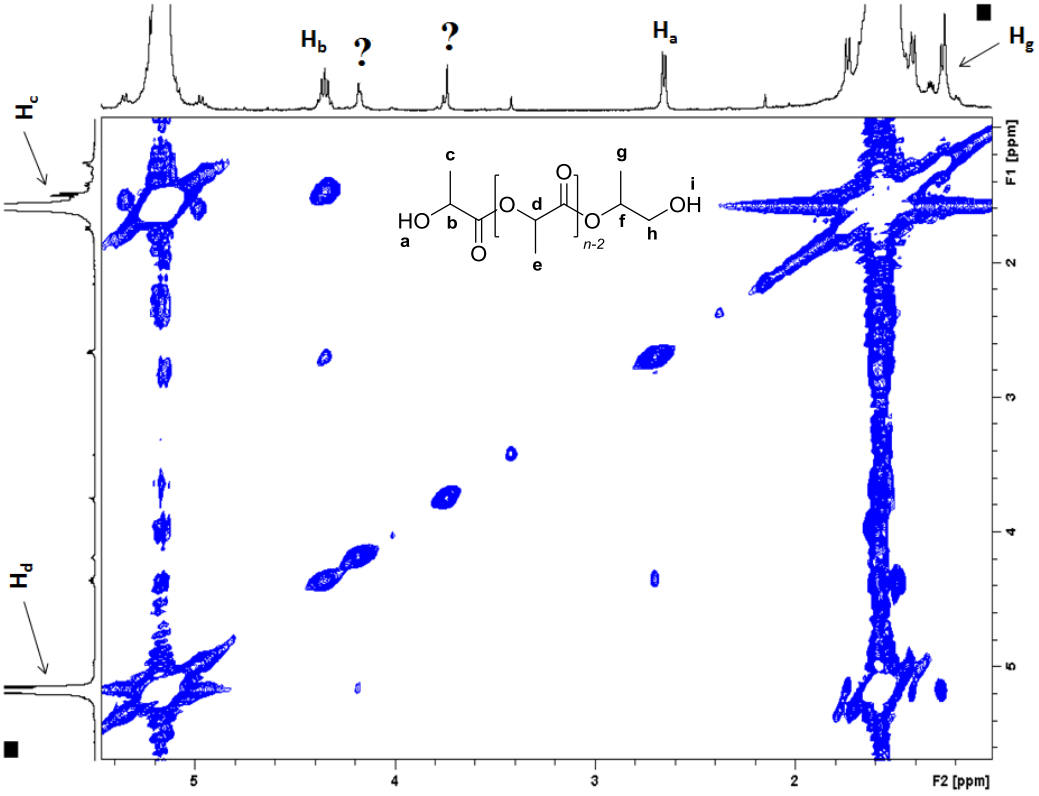

Figure 3.16 $^1H/^1H$-COSY NMR spectrum of the polymer obtained by $Nd(BH_4)_3(THF)_3$ (entry 40).

The polylactides obtained from entries 34-38, were also analyzed by MALDI-ToF MS in the linear mode (see experimental section) and the results are reported in Table 3.6. All the MALDI spectra show peak separation equal to 72 (72.06 as accurate value), which is half of the *L*-LA monomer (*i.e.* -OCH(Me)C(O)-), which is in consistence with the occurrence of transesterification reaction. In addition, no cyclic polylactide could be detected in any of the spectra, indicating that the transesterification observed it thus mainly intermolecular and not intramolecular. Using catalyst **2** (entry 35) each mass number peak was in good agreement with the calculated one assuming the α,ω-dihydroxy-terminated polymers, $H(OCH(Me)CO)_{n-1}OCH(Me)CH_2OH$ ("HO—PLA—OH"). For instance, *m/z* (observed) = 2981.105 versus *m/z* (calculated) = 2981.48 for M(*n* = 41, 41x72.06+4.03) + Na^+(22.99) (Figure 3.17). Interestingly, no aldehyde terminated group appeared to be present in that polymer, while in case of Sc (**1**) (entry 34, Appendix VI), the polymer obtained seemed to be mixed of dihydroxy and aldehyde terminations, "HO—PLA—OH" and H—PLA—H respectively. However for the PLAs initiated using complexes **3-5** (entries 36-38), only the aldehyde termination appeared and no α,ω-dihydroxy-terminated polymers could be detected.

For instance, in case of Nd (**4**), *m*/*z* (observed) = 2835.964 versus *m*/*z* (calculated) = 2835.33 for M(*n* = 39, 39x72.06+2) + Na^+(22.99) for H—PLA—H (Figure 3.18, Appendices VII and VIII for **3** and **5** complexes). In most cases (entries 35, 37, 38, 40) a minor population of polylactide with the structures H—PLA—OMe and H—PLA—OH could be detected, and could be related to the opening of a small fraction of cyclic PLA by methanol or water. Noteworthy, the presence of aldehyde signal of H—PLA—H by ^{1}H NMR was clearly detected at 9.49 ppm, for all the polylactides except the one synthesized with Sm metal (**5**) (entry 38) where no clear signal on the spectrum could be seen.

Table 3.6 Chain-end analysis of the polylactides synthesized with complexes **1**-**5** and $Mg(C_3H_5)_2(diox)_{0.06}$ and $Nd(BH_4)_3(THF)_3$.

Entry [a]	Initiator	Chain-ends obtained by MALDI-ToF [c]	Aldehyde signal δ (ppm) [d]
34	**1** (Sc)	Major: *H*-PLA-*H* *Or "HO*-PLA-*OH"* [e]	9.49
35	**2** (Y)	Major: *"HO*-PLA-*OH"* Minor: *H*-PLA-*OMe*	9.49
36	**3** (La)	Major : *H*-PLA-*H*	9.49
37	**4** (Nd)	Major : *H*-PLA-*H* Minor : *H*-PLA-*OMe*	9.49
38	**5** (Sm)	Major : *H*-PLA-*H* Minor : *H*-PLA-*OMe*	Not clear
39	$Mg(C_3H_5)_2(diox)_{0.06}$	nd [f]	-
40	$Nd(BH_4)_3(THF)_3$	Major: *"HO*-PLA-*OH"* Minor: *H*-PLA-*OH*	9.49

[a] [*L*-LA] / [M] = 100, [*L*-LA] = 2 M, solvent toluene, T = 70 °C for 30 mins. [c] Chain ends of polylactide obtained by MALDI-ToF spectra. [d] Determined by ^{1}H NMR in $CDCl_3$ of the isolated polymers. [e] For H—PLA—$CH(Me)CH_2OH$ as stated above. [f] not determined.

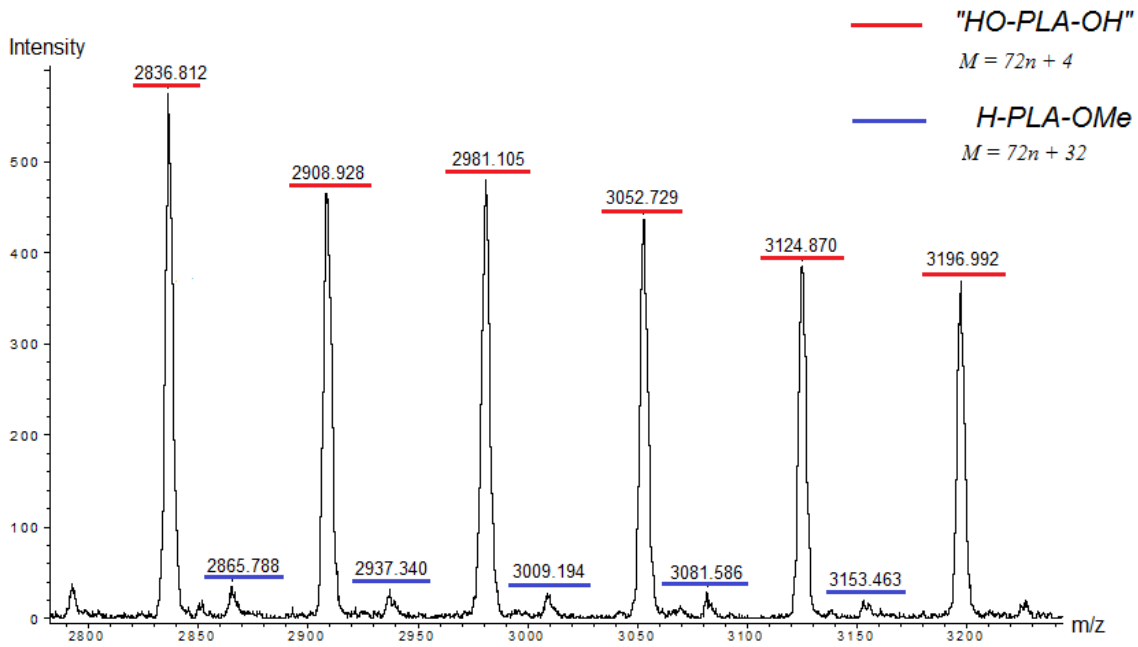

Figure 3.17 MALDI-ToF MS spectrum of polylactide obtained by using $Y(BH_4)_2(C_3H_5)(THF)_3$ (**2**) (entry 35).

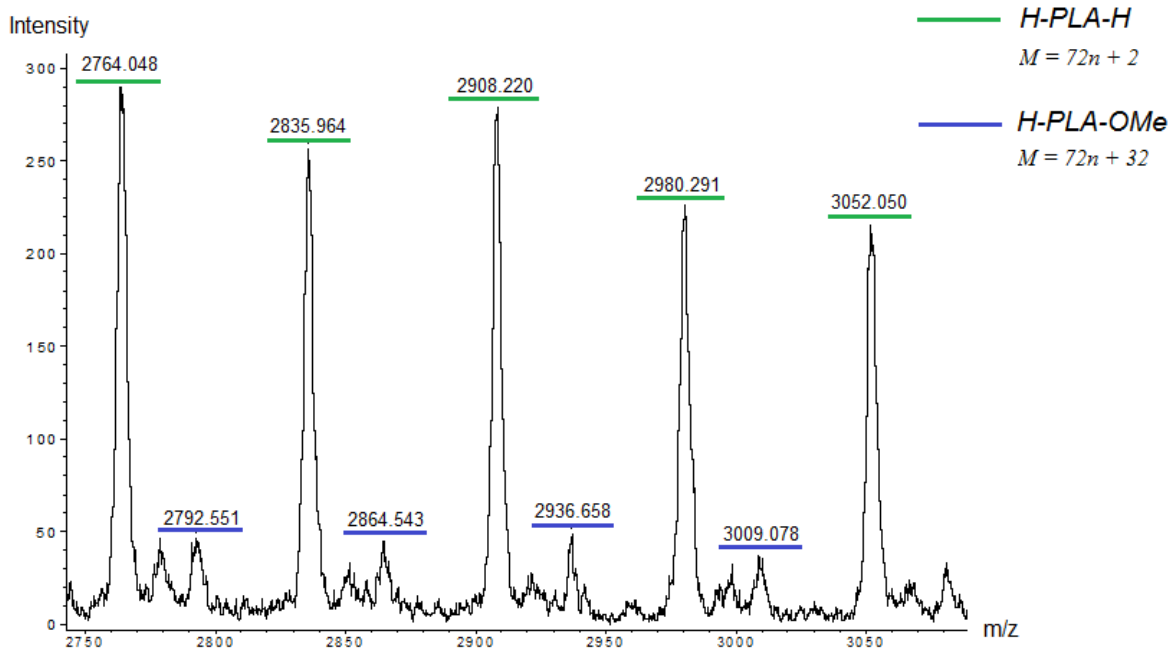

Figure 3.18 MALDI-ToF MS spectrum of polylactide obtained by using $Nd(BH_4)_2(C_3H_5)(THF)_3$ (**4**) (entry 37).

3.4 Conclusion

Neodymium complex **4** was found active and higly *trans*-selective toward the polymerisation of IP as single-component catalyst yielding 53 % of PIP in 3h. The addition of 1 equiv. of BEM gave better activity (58 % in 2 h) and higher *trans*-selectivity (95.5 % *trans*-1,4-PIP). However the addition of $Al^{i}Bu_3$ or MAO, although it gave better activity (complete conversion in 1 h) the selectivity was less (68.2 and 78.7 % respectively of *trans*-1,4-PIP). The same experiments were done with the samarium complex **5** where no reactivity was observed.

Moreover, the mixed allyl borohydride complexes **1-5** revealed to be highly efficient as initiators toward the ROP of *ε*-CL and of *L*-LA. For *ε*-CL, the conversion of 1000 equiv monomer was completed in less than 1 min with all five complexes. Nd (**4**) was the best and was able to convert 10,000 equiv. of the monomer in less than 1 min. This corresponds to an activity up to 81 x 10^6 g polymer $(mol\ Nd)^{-1}.h^{-1}$, which is the best ever reported to our knowledge for such reaction. For *L*-LA, all the reported complexes were found to be excellent initiators (TOF up to 1300 $mol_{L\text{-}LA}(mol_{Nd}.h)^{-1}$ in the case of the Nd catalyst **4**). In the presence of benzyl alcohol as a CTA, better control of the polymerisation process was observed in all cases. The catalytic performances toward *ε*-CL and *L*-LA were found to be dependent on the nature of the metal center and can be lined in the order Nd (**4**) > La (**3**) > Sm (**5**) > Y (**2**) > Sc (**1**).

Thanks to end-group NMR studies (^1H and $^{13}C\ \{^1H\}$) a coordination-insertion mechanism with initiation by the borohydride moieties was established for the polymerisation of *ε*-CL and α,ω-dihydroxy telechelic was recorded. In case of *L*-LA, the analysis of the polymers synthesized, using NMR spectroscopy (^1H, $^{13}C\ \{^1H\}$, $^1H/^1H$-COSY) and MALDI-ToF MS, revealed that the initiation preferentially took place *via* the borohydride moiety rather than *via* the allyl one. Regarding the nature of the end-groups of PLAs, MALDI-ToF spectra showed the α,ω-dihydroxy telechelic terminals "HO—PLA—OH" for PLAs initiated using Sc (**1**) or Y (**2**), however α-hydroxy ω-aldehyde termination, H—PLA—H, was detected in the case of La (**3**), Nd (**4**) and Sm (**5**).

3.5 References

[1] T. Yasuyuki, *Rubber. Chem. Technol.* **2001**, 74.

[2] J. S. Esong, B. C Haung, D. S. Yu, *J. Appl. Polym. Sci*. **2001**, *82*, 81.

[3] D. J. Kind, T. R. Hulla, *Polym. Degrad. Stabil.* **2012**, *97*, 201.

[4] R. F.Yan, *Chin .Chem. Bull.* **1991**, *1*, 1.

[5] W. Yao, J. S. Song, A. H. He, B. C. Huang, *Chin. Elast*. **1995**, *5*, 6.

[6] V. Jitchum, S. Perrier, *Macromolecules*, **2007**, *40*, 1408.

[7] D. J. Worsfold, S. Bywate, *Can. J. Chem*. **1964**, 42.

[8] J. S. Lasky, H. K. Garner, R. H. Ewart, *Ind. Eng. Chem. Prod. Res. Dev*. **1962**, *1*, 82.

[9] Z. Zhang, D. Cui, B. Wang, B. Liu, Y. Yang, *Struct. Bond.* **2010**, *137*, 49.

[10] F. Bonnet, M. Visseaux, D. Barbier-Baudry, E. Vigier, M. M. Kubicki, *Chem. Eur. J.* **2004**, *10*, 2428.

[11] N. Ajellal, L. Furlan, C.M. Thomas, O. L. Casagrande Jr., J. F. Carpentier, *Macromol. Rapid Commun*. **2006**, *27*, 338.

[12] Z. Jian, D. Cui, Z. Hou, X. Li, *Chem. Commun.* **2010**, *46*, 3022.

[13] L. N. Jende, C. O. Hollfelder, C. Maichle-Mössmer, R. Anwander, *Organometallics* **2015**, *34*, 32.

[14] D. Barbier-Baudry, N. Andre, A. Dormond, C. Pardes, P. Richard, M. Visseaux, C. J. Zhu, *Eur. J. Inorg. Chem.* **1998**, 1721.

[15] (a) S. Fadlallah, M. Terrier, C. Jones, P. Roussel, F. Bonnet, M. Visseaux, *Organometallics* 2016, *35*, 456; (b) S. Fadlallah, J. Jothieswaran, F. Capet, F. Bonnet, M. Visseaux, *Submitted to Chem. Eur. J.*

[16] Michaël Terrier's thesis: « Borohydrures de lanthanides polymérisation et copolymerisation », University of Lille 1, 2008, Dir M. Visseaux.

[17] D. Takeuchi, Stereoselective Polymerisation of Conjugated Dienes. in Encyclopedia of Polymer Science and Technology; Wiley: New York, 2013; pp 1.

[18] R. Taube, H. Windisch, H. Weissenborn, H. Hemling, H. Schumann, *J. Organomet. Chem.* **1997**, *548*, 229.

[19] M. Terrier, M. Visseaux, T. Chenal, A. Mortreux, *J. Polym. Sci. Part A: Polym. Chem.* **2007**, *45*, 2400.

[20] L. F. Sanchez-Barba, D. L. Hughes, S. M Humphrey, M. Bochmann, *Organometallics* **2005**, *24*, 5329.

[21] W. Wu, M. Chen, P. Zhou, *Organometallics* **1991**, *10*, 98.

[22] F. Bonnet, M. Visseaux, A. Pereira, D. Barbier-Baudry, *Macromolecules* **2005**, *38*, 3162.

[23] P. Zinck, M. Terrier, A. Mortreux, M. Visseaux, *Polym. Test.* **2009**, *28*, 106.

[24] W. Zheng, N. Yan, Y. Zhu, W. Zhao, C. Zhang, H. Zhang, C. Bai, Y. Hu, X. Zhang, *Polym. Chem.* **2015**, *6*, 6088.

[25] S. Maiwald, H. Weissenborm, H. Windisch, C. Sommel, G. Muller, R. Taube, *Macromol. Chem. Phys.* **1997**, *198*, 3305.

[26] S. Maiwald, H. Weissenborn, C. Sommer, G. Muller, R. Taube, *J. Organomet. Chem.* **2001**, *640*, 1.

[27] C. M. Thomas, *Chem. Soc. Rev*. **2010**, *39*, 165.

[28] R. H Platel, L. M. Hodgson, C. K. Williams, *Polym. Rev.* **2008**, *48*, 11.

[29] J. Wu, T. L. Yu., C. T. Chen, C. C. Lin, *Coord. Chem. Rev.* **2006**, *250*, 602.

[30] Y. Hu, W. A. Daoud, K. K. L. Cheuk, C. S. K. Lin, *Materials* **2016**, *9*, 133.

[31] H. R. Kricheldorf, *Chemosphere* **2001**, 49.

[32] A. C. Albertsson, I. K. Varma, *Biomacromolecules*, **2003**, *4*, 1466.

[33] O. Dechy-Cabaret, B. Martin-Vaca, D. Bourissou, *Chem. Rev.* **2004**, *104*, 6147.

[34] J. Ling, J. Shen, T. E. Hogen-Esch, *Polymer* **2009**, 3575.

[35] P. Kubisa and S. Penczek, *Prog. Polym. Sci*. **1999**, 1409.

[36] N. Ajellal, J. F. Carpentier, C. Guillaume, S. M. Guillaume, M. Helou, V. Poirier, Y. Sarazin, A. Trifonov, *Dalton Trans.* **2010**, *39*, 8363.

[37] C. K. Williams, *Chem. Soc. Rev.* **2007**, *36*, 1573.

[38] S. Asano, T. Aida, S. Inoue, *J. Chem. Soc., Chem. Commun.* **1985**, 1148.

[39] T. Aida, Y. Maekawa, S. Asano, S. Inoue, *Macromolecules* **1998**, *21*, 1195.

[40] S. Inoue, *J. Polym. Sci., Part A: Polym. Chem.* **2000**, *38*, 2861.

[41] W. M. Stevels, M. J. K. Ankoné, P. J. Dijkstra, J. Feijen, *Macromolecules* **1996**, *29*, 3332.

[42] E. Martin, P. Dubois, R. Jérôme, *Macromolecules* **2000**, *33*, 1530-1535.

[43] E. Martin, P. Dubois, R. Jérôme, *Macromolecules* **2003**, *36*, 5934.

[44] V. Poirier, T. Roisnel, J.-F. Carpentier, Y. Sarazin, *Dalton. Trans.* **2009**, 9820.

[45] M. Mazzeo, R. Tramontano, M. Lamberti, A. Pilone, S. Milione, C. Pellecchia, *Dalton. Trans.* **2013**, *42*, 9338.

[46] N. Liu, C. Yao, F. Lin, B. Liu, D. Cui, D. *Polymer* **2015**, *80*, 104.

[47] J. Kleine, H. H. Kleine, *Makromol. Chem.* **1959**, *30*, 23.

[48] T. P. A. Cao, A. Buchard, X. F. Le Goff, A. Auffrant, C. K. Williams, *Inorg. Chem.* **2012**, *51*, 2157.

[49] C. Bakewell, T. P. A. Cao, N. Long, X. F. L. Goff, A. Auffrant and C. K. Williams, *J. Am. Chem. Soc*., **2012**, 20577.

[50] C. Bakewell, A. J. P. White, N. J. Long, C. K. Williams, *Angew. Chem., Int. Ed*., **2014**, *53*, 9226.

[51] A. Arbaoui, C. Redshaw, *Polym. Chem.* **2010**, *1*, 801.

[52] C. Jérôme, P. Lecomte, *Adv. Drug. Deliv. Rev.* **2008**, *60*, 1056.

[53] Z. Hou, Y. Wakatsuki, *Coord. Chem. Rev*. **2002**, *231*, 1.

[54] I. Palard, M. Schappacher, M. Soum, S. Guillaume, *Polym. Int*. **2006**, *55*, 1132.

[55] M. T. Gamer, P. R. Roesky, I. Palard, M. Le Hellaye, S. Guillaume, *Organometallics* **2007**, *26*, 651.

[56] S. Guillaume, M. Schappacher, A. Soum, *Macromolecules*, **2003**, *36*, 54.

[57] I. Palard, A. Soum, S. Guillaume, *Macromolecules*, **2005**, *38*, 6888.

[58] F. Bonnet, A. R. Cowley, P. Mountford, *Inorg. Chem.* **2005**, *44*, 9046.

[59] Y. Nakayama, S. Okuda, H. Yasuda, T. Shiono, *React. Funct. Polym*. **2007**, *67*, 798.

[60] Y. Nakayama, K. Sasaki, N. Watanabe, Z. Cai, T. Shiono, *Polymer* **2009**, *50*, 4788.

[61] F. J. Van Natta, J. W. Hill, W. H. Carruthers, *J. Am. Chem. Soc.* **1934**, *56*, 455.

[62] T. Hayashi, *Progr. Polym. Sci*. **1994**, *19*, 663.

[63] O. Coulembier, P. Degee, J. L Hedrick, P. Dubois, *Progr. Polym. Sci.* **2006**, *31*, 723.

[64] M. Okada, *Progr. Polym. Sci*. **2002**, *27*, 87.

[65] M. Visseaux, F. Bonnet, *Coord. Chem. Rev.* **2011**, *255*, 374.

[66] P. Zinck, M. Terrier, A. Mortreux, M. Visseaux, *Polym. Test*. **2009**, *28*, 106.

[67] M. Save, M. Schappacher, A. Soum, *Macromol. Chem. Phys*. **2002**, *203*, 889.

[68] A. Kowalski, A. Duda, S. Penczek, *Macromolecules* **1998**, *31*, 2114.

[69] K. E. Uhrich, S. M. Cannizzaro, R. S. Langer, K. M. Shakessheff, *Chem. Rev.* **1999**, *99*, 3181.

[70] Berzelius. *Quoted in Dictionnaire Encyclopidique des Sciences Midicales.* **1883**, *63*, 89.

[71] J. Vonliebig, *Annalen* **1847**, *61*, 327.

[72] H. Englehardt, *Annalen* **1848**, *65*, 359.

[73] J. Wislicenus, *Annalen* **1873**, *168*, 302.

[74] P. A. Levene, G. M. Meyer, *J. Biol. Chem*. **1913**, *15*, 65.

[75] O. Meyerhof, L. Lohmann, *Biochem*. **1926**, *171*, 421.

[76] N. Ajellal, D.M. Lyubov, M.A. Sinenkov, G.K. Fukin, A.V. Cherkasov, C.M. Thomas, J.F. Carpentier, A.A. Trifonov, *Chem. Eur. J.* **2008**, *14*, 5440.

[77] R. D. Shannon, *Acta Crystallogr*. **1976**, *A32*, 751.

[78] G. G. Skvortsov, M. V. Yakovenko, P. M. Castro, G. K. Fukin, A. V. Cherkasov, J.-F. Carpentier, A. A. Trifonov, *Eur. J. Inorg. Chem.* **2007**, 3260

[79] T. V. Mahrova, G. K. Fukin, A. V. Cherkasov, A. A. Trifonov, N. Ajellal, J.-F. Carpentier, *Inorg. Chem*. **2009**, *48*, 4258.

[80] H. E. Dyer, S. Huijser, N. Susperregui, F. Bonnet, A. D. Schwarz, R. Duchateau, L. Maron, P. Mountford, *Organometallics* **2010**, *29*, 3602.

[81] J. Kratsch, M. Kuzdrowska, M. Schmid, N. Kazeminejad, C. Kaub, P. Oña-Burgos, S. M. Guillaume, P. W. Roesky, *Organometallics* **2013**, *32*, 1230.

[82] A. O. Tolpygin, G. G. Skvortsov, A. V. Cherkasov, G. K. Fukin, T. A. Glukhova, A. A. Trifonov, *Eur. J. Inorg. Chem.* **2013,** 6009.

[83] A. Marie, F. Fournier, J. C. Tabet, *Anal. Chem*. **2000**, *72*, 5106.

[84] A. E. Clark, E. J. Kaleta, A. Arora, D. M. Wolk, *Clin. Microbiol. Rev*. **2013**, *3*, 547.

[85] N. Susperregui, M. U. Kramer, J. Okuda, L. Maron, *Organometallics* **2011**, *30*, 1326.

[86] I. Palard, M. Schappacher, B. Belloncle, A. Soum, S. G. Guillaume, *Chem. Eur. J.* **2007**, *13*, 1511.

[87] M. Yuan, C. Xiong, X. Li, X. Deng, *J. of App. Polym. Sci.* **1999**, *73*, 2857.

CHAPTER 4

(CO)-POLYMERISATION STUDIES

4.1 Introduction

Copolymerisation is a valuable tool for tuning the properties of a polymeric material for a broad range of applications. However the properties of an obtained copolymer depend essentially on the chemical structure of the two monomer units and their sequence distribution in the copolymer chain which can be incorporated in random, alternating or block fashions (Figure 4.1). NMR can be used as a technique to determine the comonomers ratio in the copolymer as well as the sequence distribution of the comonomers (*e.g.* AAA, AAB, BAB, …). However, deviating from A/B copolymer to copolymers containing more than two comonomers, leads to increasing difficulty to assign their NMR spectra in the detail required for complete analysis.

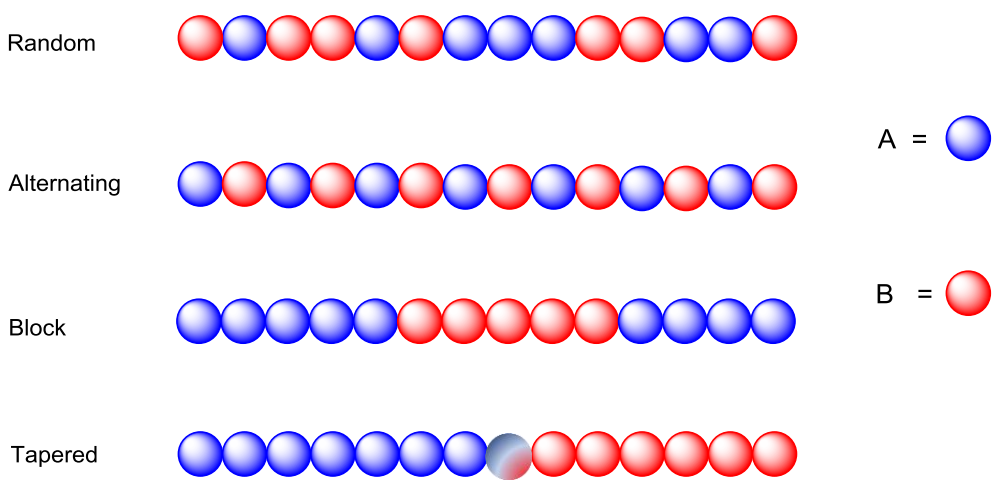

Figure 4.1 Types of A/B copolymers.

For A/B copolymer, there exist three possible types of dyads (two units) sequences, AA, BB and AB which is equivalent to BA. In addition, there are six probable triads, AAA, AAB (equivalent to BAA), BAB, ABA, ABB (equivalent to BBA) and BBB. The ability of NMR spectroscopy to detect either these dyads or triads, set up the understanding of the microstructural magnitude of the copolymer and in turn gives insights regarding its properties.

4.2 Copolymerisation of *L*-lactide and *ε*-caprolactone

4.2.1 Introduction

Poly(L-lactide) (PLA) has been known to display low elongation break value because of its high glass transition temperature and crystallinity. However, the use of these polyesters for high-value added in particular clinical uses requires high flexibility in addition to the biodegradability. The latter properties can be altered by inserting into the polymer chain a sequence with low glass transition temperature such as poly(*ε*-caprolactone) (PCL).[1] PCL for example is more permeable to drugs than PLA due to its less hydrophilicity, on the other hand, PLA has much shorter lifetime (a few weeks) than PCL (1 year) under similar conditions of degradability.[2-4] Copolymers formed from these two monomers were used for drugs delivery system and nerve guides because they are more permeable to drugs than PLA alone and at the same time they are of increasing value for biodegradable devices than PCL.[5-6] Thus, the copolymerisation of *L*-lactide (LA for this chapter) with *ε*-caprolactone (CL for this chapter) can be a promising way to give rise to copolymers with controlled mechanical properties.[7-12]

Ring-opening polymerisation (ROP) of LA and CL using metal based initiators is the most commonly route to access to such type of copolymer.[13,14] In this context several catalysts were applied, for example Al, Zn, Sn, or Mg for block copolymer[15-23] and Al, rare-earth, Zn, Ti or Sn for random copolymers.[24-32] However, the metal contaminant, bound to the chain-end, which may be harmful and not suitable in the synthesis of these polymers, must be considered for application in resorbable biomaterials and microelectronics

Block copolymers of LA and CL can be accessed through the sequential addition of monomers, where the order of monomer addition is critical. Studies of the statistical (one-pot) copolymerisation showed that controlled random copolymers of these monomers could not, in general, be achieved because the CL could not be polymerised with living PLA chain and the LA preferentially incorporate over the CL, especially using rare-earth (RE) catalytic systems.[30-36] However, recent reports revealed that the living PLA initiates the CL polymerisation using bulky salicyloadiminito[22-37] and homosalen[38] aluminium complexes, leading to true random, diblock and triblock copolymers.

Herein, we report the study of the catalytic behavior of the mixed allyl-borohydride rare-earth complexes $RE(BH_4)_2(C_3H_5)(THF)_x$ (RE = Sc, x = 2; Y, La, Nd, Sm, x = 3) toward the statistical copolymerisation of LA and CL. In addition, the microstructural properties of the obtained copolymers are discussed in detail.

4.2.2 Copolymerisation of *L*-lactide and *ε*-caprolactone using allyl-borohydride rare-earth complexes

Having explored the reactivity of these mixed allyl-borohydride complexes for the homopolymerisation of LA and CL and since the polymerisation of CL using these catalysts was very fast compared to that of LA, then, we became interested in the statistical copolymerisation of these monomers with complexes **1**-**5** as initiators.

The feed monomers ratio [LA]:[CL] was set to 100:200, 100:100 or 200:100, the reactions were carried out in toluene at 70 °C, in absence or in presence of Benzyl alcohol (BnOH) as chain transfer agent (CTA). We used ^{1}H and ^{13}C $\{^{1}H\}$ NMR spectroscopic analysis to study the conversion of the monomers, the composition and the microstructure of the copolymers synthesized. Conversion and composition were calculated by ^{1}H NMR based on the methine signals of PLA and LA (incorporated in the copolymer chain) centered at 5.15 and 5.05 ppm, respectively, and the signals of methylene protons of the PCL around 4.05, 4.13 ppm and CL (incorporated in the copolymer chain) 4.23 ppm (Figure 4.2).

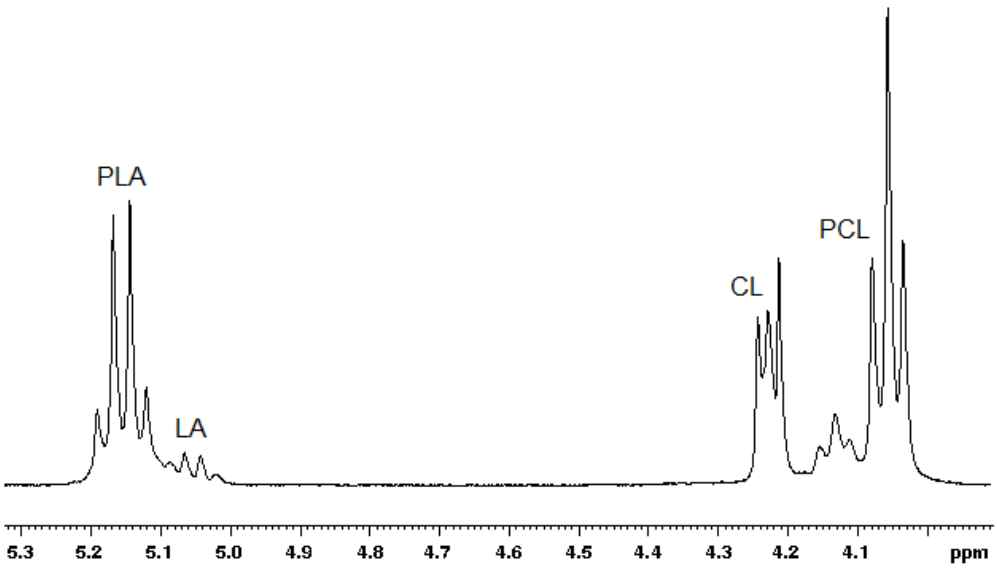

Figure 4.2 ^{1}H NMR spectrum of unwashed poly(LA-*co*-CL), enrty 3.

Representative results are gathered in Tables 4.1 and 4.2. For all experiments in the absence of CTA (entries 1-15), the conversion was found close to completeness for LA, and limited to a certain extent regarding CL, the maximum conversion reached was 67.1% with catalyst **3** (La) as initiator and 100:200 LA:CL ratio (entry 3). For an equimolar feed ratio and in the absence of CTA (entries 6-10) the conversion of CL was little in comparison (limited to 39.2 %, entry 7). This resulted in copolymers containing from 7.6 % (entry 6, Sc initiator) to 28.6 % (entry 7, Y initiator) CL incorporated. Apart from a few exceptions,[35a,37] the results are in agreement with what is generally obtained in LA/CL copolymerisation attempts under smooth experimental conditions (solution, low temperature): even though CL is much more easily homopolymerised than LA – which is the case as well in the present study (see chapter 3) – the competition between these two monomers is clearly in favor of the conversion of LA, with a difficulty to enchain two CL monomers successively. Among the hypotheses advanced to explain this result is the higher coordination ability of LA than CL to the metal center, due to its two ester groups. The dispersities (*Đ*) fall in the range 1.26-1.60 which is relatively narrow and speaks in favor of unique active species.

By doubling the initial quantity of CL (LA:CL = 100:200), higher amount of that monomer was consumed and incorporated in the copolymer, with a CL content in the final copolymer material of 34, 59, and 41 % (entries 2, 3 and 5, respectively). In the case of Sc(**1**) and Nd(**4**) as initiators, the incorporation of the CL units in the final composition of the polymer was limited to 19.1 and 25.7 % (entries 1 and 4, respectively). For a family of metals like the rare earths, the Lewis acidity as well as the ionic radius has to be taken in consideration to account for these results. However, the copolymerisation process seemed to be less controlled in the latter cases, since the size exclusion chromatography (SEC) analyses gave broader dispersities (*Đ*) (2.27, 3.16, 2.59, entries 2, 3 and 5, respectively) than with initiators **1** (1.27, entry 1); and **4** (1.51, entry 4).

Moreover, by doubling the initial quantity of LA (entries 11-15), the conversion of CL was less, as expected, and ranged from 2.8 (entry 15, Sm) to 8.7 (entry 11, Sc), and consequently less CL was inserted into the copolymer chains where the best contribution obtained was 7.6 % with catalyst **4** (entry 14).

When the copolymerisation was performed in the presence of 5 equiv. BnOH as CTA, significant changes were observed and the CL incorporation was found dramatically increased as compared to previously in absence of alcohol.

With a 100:100 feed ratio, the conversion of CL was largely improved (entries 21-25) with up to 80.9% (catalyst **2**, entry 22) and copolymers having content in CL units up to 47.5 % (entries 44 and 45) were received. This rate is among the highest reported in the case of random copolymerisation of a 1:1 LA/CL feed mixture under smooth conditions,[39] and unprecedented for a rare earth catalyst.

When the feed ratio was set to 100:200, the most spectacular effect was noticed for the yttrium initiator **2**, which allowed the production of a material containing this time 62.2% CL (entry 7, by comparison with entry 2) and with **3** (52 %, entry 18), and to a lesser extent for initiators **1** (38.1 % CL, entry 16, *vs*. entry 1) and **4** (40.4 % CL, entry 19, *vs*. entry 4). The same trend for increase in the conversion and insertion of CL was reported for 200:100 feed ratio of LA:CL (entries 26-30)

These results are in line with previous LA/CL copolymerisation studies under chain transfer conditions: the presence of an alcohol as CTA strongly modified the reactivity ratio of comonomers (as it is discussed later in this section), affording polymers richer in the less reactive one.[40,41] A similar trend had already been reported in the case of non-polar monomers.[42] This effect was less pronounced for initiators **3** and **5**.

In terms of macromolecular data, the addition of a CTA clearly improved the control of the process: unimodal SEC curves with $Đ$ range between 1.15 and 1.68 were determined by SEC, whereas the M_n values were considerably decreased as expected for a living process with reversible transfer.

Table 4.1 Solution statistical co-polymerisation of *L*-lactide and *ε*-caprolactone initiated by $Sc(BH_4)_2(C_3H_5)(THF)_2$ **1**; $Y(BH_4)_2(C_3H_5)(THF)_3$ **2;** $La(BH_4)_2(C_3H_5)(THF)_3$ **3**; $Nd(BH_4)_2(C_3H_5)(THF)_3$ **4**; $Sm(BH_4)_2(C_3H_5)(THF)_3$ **5**

Entry[a]	Initiator	[LA]:[CL]	Conversion[b]		Composition[c]		$M_{n\ SEC}$ (g/mol) [d]	Đ [d]
			%LA	%CL	%LA	%CL		
1	**1**	100:200	96.9	11.3	80.9	19.1	10000	1.27
2	**2**	100:200	95.4	28.9	66.2	33.8	13000	2.27
3	**3**	100:200	93.5	67.1	41.0	59.0	16300	3.16
4	**4**	100:200	91.5	15.3	74.3	25.7	10360	1.51
5	**5**	100:200	95.8	34.8	58.7	41.3	16000	2.59
6	**1**	100:100	97.6	8.0	92.4	7.6	10500	1.26
7	**2**	100:100	98.1	39.2	71.4	28.6	12100	1.49
8	**3**	100:100	99.4	25.5	79.6	20.4	17200	1.60
9	**4**	100:100	99.0	28.2	77.8	22.2	12200	1.38
10	**5**	100:100	97.4	7.8	92.6	7.8	18300	1.42
11	**1**	200:100	99.7	8.7	95.8	4.2	17000	1.41
12	**2**	200:100	99.8	3.5	96.6	3.4	21000	1.47
13	**3**	200:100	99.1	4.8	95.3	4.7	25000	1.49
14	**4**	200:100	98.7	8.0	92.4	7.6	23500	1.47
15	**5**	200:100	98.0	2.8	97.2	2.8	27300	1.36

[a] n(RE) = 10 µmol, [M]:[RE]= 100:1, 70 °C in toluene, reaction time 5 h. [b] Monomers conversion, determined by ^{1}H NMR of an aliquot of the reaction mixture. [c] percentage of CL and LA units in the copolymer . [d] Measured by SEC with reference to PS standards.

Table 4.2 Solution statistical co-polymerisation of *L*-lactide and *ε*-caprolactone initiated by $Sc(BH_4)_2(C_3H_5)(THF)_2$ **1**; $Y(BH_4)_2(C_3H_5)(THF)_3$ **2;** $La(BH_4)_2(C_3H_5)(THF)_3$ **3**; $Nd(BH_4)_2(C_3H_5)(THF)_3$ **4**; $Sm(BH_4)_2(C_3H_5)(THF)_3$ **5** under chain transfer agent condition.

Entry[a]	Initiator	[LA]:[CL]	Conversion[b]		Composition[c]		$M_{n\,SEC}$ (g/mol)[d]	Đ[d]
			%LA	%CL	%LA	%CL		
16	**1**	100:200	93.5	26.8	61.9	38.1	5900	1.39
17	**2**	100:200	82.3	73.5	37.8	62.2	4700	1.63
18	**3**	100:200	81.5	75.2	47.3	52.7	4100	1.68
19	**4**	100:200	87.6	29.9	59.6	40.4	5200	1.45
20	**5**	100:200	99.3	8.7	85.1	14.9	5400	1.30
21	**1**	100:100	99.2	47.2	67.7	32.3	5000	1.25
22	**2**	100:100	90.3	80.9	52.7	47.3	6800	1.30
23	**3**	100:100	88.8	80.5	52.5	47.5	5500	1.47
24	**4**	100:100	99.1	68.5	59.2	40.8	6700	1.29
25	**5**	100:100	98.9	13.7	87.8	12.2	5900	1.26
26	**1**	200:100	98.0	2.8	97.2	2.8	5400	1.17
27	**2**	200:100	99.5	16.6	85.7	14.3	5800	1.15
28	**3**	200:100	99.7	15.9	85.4	14.6	8700	1.36
29	**4**	200:100	99.9	17.0	85.2	14.8	3000	1.22
30	**5**	200:100	98.6	6.6	93.7	6.3	8000	1.37

[a] Added 5 equiv. of benzyl alcohol, n(RE) = 10 µmol, , [M]:[RE]= 100:1, 70 °C in toluene, reaction time 24 h. [b] Monomers conversion, determined by ^{1}H NMR of an aliquot of the reaction mixture. [c] percentage of CL and LA units in the copolymer . [d] Measured by SEC with reference to PS standards.

4.2.3 ^{1}H NMR structural characterization of poly(LA-*co*-CL) copolymers

The extent of random copolymerisation could be determined by ^{1}H NMR spectroscopy of isolated copolymers, through the ratio of the integrated intensity of the methine signal of the lactidyl unit at 5.0-5.25 ppm and methylene protons of the caproyl unit around 4.0-4.2 ppm (Scheme 4.1, Figure 4.3).

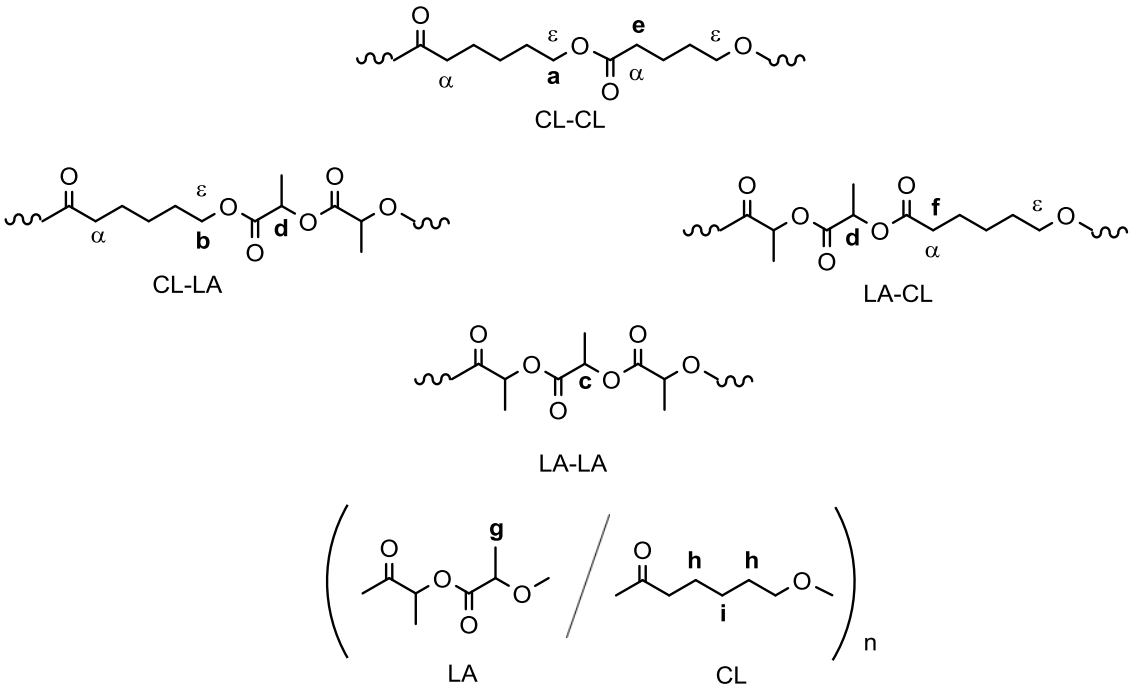

Scheme 4.1 Annotated chemical structure of poly(LA-*co*-CL).

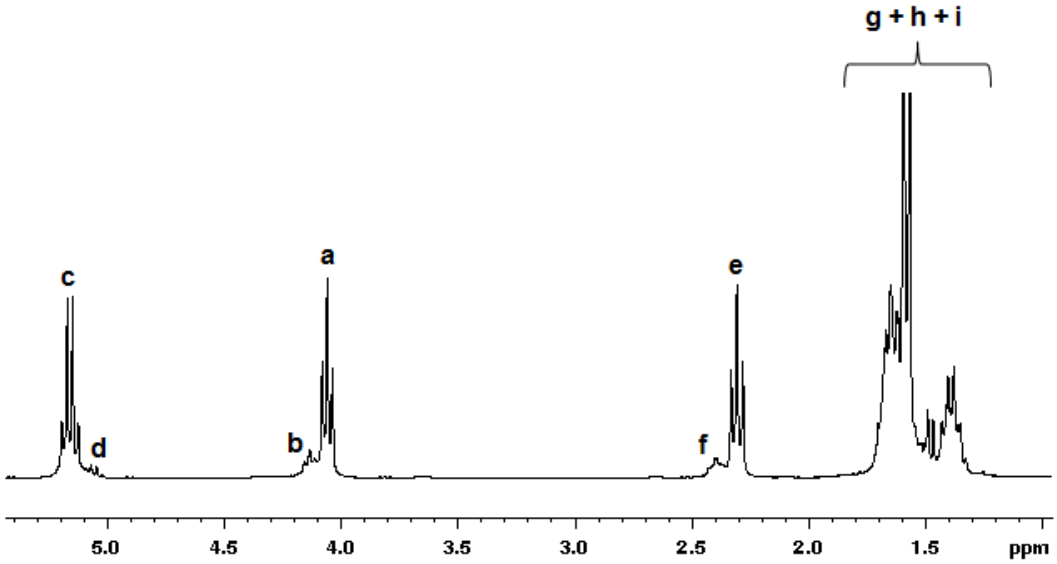

Figure 4.3 ^{1}H NMR spectrum of isolated poly(LA-*co*-CL), entry 3.

The relative molar fractions (LA-LA), (LA-CL) [which is equal to (CL-LA), so any reference to (LA-CL) dyad will be taken to mean (LA-CL) + (CL-LA)] calculated based on the assumption that the relative intensity of the hetero-methine of the lactidyl unit of (LA-CL) segment and hetero-methylene of caproyl unit of (CL-LA) segment are equal and thus: d = f, c = (c+d) – f, knowing that lactidyl contributes to two methine protons to chain. Deconvolution (Bruker software) was carried out to approximate the intensities and to obtain good correlations. Therefore, the average dyad relative molar fractions were calculated by the following:

$$(\mathrm{LA}-\mathrm{LA}) = \frac{\mathrm{c}}{\mathrm{a}+2\mathrm{b}+\mathrm{c}} \qquad eq.1$$

$$(\mathrm{LA}-\mathrm{CL}) = \frac{2\mathrm{b}}{\mathrm{a}+2\mathrm{b}+\mathrm{c}} \qquad eq.2$$

$$(\mathrm{CL}-\mathrm{CL}) = \frac{\mathrm{a}}{\mathrm{a}+2\mathrm{b}+\mathrm{c}} \qquad eq.3$$

The intensities of ε-methylene protons b and α-methylene protons f are equivalent and they were calculated based on equations 4 and 5:

$$\frac{\varepsilon(CL-LA)}{\varepsilon(PCL)} \qquad eq.4 \quad ; \quad \frac{\alpha(CL-LA)}{\alpha(PCL)} \qquad eq.5$$

The signal equivalence shows that the insertion of LA into PCL sequences and CL into PLA sequences are both possible in the one-pot copolymerisation of LA and CL. If this is not the case and the signals are not equivalent, then only homopolymerisation would be preferred to take place by the comonomers. And the difference between ε-methylene and α-methylene protons increases the probability of only homopolymerisation to occur. Scheme 4.2 represents this mechanism by which the formation of hetero-dyad b exists because of the insertion of LA into a growing chain where CL was last monomer inserted. Similarly, the hetero-dyad f only occurs when CL chain is inserted into a growing chain where the previous monomer inserted was LA.

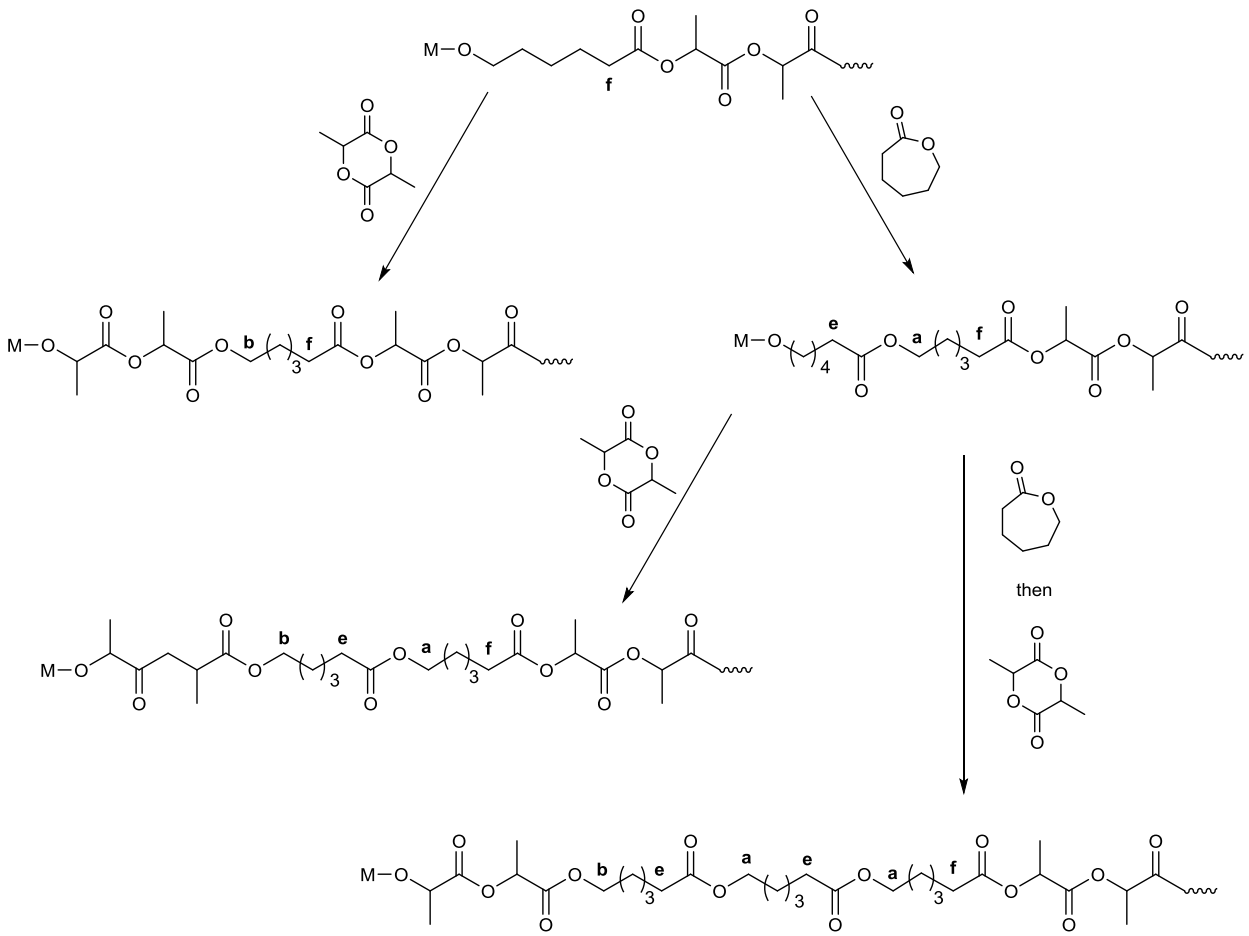

Scheme 4.2 Mechanism of formation of the hetero- and homo-dyads caused by the insertion of 1, 2 and 3 caproyl units into a growing chain [LA-$(CL)_n$-LA].

In addition equations 6-10 were employed to obtain the number-average sequence length (l_i) of LA and CL building units, the bernoullian random number-average sequence lengths $(l_i)_{random}$ and the randomness character (R): [11,43]

$$l_{LA} = \frac{2(LA)}{(LA-CL)} \qquad eq.6 \quad ; \quad l_{CL} = \frac{2(CL)}{(LA-CL)} \qquad eq.7$$

$$(l_{LA})_{random} = \frac{1}{(CL)} \qquad eq.8 \quad ; \quad (l_{CL})_{random} = \frac{1}{(LA)} \qquad eq.9$$

$$R = \frac{(l_{LA})_{random}}{l_{LA}} = \frac{(l_{CL})_{random}}{l_{CL}} = \frac{(LA-CL)}{2(LA)(CL)} \qquad eq.10$$

Where (LA) and (CL) are the two comonomers molar fractions and (LA-CL) is the LA-CL average dyad relative molar fraction.

Table 4.3 Solution statistical co-polymerisation of *L*-lactide and *ε*-caprolactone initiated by $Sc(BH_4)_2(C_3H_5)(THF)_2$ **1**; $Y(BH_4)_2(C_3H_5)(THF)_3$ **2;** $La(BH_4)_2(C_3H_5)(THF)_3$ **3**; $Nd(BH_4)_2(C_3H_5)(THF)_3$ **4**; $Sm(BH_4)_2(C_3H_5)(THF)_3$ **5**

Entry[a]	Initiator	[LA]:[CL]	Average relative molar fractions (%) [e]			Microstructural magnitude					Reactivity ratios [i]			Thermal analysis [j]	
			(LA–LA)	(LA–CL)	(CL–CL)	l_{LA} [f]	l_{CL} [g]	$(l_{LA})_{random}$	$(l_{CL})_{random}$	R [h]	r_1	r_2	$r_1 . r_2$	T_g (°C)	T_m (°C)
1	**1**	100:200	70.3	21.1	8.6	7.7	1.8	5.2	1.2	0.68	6.66	0.86	5.72	50	140
2	**2**	100:200	53.3	25.9	20.8	5.1	2.6	2.9	1.5	0.58	4.07	1.61	6.55	nd	148
3	**3**	100:200	32.6	22.2	45.1	3.7	5.3	1.7	2.4	0.46	2.94	4.06	11.9	-52	52 ;155
4	**4**	100:200	62.5	31.7	5.8	4.7	1.6	3.9	1.3	0.83	3.94	0.36	1.42	-58	-7 ;142
5	**5**	100:200	41.8	33.7	24.4	3.5	2.5	2.4	1.7	0.69	2.48	1.45	3.59	-39	44;153
6	**1**	100:100	85.9	13.0	1.1	14.2	1.2	13.1	1.0	0.92	13.21	0.16	2.11	52	138
7	**2**	100:100	47.7	47.5	4.8	3.0	1.2	3.5	1.4	1.16	2.00	0.20	0.40	58	147
8	**3**	100:100	66.0	27.1	6.9	5.9	1.5	4.9	1.3	0.83	4.87	0.51	2.48	41	152
9	**4**	100:100	57.8	40.2	2.0	3.9	1.1	4.5	1.3	1.16	2.88	0.10	0.29	10	140
10	**5**	100:100	87.3	10.5	2.2	17.6	1.4	12.8	1.1	0.77	16.62	0.42	6.98	nd	
11	**1**	200:100	91.9	7.7	0.4	24.8	1.0	23.8	1.0	0.96	23.87	0.10	2.39		
12	**2**	200:100	93.3	6.5	0.2	29.6	1.0	29.4	1.0	0.99	28.70	0.06	1.72		
13	**3**	200:100	91.7	7.2	1.1	26.5	1.3	21.2	1.0	0.80	25.47	0.30	7.64		
14	**4**	200:100	86.8	11.2	2.0	16.5	1.0	13.1	1.1	0.79	15.50	0.35	5.42		
15	**5**	200:100	94.4	5.5	0.1	35.3	1.0	35.7	1.0	1.01	34.32	0.036	1.24		

[a] n(RE) = 10 µmol, [M]:[RE]= 100:1, 70 °C in toluene, reaction time 5 h. [e] Average relative molar fractions in the copolymer determined by ^{1}H NMR. [f] Average sequence length of the lactidyl unit in the copolymer determined by ^{1}H NMR. [g] Average sequence length of the caproyl unit in the copolymer determined by ^{1}H NMR. [h] Degree of Randomness. [i] Reactivity ratios determined by ^{1}H NMR. [j] Determined by DSC.

Table 4.4 Solution statistical co-polymerisation of *L*-lactide and *ε*-caprolactone initiated by $Sc(BH_4)_2(C_3H_5)(THF)_2$ **1**; $Y(BH_4)_2(C_3H_5)(THF)_3$ **2;** $La(BH_4)_2(C_3H_5)(THF)_3$ **3**; $Nd(BH_4)_2(C_3H_5)(THF)_3$ **4**; $Sm(BH_4)_2(C_3H_5)(THF)_3$ **5** under chain transfer agent conditions.

Entry[a]	Initi-ator	[LA] : [CL]	Average relative molar fractions (%) [e]			Microstructural magnitude					Reactivity ratios [i]			Thermal analysis [j]	
			(LA–LA)	(LA–CL)	(CL–CL)	l_{LA} [f]	l_{CL} [g]	$(l_{LA})_{random}$	$(l_{CL})_{random}$	R [h]	r_1	r_2	$r_1 . r_2$	T_g (°C)	T_m (°C)
16	**1**	100:200	35.9	52.0	12.1	2.4	1.5	2.62	1.61	1.10	1.38	0.46	0.64	-16	94(br)
17	**2**	100:200	11.4	51.3	35.7	1.5	2.4	1.60	2.65	1.09	0.44	1.39	0.61	nd	
18	**3**	100:200	0.3	94.0	5.7	1.0	1.1	1.89	2.11	1.89	0.006	0.12	0.0007	-16	105(br)
19	**4**	100:200	29.3	60.5	10.2	2.0	1.3	2.47	1.67	1.26	0.97	0.34	0.33	-52	109(br)
20	**5**	100:200	72.5	25.2	2.3	6.7	1.2	6.71	1.18	0.99	5.75	0.18	1.03	nd	
21	**1**	100:100	36.0	63.5	0.5	2.1	1.0	3.1	1.5	1.45	1.13	0.02	0.03	-25;15	109(br)
22	**2**	100:100	24.0	57.6	18.4	1.8	1.6	2.1	1.9	1.15	0.83	0.64	0.53	-20	102(br)
23	**3**	100:100	10.9	83.1	6.0	1.4	1.1	2.1	1.9	1.67	0.26	0.14	0.04	nd	
24	**4**	100:100	23.4	71.6	5.0	1.6	1.1	2.5	1.7	1.48	0.65	0.14	0.09	-6	103(br)
25	**5**	100:100	76.6	22.4	1.0	7.8	1.1	8.2	1.2	1.05	6.84	0.08	0.55	nd	
26	**1**	200:100	94.4	5.5	0.1	35.3	1.0	35.7	1.0	1.01	34.32	0.04	1.37	nd	
27	**2**	200:100	72.3	26.6	1.1	6.4	1.1	7.0	1.2	1.08	5.43	0.08	0.43		
28	**3**	200:100	72.4	27.5	0.1	6.2	1.0	6.8	1.2	1.10	5.26	0.007	0.04		
29	**4**	200:100	70.8	28.7	0.5	5.9	1.0	6.8	1.2	1.13	4.93	0.03	0.15		
30	**5**	200:100	87.7	12.0	0.3	15.7	1.0	15.8	1.1	1.00	14.61	0.05	0.73		

[a] Added 5 equiv. of benzyl alcohol, n(RE) = 10 µmol, [M]:[RE]= 100:1, 70 °C in toluene, reaction time 24 h. [e] Average relative molar fractions in the copolymer determined by ^{1}H NMR. [f] Average sequence length of the lactidyl unit in the copolymer determined by ^{1}H NMR. [g] Average sequence length of the caproyl unit in the copolymer determined by ^{1}H NMR. [h] Degree of Randomness. [i] Reactivity ratios determined by ^{1}H NMR. [j] Determined by DSC.

In terms of polymer microstructure, it is clearly seen that the average sequence length and the randomness factor are greatly affected by the nature of the catalyst (metal center), by the feed ratio and by the presence/absence of an alcoholic transfer agent (BnOH). The randomness factor R takes value close to 0 in a block copolymer, close to 1 in a random one and $1 < R \leq 2$ in alternating polymers.[43]

In the absence of BnOH (entries 1-15, Table 4.3), copolymers having marked random character (R > 0.8) were synthesized, except for **1-3** and **5** as initiators (LA:CL = 100:200, entries 1-3 and 5) where intermediate values (0.46-0.69) were obtained. In turn, under CTA conditions (5 equiv. BnOH, entries 16-30, Table 4.4), the randomness factor showed a significant change and they were all superior to 1 to reach 1.89 (100:200, entry 18). This indicates a trend of moderate to high alternating character of the resulting copolymer, which is unprecedented in such reactions under smooth condition and simple catalysts without having bulky ligands - knowing that the nature of catalyst can affect the randomness of the copolymer by changing both the rate of the reaction and the sequence distribution of the comonomers, and lower temperatures favor the polymerisation of LA over that of CL forming a copolymer with higher block characters - In addition a pure random copolymer were obtained with R = 0.99 and 1.00 using the Sm catalyst **5** (entries 20 and 30, feed ratios 100:200 and 200:100 respectively) and 1.01 in case of Sc(**1**) and LA:CL ratio 200:100 (entry 26). Moreover, we found that with respect to the average molar fractions of the copolymer, the presence of alcohol in all cases (entries **16**-**30**) gave more (LA-CL) junctions compared to the experiments performed with no alcohol (for instance, 52.0, 51.3, 94.0, 60.5 %, entries 16-19, respectively, Table 4.3, instead of 21.1, 26.0, 22.2, 31.7, entries 1-4, respectively, Table 4.4). Interestingly, when the copolymerisation was performed with the lanthanum initiator (**3**) and in presence of BnOH, the LA-LA and CL-CL relative molar fraction were found to be nearly inexistent (ca 0.3 %, and 5.7 % respectively, entry 18) whereas LA-CL junctions reached 94%. Knowing that, **1**, **2** and **4** initiators display also a specific behavior, with a LA-CL ranging from 0.513 to 0.605 as preferential motives at the addition of the transfer agent (Feed ratio = 100:200 entries 16, 17 and 19). Thus, the CTA conditions have a great influence towards the LA/CL enchainments during the copolymerisation process. Furthermore, the decrease of CL or increase of LA monomer feed ratios largely affected the average relative molar fractions along the copolymers where in general decrease of LA-CL junctions was recorded and increase of LA-LA ones, apart from some exceptions (Table 4.3), moreover the

same catalytic behavior was observed when added 5 equiv. of benzyl alcohol which leaded to increase of LA-CL and decrease of LA-LA dyads compared to the experiments done with no alcoholic role in the system (Tables 4.3 and 4.4).

On the other hand, the number average sequence length l_{LA} and l_{CL} (the average length of sequences comprising only LA and CL units respectively), do provide insights to measure the tendency of a copolymer to deviate from randomness.

For example we can consider a model chain segment which consists of equal number of comonomers LA and CL, and where 12 LA–CL, 3 LA–LA, and 3 CL–CL dyads exist (Figure 4.4).

——LA—CL—LA—LA—CL—LA—CL—LA—LA—LA—CL—LA—CL—CL—LA—CL—CL—CL—LA—CL——

Figure 4.4 Copolymer model comprised of LA and CL units.

By following the equations 11 and 12[43] (which are equal to equation 6 and 7, if the comonomer and sequence abundance are expressed in molar fractions), where N is the abundance of the sequence denoted by subscript, the model chain segment is l_{LA} = 18/12 = 1.5. Similarly, l_{CL} = 1.5. Thus, l_{LA} and l_{CL}, for a 50:50 (when the contribution of both monomers in the final structure of the copolymer is equal) of purely random copolymer are both equal to 2, where $N_{LACL} = 2\ N_{LALA} = 2\ N_{CLCL}$.[43]

$$l_{LA} = \frac{2N_{LALA} + N_{LACL}}{N_{LACL}} \qquad eq.11$$

$$l_{CL} = \frac{2N_{CLCL} + N_{LACL}}{N_{LACL}} \qquad eq.12$$

Therefore, in the case of equal conversions of monomers of the same feed ratio, the l_i (where i is the symbol of the monomer studied) of truly random copolymer is 2 while in block one it is greater than 2 and in copolymer with tendency towards alternation it is less than 2, knowing that for perfectly alternating 50:50 copolymer, l_{LA} and l_{CL} are both equal to 1.[43]

Looking this way, and taking into consideration that the conversions of LA and CL were nearly equal (81.5 and 75.2 %, respectively, entry 18, Table 4.2), l_{LA} = 1.00 and l_{CL} = 1.12 (entry 8, Table 4.2) which almost indicates the perfect alternation of the two monomers. This is in accordance with the previous discussion regarding the randomness factor.

The relationship between lactide feed ratio and average length of lactidyl and caproyl units are graphically represented in Figures 4.5 and 4.6 for experiments done in the absence of BnOH and Figures 4.7 and 4.8 for the ones done under CTA conditions. The feed ratio of LA is equal to 50 in the case of LA:CL = 100:200, to 100 when the latter is equal 100:100 and to 200 for 200:100 initial equivalences of LA and CL. Generally speaking, going from LA:CL ratio of 100:200 to 100:100 to 200:100, the average lengths l_{LA} increases and l_{CL} decreases. Interestingly, in the presence of BnOH, the variation of l_{LA} (except with the Sc initiator) and of l_{CL} with the feed ratio is largely attenuated. The average l_{CL} even tends to a constant value, close to 1, especially with the larger size metal initiators.

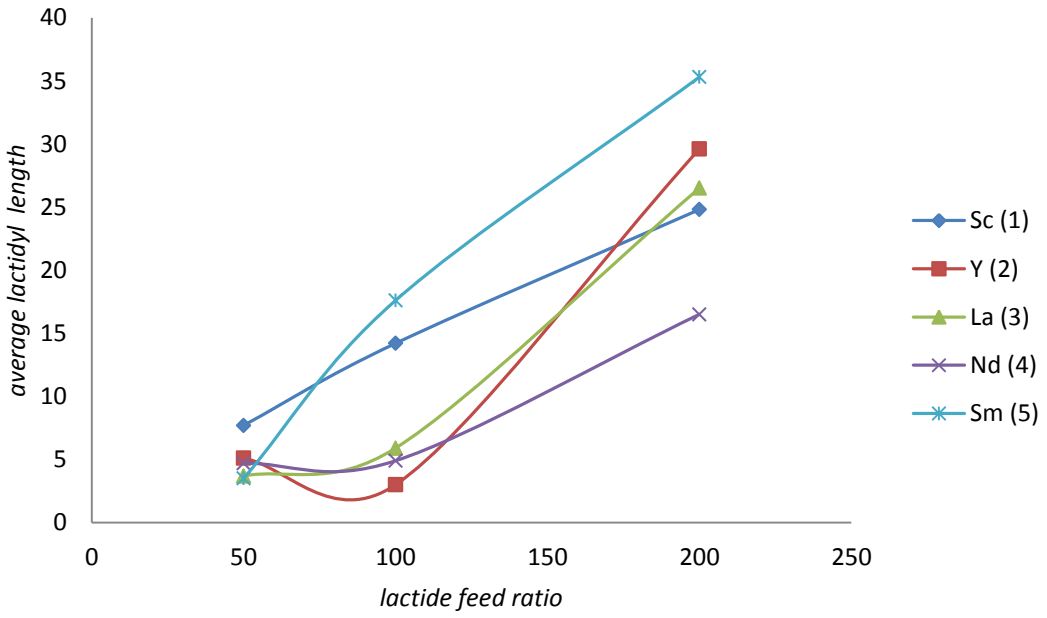

Figure 4.5 average lactidyl length with respect to lactide feed ratio for poly(LA-*co*-CL) initiated with **1**-**5** in the absence of BnOH.

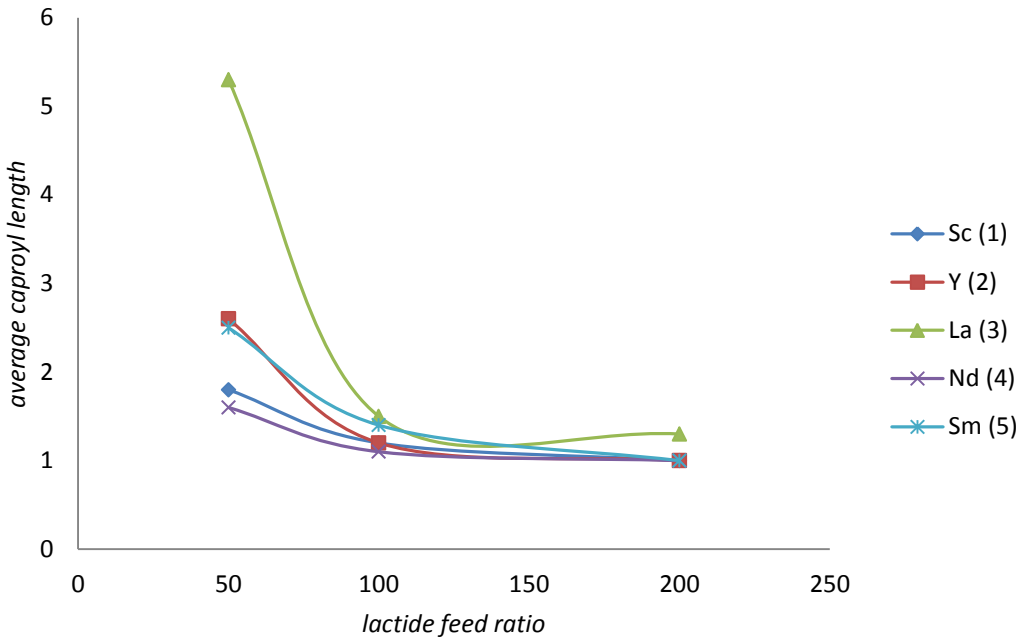

Figure 4.6 average caproyl length with respect to lactide feed ratio for poly(LA-*co*-CL) initiated with **1**-**5** in the absence of BnOH.

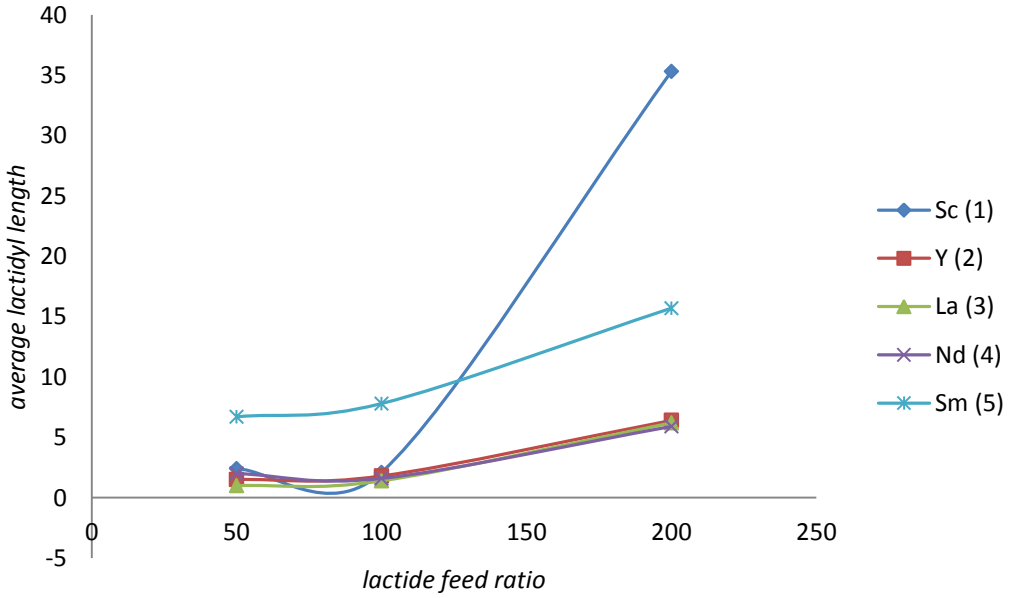

Figure 4.7 average lactidyl length with respect to lactide feed ratio for poly(LA-*co*-CL) initiated with **1**-**5** in the presence of BnOH as chain transfer agent.

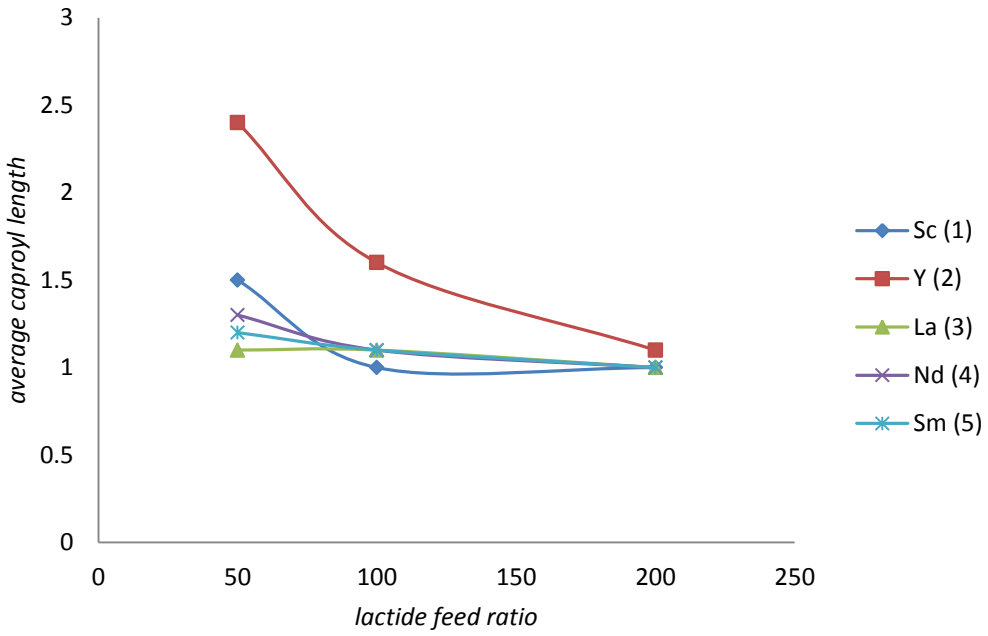

Figure 4.8 average caproyl length with respect to lactide feed ratio for poly(LA-*co*-CL) initiated with **1**-**5** in the presence of BnOH as chain transfer agent.

Another approach to predict the randomness of the copolymers was by calculating the bernoullian random number average sequence length, $(l_{LA})_{random}$ and $(l_{CL})_{random,}$ applying the bernoullian model (which is the simplest statistical model used to describe copolymerisation). Generally, these lengths are only dependent on the ratio of monomers in the medium, as it can be seen in equations 8 and 9, where the propagation of one monomer on a polymer chain is only related to the mole fraction of the second one.

It is also possible to use the NMR-derived sequence distributions of the hetero- and homo- dyads to determine the relative reactivity ratios of the two comonomers LA and CL. They provide insight into the relation between the rate constant of homo- and copolymerisation.

In general, during copolymerisation, the two reacted monomers do not incorporate into the polymeric chain in the same proportion as in the initial comonomer mixture. The reason for this is that the two monomers generally have different reactivities toward the growing chain ends, so for copolymerisation of LA and CL there are four potential reactions each defined by their own rate constant k_{xx} (Scheme 4.3):

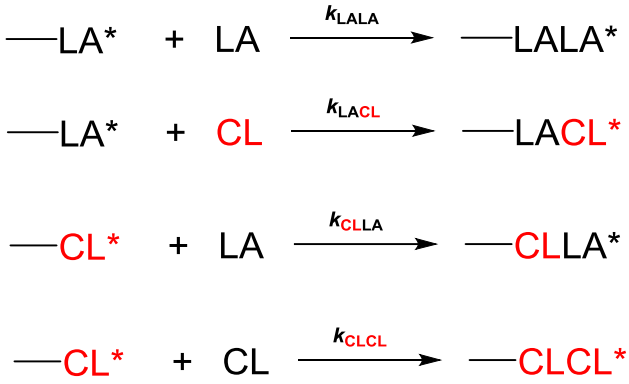

Scheme 4.3 Possible propagation reactions for the copolymerisation of LA and CL.

LA* indicates that monomer LA was the last inserted into the polymeric chain and is adjacent to the active metal center, the same definition is applied for CL*

Thus, the reactivity ratios were calculated based on traditional kinetic models according to the following equations (with an assumption that propagation of the polymerisation obeys a first-order rate equation):[23-44,45-49]

$$r_1\,(1/f) = \frac{k_{LALA}}{k_{LACL}} = \frac{2(LA - LA)}{(LA - CL)} \qquad eq.13$$

$$r_2\,(f) = \frac{k_{CLCL}}{k_{LACL}} = \frac{2(CL - CL)}{(LA - CL)} \qquad eq.14$$

$$f = \frac{(CL)}{(LA)}$$

Then, several possibilities are encountered:

- $r_1 = r_2 >> 1$ or $r_1.r_2 >> 1$ – could be attributed to a mixture of two homopolymers and very little copolymerisation. Both reactivity ratios having a high value indicates overwhelming preference for homo-monomer insertion into the active site (*ie*. LA into RE-LA*, CL into RE-CL*).
- $r_1 = r_2 > 1$ or $r_1.r_2 > 1$ - with both monomers showing a preference for homopolymerisation on the rare insertion of LA into CL, or vice versa, leads that newly inserted monomer takes preference leading to a block-copolymer.

- $r_1.r_2 \approx 1$ - an equal probability of either monomer inserting into any active center would provide conditions to generate a truly random copolymer. Note that the special case $r_1 = r_2 \approx 1$, corresponds to a random copolymer formed by Bernoullian process.
- $r_1 = r_2 \approx 0$ - with both reactivity ratios equal to zero, it suggests that insertion of LA has to be followed by insertion of monomer CL, leading to alternating copolymer.

In the absence of CTA (entries 1-15, Table 4.3) and apart from few cases, the r_1 values are all greater than 1 while r_2 values were smaller than 1, which indicates that the rate of insertion of LA into a growing PLA is preferred over the insertion of caprolactone. Which is not the case of insertion of CL into a growing polymer chain with a previously inserted CL. However, when CTA was employed in the reaction mixture (entries 16-30, Table 4.4), $r_1.r_2$ starts to take values less than or equal to 1 (the case of random copolymer) and interestingly when La initiator is used $r_1.r_2$ tends to be 0 indicating the presence of alternating sequence of LA and CL (entry 18, Table 4.4), therefore supporting the previous discussion. The same reasoning can be considered for copolymers issued from entries 23 and 24, which have a marked alternating character.

Thermal analysis

DSC analyses showed that several of the copolymers synthesized display a crystalline phase (Appendix XII). In some cases (entries 1-5, 7-9) the T_m peaks (138-155 °C) can be attributed to P(*L*-LA). The lower value in comparison with pure P(*L*-LA) (164-179 °C) is attributed to shortened P(*L*-LA) sequences. In other cases (entries 3, 5), a second T_m peak was observed, attributed to PCL, thus confirming the blocky nature of these copolymers. In thermograms of entries 21, 22, 24, 26, 28 and 29, broad endothermic transitions are noticed around 100°C, which would tend to exclude polylactide fusion. Glass transition temperatures (T_g) comprised between -67°C (PCL) and 60 °C (PLA), account for CL/LA copolymer in the amorphous phase. Such thermal behaviours call for in-depth studies of these random to alternating-like copolymers, wich could open to interesting properties for further biomedical applications.

4.2.4 ^{13}C NMR structural characterization of poly(LA-*co*-CL) copolymers

^{13}C spectroscopy is a very sensitive method toward the chemical environment of a studied nucleus and accordingly is a powerful tool to analyze microstructure of copolymer system and determine the actual average sequence length of each type of monomer sequence. Several papers discussed this issue and showed how the structure of various copolymers can be analyzed by ^{13}C NMR. Kricheldorf reported that ^{13}C NMR can be a more suitable method to analyze the polyesters than ^{1}H NMR by using the carbonyl signal of the esters used to distinguish between triad standing for three monomer units connected together.[50-56]

In particular, for the analysis of a copolymer formed of LA and CL, the triad carbonyl signals that exist in the region 175-165 ppm have been used in the calculations of the average sequence lengths.

Figure 4.10 shows the spectra of the carbonyl regions correspond to the copolymer P(LA-*co*-CL) as well as the assignments of the peaks according to the literature,[56] all peaks due to the different possible monomer sequences in the copolymer are present. It is important to note that each lactidyl unit (represented in this part as LL) stands for two lactyl units (L), because the addition of a lactidyl unit to the copolymer chain results in the incorporation of two carbonyl groups, which is not the case of the caproyl unit (represented as Cap or C in this part) (Figure 4.9).

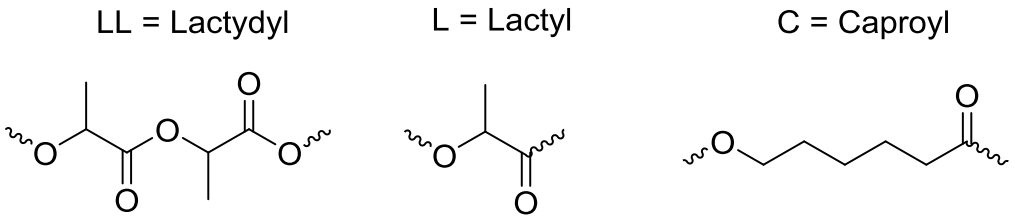

Figure 4.9 Structures of lactidyl, lactyl and caproyl units.

So there are eight main different triads, CCC, LLCC, CLLC, CCLL, LLLLLL, CLLLL, LLCLL and LLLLC. In addition there are more triad groups which exist because of

the transesterification process, *i.e*., the exchange reaction of group between different esters by redistribution of monomer sequences.

Peaks	δ (ppm)	Triad(s)
a	173.58	C<u>C</u>C
b	173.53	LL<u>C</u>C
c	172.87	C<u>C</u>LL
d	172.82	LL<u>C</u>LL
e	170.40	LLL<u>L</u>C
f	170.35	C<u>L</u>LC
g	170.29	CL<u>L</u>C
h	170.13	C<u>L</u>LLL
i	169.79	LL<u>L</u>LC, CL<u>L</u>LL
j	169.63	LL<u>LL</u>LL
k	170.90	C<u>L</u>C

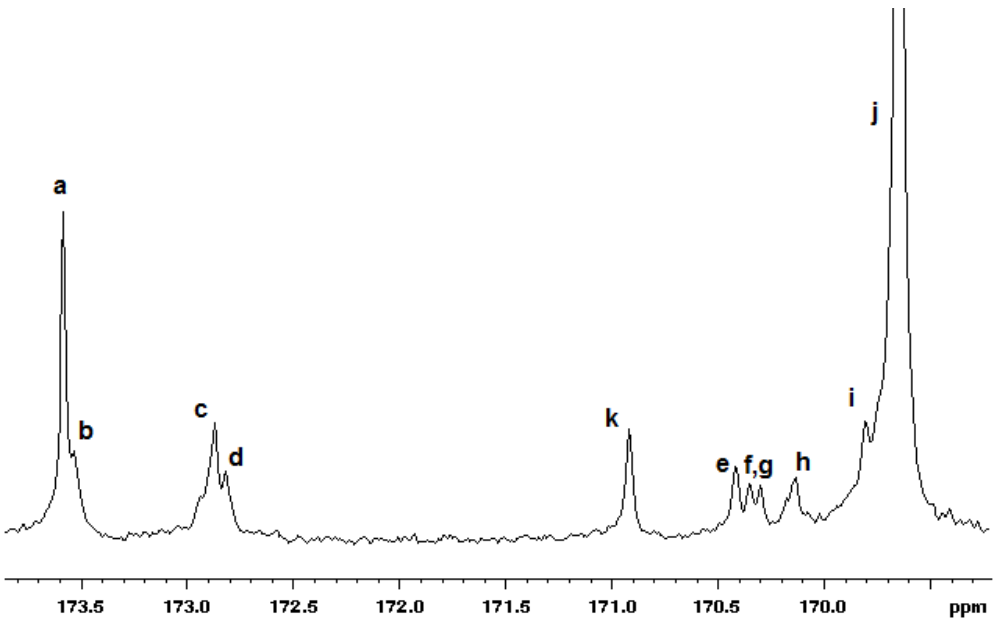

Figure 4.10 ^{13}C NMR spectrum of P(LA-*co*-CL) of entry 5, Table 4.4 and triad assignments. Underlying indicates the carbonyl group to which resonance is assigned.

In the copolymerisation of lactide and caprolactone, transesterification plays an important role and it should be taken into consideration. Two types of transesterification reaction were introduced, the first and the second modes. If lactide (LL) undergoes bond cleavage, this leads to the appearance of triad signals with even number of lactyl unit (CLLC) (first mode of transesterification) and odd number ones CLC and CLLLC (second mode of transesterification) (Scheme 4.4).[57]

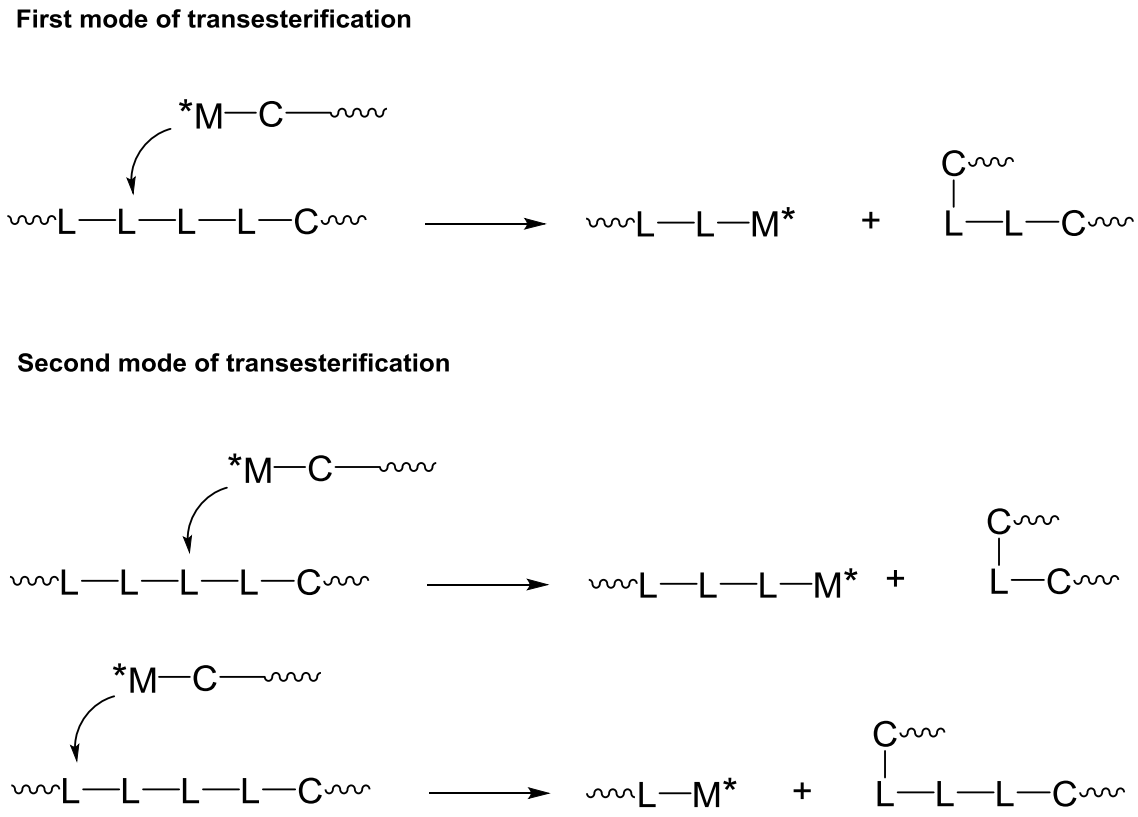

Scheme 4.4 Possible modes of transesterification.

Table 4.5 Solution statistical co-polymerisation of *L*-lactide and *ε*-caprolactone initiated by $Sc(BH_4)_2(C_3H_5)(THF)_2$ **1**; $Y(BH_4)_2(C_3H_5)(THF)_3$ **2;** $La(BH_4)_2(C_3H_5)(THF)_3$ **3**; $Nd(BH_4)_2(C_3H_5)(THF)_3$ **4**; $Sm(BH_4)_2(C_3H_5)(THF)_3$ **5**

Entry [a]	**Initiator**	**LA:CL: BnOH**	**Relative triads intensities of carbonyl signals (%)** [h]						
			(C<u>C</u>C) + (LL<u>C</u>C)	(C<u>C</u>LL) + (LL<u>C</u>LL)	(C<u>L</u>C)	(C<u>LL</u>LL)	(LL<u>LL</u>C)	(C<u>LL</u>C)	LL<u>LL</u>LL
1	1	100:200:0	2.10	4.66	0.82	7.10	7.10	0.89	77.33
2	2	100:200:0	12.09	6.60	3.20	5.40	5.40	1.63	65.67
3	3	100:200:0	24.10	5.71	3.30	2.66	2.66	0.90	60.68
4	4	100:200:0	2.03	6.38	0.83	6.56	6.56	1.07	76.64
5	5	100:200:0	13.79	7.71	3.97	4.88	4.88	2.69	62.09
6	1	100:100:0	0	2.27	0	5.36	5.36	1.67	85.34
7	2	100:100:0	0.37	2.96	0.54	5.22	5.22	1.56	84.13
16	1	100:200:5	4.93	11.10	4.24	9.26	9.26	5.02	56.20
18	3	100:200:5	6.73	22.68	11.79	11.74	11.74	8.98	28.82
19	4	100:200:5	6.12	15.97	5.98	10.40	10.40	5.21	45.92
20	5	100:200:5	2.77	11.14	0	11.24	11.24	1.72	61.89
21	1	100:100:5	1.29	4.31	0.32	6.94	6.94	0.64	79.56
22	2	100:100:5	7.93	12.01	5.48	8.00	8.00	5.50	53.08
23	3	100:100:5	3.09	21.62	9.49	13.64	13.64	8.58	29.94
24	4	100:100:5	2.58	12.05	4.87	11.14	11.14	4.75	53.47
25	5	100:100:5	0.60	4.76	0.85	7.14	7.14	1.90	77.62
27	2	100:200:5	0.73	3.70	0.83	3.52	3.52	1.13	86.57
28	3	100:200:5	0	4.19	0.43	5.48	5.48	1.04	83.39
29	4	100:200:5	0	3.06	0.31	4.56	4.56	1.13	86.38

[a] n(RE) = 10 µmol, [M]:[RE]= 100:1, 70 °C in toluene.[h] Average relative molar fractions in the copolymer determined by ^{13}C NMR.

The mentioned triads were grouped and relatively quantified in Table 4.5, allowing the calculation of the average block length (l_{LL} and l_C), reactivity ratios and the second mode transesterification degree (T_{II}) according to the following equation as described by Kricheldorf and Bero (eq. 15-20): [53,57]

$$L_{LL} = \frac{(LLLLL + LLLLC + CLLLL + CLLC)}{(CLLC + \frac{1}{2}(LLLLC + CLLLL))} \qquad eq.15$$

$$L_C = \frac{(CCC + LLCC)}{(CCLL + LLCLL)} + 1 \qquad eq.16$$

$$r_1\,(1/f) = \frac{k_{LLLL}}{k_{LLC}} = \frac{(LLLLLL + \frac{1}{2}(LLLLC + CLLLL))}{((CCLL + LLCLL) + \frac{1}{2}(LLLLC + CLLLL))} \qquad eq.17$$

$$r_2\,(f) = \frac{k_{CC}}{k_{LLC}} = \frac{(CCC + LLCC) + \frac{1}{2}(CCLL + LLCLL)}{(LLLLC + CLLLL) + \frac{1}{2}(CCLL + LLCLL)} \qquad eq.18$$

$$T_{II} = \frac{(CLC)_e}{(CLC)_R} \qquad eq.19$$

Where $(CLC)_e$ is the intensity of the CLC triad sequence from the ^{13}C NMR at 170.9 ppm, and $(CLC)_R$ is the theoretical concentration for completely random chains calculated via Bernoullian statistics.

$$(CLC)_R = \frac{k^2}{(k+1)^3} \qquad where\ k = \frac{(CL)}{(LA)} \qquad eq.20$$

Table 4.6 Solution statistical co-polymerisation of L-lactide and ε-caprolactone initiated by $Sc(BH_4)_2(C_3H_5)(THF)_2$ **1**; $Y(BH_4)_2(C_3H_5)(THF)_3$ **2;** $La(BH_4)_2(C_3H_5)(THF)_3$ **3**; $Nd(BH_4)_2(C_3H_5)(THF)_3$ **4**; $Sm(BH_4)_2(C_3H_5)(THF)_3$ **5**

Entry [a]	Initiator	LA:CL: BnOH	l_{LL} [j]	l_C [k]	r_1 [l]	r_2 [l]	$r_1.r_2$	T_{II} [m]
1	1	100:200:0	11.56	1.45	7.18	0.26	1.92	0.27
2	2	100:200:0	11.10	2.83	5.92	1.09	6.46	0.42
3	3	100:200:0	18.77	5.22	7.57	3.30	24.95	0.43
4	4	100:200:0	11.90	1.32	6.43	0.32	2.05	0.17
5	5	100:200:0	9.84	2.79	5.32	1.29	6.89	0.39
6	1	100:100:0	13.9	1	11.8	0.09	1.13	0
7	2	100:100:0	14.17	1.12	10.9	0.15	1.69	0.09
16	1	100:200:5	5.58	1.44	3.25	0.43	1.39	0.47
18	3	100:200:5	2.95	1.29	1.17	0.51	0.61	0.90
19	4	100:200:5	4.60	1.38	2.13	0.49	1.04	0.61
20	5	100:200:5	6.64	1.24	3.27	0.29	0.97	0.00
21	1	100:100:5	12.41	1.29	7.68	0.21	1.65	0.045
22	2	100:100:5	5.52	1.66	3.05	0.63	1.93	0.46
23	3	100:100:5	2.96	1.14	1.23	0.36	0.45	0.80
24	4	100:100:5	5.06	1.21	2.78	0.30	0.84	0.49
25	5	100:100:5	10.37	1.12	7.12	0.17	1.27	0.65
27	2	100:200:5	20.37	1.19	12.47	0.29	3.62	0.47
28	3	100:200:5	14.63	1	9.19	0.16	1.47	0.23
29	4	100:200:5	16.98	1	11.93	0.14	1.71	0.16

[a] n(RE) = 10 µmol, [M]:[RE]= 100:1, 70 °C in toluene. [j]Average sequence length of the lactidyl unit in the copolymer determined by ^{13}C NMR. [k]Average sequence length of the caproyl unit in the copolymer determined by ^{13}C NMR.[l] Reactivity ratios determined by ^{13}C NMR. [m] Transesterification degree.

The average sequence lengths and reactivity ratios obtained by the triad intensities of ^{13}C NMR (Table 4.6) are somewhat different from the ones obtained from the dyad intensities of ^{1}H NMR (Table 4.3), and the reason is the better accuracy of ^{13}C NMR and the detection of more monomer groups which cannot be known using the ^{1}H NMR spectra. However, the same trends can be deduced from these two sets of data and since we did not obtain in all cases ^{13}C NMR spectra with high resolution, which could allow us to calculate the intensities of the triads, we based our full interpretation and discussion (see above) on the ^{1}H NMR analysis of the isolated copolymers.

Along the experiments tabulated in Table 4.6, it is clear that the use of benzyl alcohol as CTA resulted in reduction in l_{LL} quantity which could be attributed to a decrease in incorporation of LA into the growing polymer chain with respect to CL, for example in case of Sc **1**, Nd **4** and Sm **5** catalysts and with aid of the CTA the l_{LA} length decreased from 11.56 (entry 1), 11.90 (entry 4) and 9.84 (entry 5) into 5.58 (entry 16), 4.60 (entry 19) and 6.64 (entry 20) respectively. Also under CTA condition the reactivity ratio decreased leading to $r_1.r_2$ in the range of 0.45-1.65 which is an indication to the formation of copolymers with more random character.

The second mode of transesterification (T_{II}), which stands for the CLC sequences with odd number of lactidyl units, was detected in most ^{13}C NMR spectra, except for few cases where T_{II} is negligible. The T_{II} coefficient was found to shift to higher values by adding benzyl alcohol to the system, knowing that, extending the reaction time from 5 h to 24 h can result in more transesterification in the composition of those copolymers. It should be stated that these transesterification reactions do not affect the rate of the reaction, but can cause the decrease in the molecular weight of the copolymers obtained.

4.2.5 Conclusion

The performances of the $RE(BH_4)_2(C_3H_5)(THF)_x$ (RE = Sc, x = 2; Y, La, Nd, Sm, x = 3) were studied in the random copolymerisation of *L*-Lactide and *ε*-caprolactone. The five complexes were found to be efficient towards the statistical copolymerisation of LA and CL, producing copolymers with preferential incorporation of lactide, and CL content up to 28 %

(yttrium catalyst) in the case of a 1:1 LA: CL feed. The CL units were randomly and single dispersed into the PLA backbone. When the starting quantity of CL was doubled, it was possible to incorporate higher amounts of CL, up to 59% (lanthanum catalyst), giving copolymers having a blocky character. Under CTA conditions (5 equiv BnOH), significant improvement in the control of the copolymerisation was observed: i) high CL amounts were obtained (up to 47.5 % with *L*-LA:*ε*-CL = 1:1; up to 62.2 % with *L*-LA:*ε*-CL = 1:2); ii) the CL was found statistically distributed over the PLA frame, giving a range of copolymers from random with Sc, Y, and Sm, to alternating with the larger Nd and La; iii) much narrow distributions but higher degrees (in case of 1:2 feed, by comparison with experiments done with 1:1 feed) of transesterification were finally noticed under such conditions; iv) In all cases the use of benzyl alcohol reduced l_{LA} in the polymer chain and decreased the reactivity ratios.

4.3 Copolymerisation of isoprene and ε-caprolactone

4.3.1 Introduction

High-strength polymer composites are of growing interest, but one limitation to form such products is that most polymeric mixtures are immiscible together and thus the components phase separate into different levels. In this context a variety of block copolymers are commonly used as compatibillizing agents.[58-61] For example, consider two immiscible polymers poly(A) and poly(B), the best route to compatibillize them is to use block copolymer formed of A and B monomers, i.e. poly(A)-*block*-poly(B), which should be proceeded by the blending step of poly(A), poly(B) and poly(A)-block-poly(B). Beyond this, diblock copolymer formed of polar (*ε*-caprolactone) and non-polar (diene) monomers are of particular interest and have been known and discussed for a long time. [62-73] However, the copolymerisation of IP and CL that yields polyisoprene-*block*-polycaprolactone (PIP-*b*-PCL) was limited to few records in the literature. [70-73]

Visseaux *et al.* used an ansasamarocene allyl initiator to produce diblock copolymer of 1,4-*trans*-PIP and PCL. First they synthesized the 1,4-*trans*-PIP, where the PIP grew on the allyl moiety. Next the CL was inserted onto the allyl moiety of the Sm-PIP chain and the polymerisation of the CL continues to grow via the alkoxide active species (Scheme 4.5).[70]

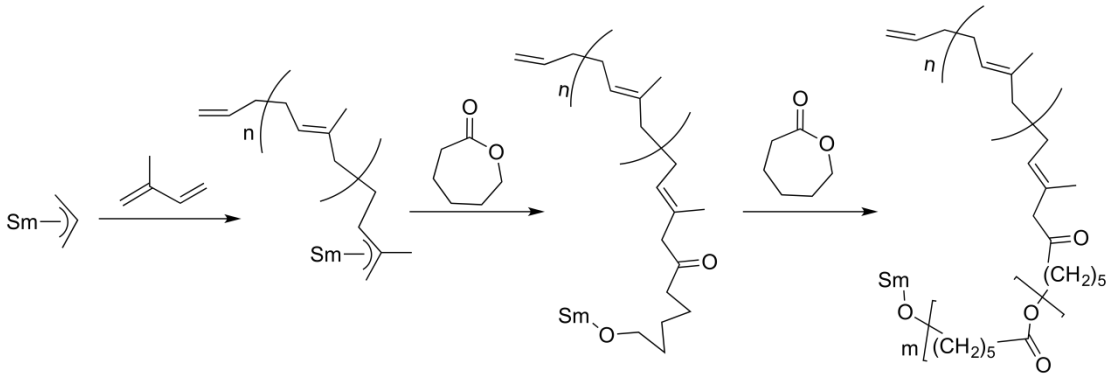

Scheme 4.5 PIP-*b*-PCL formation from ansasamaocene allyl complex (ligands omitted for clarity).[73]

Hou, Cui *et al.* used their activated cationic yttrium-polyisoprene species, to initiate the ROP polymerisation of CL affording pure diblock copolymers of poly(*cis*-1,4-IP)-*b*-PCL, with high moleculer weight up to 70300 $g.mol^{-1}$.[71]

Zhang *et al.* used a typical Ziegler-Natta catalyst system [$Nd(Oi\text{-}Pr)_3$/Al(*i*-$Bu)_2H/Me_2SiCl_2$] in conjunction with Al(*i*-$Bu)_2H$ as co-catalyst and CTA. The latter helps in polymerisation by exchanging the PIP with the catalyst and increasing the number of growing polymer chains per Nd center up to 6-8 chains.[72]

4.3.2 Copolymerisation of isoprene and ε-caprolactone using $Nd(BH_4)_2(C_3H_5)(THF)_3$

As previously mentioned, $Nd(BH_4)_2(C_3H_5)(THF)_3$ showed the ability to polymerise both IP and CL (CL stands for *ε*-caprolactone for the rest of this chapter) (chapter 3), as single component catalyst (without the aid of co-catalyst). This polymerisation ability can be attributed to the presence of two different active ligands. Isoprene polymerises on the allyl ligand while CL has the potential to polymerise on both the borohydride and allyl ligand. Although it was proved by chain end analysis using NMR spectroscopy that borohydride preferentially initiates the CL monomer, allyl group, in theory, could also initiate a small portion of CL to yield PCL small chains (oligomers) (Figure 4.11).

Therefore, we wanted to study the ability of this complex to conduct the one-pot and sequential copolymerisation of IP and CL, trying to form a block copolymer or to confirm our findings of chain end analysis of PCL.

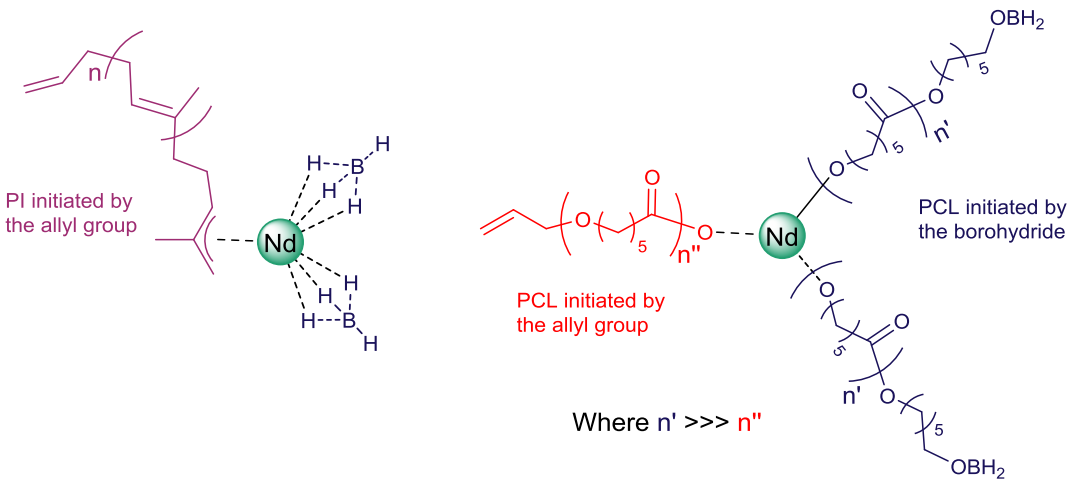

Figure 4.11 Possible growing chains of PIP and PCL on the $Nd(BH_4)_2(allyl)(THF)_x$ complex.

The polymerisation tests were conducted in toluene at 50 or 80 °C in three different ways: the sequential addition of IP followed by CL, CL followed by IP and the simultaneous addition of both monomers (Table 4.6). In theory adding isoprene first can lead to the growth of one PIP chain initiated by the allyl group of the $Nd(BH_4)_2(C_3H_5)(THF)_3$ because the borohydride on its own is not capable to initiate the polymerisation of such monomer. Then the coming CL can form two PCL chains by the two borohydride groups, and another one by the allyl group belongs to the PIP-RE species (Scheme 4.6). When caprolactone is polymerised first, there are two possibilities: i) CL polymerises on the three available different sites, thus no active initiating group left for the isoprene when added, ii) only the two borohydride starts forming PCL, so isoprene begins to grow on the allyl group as soon as it is added (Scheme 4.7). Finally, when the two monomers are mixed together in one-pot, this will result in monomers competition toward the catalyst.

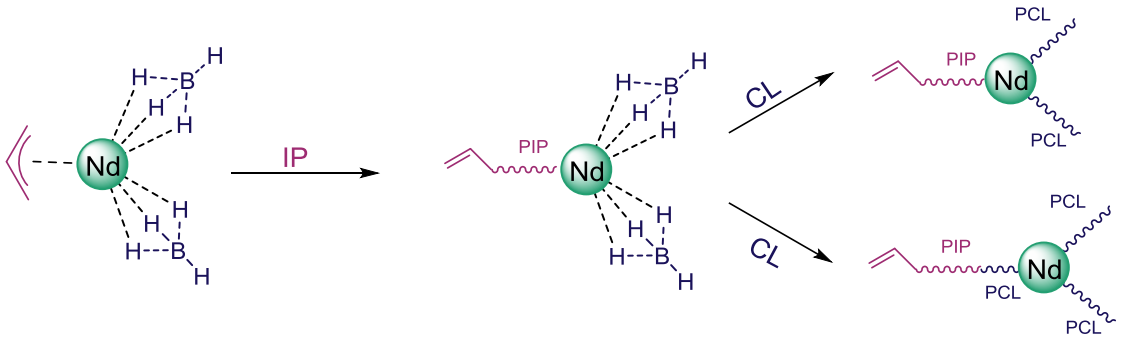

Scheme 4.6 Sequential copolymerisation of isoprene followed by ε-caprolactone.

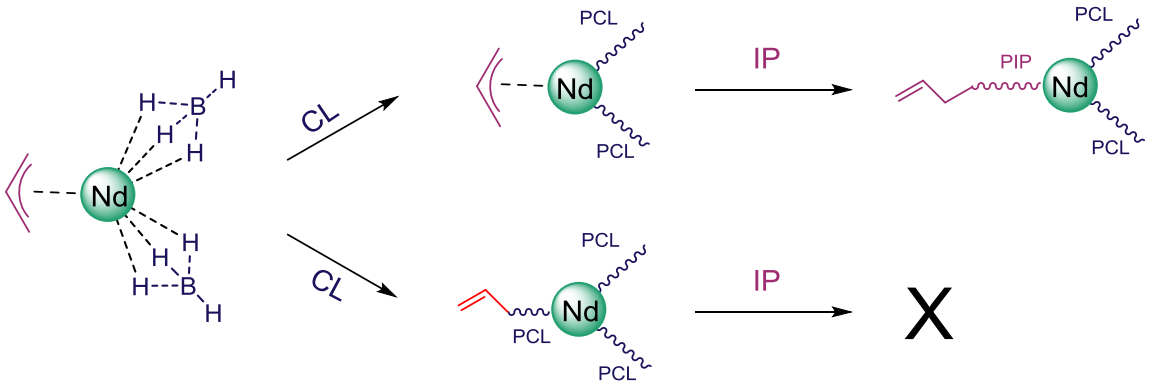

Scheme 4.7 Sequential copolymerisation of ε-caprolactone followed by isoprene.

Table 4.6 Copolymerisation of ε-caprolactone and isoprene with $Nd(BH_4)_2(allyl)(THF)_3$ complex

Entry [a]	[IP]:[CL]:[Nd]	Order of addition		Yield %	$M_{n\ SEC}$ (g/mol) [d]	Đ [d]	PIP:PCL (final polymer)	1,4-trans (cis), %
		M_1	M_2					
31	**500:500:1**	IP	CL	76	69200	2.36	1:2	91.4 (8.6)
32	**500:500:1**	CL	IP	64	19500	1.58	0:1	-
33	**500:100:1**	CL	IP	22	-	-	0:1	-
34	**500:100:1**	IP +CL (one-pot)		4.4	10700 25800	1.34 1.05	1:8	100 (0)
35[d]	**500:100:1**	IP +CL (one-pot)		11	16000	1.48	1:0.7	88.4 (5.9)
36[e]	**500:100:1**	IP +CL (one-pot)		0.7	8600	2.71	1:3	100 (0)

[a] T (IP) = 50 °C, T (CL) = 25°C, in toluene, time = 24 h . [b] Ratio given per equivalent of metal atom. [c] Determined by SEC in THF at 40 °C, uncorrected values. [d] time = 1 week [e] time = 48 h, T = 80 °C.

^{1}H NMR analysis of the isolated polymer was recorded in $CDCl_3$, to determine the found ratio of the IP and CL based on the resonances at 5.11 and 4.05 ppm (Figure 4.12). When caprolactone was added to the isoprene polymerisation system in equal equivalences (entry 31), the found ratio for the PIP:PCL in the isolated product was equal to 1:2. $M_{n\ SEC}$ was relatively high (69200 g.mol^{-1}) and dispersity index was 2.36, which is in consistent with the presence of two types of polymers in accordance with the bimodal SEC curve. The comparison of the latter to the SEC trace recorded for a PIP aliquot taken before the addition of the CL gives insight about the structure of the obtained polymer. It can be seen that the trace for PIP does not change indicating that PCL did not continue to grow on the PIP but more probably was initiated by the borohydride ligands (Figure 4.13).

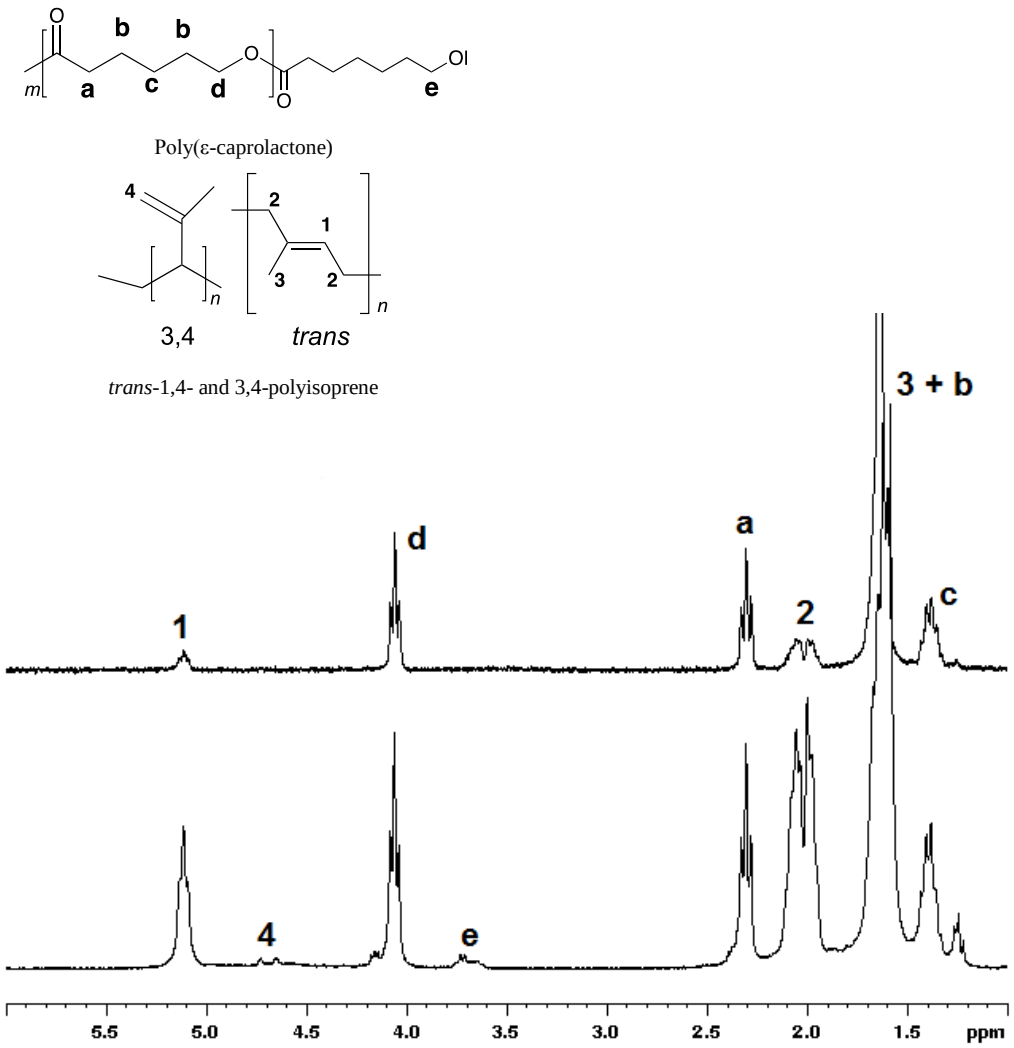

Figure 4.12 ^{1}H NMR spectra of polymers synthesized in entry 31 (bottom) and 34 (top) in $CDCl_3$.

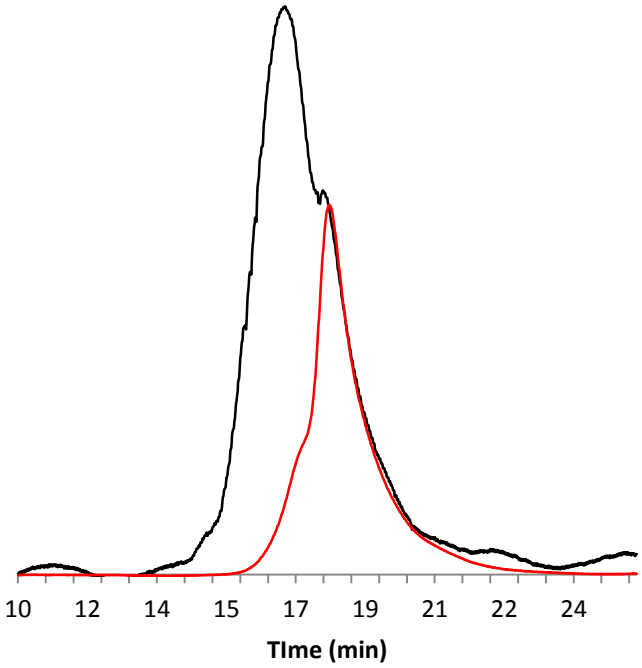

Figure 4.13 SEC curves of polymers synthesized in entry 31, before (red trace) and after (black trace) ε-caprolactone addition.

It is important to note that this method of polymerisation is different from the previously discussed ones, as there are two different active ligands with different reactivity. This is a further indication, supporting that PCL did not polymerise on the allyl group, even when there is a living polyisoprene on the allyl group. In contrast, for the case of the polymerisation using the ansasamarium allyl initiator, the reactivity of the samarium-polyisoprene group resulted in an increase in reactivity towards the CL.[70]

Then, when the polymerisation was conducted in reverse, *i.e.* addition of CL before IP (entry 32), IP was not polymerised and only PCL was produced as seen from both the ^{1}H NMR spectrum and SEC curves (Figure 4.14). This was also the case when the ansasamarocene allyl initiator was used to first polymerise CL followed by IP.[70]

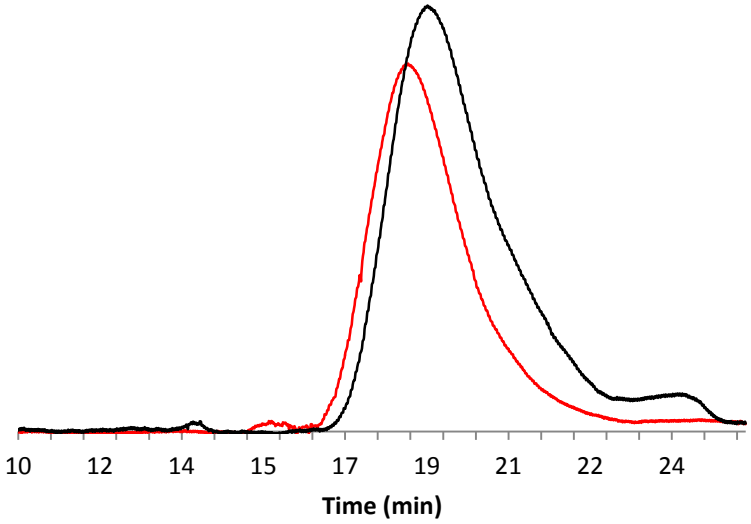

Figure 4.14 SEC curves of the polymers synthesized in entry 32, before (red trace) and after (black trace) isoprene addition.

Even when the ratio of CL was decreased relatively to IP (CL:IP ratio decreased to 100:500 from 500:500) (entry 33), IP was not polymerised and only PCL was produced. The selective polymerisation of PCL, could be due to the polar PCL growing around the catalyst and possibly coordinating to the neodymium, preventing and repelling the non-polar IP from coordinating into the neodymium center and inserting into the allyl bond.

Finally, both monomers were added at the same time as a mixture to the catalyst in the ratio of 100:500 for CL:IP (entry 34). The PIP:PCL ratio of the isolated polymer determined by ^{1}H NMR analysis was equal to 1:8 and the SEC curve was found to be bimodal which probably corresponds to the presence of both homopolymers of *trans*-1,4-IP and CL as already discussed. When the same polymerisation was allowed to react for one week at 50°C (entry 35), PIP:PCL ratio in the final polymer was found to be 1:0.7 which means that much more IP was allowed to polymerise. However, this resulted in a poor yield (11%) and very broad SEC curve displaying three populations, one of which can be contributed to the copolymer and the other two for the homopolymers (Figure 4.15). The prolonged heating could have compromised the polymerisation of both monomers. When

both the monomers were added to the catalyst and heated to 80 °C over 2 days (entry 36), there was a higher ratio of CL polymerised in comparison to IP than when heated at 50°C for 24 hours (PIP:PCL 1:0.7, entry 35). The yield was very poor (0.7 %) and also the SEC curve displayed three populations, which is similar to entry 35 where the copolymer could be formed. In all cases where IP was polymerised, the *trans*-1,4 isomer was predominantly formed, with conversion ranging from 88.4 to 100%.

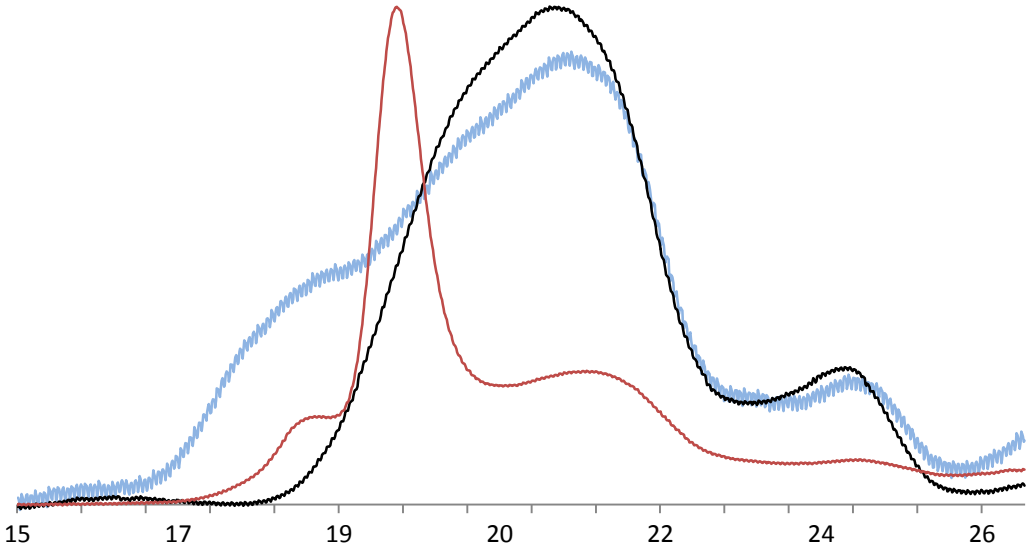

Figure 4.15 SEC curves of the polymers resulting from the polymerisations conducted with a mixture of IP and CL (entry 34 - 36). Black trace corresponds to entry 34, red trace to entry 35 and blue trace to entry 36.

4.3.3 Conclusion

$Nd(BH_4)_2(C_3H_5)(THF)_3$ has shown a unique ability to polymerise not only two different monomers, but monomers which have different polar characteristics, independently of each other, aside from probably forming a copolymer of IP and CL. Unfortunately, it displayed poor copolymerisation ability towards IP and CL. Interestingly, the ability of the catalyst to polymerise IP in the presence of CL supports the hypothesis that in the presence of CL only some RE—allyl moieties remain unreacted. In other words, this confirms the preferential reactivity of the RE—(BH_4) rather than the RE—allyl towards the ROP of CL. These

attempts at copolymerisations were different from the previously published ones as there are two active ligands as opposed to just one.

Top our knowledge, there is no other example in the literature of a catalyst that enables homopolymerisation of two different monomers in the same pot with two different chains growing.

4.4 References

[1] M. Labet, W. Thielemans, *Chem. Soc. Rev*. **2009**, *38*, 3484.

[2] Y. Shen, K. J. Zhu, Z. Shen, K. M. Yao, *J. Polym. Sci., Part A: Polym. Chem.* **1996**, *34*, 1799.

[3] A. Schindler, R. Jeffcoat, G. L. Kimmel, C. G. Pitt, M. E. Wall, R. Zweidinger, *in Contemporary Topics in Polymer Science*; *Vol. 2* (Eds: E. M. Pearce, J. R. Schaefgen) Plenum: New York, **1977**, pp. 251.

[4] K. Van Butsele, R. Jerome, C. Jerome, *Polymer* **2007**, *48*, 7431.

[5] R, Wada, S. H. Hyon, T. Nakamura, Y. Ikada, *Pharm. Res.* **1991**, *8*, 1292.

[6] M. F. Meek, K. Jansen, R. Streendam, W. van Oeveren, P. B. van Wachem, M. J. A. van Luyn, *J. Biomed. Mater. Res.* **2004**, *68A*, 43.

[7] D. Dakshinamoorthy, F. Peruch, *J. of Polym. Sci.* **2012**, *50*, 2161.

[8] K. Nalampang, R. Molloy, W. Punyodom, *Polym. Adv. Technol*. **2007**, *18*, 240.

[9] M. Leonora de Castro, S. H. Hui Wang, *Polymer Bulletin* **2003**, *51*, 151.

[10] Y. Shen, K. J. Zhu, Z. Shen, K. Yao, *Journal of Polymer Science: Part A: Polymer Chemistry* **1996**, *34*,1799.

[11] J. Fernandez, E. Meaurio, A. Chaos, A. Etxeberria, A. Alonso-Varona, J.R. Sarasua, *Polymer* **2013**, *54*, 2621.

[12] R.M. Rasal, A.V. Janorkar, D.E. Hirt, *Prog. Polym. Sci*. **2010**, *35*, 338.

[13] R. H. Platel, L. M. Hodgson, C. K. Williams, *Polym. Rev.* **2008**, *48*, 11.

[14] J. Wu, T. L. Yu, C. T. Chen, C. C. Lin, *Coord. Chem. Rev*. **2006**, *250*, 602.

[15] M. H. Huang, S. Li, J. Coudane, M. Vert, *Macromol. Chem. Phys*. **2003**, *204*, 1994.

[16] O. Jeon, S. H.Lee, S. H. Kim, Y. M. Lee, Y. H. Kim, *Macromolecules* **2003**, *36*, 5585.

[17] J. L. Wang, C. M. Dong, *Macromol. Chem. Phys*. **2006**, *207*, 554.

[18] Z. Wei, L. Liu, F. Yu, P. Wang, C. Qu, M. Qi, *Polym. Bull.* **2008**, *61*, 407.

[19] I. Barakat, P. Dubois, R. Jerome, P. Teyssie, M. Mazurek, *Macromol. Symp.* **1994**, *88*, 227.

[20] D. Tian, P. Dubois, R. Jerome, *Macromolecules* **1997**, *30*, 1947.

[21] P. J. A. IntVeld, E. M. Velner, P. V. D. Witte, J. Hamhuis, P. J. Dijkstra, J. Feijen, *J. Polym. Sci. Part A: Polym. Chem.* **1997**, *35*, 219.

[22] J. K. Kim, D. J. Park, M. S. Lee, K. J. Ihn, *Polymer* **2001**, *42*, 7429.

[23] D. Pappalardo, L. Annunziata, C. Pellecchia, *Macromolecules* **2009**, *42*, 6056.

[24] P. Vanhoorne, Ph. Dubois, R. Jerome, Ph. Teyssie, *Macromolecules* **1992**, *25*, 37.

[25] Y. Shen, K. J. Zhun, Z. Shen, K. M. Yao, *J. Polym. Sci. Part A: Polym. Chem.* **1996**, *34*, 1799.

[26] M. Bero, J. Kasperczyk, *Macromol. Chem. Phys*. **1996**, *197*, 3251.

[27] G. Kister, G. Cassanas, M. Bergounhon, D. Hoarau, M. Vert, *Polymer* **2000**, *41*, 925.

[28] F. Fay, E. Renard, V. Langlois, I. Linossier, K. Vallee-Rhel, *Eur. Polym. J*. **2007**, *43*, 4800.

[29] L. Calandrelli, A. Calarco, P. Laurienzo, M. Malinconico, O. Petillo, G. Peluso, *Biomacromolecules* **2008**, *9*, 1527.

[30] A. J. Chmura, M. G. Davidson, M. D. Jones, M. D. Lunn, M. F. Mahon, A. F. Johnson, P. Khunkamchoo, S. L. Roberts, S. S. F. Wong, *Macromolecules* **2006**, *39*, 7250.

[31] C. X. Song, X. D. Feng, *Macromolecules* **1984**, *17*, 2764.

[32] C. Jacobs, Ph. Dubois, R. Jerome, P. Teyssie, *Macromolecules* **1991**, *24*, 3027.

[33] X. Deng, Z. Zhu, Ch. Xiong,; L. Zhang, *J. Polym. Sci. Part A: Polym. Chem.* **1997**, *35*, 703.

[34] D. Cui, T. Tang, W. Bi, J. Cheng, W. Chen, B. Huang, *J. Polym. Sci. Part A: Polym. Chem.* **2003**, *41*, 2667.

[35] F. Stassin, R. Jerome, *J. Polym. Sci. Part A: Polym. Chem.* **2005**, *43*, 2777.

[36] L. Fan, Y. B. Xiong, H. Xu, Z. Q. Shen, *Eur. Polym. J*. **2005**, *41*, 1647.

[37] M. Florczak, J. Libiszowski, J. Mosnacek, A. Duda, S. Penczek, *Macromol. Rapid Commun*. **2007**, *28*, 1385.

[38] N. Nomura, A. Akita, R. Ishii and M. Mizuno, *J. Am. Chem. Soc.* **2010**, *132*, 1750.

[39] A. Pilone, N. De Maio, K. Press, V. Venditto, D. Pappalardo, M. Mazzeo, C. Pellecchia, M. Kolb, M. Lamberti, *Dalton Trans*. **2015**, 44, 2157.

[40] L. Li, B. Liu, D. Liu, C. Wu, S. Li, D. Cui, *Organometallics* **2014**, *33*, 6474 and refs cited therein.

[41] C. Bonné, A. Pahwa, C. Picard, M. Visseaux, *Inorg. Chim. Acta* **2017** *455*, 521.

[42] A. Valente, P. Zinck, A. Mortreux, M. Visseaux, *J. Polym. Sci. Part A* **2011**, *49*, 1615.

[43] I. R. Herbert, *Statistical Aanalysis of Copolymer Sequence Distribution, in NMR Spectroscopy of Polymers* (Eds: R. N. Ibbet), **1993**, pp. 50.

[44] D. J. Darensbourg, O. Karroonnirun and S. J. Wilson, *Inorg. Chem.* 2011, **50**, 6775-6787.

[45] P. C. Painter and M. M. Coleman, *Spectroscopy and the Characterization of Chain Microstucture*, in *Essentials of Polymer Science and Engineering*, DEStech Publications, Inc, **2008**, pp. 167.

[46] Y. Chen and A. Sen, *Macromolecules* **2009**, *42*, 3951.

[47] A. M. V. Herk and T. Dröge, *Macromol. Theory Simul.* **1997**, *6*, 1263.

[48] M. Fineman and S. D. Ross, *J. Polym. Sci.* **1950**, *5*, 259.

[49] T. Kelen and F. Tudos, *J. Macromol. Sci. Chem.* **1975**, ***A9***, 1.

[50] H. R. Kricheldorf, I. Kreiser, *Makromol. Chem.* **1987**, *188*, 1861.

[51] H. R. Kricheldorf, T. Mang, J. M. Jonte, *Makromol. Chem*. **1985**, *186*, 955.

[52] F. Chabot, M. Vert, S. Chapelle, P. Granger, *Polymer* **1983**, *24*, 53.

[53] H. F. Kricheldorf, J. M. Jonte, M. Berl, *Makromol. Chem., Suppl*. **1985**, *12*, 25.

[54] D. W. Grijpma, G. J. Zondervan, A. Pennings, *J. Polym. Bull*. **1991**, *25*, 327.

[55] D. W. Grijpma, A. J. Pennings, *Polym. Bull*. **1991**, *25*, 335.

[56] J. Kasperczyk , M. Bero, *Makromol. Chem*. **1991**, *192*, 1777.

[57] J. Kasperczyk , M. Bero, *Makromol. Chem*. **1993**, *194*, 913.

[58] H. Zhao, B. Huang, *J.Polym. Sci. Part B: Polym. Phys.* **1998**, *36*, 85.

[59] D. R. Paul, S. Newman, *Polymer Blends Vol. 2*, Acadmic Press, New York, **1978**.

[60] A. Padwa, *Prog. Polym. Sci.* **1989**, *14*, 811.

[61] R. Israels, D. P. Foster, A. C. Balazs, *Macromolecules* **1995**, *28*, 218.

[62] K. Nobutoki, H. Sumitomo, *Bull. Chem. Soc. Jpn.* **1967**, *40*, 1741.

[63] W. H. Sharkey (to du Pont Company), US. Pat. 3,557,255 Jan. 19, **1971**.

[64] R. P. Foss (to du Pont Company) US. Pat. 3,821,331 June 28,**1974**.

[65] H. L. HSIEH, *J. of App. Polym. Sci.* **1978**, *22*, 1119.

[66] E. Buzdugan, P. Ghioca, N. Stribeck, E. J. Beckman, S. Serban, *Macromol. Mater. Eng.* **2001**, *286*, 497.

[67] V. Balsamo, R. Stadler, *Macromolecules* **1999**, *32*, 3994.

[68] S. Nojima, N. Nikuchi, A. Rohadi, S. Tanimoto, S. Sasaki, *Macromolecules* **1999**, *32*, 3727.

[69] L. Freibe, O. Nuyken, H, Windisch, W. Obrecht, *Macromol. Mater. Eng.* **2003**, *288*, 484.

[70] D. Barbier-Baudry, F. Bonnet, A. Dormond, E. Finot, M. Visseaux, *Macromol. Chem. Phys.* **2002**, *203*, 1194.

[71] L. Wang, D. Cui, Z. Hou, W. Li , Y. Li, *Organometallics* **2011**, *30*, 760.

[72] F. Wang, C. Y. Zhang, Y. M. Hu, X. Y. Jia, C. X. Bai, X. Q. Zhang, *Polym* **2012**, *53*, 6027

[73] C. Yao, D. Liu, P. Li, C. Wu, S. Li, B. Liu, D. Cui, *Organometallics* **2014**, *33*, 684.

[74] C. K. Williams, *Chem. Soc. Rev.*, **2007**, *36*, 1573.

CHAPTER 5

PHOSPHASALEN RARE-EARTH BOROHYDRIDE COMPLEXES

5.1 Introduction to metal-Salen Schiff base complexes

5.1.1 Ligands synthesis and coordination chemistry

A Schiff base (also known as imine or azomethine), named after Hugo Schiff,[1] is a compound displaying a general structure $(R^1)(R^2)C=N(R)$ (Figure 5.1). It is a nitrogen analogue of an aldehyde or ketone in which the carbonyl group is replaced by an imine or azomethine group. It is formed from the condensation of primary amine and aldehyde.[2]

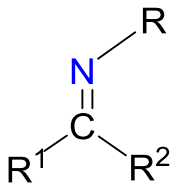

Figure 5.1 General structure of Schiff base; R, R^1 or/and R^2 = alkyl or aryl.

The condensation of 2 equiv. of salicylaldehyde with 1,2-diamines leads to the formation of a highly important class of ligands known as "Salen". Salicylaldehydes with different substituents can be obtained by introducing a formyl group into the corresponding phenol derivative (Scheme 5.1). The variation of the substituents on the diamine linkage, phenoxide rings or on the carbon of the imine function extends largely this class of ligands.[3-5]

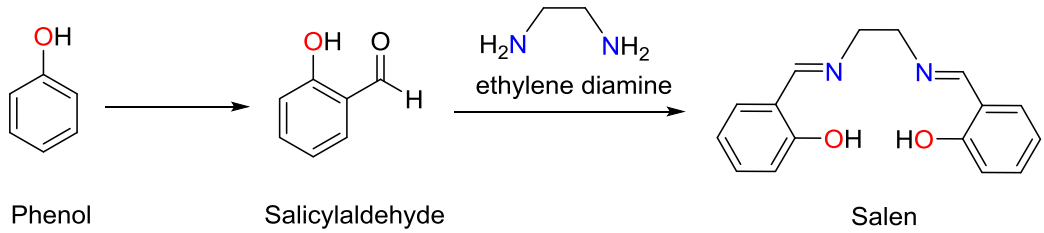

Scheme 5.1 Preparation of non-substituted Salen ligand.

Although the term "Salen" was originally used only to describe the tetradentate Schiff bases derived from ethylene diamine, the more general term Salen-type is used in the

literature to describe the class of [O,N,N,O] tetradentate Schiff base ligands (Figure 5.2, A, B, C). Interestingly, a second generation of Salen ligands was synthesized later by introducing asymmetric centers at different places on the molecule.[6] Recently, a new pentadentate congener of the type [O,N,O,N,O] was synthesized (Figure 5.2, D).[7]

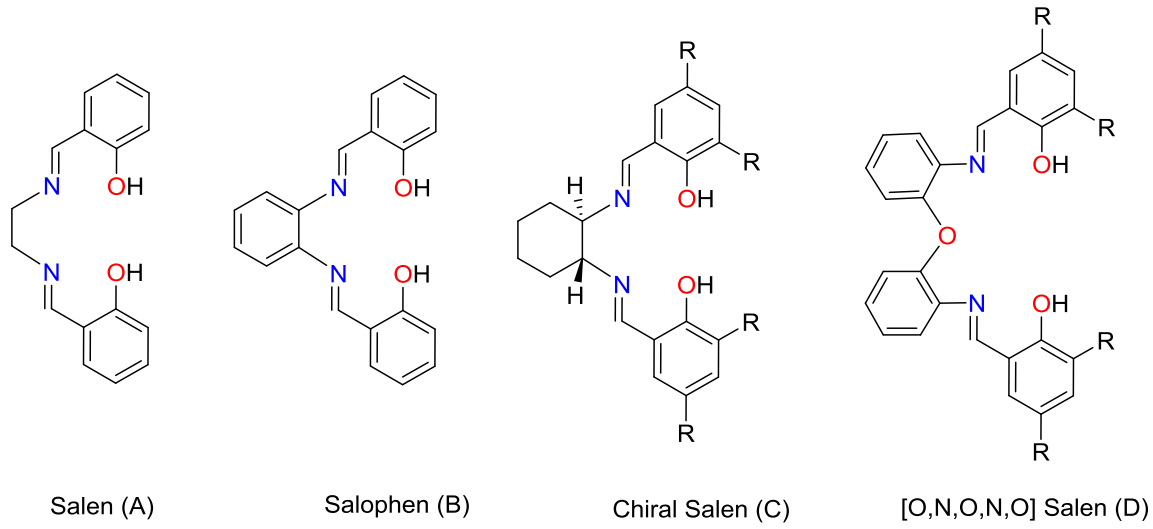

Figure 5.2 Various examples of Salen ligands.

Salen ligands are particularly suitable for the coordination of metal complexes, due to the ease of the reaction conditions and the variety of chiral amines and aldehydes available as precursors. The double deprotonation of Salens yields tetradentate dianionic ligands which have the ability to bind strongly to a metal center through the phenoxide and imine groups. Salen ligands were first introduced in transition metal complexes. The list includes among other, metals such as Mn,[8] Cr,[9] Co,[10] V,[11] Cu [12] Ti,[13] Ru,[14] Pd,[15] Au,[16] Zn[17] and Al.[18] Depending on the coordination mode of the tetradentate [O,N,N,O] or pentadentate N_2O_2X ligands around the metal center, the complexes exhibit a distorted square planar or square pyramidal geometry.[19-22]

Aftrewards, Salen ligands were involved in the synthesis of rare-earth (RE) based complexes. The field was first investigated nearly two decades ago by Ovitt and Coates who synthesized the yttrium complex $[(R)(SalBinap)YO(CH_2)_2\text{-}NMe_2]_2$ [23,24] and used it as an initiator in the ROP of *meso*-lactide, showing moderate activity along with poor tacticity control.[23,24] Some years later, several complexes were designed in this purpose, and they showed beneficial use in polymerisation catalysis (Figure 5.3).[25-28]

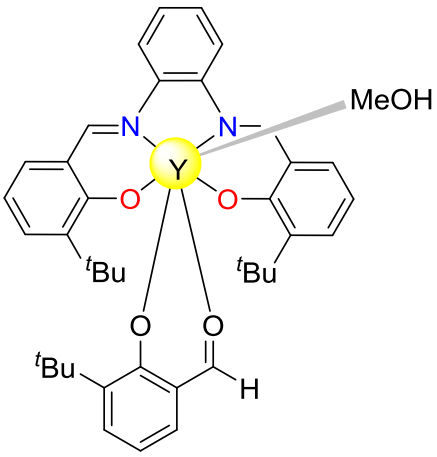

• *poly(cyclohexene)carbonate selectivity > 99.1 %* [25]
• *> 99 % carbonate linkages* [25]

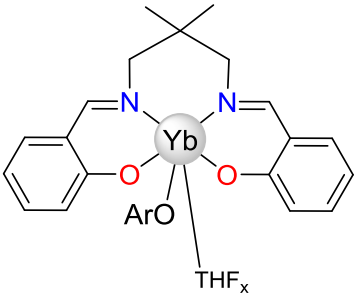

• *heretotactic poly(lactide), P_r up to 0.85* [26]

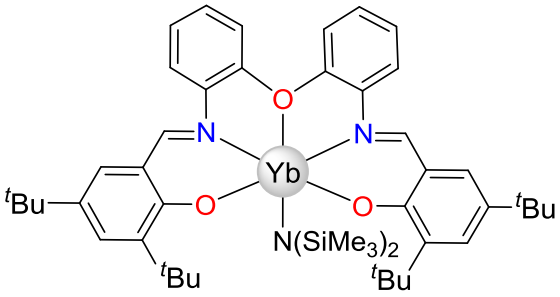

• *heretotactic poly(lactide), P_r up to 0.90* [27]

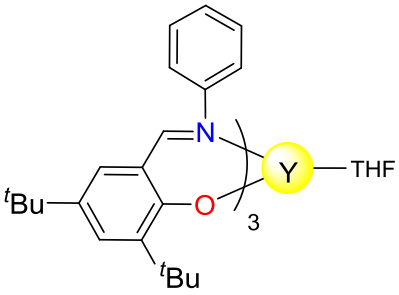

• *Co-catalyst: Al(^{i}Bu)$_3$*
⟹ *poly(n-octyloxyallene), yield 100 %* [28]

Figure 5.3 Representative examples of Salen rare-earth complexes used as polymerisation initiators.

The complexation takes place *in situ* by reaction between the Salen ligand and well-defined metal precursors. In a general manner, five different routes are available for the preparation of Salen metal-based complexes (Scheme 5.2).[4]

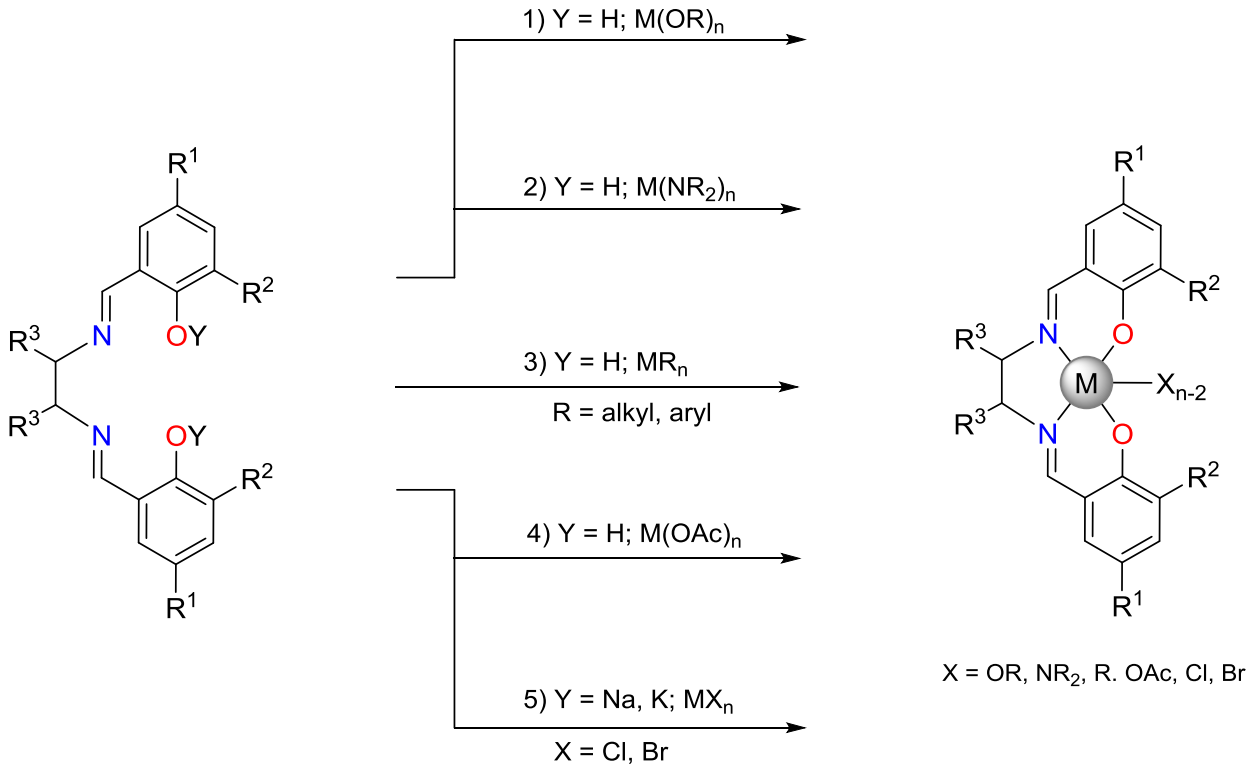

Scheme 5.2 Preparation of Salen metal-based complexes.[4]

Route 1 requires the use of metal alkoxides, $M(OR)_n$ (M = Ti, Zr). These compounds are commercially available and easy to handle, in contrast to RE derivatives which are more problematic because of their high sensitivity to moisture. Although, metal Schiff bases having alkoxide ligands are sensitive to water traces, producing various, μ-oxo, species.

Route 2 consists in the use of metal amides, $M(NMe_2)_4$ (M = Ti, Zr). The reaction proceeds via the elimination of the acidic proton of the phenol ring and the formation of the volatile $NHMe_2$. $M(NMe_2)_4$ are considered as highly suitable precursors for the preparation of complexes of early transition metal. $RE(NTMS_2)_3$ may also be considered here (TMS = $SiMe_3$).

In Route 3, metal alkyls are used to form Salen complexes bearing alkyl ligand in clean and effective way by direct exchange reaction. Various metals alkyls have been used for this reaction, such as $AlMe_3$, $GaMe_3$, $InMe_3$, which are commercially available. Several complexes of the type $M(Mesityl)_n$ (M = Fe, Mn, V, Cu, Mesityl = 2,4,6-trimethylbenzene)

compounds were produced. Noteworthy, the synthesis of mesityl complexes can be difficult due to their sensitivity.

Route 4 involves metal acetates, $M(OAc)_2$ (M = Ni, Cu, Co), the reaction being conducted under reflux conditions.

Route 5 is a two-step reaction involving the deprotonation of the Salen ligand followed by the reaction with metal halides. The deprotonation can be done using NaH or KH in excess, generally a coordinating solvent such as THF is recommended for such reactions, and the excess of NaH or KH can be removed easily by filtration. Deprotonation can also occur using BuLi or MeLi, however, lithium alkyls can attack the imine group of the Schiff base.

5.1.2 Configurations and conformations

The geometry of the Salen ligands around the metal center, in addition to their electronic properties, largely affects the catalytic activities of the resulting complexes. The presence of imine function connected to the phenoxide ring brings rigidity to the ligand, which renders the geometry of the complex more controlled, thus with less flexibility which is detrimental to many catalytic conformations. However, the rigidity can be overcome by adding two sp^3 carbons to the diamine backbone. The [O,N,N,O] ligand can adopt many configurations when it is coordinated to the metal center (Figure 5.4): i) *trans*-configuration, in which the [O,N,N,O] occupies all the four equatorial positions and the two ancillary ligands (Z and W) occupy two apical positions, ii) *cis-α* in which the two ancillary ligands take two equatorial positions, and *cis-β* where they occupy one apical and one equatorial positions.[29] It is important to note that the major configuration observed for Salen complexes is *trans*, with two typical ones, *stepped* and *umbrella* configurations depending on the substituents on the diamine backbone. [4,6]

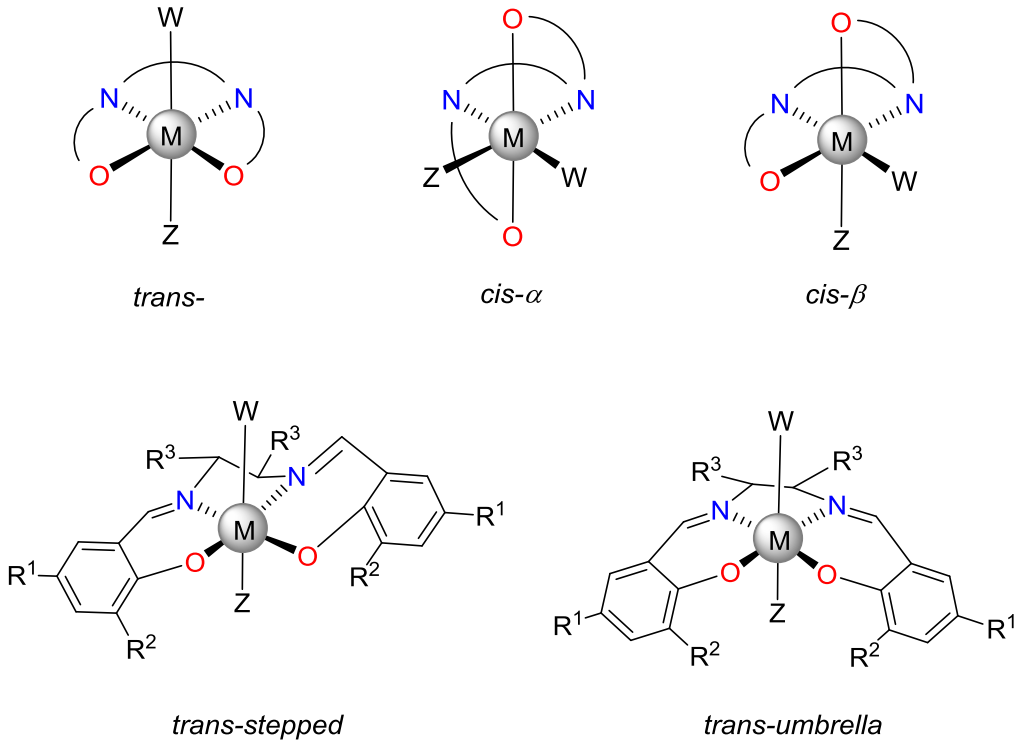

Figure 5.4 Configurations and conformations of Salen complexes.[29]

Furthermore, the steric factor from the ancillary ligands has a strong effect on the conformation of the Salen ligands. For instance *trans-stepped* complexes can exist as two possible conformations which are in equilibrium. The introduction of a chiral element in Z shifts the equilibrium to one side (Figure 5.5).

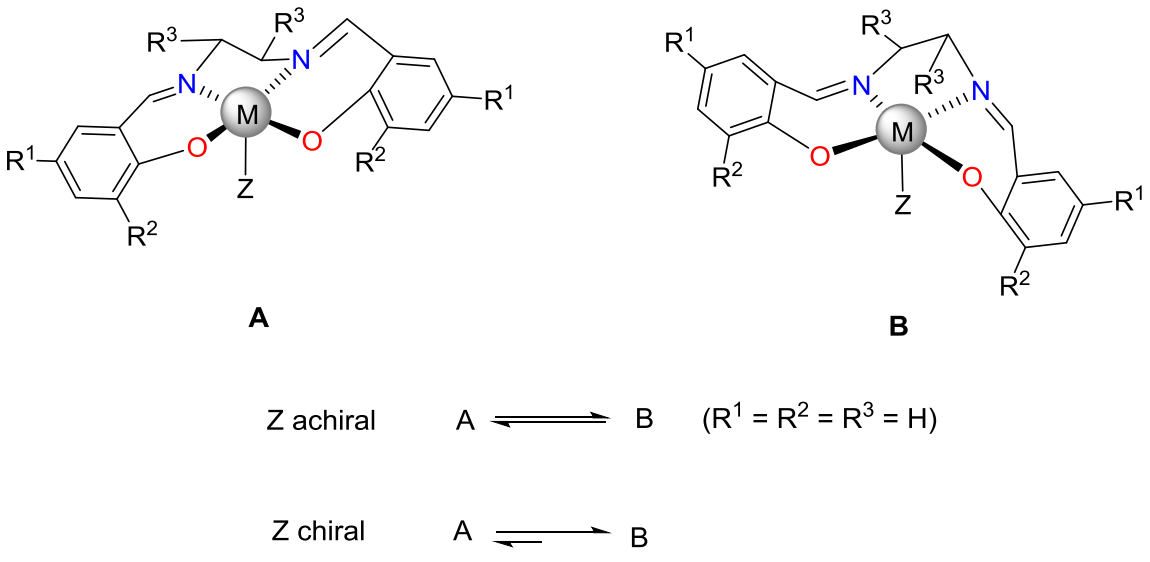

Figure 5.5 Influence of ancillary ligands to the conformation of Salen.[29]

Moreover, when the ancillary ligand is multidentate, like acetylacetonate or oxalate (bidentate ligands), they change the configuration from *trans* to *cis*, as in the case of the Co(II) Salen complexes.[30,31] However, Salen complexes of some metals prefer the *cis*-configuration, in the presence or absence of multidentate ancillary ligand.

In addition, the coordinating solvent can affect the final configuration of Salen complexes. For example, zirconium and hafnium Salen complexes form seven-coordinated pentagonal bipyramidal geometry, in which one THF molecule occupies an equatorial position along with the Salen ligands in *trans*-configuration. However, heating in toluene removes the THF molecule and leads to an octahedral geometry with *cis-β* configuration of the resulting compound (Scheme 5.3).[32]

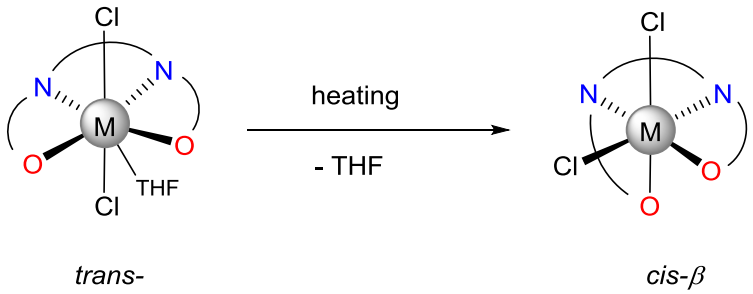

Scheme 5.3 T*rans-cis* configurations transition of zirconium and hafnium Salen complexes.[29]

Later, new Salan ligands were developed having one or two amine functions instead of imine (Figure 5.6). The change of the double bond C=N in the imine group of the Salen to a single one in the amine group of Salan gave to the [O,N,N,O] more flexibility which lead to the formation of *cis*-complexes.[33,34,47]

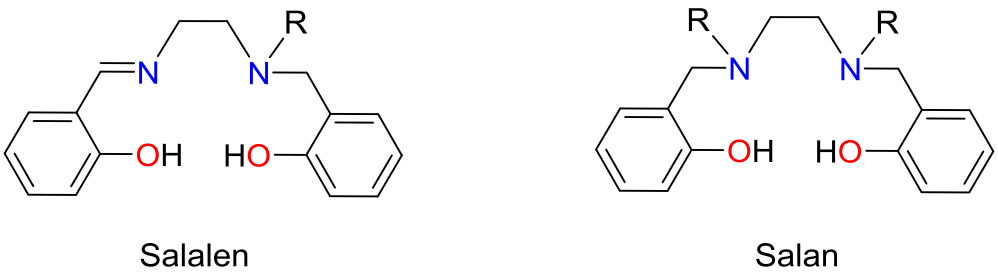

Figure 5.6 Structures of Salalen and Salan ligands.

An important progress in this field was done by Auffrant, Le Floch *et al.* [35,36] who synthesized a new Salen-based ligand replacing the imines with iminophosphorane, so called phosphasalen ligand (Figure 5.7). The P=N bond in the latter is not a real double bond, which renders the ligand more flexible and allows it to rotate around the metal center. In addition, electronic properties of P=N are very different from imine, amine or amide.[37-39]

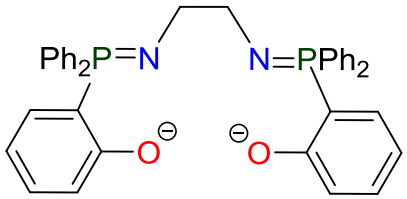

Figure 5.7 Structure of the phosphasalen ligand.[35]

Simultaneously, Diaconescu *et al.* developed a new ferrocene diphosphazene ligand based on Staudinger reaction of diazidoferrocene and a phosphinophenol (Scheme 5.4).[40] Although the ligand has two iminophosphoranes and two phenoxides, the electronic and steric properties are different from the phosphasalen ligands, due to the presence of ferrocenediyl linker instead of ethylene.

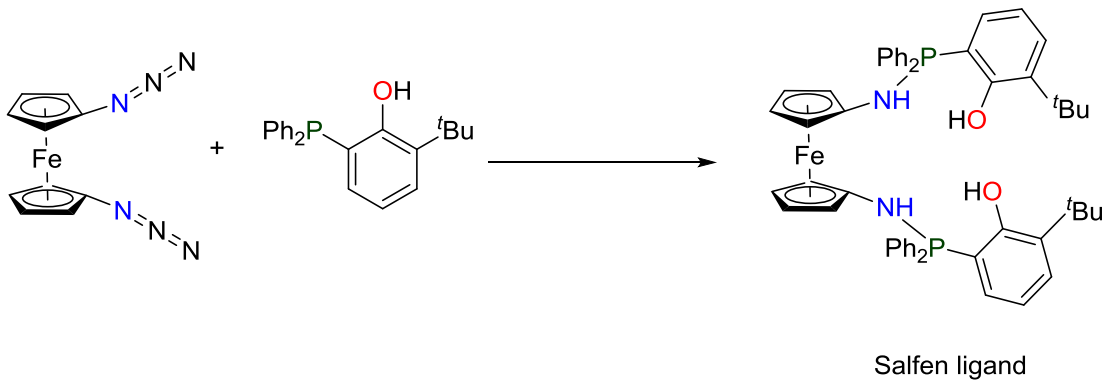

Scheme 5.4 Synthesis of ferrocene diphosphazene.[40]

5.2 Phosphasalen rare-earth complexes

5.2.1 Synthesis of phosphasalen ligands

5.2.1.1 Non-substituted phosphasalen ligand

As mentioned previously, a phosphasalen ligand is a Salen that contains iminophosphorane function instead of imine. The chemistry of iminophosphoranes is a relatively new area in chemistry which still needs to be thoroughly explored. The first iminophosphoranes were synthesized by Staudinger and Meyer in 1919.[41] There are three main ways to access such compounds, which are the Staudinger, the Kirsanov[42,43] and the aza-Mitsunobu reactions.[44,45]

To synthesize the phosphasalen proligands (LH_4, Scheme 5.5) the authors followed the Kirsanov reaction (Scheme 5.5).[35,36] *o*-diphenylphosphinophenol was first obtained from phenol following literature procedure,[46,47] followed by the deprotection in HCl-saturated MeOH. The reaction between ethylenediamine (0.5 equiv.) and *o*-diphenylphosphinophenol (1 equiv.) in the presence of tributylamine (1 equiv.) in CH_2Cl_2 at room temperature (RT) yielded the non-substituted phosphasalen proligand LH_4. The structure of LH_4 was confirmed by ^1H and ^{31}P NMR spectroscopy in $CDCl_3$ (it showed poor solubility in most of NMR solvents), elemental and X-ray analysis.

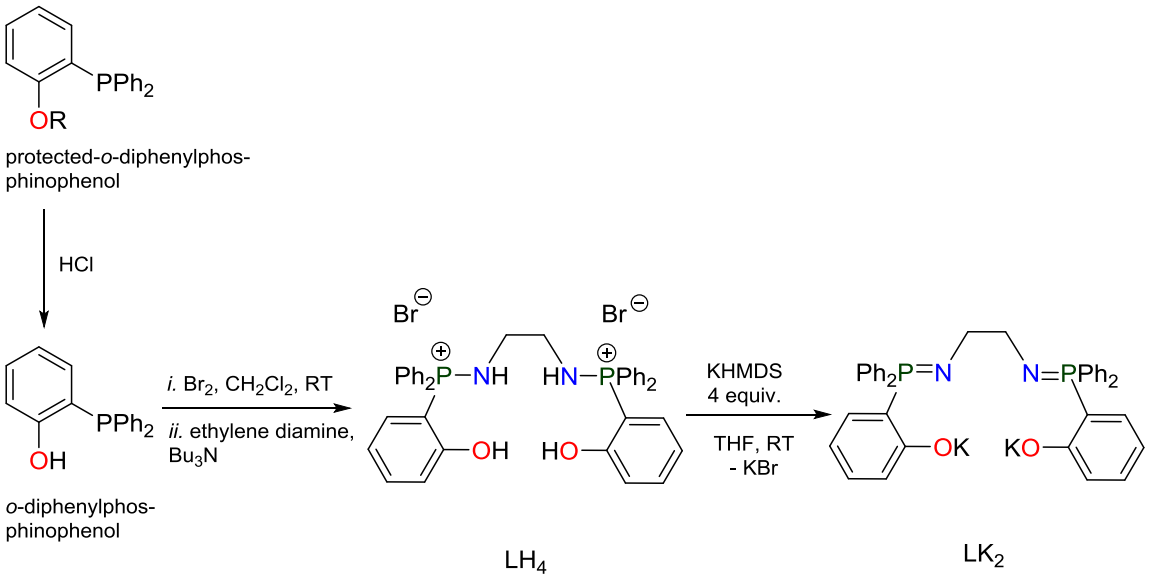

Scheme 5.5 Preparation of non-substituted phosphasalen ligand.[29]

The resonance of the phosphorus atoms of LH_4 appeared as a singlet at 39.3 ppm according to ^{31}P $\{^1H\}$ NMR spectroscopy in $CDCl_3$, which is in the range of the signals for bidentate phenolaminophosphonium salts.[48] In the ^1H NMR spectrum, the bridging ethylene protons appeared as a doublet with a chemical shift ($\delta(CDCl_3)$ = 3.43 ppm) similar to the one observed for bis(phosphine-aminophosphonium) salts featuring such ethylene diamine linker.[49]

LH_4 was deprotonated using 4 equiv. of potassium hexamethyldisilazide (KHMDS) in THF at RT. The end of the reaction was monitored by *in situ* ^{31}P $\{^1H\}$ NMR in $[D_8]$THF, the completeness of the deprotonation and the formation of the phosphasalen ligands LK_2 (99 %) being indicated by the appearance of a singlet at 18.6 ppm. This synthetic procedure is very useful as it produces high yield of pure product and is suitable for the preparation of phosphasalen ligands with a range of substituents on the phenoxide rings or diamine backbone.

5.2.1.2 Substituted phosphasalen ligands

Variation of the nature of the substituents at the *ortho*-phenolate positions and changing the group linking the two iminophosphonium groups have a large influence on the coordination of these ligands to the metal complexes, and can favor the formation of mononuclear over binuclear complexes or *vice versa*, knowing that non-substituted ligands coordinate to form bimetallic species. The authors chose to develop mostly substituted phosphasalen ligands with *tert*-butyl substituents on *ortho*- and *para*- positions of the phenoxide rings and various linkers for the diamine backbone (Figure 5.8).[36]

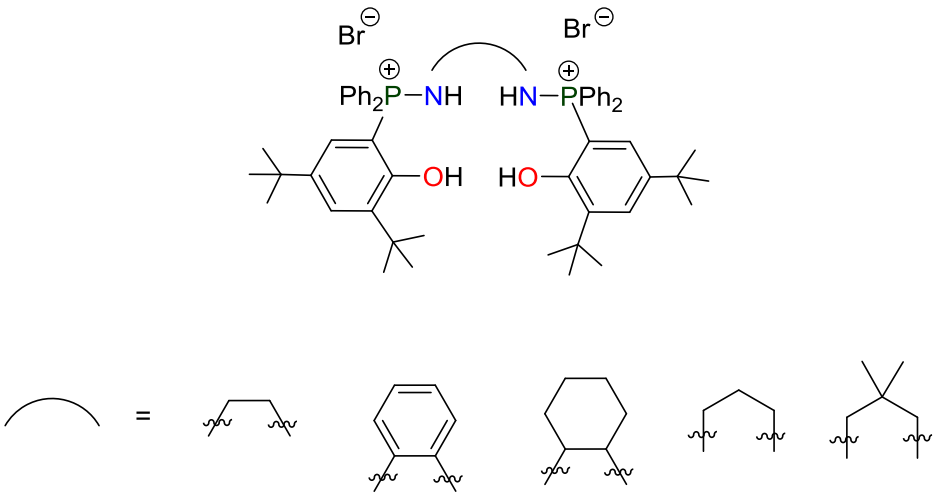

Figure 5.8 Substituted phosphasalen ligands.[29]

In this section we show only the synthesis of phosphasalen ligand with ethylene diamine or phenyl diamine linkage, as these ligands in particular will be used in our study (Scheme 5.6). The proligands L^1H_4 and L^2H_4 were synthesized from 2,4-di-tert-butyl-6-phosphinophenol by the Kirsanov reaction with dibromine and ethyl diamine (L^1H_4) or phenyl diamine (L^2H_4) in dichloromethane, using DABCO (1,4-diazabicyclo[2.2.2]octane) as the base at RT. The dichloromethane was evaporated then the proligands were extracted with THF in order to separate them from the insoluble DABCO salts. THF was evaporated and the solid was washed with THF (L^1H_4) or Et_2O (L^2H_4), leading to, the product was isolated as powdered corresponding to L^1H_4 (71%) and L^2H_4 (72 %) according to NMR spectroscopy and elemental analysis. In ^{31}P $\{^1H\}$ spectroscopy the phosphorus atoms of L^1H_4 appear as a singlet at $\delta(CDCl_3)$ = 40.3 ppm and that of L^2H_4 at $\delta([D_8]THF)$ = 39 ppm, which are very close to the value reported for the non-substituted LH_4 ($\delta(CDCl_3)$ = 39.3 ppm).

Upon reaction with 4 equiv. of KHMDS in THF, L^1H_4 and L^2H_4 were easily deprotonated to give the corresponding anionic phosphasalen ligands, L^1K_2 and L^2K_2 (Scheme 5.6). The completion of the reaction was monitored by the apparition of a unique singlet by ^{31}P $\{^1H\}$ NMR (δ = 20.6 ppm for L^1K_2, 13.2 ppm for L^2K_2). After removal of KBr by filtration, evaporation of THF and washing with petroleum ether to remove HMDS, phosphasalen ligand L^1K_2 was obtained as a white solid in 78 % yield. In ^1H NMR spectrum, the bridging ethylene protons of L^1K_2 appeared as a virtual triplet at $\delta([D_8]THF)$ = 3.20 ppm, due to coupling with two phosphorus atoms. In the published manuscript, the authors did not

isolate L^2K_2, instead they used it *in situ* to react with a proper precursor to form new complexes.[29]

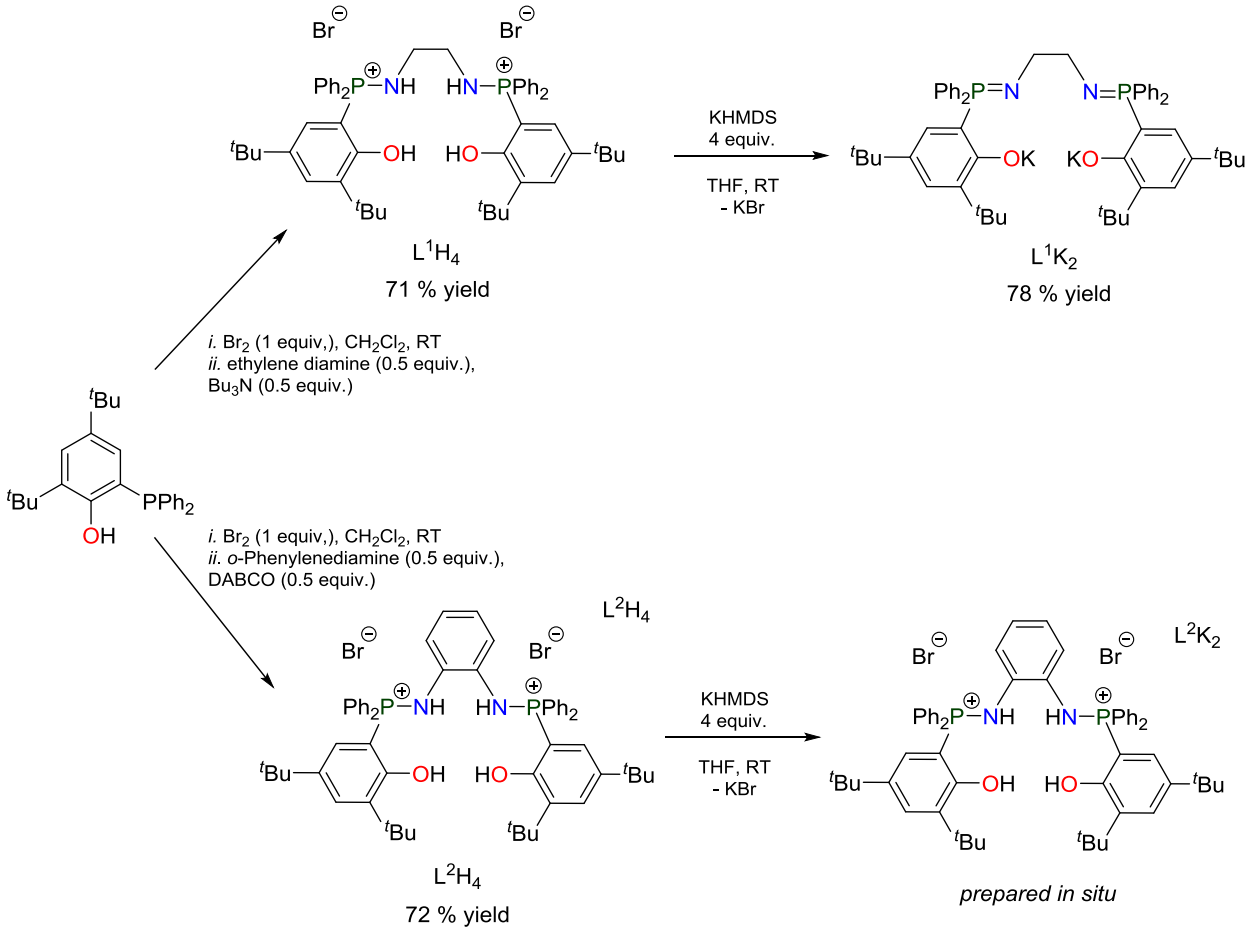

Scheme 5.6 Synthesis of substituted phosphasalen ligand.[29]

5.2.2 Synthesis of yttrium phosphasalen complexes

5.2.2.1 Synthesis using isolated anionic phosphasalen

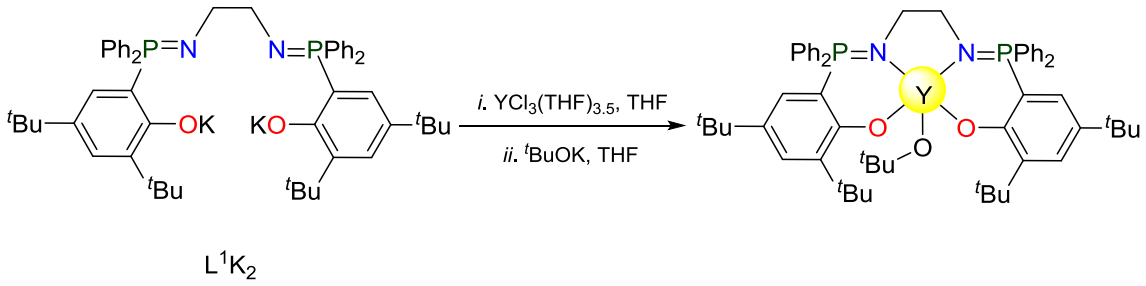

Scheme 5.7 Synthesis of Yttrium phosphasalen complex using isolated anionic phosphasalen ligand.

The complex $L^1Y(O^tBu)$ was prepared by the authors from the phosphasalen ligand L^1K_2 with sterically hindered *tert*-butyl substituents on the phenoxide ring and with a *tert*-butyl alkoxide group (Scheme 5.7).[35] Noteworthy, when phosphasalen with hydrogen substituent on the phenolate ring was used, the complex produced was in a dimeric form. In that context, the L^1K_2 was consciously designed to prevent dimerization and enable isolation of a mononuclear yttrium alkoxide complex. Moreover, in order to achieve well defined monomeric complexes, the diamine bridge must not be too large, otherwise it may coordinate two yttrium centers as shown in Figure 5.9.[29]

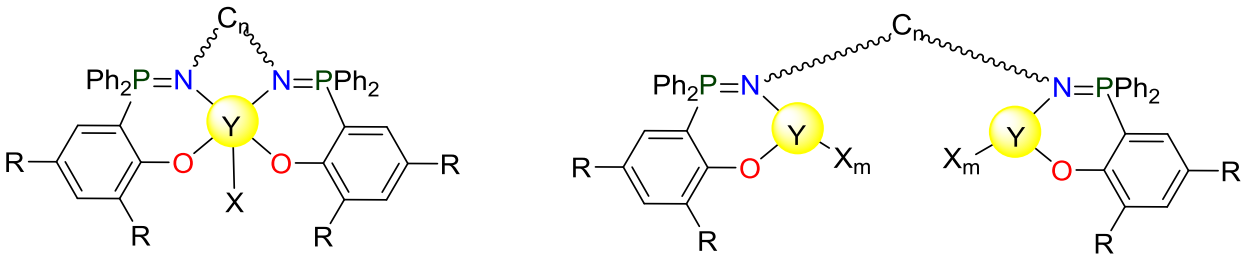

Figure 5.9 Small diamine bridge, monomeric yttrium phosphasalen complex (left). Small diamine bridge, one phosphasalen ligand coordinated to two yttrium centers (right).[29]

Reaction of ligand L^1K_2 with $YCl_3(THF)_{3.5}$ in tetrahydrofuran resulted in immediate precipitation of a white product. The reaction was monitored by $^{31}P\ \{^1H\}$ NMR showing the complete disappearance of the free ligand signal at 20.6 ppm. One equiv. of potassium tert-butoxide was then added to yield $L^1Y(O^tBu)$ in quantitative yield 97 %.

5.2.2.2 Synthesis via *in situ* preparation of the ligand

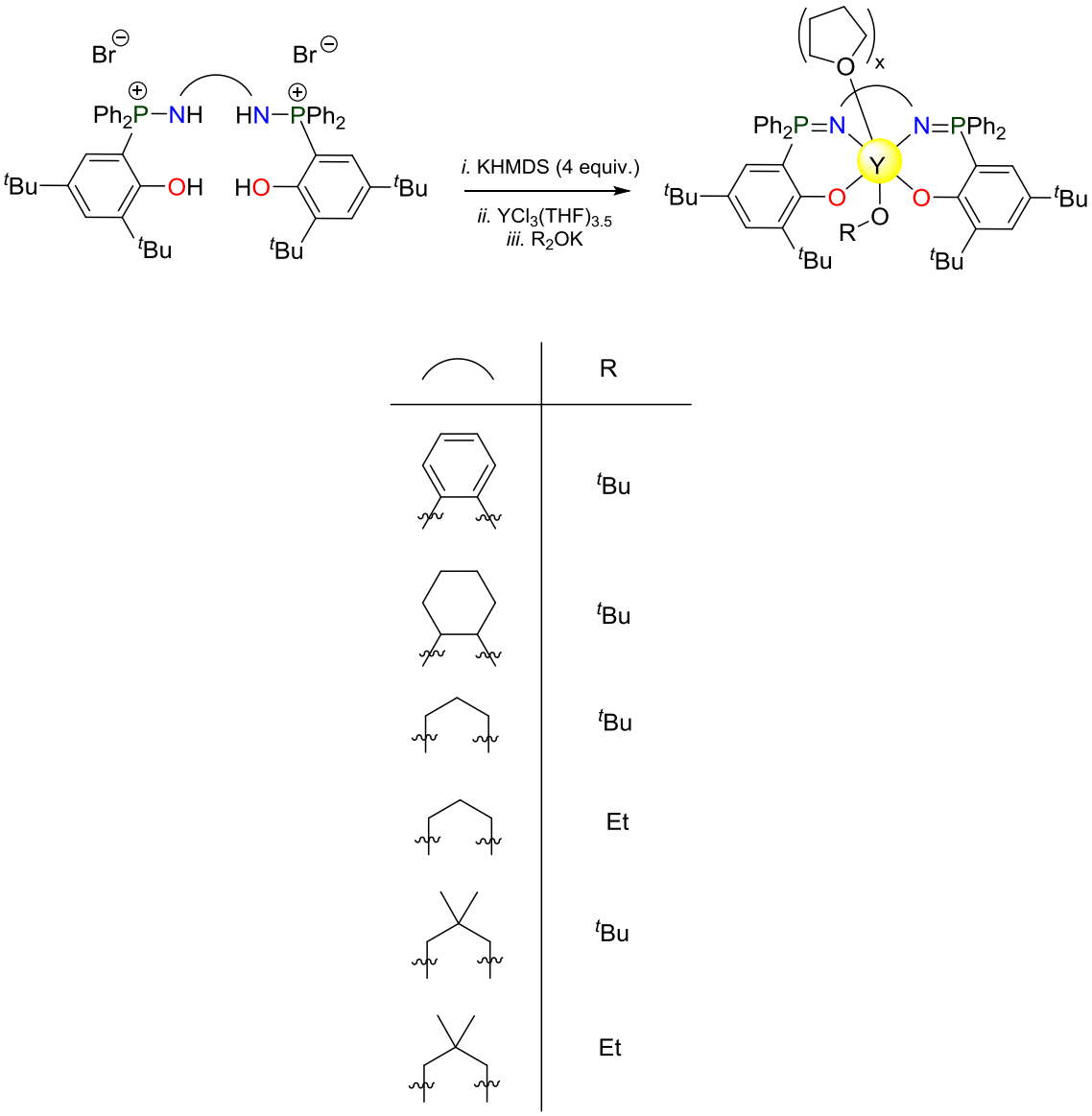

Scheme 5.8 Synthesis of yttrium phosphasalen complexes including the *in situ* preparation of the anionic phosphasalen ligand.[36]

The addition of 4 equiv. of KHMDS onto the aminophosphonium salt in THF gave cloudy colorless solutions, indicating the formation of the anionic phosphasalen ligands (Scheme 5.8). Completeness of the reaction was checked by $^{31}P\{^{1}H\}$ NMR which was used to monitor the reactions. In general, the spectra showed singlets in much higher field compared to the signals of phosphasalen proligands.[36]

The insoluble potassium salts was removed by centrifugation, then followed by the addition of the yttrium tris(chloride) ,$YCl_3(THF)_{3.5}$, which gave a product that had one singlet at lower field in $^{31}P\{^1H\}$ NMR spectra, compared to the phosphasalen ligands. This indicated the formation of yttrium phosphasalen complexes.[36]

Finally, the nucleophilic substitution using potassium *tert*-butoxide or ethoxide yielded the phosphasalen yttrium alkoxide complexes, with in general upfield shift in $^{31}P\{^1H\}$ NMR spectra. Evaporation of the volatiles and recrystallisation in cyclohexane gave the products as colorless crystals or white solids. All the complexes have been fully characterized by NMR and elemental analysis, including by X ray diffraction for some of them.[36]

5.3 Rare-earth borohydride phosphasalen complexes

Rare-earth (RE) metal phosphasalen complexes were shown to be efficient initiators for the ROP of cyclic esters, displaying higher activities than those of rare-earth Salen analogues, the latter being well known to be part of the most active initiators for this reaction. The higher electron donation of phosphasalen ligands was advanced to account for such properties.[50] For instance, phosphasalen complexes were reported as highly *iso*-selective or *hetero*-selective initiators for the for *rac*-lactide polymerisation due to their ability to change the structure of the phosphasalen ligand or the metal size.[35,36,51,52]

In that context, our research group started a collaboration with Dr Auffrant from the LCM laboratory of Polytechnic School of the University of Paris-Saclay, in order to develop new rare-earth phosphasalencomplexes bearing a borohydride ligand instead of the alkoxy one, because of the well-known versatile ability of borohydride initiators, in order to conduct the polymerisation of polar [53-57] and non-polar [58-60] monomers (knowing that, that for non-polar monomers it requires the presence of co-catalyst in the reaction system). In that purpose, we used the already published tetradentate ligands L^1H_4, L^2H_4 and the new tridentate L^3H_2 (Figure 5.10, Scheme 5.10) with the aim to the synthesis of new rare-earth borohydride complexes, these three ligands having been synthesized in LCM laboratory in Palaiseau.

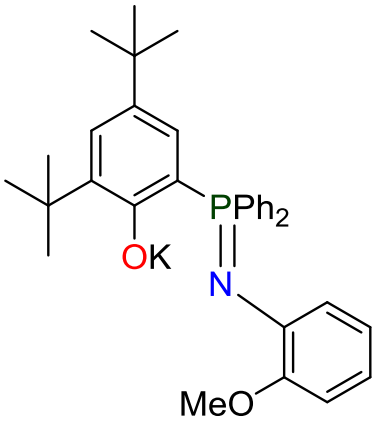

Figure 5.10 Structure of deprotonated ligand L^3K.

The deprotonation of the phosphasalen proligands L^1H_4 and L^2H_4 was conducted following the already reported procedure and was confirmed by ^1H NMR and $^{31}P\{^1H\}$ NMR (see section 5.2.1.2, Appendices IX and X). L^1K_2 and L^2K_2 were then reacted with the homopleptic trisborohydrides, $RE(BH_4)_3(THF)_x$ (RE = Sc, x = 2; Y, Nd, x = 3) *via* salt metathesis in THF at RT for 18 h (Scheme 5.9).

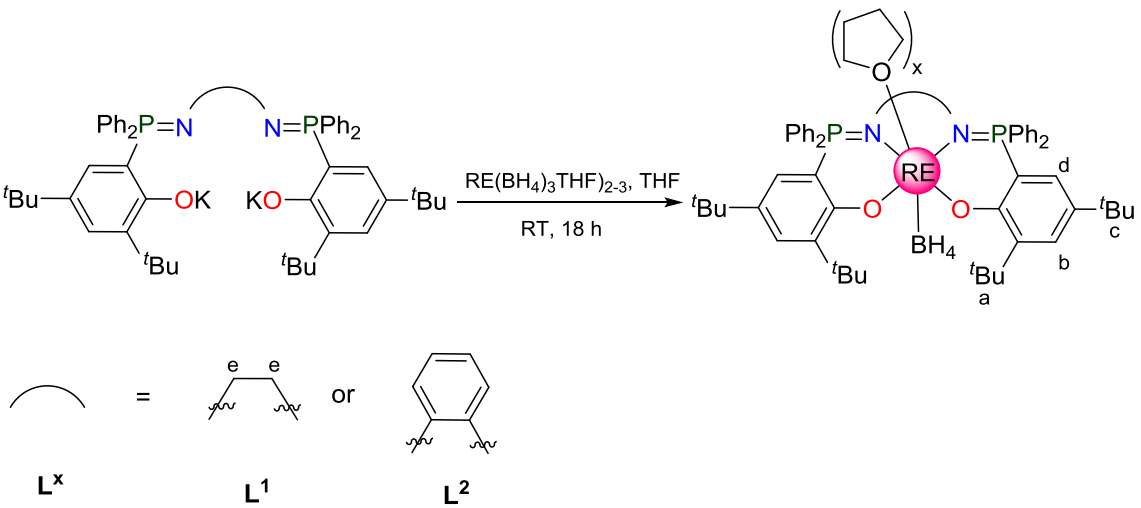

Scheme 5.9 Synthesis of rare-earth phosphasalen complexes with borohydride group.

Upon addition of THF by distillation to $Y(BH_4)_3(THF)_3$and K_2L_1 ligand which were introduced in a Schleck in the glove box in equimolar ratio, a pale-yellow solution was formed, which became darker with time. The mixture was left to react at room temperature for 18 h to complete the reaction. Removal of insoluble salts by filtration and evaporation of the volatiles yielded a pale-yellow solid with 82 % yield corresponding to the formula

$L^1Y(BH_4)(THF)_x$ (**11**) according to ^1H and ^{31}P NMR spectroscopy analysis. $^{31}P\{^1H\}$ NMR in $[D_8]$THF showed complete consumption of the ligand, as only one single peak at 31 ppm was present and at higher chemical shift compared to the potassium ligand L_1K_2 (20.6 ppm). This suggested the formation of the expected phosphasalen yttrium complex **11**. The resonances obtained by ^1H NMR in $[D_8]$THF were very similar to the ones obtained for the complex $L^1Y(OR)$ reported by Auffrant *et al.*.[35] This was in agreement with the substitution of two borohydride groups by the tetradentate ligand and the formation of monoborohydride yttrium phosphasalen complex.

A crop of colorless mono-crystals, suitable for X-ray diffraction analysis, was obtained from a concentrated THF solution of **11** at –20°C.

Despite the rather low quality of the crystals (Figure 5.11), it was possible to confirm the obtaining of the expected structure $L^1Y(BH_4)(THF)$. The mono-THF solvated complex adopts square bipyramidal geometry with four coordinating atoms [O,N,N,O] of the phosphasalen ligand (L^1) forming the basal plane. The yttrium center is slightly out the basal plane, similar to the case of $L^1Y(OR)$ which recorded as square pyramidal geometry. The values of the angles N1—Y—O1 and N2—Y—O2 are not accurate enough to be given.

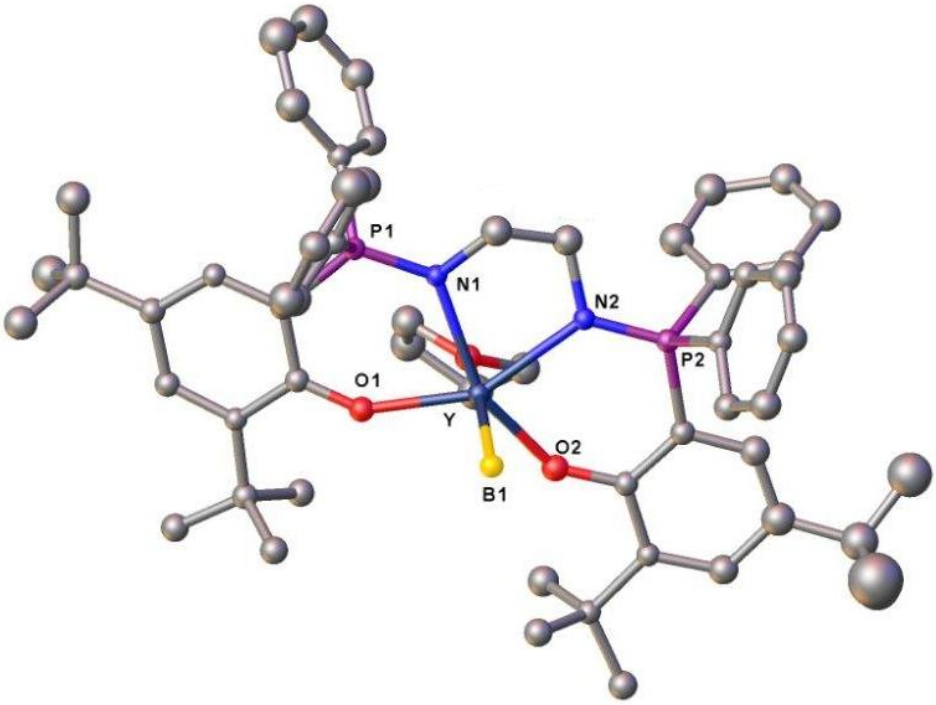

Figure 5.11 ORTEP view of complex $L^1Y(BH_4)(THF)$ **11.** Hydrogens are omitted for clarity.

The X-ray structure showed the presence of one borohydride group, although, it was not possible to locate the hydrogen atoms. The BH_4 group along with the THF molecule, occupies the axial position. Noteworthy, the [O,N,N,O] of the phosphasalen ligand adopts the *trans*-configuration in which also the [O,N,N,O] occupy all the four equatorial positions. This is consistent with what mostly observed for Salen complexes.[4,6]

The same reaction conducted with smaller ionic size precursor, $Sc(BH_4)_3(THF)_2$ and L^1K_2 was undertaken. The addition of THF to the reactants mixture yielded a pale-yellow solution which got darker with time. After removal of the volatiles, the product obtained was a yellow powder in aspect. The ^1H NMR of this product in [D_8]THF confirmed the formula $L^1Sc(BH_4)(THF)_x$ (**12**) and the peaks obtained for the coordinated phosphasalen ligand were in accordance with what previously observed except the ethyl diamine signal separated into two signals each corresponding to two hydrogen at 3.08 and 3.33 ppm (Figure 5.12). However, the ^{31}P {^1H} NMR of the product in [D_8]THF obtained from several syntheses trials gave spectra with more than four peaks with different intensities.

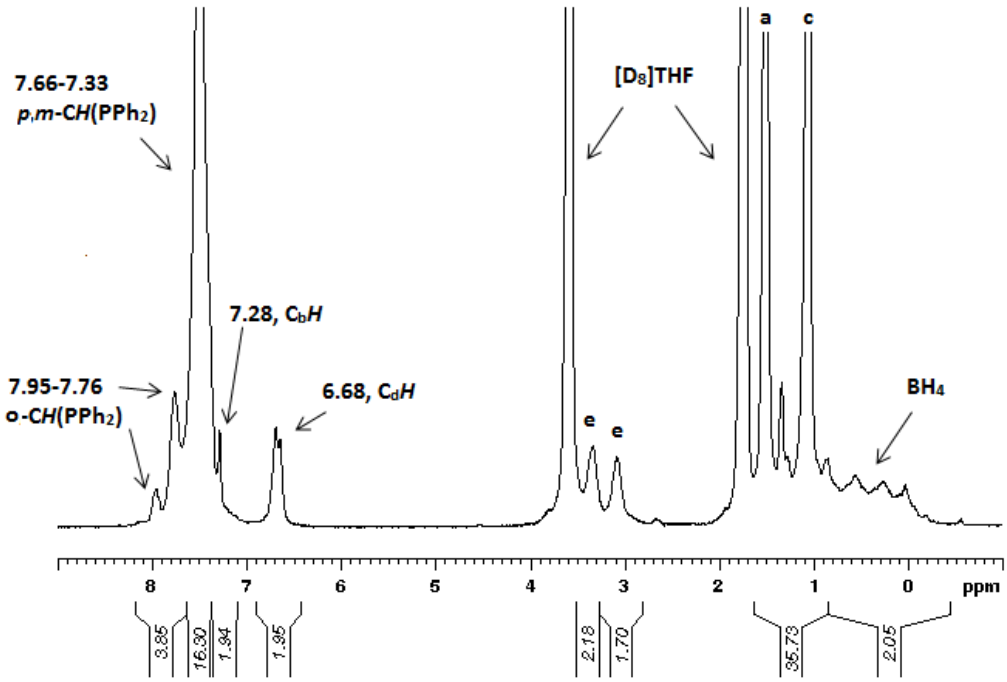

Figure 5.12 ^1H NMR of $L^1Sc(BH_4)(THF)_x$ **12** in [D_8]THF.

X-ray colorless crystals, suitable for X-Ray diffraction analysis, were grown from a saturated THF solution of $L^1Sc(BH_4)(THF)_x$ at –20°C. The structure was in agreement with the expected formula $L^1Sc(BH_4)(THF)$, with one THF molecule per Sc atom as obtained for

Y metal, showing a distorted octahedral geometry (Figure 5.13). Despite the low quality of the cristal, it was clear that the phosphasalen ligand was coordinated to the Sc center by the [O,N,N,O] atoms. However, we were not able to clearly identify the boron atom of the borohydride group (the same for the hydrogen atoms) connected to it. There was an uncertainty on this atom, which could be partly replaced in the crystalline network by an electron-rich atom such as Br. Several syntheses and re-crystallization procedures always conducted to the same problem.

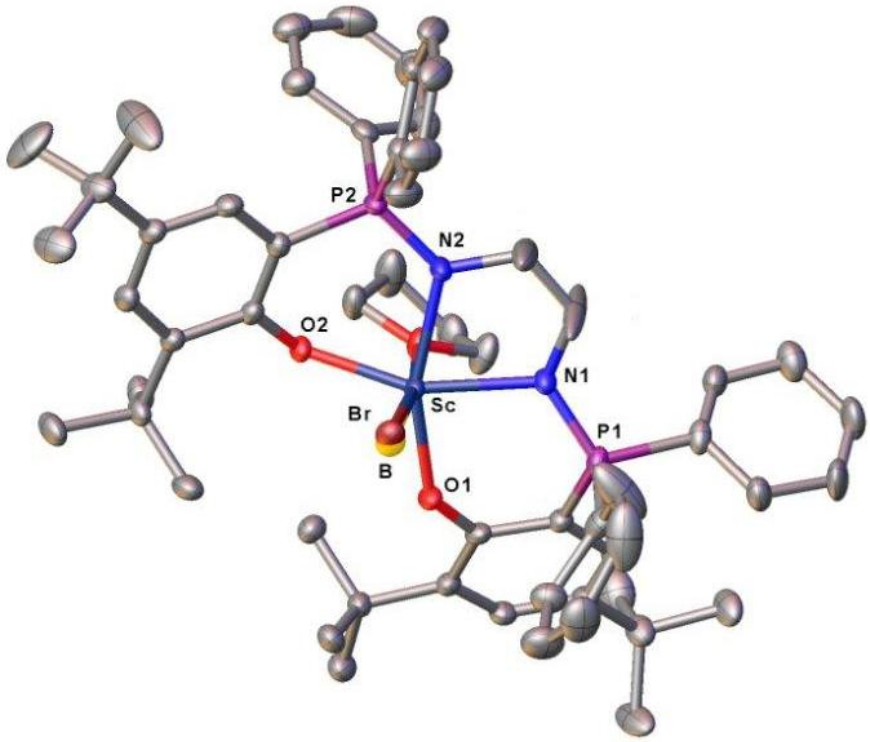

Figure 5.13 ORTEP view of complex $L^1Sc(BH_4)(THF)$ **(12).** Hydrogens are omitted for clarity.

The reaction of L^1K_2 and L^2K_2 with the paramagnetic neodymium trisborohydride, $Nd(BH_4)_3(THF)_3$ were also performed. A blue colored solution was formed with both ligands upon addition of THF to the reagents. The coordination of L^1 and L^2 to the neodymium center was settled by ^{31}P $\{^1H\}$ NMR in $[D_8]$THF which showed the appearance of one single peak at 54.3 and 49.4 ppm, respectively (Figures 5.14 and 5.15). The complete analysis of the ^1H NMR spectra, for both neodymium phosphasalen complexes obtained, was not possible due the intrinsic paramagnetism of neodymium metal, although the borohydride signal was clear at 41.9 ppm with L^1K_2, and at 38.8 ppm. We were able to obtain X-Ray quality crystals of both compounds from a concentrated THF solution at -20°C, but several trials to analyze

them by X-ray failed as the compounds were very sensitive and decomposed readily as soon as they were taken outside of the glove box in fluorinated grease. The elemental analysis of the product obtained by reaction of L^1K_2 and $Nd(BH_4)_3(THF)_3$ does not fit with the calculated values for a neutral form complex of formula $L^1Nd(BH_4)(THF)_x$, however, about it corresponds to the formation of an anionic "ate" potassium complex of formula $K[L^1Nd(BH_4)_2(THF)_2]$ (**13**) : C 62.7 % (calcd 62.46 %), H 7.53 % (calcd 7.44 %), N 2.63 % (calcd 2.35 %) for $C_{62}H_{88}B_2N_2NdO_4P_2K$.

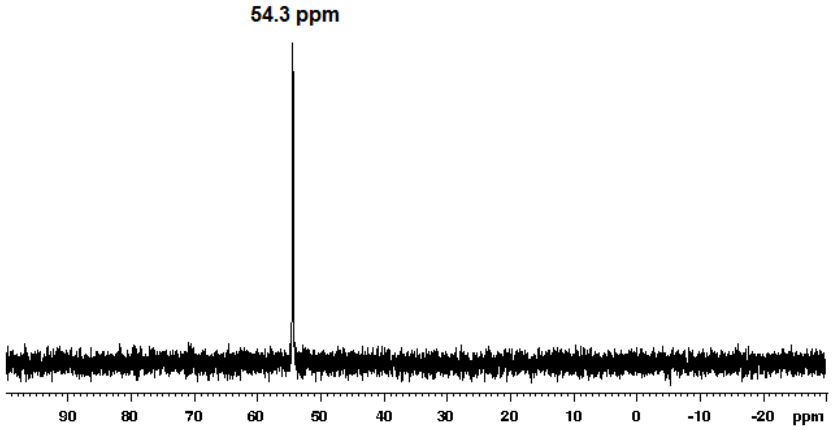

Figure 5.14 ^{31}P $\{^1H\}$ NMR in $[D_8]THF$ of the compound resulting from the reaction between L^1K_2 and $Nd(BH_4)_3(THF)_3$.

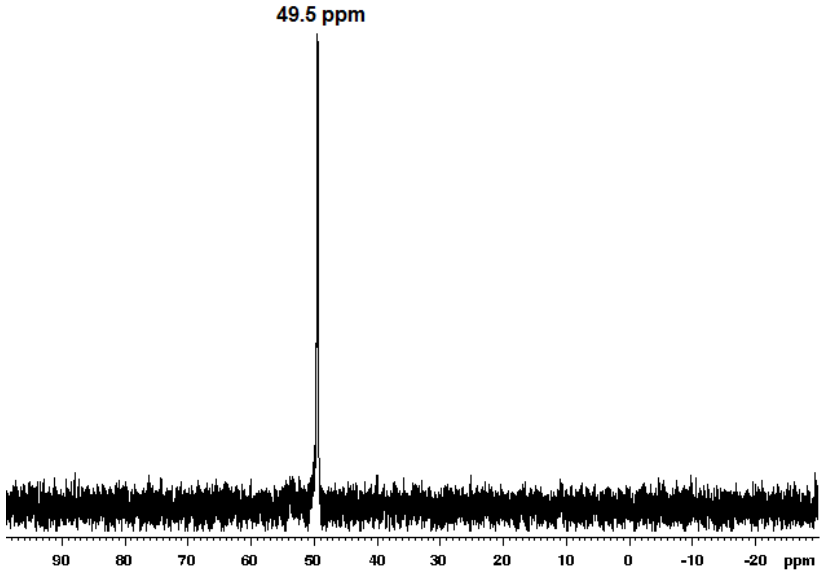

Figure 5.15 ^{31}P $\{^1H\}$ NMR in $[D_8]THF$ of the compound resulting from the reaction between L^2K_2 and $Nd(BH_4)_3(THF)_3$.

Finally, the complexation reaction between the tridentate iminophosphonium ligand L^3H_2 and $Y(BH_4)_3(THF)_3$ was studied (Scheme 5.10). In contrast to L^1H_4 and L^2H_4, the deprotonation of the proligand L^3H_2 was performed *in situ* by the reaction of 2 equiv. of KHMDS in THF at RT for 18 h, leading to the formation of a pale yellow solution. The time of completion of the deprotonation reaction was checked by ^1H and $^{31}P\{1H\}$ NMR analysis of NMR-scale reactions of the former reactants in $[D_6]$benzene. In $^{31}P\ \{^1H\}$ NMR, the signal of the free ligand at 33 ppm completely disappeared, instead a new signal formed at 12 ppm. Moreover, the resonances obtained by ^1H NMR perfectly matched with the deprotonated ligand (Figure 5.10).

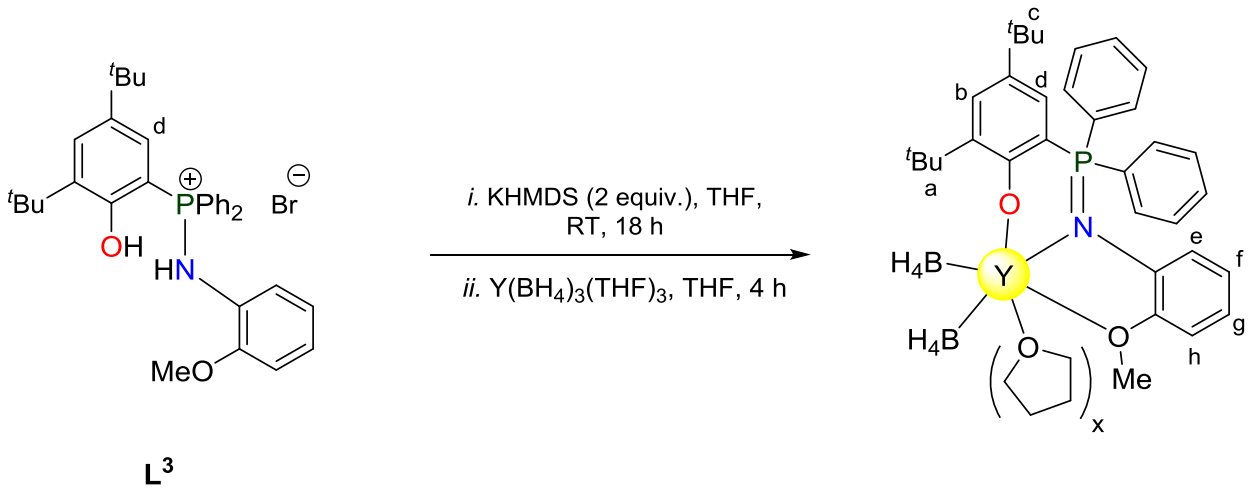

Scheme 5.10 Synthesis of yttrium iminophosphonium borohydride complex **14**.

After a 18 h reaction time at RT, an equimolar amount of $Y(BH_4)_3(THF)_3$ in solution in THF was added dropwise to the pale yellow solution. The reaction was left to stir for 4h at RT. Trials to separate the non-soluble salts from the desired product in THF were unsuccessful. Toluene was indeed necessary to extract the product apart from the salt. Evaporation of the volatiles yielded a pale yellow solid in 90 % yield which corresponded to the formula $L^3Y(BH_4)(THF)_x$ (**14**) as confirmed with ^1H and ^{31}P NMR spectroscopy analysis. Completeness of the reaction was checked by $^{31}P\ \{^1H\}$ NMR spectra which showed only one singlet at lower field compared to the signals of aminophosphonium salt in the proligands (29.8 ppm instead of 12 ppm). Furthermore, the ^1H NMR in $[D_6]$benzene (Figure 5.16) gave another evidence of the coordination of the ligand and formation of yttrium phosphasalen complex with two borohydride groups (at 1.39 ppm), signals relative to THF coordinated to

the yttrium center at 3.67 and 1.25 ppm in addition to the presence of residual toluene molecule even after drying for prolonged time and heating at 50 °C.

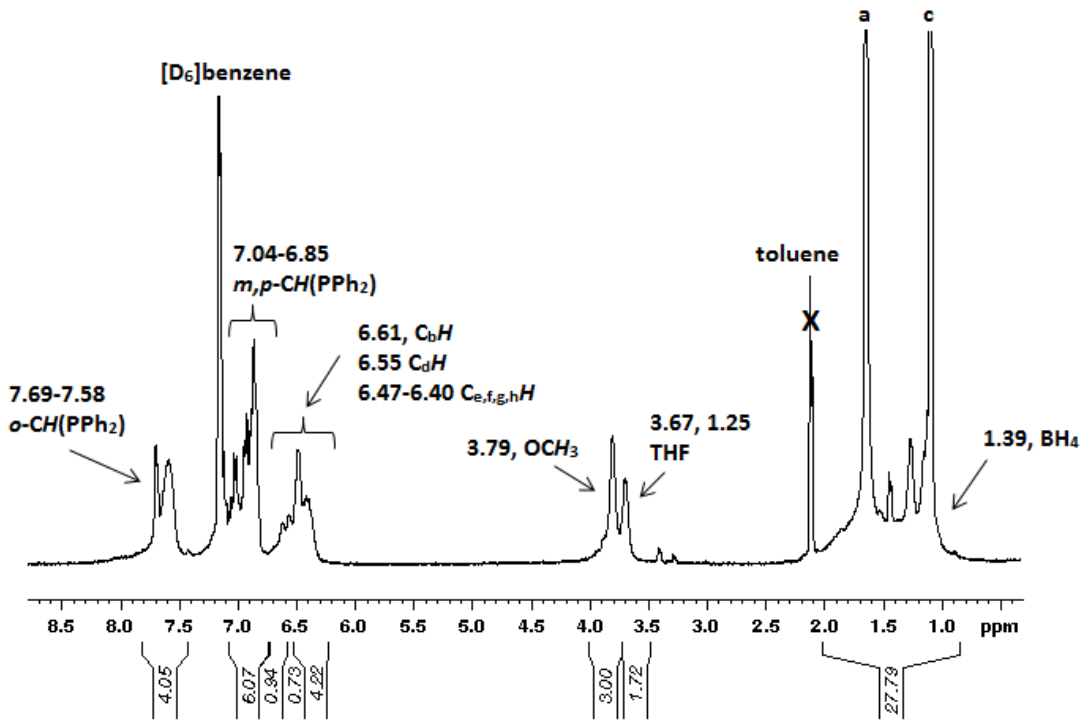

Figure 5.16 ^{1}H NMR of $L^{3}Y(BH_4)_2(THF)_x$ **14** in [D_6]benzene.

Colorless crystals suitable for X-ray diffraction analysis were grown from concentrated toluene solution at -20 °C. The same problem of identification/localization of the borohydride group was encountered. The X-ray structure showed the presence of one BH_4 group coordinated to the yttrium center, however another group (probably Br) that we were not able to identify was present. The iminophosphonium ligand was found to bind to the yttrium center through the nitrogen and the two oxygen atom.

As a preliminary study, the reactivity of complex **13** was assessed toward the polymerisation of isoprene in combination with ^{n}BuMgEt (BEM). It was found to be slightly active, yielding 33 % of the polymer after 48 h reaction time. The M_n value of the isolated polyisoprene determined by SEC (25400 g.mol^{-1}) is close to the expected molar mass (36000 g.mol^{-1}), along with a rather narrow dispersity ($Đ$ = 1.44), which is in consistent with the growth of one polymer chain per neodymium center. Interestingly as well, the polymer displayed a highly *trans*-stereoregular microstructure with 93 % of *trans*-units (2.4 % *cis*- and 4.6 % 3,4-units) as determined by ^{1}H and ^{13}C NMR analysis (Appendix XI). As a

comparison, the activity of catalyst **13** was lower than that previously observed for the $Nd(BH_4)_3(THF)_3$/BEM catalytic system (60 % yield in 2 h at 50 °C), as well as the *trans*-stereoselectivity (95.5 %).[61,62] Other tests were not performed for the reasons discussed previously.

5.4 Conclusion

The Phosphasalen ligand is the analogous of the Salen with iminophosphorane function instead of the imine one. Taking into account the previous work from Dr Auffrant's reaserach group with such ligands to build high catalytic performance phosphasalen rare-earth complexes, we were interested in developing new catalysts of that type bearing in the borohydride group. The previously reported phosphasalen proligand (L^1H_4 and L^2H_4) were deprotonated using KHMDS in addition to the new tridentate L^3H_2 ligand. Among the different rare-earths, the coordination study was attempted with $RE(BH_4)_3(THF)_x$ (RE = Sc, x = 2; Y, Nd, x=3) with L^1K_2 (RE = Sc, Y, Nd), L^2K_2 (RE = Nd) and L^3K (RE = Y). In all cases the ligand was found to be coordinated to the rare-earth center as evidenced by ^1H and/or ^{31}P NMR spectroscopy. Detailed and unambiguous analysis of the ^1H NMR spectra in the case of neodymium metal was not possible. However, the formation of the complexes $L^1RE(BH_4)(THF)_x$ (RE = Sc and Y) and $L^3Y(BH_4)_2(THF)_x$ was confirmed by ^1H and $^{31}P\{^1H\}$ NMR, except for the scandium metal, which was confirmed only by ^1H NMR. Although the coordination environment was established, attempts to determine the exact structure by X-ray failed for $L^1Sc(BH_4)(THF)_x$ and $L^3Y(BH_4)_2(THF)_x$ where presumably bromide and boron atoms exist in different occupation ratios. The structure of $L^1Y(BH_4)(THF)$ was determined by X-ray structural analysis and showed that [O,N,N,O] of the L^1 phosphasalen ligand adopts the common *trans*-configurations around the yttrium center. The catalytic activity of the "ate" complex $K[L^1Nd(BH_4)_2(THF)_2]$ (as determined by elemental analysis) was tested in the isoprene polymerisation and 93 % of 1,4-*trans*-polyisoprene was obtained.

5.5 References

[1] H. Schiff, *Mittheilungen aus dem universitatslaboratorium in Pisa: Eine neuereihe organischer basen. Justus Liebigs Ann Chem* **1864**, *131*, 118.

[2] M. da Silva Cleiton, L. da Silva Daniel, V. Modolo Luzia, B. Alves Rosemeire, A. de Resende Maria, V. B. Martins Cleide, A. de Fatima, *JAR* **2011**, *2*, 1.

[3] L. Canali, D. C. Sherrington, *Chem. Soc. Rev.* **1999,** *28*, 85.

[4] P. G. Cozzi, *Chem. Soc. Rev.* **2004,** *33*, 410.

[5] C. Baleizao, H. Garcia, *Chem. Rev.* **2006,** *106*, 3987.

[6] T. Synlett Katsuki, **2003**, 281 and refs. Therein.

[7] Y. Cui, W. Gu, Y. Wang, B. Zhao, Y. Yao, Q. Shen, *Catal. Sci. Technol*. **2015**, *5*, 3302.

[8] L. Xiao-Aian, L. Nan, *Shandong Huagong* **2011**, *40(1)*, 34.

[9] M. Bandini, P. G. Cozzi, A. Umani-Ronchi, *Chem. Comm*. **2002**, *9* , 919.

[10] J. Chengjun, C. Zhirong, *Huaxue Jinzhan* **2008**, *20(9)*, 1294.

[11] Z. Liu, F. C. Anson, *Inorg Chem.* **2000**, *39(2)*, 274.

[12] S. Yuichi, *Pure app. Chem* **2014**, *86(2)*, 163.

[13] K. Joo-Ho, K. Geon-Joong, *Stu. Sur. Sci, Catal.* **2001**, 3646.

[14] H. Shimizu, T. Katsuki, Chem. Lett. **2003**, *32(6)*, 480.

[15] S. R. Borhade, S. B. Waghmode, *tetrahedron lett*. **2008**, *49(21)*, 3423.

[16] T. Chen, C. Cai, *Catal. Comm*. **2015**, *65*, 102.

[17] A. W. *Dalton Trans.* **2009**, *24*, 4635.

[18] J. A. Castro-Osma, M. North, W. K. Offermans, W. Leitner, T. E. Mueller, *ChemSusChem.* **2016**, *9(8)*, 791.

[19] W. Zhang, J. L. Loebach, S. R. Wilson, E. N. Jacobsen, *J. Am. Chem. Soc.* **1990**, *112*, 2801.

[20] R. Irie, T, Hashihayata, T. Katsuki, M. Akita, Y. Moro-oka, *Chem. Lett.* **1998**, 1041.

[21] K. B. Hansen, J. L. Leighton, E. N. Jacobsen, *J. Am. Chem. Soc.* **1996**, *118*, 10924.

[22] P. J. Pospisil, D. H. Carsten, E. N. Jacobsen, E. N. *Chem. Eur. J.* **1996**, *2*, 974.

[23] T. M. Ovitt, G. W. Coates, *J. Am. Chem. Soc.* **1999,** *121(16),* 4072.

[24] T. M. Ovitt, G. W. Coates, *J. Am. Chem. Soc.* **2002,** *124(7),* 1316.

[25] A. Decortes, R. M. Haak, C. Martín, M. M. Belmonte, E. Martin, J. Benet-Buchholz, A. W. Kleij, Macromol. **2015**, *48*, 8197.

[26] W. Gu, P. Xu, Y. Wang, Y. Yao, D. Yuan, Q. Shen, *Organometallics* **2015**, *34*, 2907.

[27] Y. Cui, W. Gu, Y. Wang, B. Zhao, Y. Yao, Q. Shen, *Catal. Sci. Technol.* **2015**, *5*, 3302.

[28] J. Jiao, W. Zhu, X. Ni, Z. Q. Shen, *Chem. Sci. China*. **2013**, *56*, 970.

[29] T. P. A. Ca, *Coordination chemistry and catalysis with mixed ligands associating iminophosphorane to tiolate or phenolate*, Ecole Polytechnique, **2012**.

[30] M. Calligar, L. Randacci, G. Nardin, *Coord. Chem. Rev.* **1972,** *7*, 385.

[31] M. Calligar, G. Manzini, L. Randacci, G. Nardin, *J. Chem. Soc.- Dalton Trans.* **1972,** *4*, 543.

[32] F. Corazza, E. Solari, C. Floriani, A. Chiesivilla, C. Guastini, *J. Chem. Soc.- Dalton Trans.* **1990,** *4*, 1335.

[33] K. Matsumoto, T. Oguma, T. Katsuki, *Angew. Chem. Int. Ed.* **2009,** *48*, 7432.

[34] Y. Sawada, K. Matsumoto, S. Kondo, H. Watanabe, T. Ozawa, K. Suzuki, B. Saito, T. Katsuki, *Angew. Chem. Int. Ed.* **2006,** *45*, 3478.

[35] T. P. A. Cao, A. Buchard, X. F. Le Goff, A. Auffrant, C. K. Williams, *Inorg. Chem.* **2012**, *51*, 2157.

[36] C. Bakewell, T. P. A. Cao, X. F. Le Goff, N. J. Long, A. Auffrant, C. K. Williams, *Organometallics* **2013**, *32*, 1475.

[37] L. Pauling, *Nature of the chemical bond*. 3rd ed.; Cornell University Press: New York, **1960**.

[38] J. P. Foster, F. Weinhold, *J. Am. Chem. Soc.* **1980,** *102*, 7211.

[39] A. E. Reed, L. A. Curtiss, F. Weinhold, *Chem. Rev.* **1988,** *88*, 899.

[40] E. M. Broderick, P. S. Thuy-Boun, N. Guo, C. S. Vogel, J. Sutter, J. T. Miller, K. Meyer, P. L. Diaconescu, *Inorg. Chem.* **2011,** *50*, 2870.

[41] H. Staudinger, J. Meyer, *Helv. Chim. Acta* **1919,** *2*, 635.

[42] A. V. Kirsanov, *Isv. Akad. Nauk. SSSR* **1950**, 426.

[43] L. Horner, H. Oediger, *Justus Liebigs Annalen der Chemie* **1959,** *627*, 142.

[44] O. Mitsunobu, *Synthesis* **1981**, 1.

[45] O. Mitsunobu, M. Yamada, *Bull. Chem. Soc. Jpn*. **1967**, *40*, 2380.

[46] D. J. Darensbourg, R. R. Poland, A. L. Strickland, *J. Polym. Sci., Part A: Polym. Chem.* **2012,** *50*, 127.

[47] T. Kunisu, T. Oguma, T. Katsuki, *J. Am. Chem. Soc.* **2011,** *133*, 12937.

[48] A. Steiner, S. Zacchini, P. I. Richards, *Coord. Chem. Rev.* **2002,** *227*, 193.

[49] A. Buchard, B. Komly, A. Auffrant, X. F. Le Goff, P. L. Floch, *Organometallics* **2008,** *27*, 4380.

[50] T. M. Ovitt, G. W. Coates, *J. Am. Chem. Soc*., **1999**, *121*, 4072.

[51] C. Bakewell, T. P. A. Cao, N. Long, X. F. L. Goff, A. Auffrant and C. K. Williams, *J. Am. Chem. Soc*., **2012**, 20577.

[52] C. Bakewell, A. J. P. White, N. J. Long, C. K. Williams, *Angew. Chem., Int. Ed*., **2014**, *53*, 9226.

[53] M. Visseaux, F. Bonnet. *Coord. Chem. Rev.* **2011**, *255*, 374.

[54] S. M. Guillaume, M. Schappacher, A. Soum, *Macromolecules* **2003**, *36*, 54.

[55] M. Aurelien, F. Bonnet, M. Visseaux, L. Maron, J. Takats, M. J. Ferguson, X. F. Le Goff, F. Nief, *Chem Comm*, **2011**, *47*, 12203.

[56] F. Bonnet, F. Stoffelbach, G. Fontaine, S. Bourbigot, *RSC Advances*. **2015**, *5*, 31303.

[57] F. Bonnet, A. R. Cowley, P. Mountford, *Inorg. Chem.* **2005**, *44*, 9046.

[58] F. Bonnet, C. Da Costa Violante, P. Roussel, A. Mortreux, M. Visseaux, *Chem. Comm.* **2009,** *23*, 3380.

[59] F. Bonnet, M. Visseaux, A. Pereira, F. Bouyer, D. Barbier-Baudry, *Macromol. Rapid Comm*. **2004**, *25*, 873.

[60] A. Valente, G. Stoclet, F. Bonnet, A. Mortreux, M. Visseaux, P. Zinck., *Angew. Chem. Int. Ed.* **2014**, *53*, 4638.

[61] F. Bonnet, M. Visseaux, A. Pereira, D. Barbier-Baudry, *Macromolecules* **2005**, *38*, 3162.

[62] P. Zinck, M. Terrier, A. Mortreux, M. Visseaux, *Polym. Test.* **2009**, *28*, 106.

GENERAL CONCLUSION AND FUTURE PERSPECTIVES

General conclusion and future perspectives

This work describes the synthesis of new organometallic compounds of the rare earths, their full caracterisation including their molecular structure, and in deep study of their chemical reactivity. They have been used as catalysts to perform the polymerisation of several kinds of monomers, affording copolymers with a wide range of potentialities for further utilizations.

New mixed allyl-borohydride rare-earth complexes of formula $RE(BH_4)_2(C_3H_5)(THF)_x$ (RE = Sc (**1**), x = 2; Y (**2**), La (**3**), Nd (**4**), Sm (**5**), x = 3) were synthesized by reacting the corresponding $RE(BH_4)_3(THF)_x$ with half an equivalent of $Mg(C_3H_5)_2(L)_n$ (L = THF or dioxane). X-Ray structure analysis revealed in all cases monomeric structures with two κ^3 (H) BH_4, one η^3 (C) π-allyl ligands and three THF molecules, except for scandium complex which is five coordinated with only two THF in its coordination sphere. The access to the mono(allyl) bis(borohydride) scandium complex was also shown to be possible by using the Grignard reagent $(C_3H_5)MgX$ (X = Cl or Br) instead of $Mg(C_3H_5)_2(L)_n$. This second synthetic route removes a reaction step as it allows the use of the commercially available Grignard reagent instead of $Mg(C_3H_5)_2(L)_n$ (L = THF or dioxane).

The synthesis of the bis(allyl) derivatives $RE(BH_4)(C_3H_5)_2(THF)_x$ (RE = Sc, Y, La, Nd, Sm) was also investigated, by trying to substitute two borohydride ligands of $RE(BH_4)_3(THF)_x$ using $Mg(C_3H_5)_2(L)_n$ (L =THF or dioxane) or the Grignard reagent. Most of these various reaction attempts led to the formation of the either mono(allyl) bis(borohydride) derivative, tris(allyl)RE complexes or incurable mixtures of unidentified products. The most promising result was the formation of the bis(allyl) complex via the reaction between $(C_3H_5)MgX$ (X = Cl or Br) and $RE(BH_4)_3(THF)_x$ (RE = Sc, Y). Therefore, bis(allyl) mono(borohydride) complexes could potentially be synthesized *in situ* and then be used towards polymerisation.

The reactivity of complexes **1**-**5** was studied towards various molecules, in order to compare the reactivity of the two potential active groups linked to the rare-earth metal, borohydride and allyl. Reactions were conducted with benzophenone, phenylsilane, triethylsilane, cyclopentadienes (Cp^RH, where Cp = C_5Me_4, R = H or ethyl) and 1,4,7-

Trimethyl-1,4,7-triazacyclononane (N_3) at room temperature in either [D_6]benzene or [D_8]THF depending on the solubility of the complexes. In the case of the diamagnetic complexes **1**-**3**, the analysis of the ^{1}H NMR spectra of the reactivity reactions was easy to achieve while for the paramagnetic complexes **4** and **5** and apart from few reactions, many high- and low-field signals were observed in the ^{1}H NMR spectra, of which no unambiguous assignment could be carried out. It was shown that:

- The C=O bond of benzophenone inserted successfully into the RE—allyl bond, yielded the alkoxy compound RE(OC(allyl)Ph_2)(BH_4)$_2$(THF)$_x$ (RE = Sc, Y and La).

- (Cp^R)Nd(BH_4)$_2$(THF)$_x$ (Cp = C_5Me_4, where R = H or Et) was cleanly produced when complex **4** was reacted with Cp^RH (R = H or Et, respectively).

- In addition, the reaction between N_3 and complexes **1**-**5**, showed that the THF ligands were successfully substituted with the tridentate N_3 ligand, to give a N_3 substituted complex

In a general manner, it was shown that the allyl moiety was found to be more reactive than the borohydride for insertion of small molecules.

Complexes Nd (**4**) and Sm (**5**) were tested towards the polymerisation of isoprene (IP). Complex **4** was found to be highly active (53 % yield in 3 h) and *trans*-selective (92.2 %) as a single component catalyst (due to the presence in the complex of a Nd—allyl bond) or in combination with magnesium co-catalysts, whereas the same experiments done with its samarium analogue showed no reactivity at all, in line with the well-known “neodymium effect”. The presence of a magnesium co-catalyst with catalyst **4** in the reaction medium proved its beneficial role as higher activity (58 % yield in 2 h) and *trans*-selectivity (95.5 %) were obtained.

All five complexes **1**-**5** were shown to be excellent initiators toward the Ring Opening polymerisation (ROP) of ε-caprolactone (*ε*-CL) and of *L*-lactide (*L*-LA). Nd-based complex (**4**) was once again found to afford the highest activities towards both monomers and was able to convert 10,000 equiv. of the *ε*-CL in less than 1 min. This corresponds to an activity

up to 81 x 10^6 g polymer (mol Nd)$^{-1}$.h^{-1}, which is the best ever reported to our knowledge for such reaction conducted with a RE-based catalyst. Regarding *L*-LA monomer, TOF up to 1300 mol$_{L\text{-LA}}$(mol$_{Nd}$.h)$^{-1}$ in the case of the Nd-based catalyst **4** was recorded. In the presence of benzyl alcohol as a Chain Transfer Agent (CTA), a better control of the *L*-LA polymerisation process was observed in all cases. Moreover, the catalytic performances toward *ε*-CL and *L*-LA were found to be dependent on the nature of the metal center and ranged in the order Nd (**4**) > La (**3**) > Sm (**5**) > Y (**2**) > Sc (**1**).

End-group NMR studies (^{1}H and ^{13}C {^{1}H}) of the PCLs synthesized revealed, as already known, coordination-insertion mechanism with initiation by the borohydride moiety for the polymerisation of *ε*-CL where α,ω-dihydroxy telechelic was recorded. In case of *L*-LA, the analysis of the polymers synthesized, using NMR spectroscopy (^{1}H, ^{13}C {^{1}H}, ^{1}H/^{1}H-COSY) and MALDI-ToF MS, revealed that the initiation preferentially took place *via* the borohydride ligand rather than *via* the allyl one. Regarding the second end-group, it was shown that the formation of the dihydroxy-telechelic PLA from a borohydride initiation is not as exclusive as in the case of the polymerisation of *ε*-CL, as claimed until know by several authors. Under specific experimental conditions, aldehyde terminations could be observed.

Knowing that the copolymerisation of *L*-LA with *ε*-CL can be a promising way to give rise to copolymers with controlled mechanical properties, we tested the five complexes (**1**-**5**) towards the statistical copolymerisation of *L*-LA and *ε*-CL. In the case of a 1:1 *L*-LA:*ε*-CL feed, the copolymers produced contained preferentially *L*-LA moieties, with up to 28 % of *ε*-CL content when using Y complex (**2**), and mostly random character along the copolymer backbone. When the starting quantity of *ε*-CL was doubled, it was possible to incorporate higher amounts of *ε*-CL, up to 59 % when using La complex (**3**), affording copolymers displaying a blocky character. Under CTA conditions (5 equiv. BnOH), significant improvement in the control of the copolymerisation was observed: i) high *ε*-CL contents were obtained in the final copolymers (up to 47.5 % with *L*-LA:*ε*-CL = 1:1; up to 62.2 % with *L*-LA:*ε*-CL = 1:2); ii) the *ε*-CL was found statistically distributed over the PLA frame, giving rise to a range of copolymers from random with Sc, Y, and Sm, to alternating with the larger Nd and La metals; iii) much narrower distributions despite a non-negligible degree of transesterification were finally noticed under such conditions, iv) in all cases the use of

benzyl alcohol reduced average sequence length of *L*-LA in the polymer chain and decreased the reactivity ratios.

The Nd complex (**4**) also showed rare ability to polymerise both IP and *ε*-CL monomers independently of each other, aside from forming a copolymer of IP and CL unit. Although, it displayed poor copolymerisation ability towards IP and CL, to our knowledge this is the first example of catalyst enables the homopolymerisation of two different monomers with different polar characteristics in the same pot with two different chains growing. Furthermore, in case of sequential polymerisation the catalyst polymerised IP in the presence of *ε*-CL, giving evidences that PCL did not polymerise on the allyl group (the same when a living polyisoprene chain is present on the allyl group). This is a further indication that RE—allyl bond remained unreacted towards cyclic esters, which confirms our conclusions following NMR chain-ends analysis on the final polymers.

Finally, attempts of synthesis of phosphasalen rare-earth-based complexes were conducted on two already published tetradentate phosphasalen ligands with different types of amine linkage (L^1K_2 and L^2K_2) and new tridentate one (L^3K), by reacting $RE(BH_4)_3(THF)_x$ (RE = Sc, x = 2; Y, Nd, x=3) with L^1K_2 (RE = Sc, Y, Nd), L^2K_2 (RE = Nd) and L^3K (RE = Y). In all cases the ligands were found to coordinate the rare-earth centers as evidenced by ^1H and ^{31}P NMR spectroscopy. Detailed and unambiguous analysis of the ^1H NMR spectra in the case of neodymium metal was not possible. However, the formation of the complexes $L^1RE(BH_4)(THF)_x$ (RE = Y (**11**) and Sc (**12**)) and $L^3Y(BH_4)_2(THF)_x$ (**14**) was confirmed by ^1H and ^{31}P $\{^1H\}$ NMR, except for **12** which was confirmed only by ^1H NMR. Mono-crystals were obtained for all the complexes, but attempts to analyze their corresponding exact structure failed due to either the high sensitivity of the compounds (for the two Nd complexes) or the existence of bromide and boron atoms attached to the rare-earth center at the same place in different occupation ratios (for **11**, **12** and **14**). The catalytic activity of the "ate" complex $K[L^1Nd(BH_4)_2(THF)_2]$ (**13**) (as determined by elemental analysis) was tested for the isoprene polymerisation and 93 % of 1,4-*trans*-polyisoprene was obtained in good yield.

Future research objectives will include the following:

i. Synthesis of $RE(C_3H_5)_2(BH_4)(THF)_x$ (RE = Sc, Y) *in situ*, then testing their activities toward the polymerisation of IP in the absence or presence of a bronsted acid, such as $[HNMe_2Ph][B(C_6F_5)_4]$.Moreover, such complexes can be applied in the *L*-LA and *ε*-CL polymerisations.

ii. Synthesis of new N_3 coordinated complexes $(N_3)RE(BH_4)_2(C_3H_5)$ (RE = Y, La, Nd) then trying to grow up mono-crystals in an attempt to determine the structure by X-ray analysis. Such complexes are interesting to study in the polymerisation of IP alone as single components or in the presence of co-catalysts (BEM as alkylating agent, borate/aluminum alkyls).

iii. Synthesis of $Cp^*RE(BH_4)(C_3H_5)$ starting from $Cp^*RE(BH_4)_2$. By the generalization of the procedure used to prepare the mixed allyl-borohydride complexes of the rare earths.

iv. In addition, functionalization experiments of a growing polyisoprene chain by benzophenone can be done, this was investigated by the reactivity reactions of complexes **1-5** with benzophenone where C=O found to be inserted successfully into the RE—allyl moiety.

v. Work is in progress to determine the unidentified peaks displayed by ^1H NMR of the PLAs produced using $RE(BH_4)_2(C_3H_5)(THF)_x$ as well as $RE(BH_4)_3(THF)_x$ (RE = Sc, Y, La, Nd, Sm). And in turn, identifying the exact structures of the chain-ends of PLAs.

vi. Finally, regarding the phosphasalen rare-earth borohydride complexes, a new synthetic route can be established by which the chloride complex, $(phosphasalen)RECl_x$ being synthesized first from the reaction of $RECl_3$ and the anionic phosphasalen ligands (L^1K_2, L^2K_2 or L^3K), then the formation of the borohydride analogs *in situ* by the addition of $NaBH_4$ which can be tested directly in the polymerisation experiments.

EXPERIMENTAL PART

6.1 Syntheses and analyses techniques

All experiments were performed under an inert atmosphere using Schlenk techniques on a single Schlenk line or in a dry solvent-free glovebox (Jacomex O_2 <1 ppm, H_2O <4 ppm).

^{1}H, ^{13}C, COSY, HSQC and HMBC NMR spectra of the polymers were recorded on a Bruker Avance 300 MHz instrument at 300 K in $CDCl_3$. The spectra of organometallic complexes and reagents were also recorded on the same instrument either in [D_6]benzene or [D_8]THF. The chemical shifts (in ppm) were determined using residual signals of the deuterated solvents as gathered by Fulmer *et al.*.[1]

Elemental analyses of the complexes were performed at the London Metropolitan University on a Carlo Erba 1108 Elemental Analyzer instrument.

Size exclusion chromatography (SEC) analysis of the polymers and copolymers were performed in THF as the eluent at 40 °C (1 mL.min^{-1}) with a Waters SIS HPLC pump, a Waters 410 refractometer, and Waters Styragel columns (HR2, HR3, HR4, and HR5E) calibrated with polystyrene standards, with the following corrections : for *trans*-polyisoprene (PIP) $M_n(SEC) = M_n(PS) \times 0.5$ (*trans*-PIP),[2] poly(ε-caprolactone) (PCL) $M_n(SEC) = M_n(PS) \times 0.56$ (PCL),[3] and poly(L-lactide) (PLA) $M_n(SEC) = M_n(PS) \times 0.58$ (PLA).[4]

MALDI-ToF (matrix-assisted laser desorption and ionization time-of-flight) analyses of the polymer materials were performed at the University of Paris VI by (MALDI-ToF) using a Bruker autoflex III smartbeam mass spectrometer, equipped with the laser that produces pulses at 337 nm using dithranol as a matrix and NaI as cationizing agent. Spectra were recorded in linear mode at an accelerating potential of 20 kV. Samples were prepared by dissolving the polymer in THF at a concentration of 2-5 mg.mL^{-1}. A 10 µL aliquot of this solution was mixed with 20 µL of matrix solution and 10 µL of NaI solution (both at 20 mg.mL^{-1} in THF). Standards (polystyrenes of known structure, purchased from Polymer Standards Service) were used to calibrate the mass scale.

Single-crystal X-rays measurements were performed at 100 K. Data were collected using an Apex II CCD 4K Bruker diffractometer (λ = 0.71073 Å). The structures were solved using SHELXT[5] and refined by least-squares procedures on F2 using SHELXL.[6]

Differential scanning Calorimetry (DSC) measurements were determined with a Setaram Evo131 DSC apparatus with a heating rate of 10°/min on 40–80 μm granulometry glass powder. Thermal treatments at -100-260 °C were applied to determine the glass transition (T_g), onset (T_m) and maximum (T_c) crystallization temperatures.

6.2 Commercial reagents

6.2.1 Solvents

THF, diethyl ether, pentane, dioxane and toluene were first purified through alumina column (Mbraun solvent system), then dried over sodium/benzophenone ketyl, degassed, and stored in solvent pots/ampoules under static vacuum. Methanol, ethanol, acetone, chloroform, isopropanol and dichloromethane were purchased from VWR chemicals and used as received. [D_6]benzene and [D_8]THF, both purchased from Eurisotop, were dried over NaK alloy and sodium/benzophenone ketyl respectively, then degassed and stored in an ampoule under static vacuum. $CDCl_3$ purchased from Eurisotop was used as received.

6.2.2 Monomers

L-lactide (*L*-LA), purchased from Purac, was purified by recrystallization from a hot (80 °C), concentrated ^{i}PrOH solution, followed by two subsequent recrystallizations in hot (105 °C) toluene.

Isoprene (IP) and ε-caprolactone (ε-CL), purchased from Sigma-Aldrich, were dried over calcium hydride, distilled twice, and stored over activated molecular sieves (3 Å) in the glovebox. The purity of isoprene after treatment was checked by performing one standard polymerisation test using $Nd(BH_4)_3(THF)_3$ associated to 1 equiv. Mg(^{n}Bu)(Et) (BEM) as the

catalyst.[7] The expected yield is of 92 % in 3 h at 50 °C. If the yield is low, it is considered that isoprene contains impurities. Thus, redistilled and degassed again. The purity of ε-caprolactone was checked by performing one standard polymerisation using $Nd(BH_4)_2(C_3H_5)(THF)_3$ in THF at room temperature (RT) along with a monomer over catalyst ratio of 1000. The reaction time for full conversion should be less than 20 sec at RT.

6.2.3 Rare earths precursors

$NdCl_3(THF)_2$, pale blue powder purchased from Rhodia, was used as received. $ScCl_3$, YCl_3, $LaCl_3$ and $SmCl_3$, white powders purchased from Strem Chemicals, were used as received.

6.2.4 Other reagents

$Al(^iBu)_3$ (pure), MAO (10 wt % in toluene), allylmagnesium bromide (1.0 M in diethylether), allylmagnesium chloride (2.0 M in THF), purchased from Sigma-Aldrich and Butylethylmagnesium, purchased from Texas Alkyls (BEM, 20 wt % in hexane) were used as received.

1,2,3,4-tetramethylcyclopentadiene ($C_5Me_4H_2$), 1-ethyl-2,3,4,5-tetramethylcyclopentadienyl [$C_5Me_4(CH_2CH_3)$], 1,4,7-trimethyl-1,4,7-triazacyclononane (N_3) and sodium borohydride ($NaBH_4$) purchased from Sigma-Aldrich were stored in the glove box and used as received, except the cyclopentadienyl derivatives, which were stored under activated molecular sieves.

Phenylsilane and triethylsilane purchased from Sigma-Aldrich were dried over activated molecular sieves prior to storage in the glovebox. Benzophenone purchased from Acros Chemicals and sublimed under vacuum at 50 °C prior to use. Potassium bis(trimethylsilyl)amide (KHMDS) from Sigma-Aldrich was used as received.

6.3 Typical polymerisation experiments

6.3.1 Polymerisation of *L*-lactide

Typical L-LA polymerisation experiment is given as an example (entry 14, Table 3.3, section 3.2.2). Purified *L*-LA (0.5 g, 3.5 mmol) and the catalyst $Nd(BH_4)_2(C_3H_5)(THF)_3$ (3 mg, 7 µmol) were weighed and mixed together in a Schlenk in a glovebox. Toluene (1.75 ml) was added to the mixture. The solution was further stirred at 70 °C for 30 min outside of the glovebox. The highly viscous medium was then dissolved in non-anhydrous chloroform in order to quench the reaction. An aliquot of the resulting solution was taken and evaporated to dryness to determine the extent of conversion by ^1H NMR measurements in $CDCl_3$ (99 %). The PLLA in solution in chloroform was then poured in methanol (200 ml), filtered out and dried under vacuum before being analyzed by SEC.

6.3.2 Polymerisation of ε-caprolactone

Typical ε-CL polymerisation experiment is given as an example (entry 10, Table 3.2, section 3.2.1). In a glove box, $Nd(BH_4)_2(C_3H_5)(THF)_3$ (3.75 mg, 8.7 µmol) was dissolved in 1 mL of dry and degassed THF. ε-CL (1 ml, 8.7 mmol) was then added. The solution turned green within few seconds and the reaction was carried out at RT for a given time (typically 15 seconds, immediate reaction), after which the medium was completely solid. The polymer was dissolved in non-anhydrous THF. The solution was then poured in a large amount of methanol (400 ml), filtered and dried under vacuum before being analyzed by SEC.

6.3.3 Polymerisation of isoprene

Typical IP polymerisation experiment is given as an example (entry 4, Table 3.1, section 3.1). In a glove box, $Nd(BH_4)_2(C_3H_5)(THF)_3$ (4.3 mg, 10 µmol) was dissolved in 1 mL of dry and degassed toluene. 10 equivalents of $Al(^iBu)_3$ (d = 0.786, 25 µL, 10 µmol) were added via a micro-syringe. Isoprene (1 ml, 10 mmol) was then added. The solution turned green within few minutes and the reaction was carried out at 50 °C for a given time (typically 1 h) outside

of the glovebox, after which the medium was completely solid. The reaction was quenched by addition of some methanol drops and a small amount of THF. Polymers were precipitated in methanol (200 ml) containing butylated hydroxytoluene (BHT) as stabilizer, filtered and dried under vacuum before being analyzed by SEC.

6.3.4 Random copolymerisation of *L*-lactide and *ε*-caprolactone

Typical experiment is given as an example (entry 4, Table 4.1, section 4.2). *L*-LA (0.14 g, 1 mmol), *ε*-CL (0.11 ml, 1 mmol) and the catalyst $Nd(BH_4)_2(C_3H_5)(THF)_3$ (4.6 mg, 10 μmol) were weighed and mixed together in a Schlenk in a glovebox. Toluene (1 ml) was added to the mixture. The solution was further stirred at 70 °C for a given time (typically 5 h) outside of the glovebox. The viscous medium was then dissolved in non-anhydrous THF. An aliquot of the resulting solution was taken and evaporated to dryness to determine the extent of conversions by ^1H NMR measurements in $CDCl_3$. The copolymer in solution in THF was then poured in cold diethyl ether (50 ml), filtered out and dried under vacuum before being analyzed by SEC.

6.3.5 Random copolymerisation of isoprene and *ε*-caprolactone

Typical experiment is given as an example (entry 34, Table 4.6, section 4.3). In a glovebox, $Nd(BH_4)_2(C_3H_5)(THF)_3$ (4.3 mg, 10 μmol) was dissolved in toluene (2 mL). In a separate vial, a mixture of *ε*-caprolactone (0.11 mL, 1 mmol) and isoprene (0.5 mL, 5 mmol) was prepared. The monomers mixture was added to the catalyst solution before being stirred at 50 ^oC for a given time (typically 24 h) outside of the glovebox. A few drops of non-anhydrous THF were then added to the light green solution. The polymers solution was poured in ethanol (50 mL) containing a small amount of BHT, filtered out and dried under vacuum before being analyzed by SEC.

6.3.6 Polymerisation of isoprene followed by *ε*-caprolactone

Typical experiment is given as an example (entry 31, Table 4.6, section 4.3). In a glovebox, $Nd(BH_4)_2(C_3H_5)(THF)_3$ (4.3 mg, 10 μmol) was dissolved in toluene (0.5 mL). Isoprene (0.5 mL, 5 mmol) was added whilst stirring. The mixture was stirred and heated at 50 ^oC for 24 h outside of the glovebox. The vessel was then taken back into the glovebox where toluene (3 mL) was added and an aliquot of the reaction was taken. Methanol was added to the aliquot until a permanent white precipitate was formed. The white solid was dried under vacuum in order to perform ^1H NMR and SEC analysis of the sample. *ε*-Caprolactone (0.55 mL, 5 mmol) was then added to the rest of the reaction whilst stirring. The resulting mixture was allowed to stir at RT until the solution reached maximum viscosity (*i.e.* when the solution became a solid). The highly viscous medium was dissolved in non-anhydrous THF and poured in ethanol (100 mL). The polymer was filtered out and dried under vacuum before being analyzed by SEC.

6.3.7 Polymerisation of *ε*-caprolactone followed by isoprene

Typical experiment is given as an example (entry 32, Table 4.6, section 4.3). In a glovebox, $Nd(BH_4)_2(C_3H_5)(THF)_3$ (4.3 mg, 10 μmol) was dissolved in toluene (0.5 mL). ε-caprolactone (0.55 mL, 5 mmol) was added whilst stirring and allowed to stir overnight at RT. An additional amount of toluene (1 mL) was added, followed by isoprene (0.5 mL, 5 mmol) whilst stirring and the final mixture was stirred and heated at 50 ^oC for 22 h outside of the glovebox. Non-anhydrous THF (3 drops) was added to the green solution and the final solution was poured in ethanol (100 mL), filtered out and dried under vacuum before being analyzed by SEC.

6.4 Organometallic syntheses

6.4.1 Starting materials

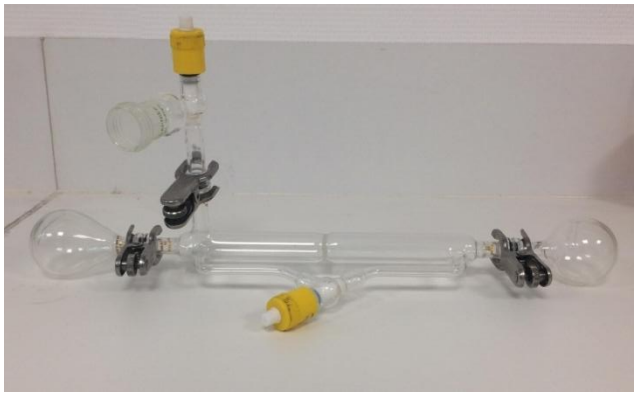

Figure 6.1 Vessel used in scale up synthesis of organometallic compounds.

- **$RE(BH_4)_3(THF)_x$ (RE = Sc, x = 2; Y, La, Nd, Sm, x = 3)**

In the glove box, $NaBH_4$ and anhydrous $RECl_3$ were weighed in a round bottom flask, which was further connected to a vessel containing a filtration system (Figure 6.1) . The vessel was then connected to the vacuum line and 50 mL of dry THF was cold-distilled under vacuum into the flask. The flask was left to stir and heat under reflux at 75 ^oC for 24 h (RE = Nd), 48 h (RE = Sm) and three days (RE = Sc, Y and La). The resulting solution was filtered and the salts were washed twice using THF. The product was dried under vacuum to form a solid. ^1H NMR ([D_6]benzene, 300 MHz, 20 ^oC): $\delta_{(BH4)}$: 100.25 (RE = Nd); -10.25 (RE = Sm); 1.45 (RE = Sc); 1.31 (RE = Y) and 1.88 (RE = La). The number of coordinated THF molecules on the final product was determined by ^1H NMR analysis and was generally found to be x = 2 for RE = Sc and x = 3 for RE = Y, La, Sm and Nd. In order to check the absence of residual chloride in the complexes $RE(BH_4)_3(THF)_x$, a test was performed systematically when a new batch of product was synthesized. A hemolysis tube was charged with the rare-earth tris(borohydride) and potassium hydroxide (KOH). The mixture was melted using heat gun until foam produced. Little amount of distilled water was added. Diluted nitric acid solution (1M) was added until the solution become clear with acidic PH. Then, few drops of silver

nitrate solution (1M) were added, leading to the formation of a white precipitate in the case of a complex containing traces of chloride.

- **$Mg(C_3H_5)_2(diox)_{0.06}$**

This synthesis was performed according to literature procedure.[8-10] In a glovebox, $(C_3H_5)MgBr$ (20 mL) was added to a 100 mL two-necked round bottom flask. Dioxane (2.4 mL) was added to a small round bottom flask that was then connected to the two-necked round bottom flask. Ether (~ 50 mL) was first distilled into the smaller flask and then into the main flask. Dioxane was slowly added to the $(C_3H_5)MgBr$ in diethyl ether solution, which turned the grey solution into a cloudy solution with white precipitate. The reaction was left under stirring for 1.5 hours. The reaction was allowed to separate for 10 minutes before filtration. Additional ether (approx. 25 mL) was used to wash the salt twice and the solid was left to filter overnight. The product was dried under vacuum to form an off-white solid (yield = 32 %). ^1H NMR ([D_6]benzene, 300 MHz, 20 ^oC): δ = 6.85 (q, CH, 1H); 3.36 (traces of dioxane); 3.04 (d, CH_2, 4H).

6.4.2 Synthesis of mono(allyl) bis(borohydride) rare-earth complexes

- **$Sc(BH_4)_2(C_3H_5)(THF)_3$**

$Sc(BH_4)_3(THF)_2$ (0.2 g, 0.88 mmol) and $Mg(C_3H_5)_2(dioxane)_{0.06}$ (0.049 g, 0.44 mmol) were weighed in a vessel in a glove box. The vessel was connected to the vacuum line and 30 mL of dry THF was cold-distilled under vacuum into the flask. After 4 h stirring at RT, a dark green solution was obtained with few white salts. The solution was filtered and concentrated to 5 mL. A Crop of green single crystals suitable for XRD analysis were grown from this THF solution at -20 °C. Several crystallizations at -20°C afforded more green crystals leading to a global yield of 60 %. ^1H NMR ([D_8]THF, 300 MHz, 20 °C): δ = 6.13 (p, 1H, CH); 2.90 (d, 4H, $2CH_2$); and -0.15 (br s, 8H, $2BH_4$). Elemental analysis: C 50.60 % (calcd 50.83 %), H 11.40 % (calcd 11.25 %) for $ScC_{11}H_{29}B_2O_2$ (bis-THF adduct). X-Ray data: $Sc(BH_4)_2(C_3H_5)(THF)_2$ crystallizes in the space group C 2/c with a = 12.6534(4), b = 10.4491(3), c = 12.5453(4) Å, α = 90°, β = 114.699(2)°, γ = 90°, and V = 1506.95 $Å^3$ (X Ray analysis performed at 100(1) K). Data were collected at 100(1) K on a Bruker Smart

Apex CCD 4K system. The structure was solved by charge flipping methods using superflip software,[11] and least-square refined with JANA2006 software.[12] CCDC 1537163.

- **$Y(BH_4)_2(C_3H_5)(THF)_2$**

$Y(BH_4)_3(THF)_3$ (0.25 g, 0.7 mmol) and $Mg(C_3H_5)_2(dioxane)_{0.06}$ (0.042 g, 0.4 mmol) were weighed in a vessel in a glove box. The vessel was connected to the vacuum line and 30 mL of dry THF was cold-distilled under vacuum into the flask. After 2 h stirring at RT, a yellow solution was obtained with few white salts. The THF was removed all under dynamic vacuum and 30 mL of dry toluene was cold-distilled into the vessel. The mixture further stirred for 1 h leading to an off-pale brown insoluble product and yellow solution. The yellow solution was filtered and the off-pale brown compound was washed two times with toluene. Toluene was removed under vacuum then 5 mL of THF was added by distillation. A Crop of pale yellow single crystals suitable for XRD analysis were grown from this THF solution at -20 °C. Several crystallizations at -20°C afforded yellow crystals with global yield of 65 %. ^{1}H NMR ([D_6]benzene, 300 MHz, 20 °C): δ = 6.06 (p, 1H, CH); 3.60 (s THF); 3.16 (d, 4H, $2CH_2$); and 1.32 (br s, 8H, $2BH_4$); 1.15 (s, THF). ^{1}H NMR ([D_8]THF, 300 MHz, 20 °C): δ = 6.16 (p, 1H, CH); 2.90 (d, 4H, $2CH_2$); and 0.42 (br s, 8H, $2BH_4$). Elemental analysis: C 40.54 (calcd 40.36 %), H 9.65 % (calcd 9.41 %) for $YC_9H_{25}B_2O_{1.5}$ (1.5 THF adduct). X-Ray data: $Y(BH_4)_2(C_3H_5)(THF)_3$ crystallizes in the orthorhombic space group P 21/n with a = 9.6091(7), b = 13.7956(11), c = 14.7135(11) Å, α = 90° , β = 90.026(5)°, γ= 90°, and V = 1950.47Å^3 (X Ray analysis performed at 100(1) K). Data were collected at 100(1) K on a Bruker Smart Apex CCD 4K system. The structure was solved by charge flipping methods using superflip software, [11] and least-square refined with JANA2006 software [12]. CCDC 1537165.

- **$La(BH_4)_2(C_3H_5)(THF)_3$**

$La(BH_4)_3(THF)_3$ (0.25 g, 0.6 mmol) and $Mg(C_3H_5)_2(dioxane)_{0.06}$ (0.035 g, 0.3 mmol) were weighed in a vessel in a glove box. The vessel was connected to the vacuum line and 30 mL of dry THF was cold-distilled under static vacuum into the flask. After 4 h stirring at RT, a yellow solution was obtained with few white salts. The yellow solution was filtered and

concentrated to 5 mL. A Crop of pale yellow single crystals suitable for XRD analysis were grown from this THF solution at -20 °C. Several crystallizations at -20°C afforded more green crystals leading to a global yield of 89%. ^{1}H NMR ([D_8]THF, 300 MHz, 20 °C): δ = 6.20 (s, 1H, CH); 2.95 (d, 4H, 2CH_2); and 0.65 (br s, 8H, BH_4). Elemental analysis: after 3 days storage at RT in the glove box, C 36.50 % (calcd 37.34 %), H 8.20 % (calcd 8.26 %) for $LaC_{11}H_{29}B_2O_2$ (bis-THF adduct); after one week storage at RT in the glove box, C 34.85 % (calcd 34.01 %), H 7.94 % (calcd 7.93 %) for $LaC_9H_{25}B_2O_{1.5}$ (1.5 THF adduct). X-Ray data: $La(BH_4)_2(C_3H_5)(THF)_3$ crystallizes in the orthorhombic space group Pbcn with a = 9.8255(6), b =14.8773(9) , c = 13.9240(9) Å, α = β = γ = 90°, and V = 2035.37 Å^3 (X Ray analysis performed at 100(1) K). Data were collected at 100(1) K on a Bruker Smart Apex CCD 4K system. The structure was solved by charge flipping methods using superflip software, [11] and least-square refined with JANA2006 software [12]. CCDC 1537164.

- **$Nd(BH_4)_2(C_3H_5)(THF)_3$**

$Nd(BH_4)_3(THF)_3$ (0.812 g, 2 mmol) and $Mg(C_3H_5)_2(THF)_3$ (0.194 g, 0.6 mmol) were weighed in a vessel in a glove box. The vessel was connected to the vacuum line and 50 mL of dry THF was cold-distilled under vacuum into the flask. After 2 h stirring at RT, a dark green solution was obtained with few white salts. The green solution was filtered and the salts washed once. The THF was evaporated under vacuum until forming a concentrated solution of 5 mL. A crop of green single crystals suitable for XRD analysis were grown from this THF solution at -20 °C. Several crystallizations at -20°C afforded more green crystals leading to a global yield of 60 %. ^{1}H NMR ([D_6]benzene, 300 MHz, 20 °C): δ = 91.9 (br s, 8H, 2BH_4); 22.6 (s, 1H, CH); 13.1 (s, 2H, CH_2); 1.28 (s, 2H, CH_2'); – 2.47 (s, THF); – 5.69 (s, THF). ^{1}H NMR ([D_8]THF, 300 MHz, 20 °C): δ = 88.5 (br s, BH_4); 30.3 (s, 1H, CH); 9.9 (s, 2H, CH_2); ~ 1 (s, 2H, CH_2'). Elemental analysis: C % 41.60 (calcd 41.77), H % 9.02 (calcd 8.65) for $NdC_{15}H_{37}B_2O_3$. X-Ray data: $Nd(BH_4)_2(C_3H_5)(THF)_3$ crystallizes in the orthorhombic space group P 21/n with a = 99.7322(4), b = 13.8301(5), c = 14.8354(6) Å, α = 90°, β = 90.720(2)°, γ = 90°, and V = 1996.65 Å^3 (X Ray analysis performed at 100(1) K). Data were collected at 100(1) K on a Bruker Smart Apex CCD 4K system. The structure was solved by charge flipping methods using superflip software, [11] and least-square refined with JANA2006 software [12]. The crystal is composed of two twin domains (69.8% *vs* 30.2%) related the one to the other by a 180° rotation along the *c* axis. The model based on 3064 reflections (I >

3.0σ(I), Rint = 0.064), total number of reflections = 76524, converged to a final R1 = 3.77 % (wR1 = 4.58%). CCDC 1421982.

- **$Sm(BH_4)_2(C_3H_5)(THF)_3$**

$Sm(BH_4)_3(THF)_3$ (0.25 g, 0.58 mmol) and $Mg(C_3H_5)_2(THF)_{1.5}$ (0.06 g, 0.29 mmol) were weighed in a vessel in a glove box. The vessel was connected to the vacuum line and 50 mL of dry THF was cold-distilled under vacuum into the flask. After 2 h stirring at RT, a dark violet solution was obtained with few white salts. The THF was removed all under dynamic vacuum and 50 mL of dry toluene was cold-distilled into the vessel. The mixture further stirred for 1 h at RT leading to an off-brown insoluble product and violet solution. The violet solution was filtered and the off-brown compound was washed two times with toluene. Toluene was removed under vacuum then 5 mL of THF and 1 mL pentane were distilled respectively. Violet single crystals suitable for XRD analysis were grown. Several crystallizations at -20°C afforded more green crystals leading to a global yield of 83%. ^{1}H NMR ([D_6]benzene, 300 MHz, 20 °C): δ = 15.8 (s, 2H, CH_2'); 11.2 (s, 2H, CH_2); 9.6 (s, 1H, CH); 2.0 (s, THF); 0.4 (s, THF); – 11.8 (br s, 8H, $2BH_4$). ^{1}H NMR ([D_8]THF, 300 MHz, 20 °C): δ = 11.4 (s, 4H, $2CH_2$); 8.9 (s, 1H, CH); – 22 (br s, 8H, $2BH_4$). Elemental analysis: C % 40.93 (calcd 41.2), H % 8.60 (calcd 8.5) for $NdC_{15}H_{37}B_2O_3$. X-Ray data: $Sm(BH_4)_2(C_3H_5)(THF)_3$ crystallizes in the orthorhombic space group P 21/n with a = 9.382(7), b = 14.173(10), c = 14.497(10) Å, α = 90°, β = 90.180(3)°, γ = 90°, and V = 1927.67 Å3 (X Ray analysis performed at 100(1) K). Data were collected at 100(1) K on a Bruker Smart Apex CCD 4K system. The structure was solved by charge flipping methods using superflip software,[11] and least-square refined with JANA2006 software [12] .The model based on 4435 reflections (I > 3.0σ(I), Rint = 0.020), total number of reflections = 15804, converged to a final R1 = 4.00 % (wR1 = 5.10 %). CCDC 1421983.

6.4.3 Attempts of synthesis of bis(allyl) mono(borohydride) rare-earth complexes

- **$Sc(BH_4)(C_3H_5)_2(THF)_x$**

From $Mg(C_3H_5)_2$

$Sc(BH_4)_3(THF)_2$ (0.1 g, 0.44 mmol) and $Mg(C_3H_5)_2(dioxane)_{0.06}$ (0.049 g, 0.44 mmol) were weighed in a vessel in a glove box. The vessel was connected to the vacuum line and 15 mL of dry THF was cold-distilled under vacuum into the flask. After 4 h stirring at RT, a dark green solution was obtained with few white salts. The solution was filtered. The THF was evaporated and the solid dried under vacuum to give a green pasty product, yield 64 %. The product was found to be only partially soluble in $[D_6]$benzene so the NMR analysis was conducted in $[D_8]$THF. ^{1}H NMR ($[D_8]$THF, 300 MHz, 20 °C): δ = 6.10 (p, 1H, CH); 3.01 (d, 4H, $2CH_2$); and -0.16 (br s, 8H, $2BH_4$). This is in accordance with formation of $Sc(BH_4)_2(C_3H_5)(THF)_x$ and not the expected product.

From $(C_3H_5)MgBr$

$Sc(BH_4)_3(THF)_2$ (0.1 g, 0.44 mmol) was weighed in a round-bottomed flask in a glove box**.** 10 mL of dry THF was added followed by $(C_3H_5)MgBr$ (0.92 mL, 0.88 mmol) drop by drop. After 3 h stirring at RT, a brown-green solution was obtained with white salts. The yellow solution was filtered and the salts washed once. THF was evaporated and the solid dried under vacuum to give a green pasty product, yield 71 %. The product was found to be only partially soluble in $[D_6]$benzene so the NMR analysis was conducted in $[D_8]$THF. ^{1}H NMR ($[D_8]$THF, 300 MHz, 20 °C): δ = 6.15 (p, 1H, CH); 2.94 (d, 4H, $2CH_2$); and -0.20 (br s, 8H, $2BH_4$). This is in accordance with formation of $Sc(BH_4)_2(C_3H_5)(THF)_x$ and not the expected product.

Following this attempt which was unsuccessful, this reaction was tested using toluene as the solvent instead of THF. Unfortunately, ^{1}H NMR spectra displayed no signals relative to the presence of the allyl group in the complex.

From $(C_3H_5)MgCl$

In a glovebox, $[D_6]$benzene (0.5 ml) was added to $Sc(BH_4)_3(THF)_2$ (10 mg, 0.044 mmol) in an NMR tube equipped with a Young valve. $(C_3H_5)MgCl$ (44.2 µL, 0.088 mmol) was then added resulting in a dark brown solution with dark brown precipitate. The ^{1}H NMR was

recorded after a day. ^{1}H NMR ([D_6]benzene, 300 MHz, 20 ^{o}C): δ = 6.8 (p, 1H, CH); 3.0 (d, 4H, $2CH_2$); 0.5 (br s, 8H, $2BH_4$). This is in accordance with formation of $Sc(BH_4)_2(C_3H_5)(THF)_x$ and not the expected product.

- **$Y(BH_4)(C_3H_5)_2(THF)_x$**

From $Mg(C_3H_5)_2$

$Y(BH_4)_3(THF)_2$ (0.14 g, 0.4 mmol) and $Mg(C_3H_5)_2(dioxane)_{0.06}$ (0.055 g, 0.48 mmol) were weighed in a vessel in a glove box. The vessel was connected to the vacuum line and 15 mL of dry THF was cold-distilled under vacuum into the flask. After 2 h stirring at RT, a yellow solution was obtained with few white salts. The solution was filtered. The THF was evaporated and the solid dried under vacuum to give a yellow pasty product, yield 81 %. The product was found to be only partially soluble in [D_6]benzene so the NMR analysis was conducted in [D_8]THF. ^{1}H NMR ([D_8]THF, 300 MHz, 20 °C): δ = 6.11 (p, 1H, CH); 2.74 (d, 4H, $2CH_2$); and -2.0 (br s, 8H, $2BH_4$). This is in accordance with formation of $Y(BH_4)_2(C_3H_5)(THF)_x$ and not the expected product.
Another synthesis was conducted using 2.2 equiv. of $Mg(C_3H_5)_2(dioxane)_{0.06}$ (0.098 g, 0.88 mmol) instead of 1.2 equiv. Unfortunately ^{1}H NMR showed the presence of two allyl and two borohydride groups**.**

From $(C_3H_5)MgBr$

$Y(BH_4)_3(THF)_3$ (0.1 g, 0.29 mmol) was weighed in a round-bottomed flask in a glove box. 10 mL of dry THF was added and then $(C_3H_5)MgBr$ (0.6 mL, 0.58 mmol) dropwise. After 1.5 h stirring at RT, a yellow solution was obtained with white salts. The yellow solution was filtered and the salts washed once. THF was evaporated and the solid dried under vacuum to give a yellow pasty product, yield 78 %. The product was found to be only partially soluble in [D_6]benzene so the NMR analysis was conducted in [D_8]THF. ^{1}H NMR ([D_8]THF, 300 MHz, 20 °C): δ = 6.49 (Major 84%, p), 6.19 (Minor 16%, p) (2H, 2CH); 3.03 (Major 84%, d), 2.90 (Minor 16%, d) (8H, $4CH_2$); and -0.12 (br s, 8H, BH_4). Minor and major products were formed instead of the expected product.

Other conditions were tested at the NMR scale using an excess of $(C_3H_5)MgBr$ (2.2 equiv.) and reaction time of 3 h. ^1H NMR displays a mixture of allylic compounds with major and minor signals. Adding 2 equiv. of tmeda to the previous mixture yielded oily yellowish product contained no allyl group.

From $(C_3H_5)MgCl$

$Y(BH_4)_3(THF)_3$ (0.1 g, 0.29 mmol) was weighed in a round-bottomed flask in a glove box. 10 mL of dry THF was added and then $(C_3H_5)MgCl$ (0.6 mL, 0.58 mmol) dropwise. After 1.5 h stirring at RT, a yellow solution was obtained with white salts. The yellow solution was filtered and the salts washed once. THF was evaporated and the solid dried under vacuum to give a yellow pasty product, yield 75 %. The product was found to be only partially soluble in $[D_6]$benzene so the NMR analysis was conducted in $[D_8]$THF. ^1H NMR ($[D_8]$THF, 300 MHz, 20 °C): δ = 6.42 (Minor 13%, p), 6.18 (Major 87%,p) (2H, 2CH); 2.92 (Minor 13%, d), 2.38 (Major 87%, d) (8H, $4CH_2$); and -0.29 (br s, 8H, $2BH_4$). Minor and major product were formed instead of the expected product.

From $Y(C_3H_5)_3$ and $Y(BH_4)_3(THF)_3$

YCl_3 (3.0 mg, 0.015 mmol) was added into an NMR tube equipped with a Young valve in a glovebox. $[D_8]$THF was distilled into the tube. $(C_3H_5)MgBr$ (50 µL, 0.045 mmol) was then added and the reaction was left for 3 days at RT. Then,$Y(BH_4)_3(THF)_3$ (5.3 mg, 0.015 mmol) was added and the tube was heated for an hour at 50 ^oC. ^1H NMR ($[D_8]$THF, 300 MHz, 20 ^oC): 6.21 (m, 2H, 2CH); 2.38 (d, 8H, $4CH_2$); -0.29 (br s, 4H, BH_4).The signals correspond to $Y(C_3H_5)_3$ and $Y(BH_4)_3(THF)_3$ unreacted.

From $Y(C_3H_5)_3$ and $NaBH_4$

In the glovebox, YCl_3 (10.0 mg, 0.05 mmol) was added into an NMR tube equipped with a Young valve. $[D_8]$THF was distilled into the tube and then $(C_3H_5)MgBr$ (0.15 mL, 0.15 mmol) was added and the reaction was left for 3 days at RT. $NaBH_4$ (3.8 mg, 0.1 mmol) was then added followed by another addition of $NaBH_4$ (1.9 mg, 0.05 mmol) of resulting in a orange solution with a grey precipitate. The ^1H NMR was recorded after a day at RT. ^1H

NMR ([D_8]THF, 300 MHz, 20 ^oC): 6.20 (m, H, CH); 2.37 (d, 4H, $2CH_2$). The signals correspond to $Y(C_3H_5)_3$ unreacted.

- **$La(BH_4)(C_3H_5)_2(THF)_x$**

[D_8]THF (0.5 ml) was added through distillation to $La(BH_4)_3(THF)_3$ (8.8 mg**,** 0.022 mmol) and $Mg(C_3H_5)_2(dioxane)_{0.06}$ (3.75 mg, 0.033 mmol) in an NMR tube equipped with a Young valve. ^1H NMR spectroscopy of the yellow solution was recorded after 3 h at RT. ^1H NMR ([D_8]THF, 300 MHz, 20 °C): δ = 6.04 (p, 1H, CH); 2.63 (d, 4H, $2CH_2$); and 0.11 (br s, 8H, 2 BH_4). This is in accordance with formation of $La(BH_4)_2(C_3H_5)(THF)_x$ and not the expected product.

Other conditions were tested using 2 equiv. $Mg(C_3H_5)_2(dioxane)_{0.06}$ (5 mg, 0.044 mmol) and 2.5 equiv. $Mg(C_3H_5)_2(dioxane)_{0.06}$ (6.2 mg, 0.055 mmol) instead of 1.5 equiv. Unfortunately, ^1H NMR showed the presence of two allyl and two borohydrides groups.

- **$Sm(BH_4)(C_3H_5)_2(THF)_x$**

From $Mg(C_3H_5)_2$

$Sm(BH_4)_3(THF)_3$ (0.19 g, 0.45 mmol) and $Mg(C_3H_5)_2(dioxane)_{0.06}$ (0.05 g, 0.45 mmol) were weighed in a vessel in a glove box. The vessel was connected to the vacuum line and 30 mL of dry THF was cold-distilled under vacuum into the flask. After 2 h stirring at RT, a red solution was obtained with few white salts. The solution was filtered. The red solution was filtered and concentrated to 5 mL. A Crop of red single crystals suitable for XRD analysis were grown from this THF solution at -20 °C and showed the presence of two BH_4 and one allyl groups. THF was removed and the solid dried under vacuum to give a red pasty solid, yield 60 %. ^1H NMR ([D_6]benzene, 300 MHz, 20 °C): δ = 16.06 (s, 2H, CH_2'); 11.18 (s, 2H, CH_2); 9.70 (s, 1H, CH); 1.55 (s, THF); 0.18 (s, THF); – 11.75 (br s, 8H, BH_4). This is in accordance with formation of $Sm(BH_4)_2(C_3H_5)(THF)_x$ and not the expected product.

From $Sm(BH_4)_2(C_3H_5)(THF)_x$

$Sm(BH_4)_2(C_3H_5)(THF)_3$ (0.24 g, 0.54 mmol) and $Mg(C_3H_5)_2(dioxane)_{0.06}$ (0.03 g, 0.27 mmol) were weighed in a vessel in a glove box. The vessel was connected to the vacuum line and 30 mL of dry THF was cold-distilled under vacuum into the flask. After 2 h stirring at RT a red solution was obtained with few white salts. The solution was filtered. THF was evaporated and the solid dried under vacuum to give a red pasty product, yield 82 %. ^{1}H NMR ([D_8]THF, 300 MHz, 20 °C): δ = 6.26 (p, 1H, CH); 2.36 (d, 4H, $2CH_2$). This result is in accordance of formation of $Sm(C_3H_5)_3(THF)_x$ and not the expected product.

6.4.4 NMR synthesis of tris(allyl) yttrium complex

From YCl_3

YCl_3 (3.0 mg, 0.015 mmol) was added into an NMR tube equipped with a Young valve in a glovebox. [D_8]THF (0.5 ml) was distilled into the tube and then $(C_3H_5)MgBr$ (50 µL, 0.045 mmol) was added, resulting in an orange solution with a grey precipitate. The ^{1}H NMR was recorded after a day at RT. ^{1}H NMR ([D_8]THF, 300 MHz, 20 ^{o}C): δ = 6.20 (p, 1H, CH); 2.33 (d, 4H, $2CH_2$). The signals corresponds to $Y(allyl)_3$.

From $Y(BH_4)_3(THF)_2$

$Y(BH_4)_3(THF)_2$ (3.5 mg, 0.01 mmol) was added into an NMR tube equipped with a Young valve in a glovebox. [D_8]THF (0.5 ml) was distilled into the tube and then $(C_3H_5)MgBr$ (30 µL, 0.03 mmol) was added, resulting in an orange solution with a grey precipitate. The ^{1}H NMR was recorded after a day at RT. ^{1}H NMR ([D_8]THF, 300 MHz, 20 ^{o}C): δ = 6.18 (m, 3H, 3CH); 2.31 (d, 12H, $6CH_2$); -0.31 (br s, 4H, BH_4). The expected product was not formed.

6.4.5 Synthesis of phosphasalen rare-earth borohydride complexes

L^1K_2 (Appendix IX). This synthesis was performed according to literature procedure.[13,14] Potassium bis(trimethylsilyl)amide (KHMDS) (1.19 g, 6 mmol) was added to a suspension of

the aminophosphonium salt L^1H_4 (1.5 g, 1.5 mmol) in THF (50 ml) at RT. After 18h a cloudy solution was formed. The white potassium bromide by-product was removed by filtration. Volatiles were removed in vacuum, and the residue was washed with pentane (10 ml) and dried in vacuum to give a white solid, yield 90 %. $^{31}P\{1H\}$ NMR ([D_8]THF, 300 MHz, 20 ^oC): δ = 20.38 (s, P^V). ^1H NMR ([D_8]THF, 300 MHz, 20 ^oC): δ = 7.54−7.48 (m, 8H, *o*-C*H*(PPh_2)); 7.41−7.36 (m, 8H, *m*-C*H*(PPh_2)); 7.34−7.30 (d, 4H, *p*-C*H*(PPh_2)); 7.14 (m, 2H, 2H, $2C_bH$), 6.02 (d, 2H, $2C_dH$); 3.42 (m, 4H, N−CH_2−CH_2−N); 1.48 (s, 18H, $C_aC(CH_3)_3$); 0.90 (s, 18H, $C_bC(CH_3)_3$).

L^2K_2 (Appendix X). This synthesis was performed according to literature procedure.[13,14] KHMDS (0.57 g, 2.8 mmol) was added to a suspension of the aminophosphonium salt L^2H_4 (0.74 g, 0.7 mmol) in THF (25 ml) at RT. After18 h a cloudy solution was formed. The white potassium bromide byproduct was removed by filtration. Volatiles were removed in vacuum, and the residue was washed with pentane (5 ml) and dried in vacuum to give a white solid, yield 93 %. $^{31}P\{1H\}$ NMR ([D_8]THF, 300 MHz, 20 ^oC): δ = 12.22 (s, P^V). ^1H NMR ([D_8]THF, 300 MHz, 20 ^oC): δ = 7.79 (m, 8H, *o*-C*H*(PPh_2)); 7.48−7.27 (m, 12H, *p,m*-C*H*(PPh_2)); 7.17 (m, 2H, $2C_bH$); 6.62 (m, 4H, N−C*H*(Ph)−N); 6.06 (d, 2H, $2C_dH$); 1.25 (s, 18H, $C_aC(CH_3)_3$); 1.05 (s, 18H, $C_bC(CH_3)_3$.

$L^1Sc(BH_4)(THF)_x$. $Sc(BH_4)_3(THF)_2$ (0.077 g, 0.33 mmol) and L^1K_2 (0.3 g, 0.33 mmol) were weighed in a vessel in a glove box. The vessel was connected to the vacuum line and 30 mL of dry THF was cold-distilled under vacuum into the flask. After 18 h stirring at RT, a pale yellow solution was obtained with white salts. The pale yellow solution was filtered and the salts washed once. The solution was then concentrated to 5 mL. A crop of colorless crystals suitable for XRD analysis were grown from this THF solution at -20 °C. THF was removed and the solid dried under vacuum to give a pale yellow solid powder, yield 91 %. $^{31}P\{1H\}$ NMR ([D_8]THF, 300 MHz, 20 ^oC): δ = 32.8, 30.1, 29.50, 27.1, 26.4 (s, PV). ^1H NMR ([D_8]THF, 300 MHz, 20 ^oC): δ = 7.95−7.76 (d, 4H, *p*-C*H*(PPh_2)); 7.66−7.33 (m, 16H, o,*m*-C*H*(PPh_2)); 7.28 (d, 2H, C_bH); 6.68 (dd, 2H, C_dH); 3.33 (m, 2H, N−CH_2−CH_2−N); 3.07 (m, 2H, N−CH_2− CH_2−N); 1.49 (s, 18H, C_a−C(CH_3)$_3$); 1.04 (s, 18H, C_c−C(CH_3)$_3$); 0.46 (br s, 4H, BH_4).

$L^1Y(BH_4)(THF)_x$. $Y(BH_4)_3(THF)_3$ (0.15 g, 0.33 mmol) and L^1K_2 (0.3 g, 0.33 mmol) were weighed in a vessel in a glove box. The vessel was connected to the vacuum line and 30 mL of dry THF was cold-distilled under vacuum into the flask. After 18 h stirring at RT, a pale yellow solution was obtained with white salts. The pale yellow solution was filtered and the salts washed once. The THF was evaporated under vacuum until forming a concentrated solution of 5 mL. A Crop of colorless single crystals suitable for XRD analysis were grown from this THF solution at -20 °C. THF was removed and the solid dried under vacuum to give a pale yellow solid powder, yield 82 %. $^{31}P\{1H\}$ NMR ([D_8]THF, 300 MHz, 20 ^oC): δ = 31 (s, P^V). ^1H NMR ([D_8]THF, 300 MHz, 20 ^oC): δ = 7.63 (m, 4H, *p*-C*H*(PPh_2)), 7.48 (m, , 8H, o-C*H*(PPh_2)), 7.40 (m, 8H, *m*-C*H*(PPh_2)), 7.20 (m, 2H, C_bH), 6.60 (dd, 2H, C_dH), 3.18 (m, 4H, N−CH_2−CH_2−N), 1.37 (s, 18H, C_a−C(CH_3)$_3$), 1.055 (s, 18H, C_c−C(CH_3)$_3$), 0.72 (br s, 4H, BH_4).

$L^1Nd(BH_4)(THF)_x$. $Nd(BH_4)_3(THF)_3$ (0.14 g, 0.33 mmol) and L^1K_2 (0.3 g, 0.33 mmol) were weighed in a vessel in a glove box. The vessel was connected to the vacuum line and 30 mL of dry THF was cold-distilled under vacuum into the flask. After 18 h stirring at RT, a pale blue solution was obtained with white salts. The pale blue solution was filtered and the salts washed once. The THF was evaporated under vacuum until forming a concentrated solution of 5 mL. A Crop of pale blue crystals suitable for XRD studies were grown from this THF solution at -20 °C but they were too sensitive and decomposed when taken out of the glove box in fluorinated grease. THF was removed and the solid dried under vacuum to give a blue solid powder, yield 77 %. $^{31}P\{1H\}$ NMR ([D_8]THF, 300 MHz, 20 ^oC): δ = 31 (s, P^V). ^1H NMR ([D_8]THF): Assignment of signals in detail could not be performed due to the paramagnetism of neodymium (III).

$L^2Nd(BH_4)(THF)_x$. $Nd(BH_4)_3(THF)_3$ (0.14 g, 0.33 mmol) and L^2K_2 (0.3 g, 0.33 mmol) were weighed in a vessel in a glove box. The vessel was connected to the vacuum line and 30 mL of dry THF was cold-distilled under vacuum into the flask. After 18 h stirring at RT, a pale blue solution was obtained with white salts. The pale blue solution was filtered and the salts washed once. The THF was evaporated under vacuum until forming a concentrated solution of 5 mL. A Crop of pale blue crystals suitable for XRD studies were grown from this THF solution at -20 °C but they were too sensitive anddecomposed when taken out of the glove box in fluorinated grease . THF was removed and the solid dried under vacuum to give a blue

solid powder, yield 95 %. $^{31}P\{1H\}$ NMR ([D_8]THF, 300 MHz, 20 °C): δ = 49.5 (s, P^V). ^1H NMR ([D_8]THF): Assignment of signals in detail could not be performed due to the paramagnetisim of neodymium (III).

$L^3Y(BH_4)_2(THF)_x$. KHMDS (0.33 g, 1.68 mmol) and L^3H_2 (0.5 g, 0.84 mmol) were weighed in a vessel in a glove box. The vessel was connected to the vacuum line and 40 mL of dry THF was cold-distilled under vacuum into the flask. After 18 h stirring at RT, a cloudy solution was obtained with white salts. $Y(BH_4)_3(THF)_3$ (0.29 g, 0.84 mmol) in THF(10 ml) solution was added dropwise giving a pale blue solution. After 4 h stirring at RT, the volatiles were removed and 50 ml of dry toluene was cold-distilled under vacuum into the flask. The toluene was evaporated under vacuum until forming a concentrated solution of 5 mL. A Crop of colorless crystals suitable for XRD studies were grown from this THF solution at -20 °C. Toluene was removed and the solid dried under vacuum to yield a pale yellow solid powder 90 %. $^{31}P\{1H\}$ NMR ([D_8]THF, 300 MHz, 20 °C): δ = 29.8 (s, P^V). ^1H NMR ([D_8]THF, 300 MHz, 20 °C): δ = 7.69-7.58 (m, 4H, *o*-C*H*(PPh_2)); 7.04-6.85 (m, 6H, *m,p*-C*H*(PPh_2)); 6.61 (m, 1H, C_bH); 6.55 (m, 1H, C_dH); 6.47-6.40 (m, 4H, $C_{e,f,g,h}H$(Ph)); 3.79 (s, 3H, OCH_3); 3.67 (traces of THF), 1.64 (s, 9H, C_a–$C(CH_3)_3$); 1.08 (s, 9H, C_c–$C(CH_3)_3$); 1.39 (br s, 4H, BH_4); 1.25 (traces of THF).

6.5 Reactivity experiments of the mono(allyl) bis(borohydride) rare-earth complexes with various reagents

6.5.1 Benzophenone

$Sc(BH_4)_2(C_3H_5)(THF)_2$ and benzophenone. [D_8]THF (0.5ml) was added through distillation to $Sc(BH_4)_2(C_3H_5)(THF)_2$ (3.7 mg**,** 14 μmol) and benzophenone (2.5 mg, 14 μmol) in an NMR tube equipped with a Young valve. ^1H NMR spectroscopy of the greenish-brown solution was recorded after 3 h at Rt. ^1H NMR ([D_8]THF, 300 MHz, 20 °C): δ = 7.45-7.11 (Phenyl rings, 10H), 5.91 (m, 1H, CH_δ); 5.05 (m, 1H, CH_β); 4.92 (m, 1H, CH_γ); 3.08 (m, 2H, $2CH_\alpha$); 0.39 (BH_4). This is in accordance with formation of $Sc(OC(C_3H_5)Ph_2)(BH_4)_2(THF)_x$.

$Y(BH_4)_2(C_3H_5)(THF)_3$ and benzophenone. [D_8]THF (0.5 ml) was added through distillation to [D_8]THF was added through distillation to $Y(BH_4)_2(C_3H_5)(THF)_3$ (5.3 mg**,** 14 μmol) and benzophenone (2.5 mg, 14 μmol) in an NMR tube equipped with a Young valve. ^{1}H NMR spectroscopy of the colourless solution was recorded after 3 h at RT. ^{1}H NMR ([D_8]THF, 300 MHz, 20 ^{o}C): δ = 7.45 (*o*-C_6H_5); 7.14 (*m*-C_6H_5); 7.01 (*p*-C_6H_5); 5.88 (m, 1H, CH_δ); 4.88 (m, 1H, CH_β); 4.75 (m, 1H, CH_γ); 3.13 (m, 2H, $2CH_\alpha$); 0.423 (BH_4). This is in accordance with formation of $Y(OC(C_3H_5)Ph_2)(BH_4)_2(THF)_x$.

$La(BH_4)_2(C_3H_5)(THF)_3$ and benzophenone. [D_8]THF (0.5 ml) was added through distillation to $La(BH_4)_2(C_3H_5)(THF)_3$ (5.9 mg**,** 14 μmol) and benzophenone (2.5 mg, 14 μmol) in an NMR tube equipped with a Young valve. ^{1}H NMR spectroscopy of the orange-brown solution was recorded after 3 h at RT. ^{1}H NMR ([D_8]THF, 300 MHz, 20 ^{o}C): δ = 7.43 (*o*-C_6H_5); 7.14 (*m*-C_6H_5); 7.02 (*p*-C_6H_5); 5.84 (m, 1H, CH_δ); 4.91 (m, 1H, CH_β); 4.79 (m, 1H, CH_γ); 3.07 (m, 2H, $2H_\alpha$); 0.85 (BH_4). This is in accordance with formation of $La(OC(C_3H_5)Ph_2)(BH_4)_2(THF)_x$.

$Nd(BH_4)_2(C_3H_5)(THF)_3$ and benzophenone. [D_6]benzene (0.5 ml) was added to $Nd(BH_4)_2(C_3H_5)(THF)_3$ (3.5 mg, 8 μmol) and benzophenone (1.5 mg, 8 μmol) in an NMR tube equipped with a Young valve. ^{1}H NMR spectroscopy of the green solution was recorded after 6 hours. ^{1}H NMR ([D_6]benzene, 300 MHz, 20 ^{o}C): δ = 90.00 (br s, BH_4); 35.56 (s); 33.93 (s); 28.82 (s); 27.81 (s); 18.19 (s); 16.13 (s); 10.94 (s); 10.48 (s); 10.01 (s); 9.67 (s); 7.48 (m); 6.20 (m); 5.76 (m); 5.01 (m); 4.72 (m); 4.42 (s); 4.07 (m); 3.49 (m); 3.26 (m); 2.98 (m); 0.47 (br s);-2.02 (s); -3.70 (s); -5.70 (br s). Assignment of signals in detail could not be performed due to the paramagnetism of neodymium (III).

$Sm(BH_4)_2(C_3H_5)(THF)_3$ and benzophenone. [D_8]THF (0.5 ml) was added through distillation to $Sm(BH_4)_2(allyl)(THF)_3$ (6.1 mg, 14 μmol) and benzophenone (2.5 mg, 14 μmol) in an NMR tube equipped with a Young valve. ^{1}H NMR spectroscopy of the colourless solution and white precipitate was recorded after 3 h at RT. ^{1}H NMR ([D_8]THF, 300 MHz, 20 ^{o}C): δ = 9.63 (s); 9.10 (m);8.59 (m); 7.52 - 7.10 (C_6H_5, 10H); 6.33 (s); 5.91 (s); 5.43 (m); 5.15 (m); 4.98 (s); 4.69 (m); -0.16 (br s); -6.15 (br s). Assignment of signals in detail could not be performed due to the paramagnetism of samarium (III).

6.5.2 Cyclopentadienes (Cp^RH, Cp = C_5Me_4, R = H or Et)

$Nd(BH_4)_2(C_3H_5)(THF)_3$ and Cp^HH. [D_6]benzene (0.5 ml) was added to Cp^HH (1.4 µL, 0.009 µmol) in an NMR tube equipped with a Young valve. followed by the addition of $Nd(BH_4)_2(C_3H_5)(THF)_3$ (3.9 mg, 9 µmol). ^{1}H NMR spectroscopy of the light green solution was recorded after 1 day at RT. ^{1}H NMR ([D_6]benzene, 300 MHz, 20 ^{o}C): δ = 92.6 (br s, BH_4); 9.36 (s, 6H, $2CH_3$); 7.56 (s, 6H, $2CH_3$); 5.71 (m, 1H, CH); 4.97 (m, 2H, CH_2); 1.54 (m, 3H, CH_3); -0.70 (s, THF); - 1.86 (s, THF). This is in accordance with formation of $(Cp^H)Nd(BH_4)_2(THF)_x$.

$Nd(BH_4)_2(C_3H_5)(THF)_3$ and $Cp^{Et}H$. [D_6]benzene (0.5 ml) was added to $Cp^{Et}H$ (1.5 µL, 8 µmol) in an NMR tube equipped with a Young valve, followed by the addition of $Nd(BH_4)_2(C_3H_5)(THF)_3$ (3.5 mg, 8 µmol). ^{1}H NMR spectroscopy of the light green solution was recorded after 1 day. ^{1}H NMR ([D_6]benzene, 300 MHz, 20 ^{o}C): δ = 96.2 (br s, BH_4); 8.62 (s, 6H, $2CH_3$); 8.22 (s, 6H, $2CH_3$); 6.76 (m, 2H, CH_2); 5.71 (m, 1H, CH); 4.97 (m, 2H, CH_2); 2.64 (m, 3H, CH_3); 1.55 (m, 3H, CH_3); -0.79 (s, THF); - 2.41 (s, THF). This is in accordance with formation of $(Cp^{Et})Nd(BH_4)_2(THF)_x$.

6.5.3 Phenylsilane

$Nd(BH_4)_2(C_3H_5)(THF)_3$ and phenylsilane. $Nd(BH_4)_2(C_3H_5)(THF)_3$ (5.2 mg, 12 µmol) was added to an NMR equipped with a Young valve followed by [D_6]benzene (0.5 ml) in a glovebox. Once all the crystals were dissolved, phenylsilane (1.5 µL, 12 µmol) was added and a ^{1}H NMR of the green solution was recorded after 20 hours at RT. One more equivalent of phenylsilane (1.5µL, 12 µmol) was added and the tube was heated at 50 ^{o}C for 6 days. This resulted in a yellow solution with brown precipitate. ^{1}H NMR ([D_6]benzene, 300 MHz, 20 ^{o}C): δ = 99.4 (br s, BH_4); 7.38-7.10 (m, phenyl rings); 5.74 (m); 4.97 (m); 4.51 (m); 4.23 (s, Si-H); 3.90 (s); 3.5 (s); 2.33 (br s, THF); 1.17 (br s, THF). Assignment of signals in detail could not be performed due to the paramagnetism of neodymium (III). The expected product seemed not to be formed. Propene was produced; in addition no signal indicating the formation of Si-allyl was recorded.

6.5.4 Triethylsilane

$Nd(BH_4)_2(C_3H_5)(THF)_3$ and triethylsilane. Triethylsilane (1.4 µL, 8.74 µmol) was added to [D_6]benzene (0.5 ml) in an NMR tube equipped with a Young valve in a glovebox. $Nd(BH_4)_2(C_3H_5)(THF)_3$ (3.9 mg, 8.74 µmol) was added and a ^{1}H NMR was recorded after 1 day at RT. One more equivalent of triethylsilane (1.4 µL, 8.74 µmol) was added and then heated at 50 ^{o}C for 4 days. This resulted in a yellow solution with brown precipitate. ^{1}H NMR ([D_6]benzene, 300 MHz, 20 ^{o}C): δ = 101.6 (br s, BH_4); 23.18 (s, CH); 13.68 (s, CH_2); 5.73 (m); 5.00 (m); 3.89 (s, Si-H); 1.55 (m); 0.97 (m, Si$CH_2$$CH_3$); 0.55 (m, $SiCH_2CH_3$); - 0.43 (br s, THF); -1.22 (br s, THF). Assignment of signals in detail could not be performed due to the paramagnetism of neodymium (III). The expected product seemed not to be formed. Propene was produced; in addition no signal indicating the formation of Si-allyl was recorded.

6.5.5 1,4,7-Trimethyl-1,4,7-triazacyclononane (N_3)

$Sc(BH_4)_2(C_3H_5)(THF)_2$ and N_3. [D_8]THF (0.5 ml) was added through distillation to $Sc(BH_4)_2(C_3H_5)(THF)_2$ (2 mg, 8 µmol) in an NMR tube equipped with a Young valve. The N_3 ligand (1.6 µL, 8 µmol) was then added. ^{1}H NMR of the brown solution with brown precipitate was recorded after 6 hours at RT. ^{1}H NMR ([D_8]THF, 300 MHz, 20 ^{o}C): δ = 6.27 (m, C*H*) 3.26 (m, 6H, 6CH, Sc-N_3); 2.90 (m, 6H, 6CH' and 9H, $3CH_3$ overlap, Sc-N_3); 2.63 (m, free N_3); 2.30 (m, free N_3); 0.66 (m, 8H, $2BH_4$). The signals of the 4 hydrogens relative to the allyl signal ($2CH_2$) are overlapped with the signals from coordinated N_3. The expected product $Sc(BH_4)_2(C_3H_5)(N_3)$ seemed to be formed.

$Y(BH_4)_2(C_3H_5)(THF)_3$ and N_3. [D_8]THF (0.5 ml) was added through distillation to $Y(BH_4)_2(C_3H_5)(THF)_3$ (2.7 mg, 7 µmol) in an NMR tube equipped with a Young valve. The N_3 ligand (1.4 µL, 7 µ mol) was then added. ^{1}H NMR of the colorless solution with white precipitate was recorded after 6 hours at RT.^{1}H NMR ([D_8]THF, 300 MHz, 20 ^{o}C): δ = 3.11 (m, CH_2, Y-N_3); 2.89 (m, CH'_2, Y-N_3); 2.83 (m, CH_3, Y-N_3); 2.63 (m, free N_3); 2.30 (m, free N_3); 0.56 (m, BH_4). The signals of the 4 hydrogens relative to the allyl signal ($2CH_2$) are overlapped with the signals from coordinated N_3. The expected product $Y(BH_4)_2(C_3H_5)(N_3)$ seemed to be formed.

$La(BH_4)_2(C_3H_5)(THF)_3$ and N_3. $[D_8]$THF (0.5 ml) was added through distillation to $La(BH_4)_2(C_3H_5)(THF)_3$ (3 mg, 7 μmol) in an NMR tube equipped with a Young valve. The N_3 ligand (1.4 μL, 7 μmol) was then added. ^{1}H NMR of the colorless solution with white precipitate was recorded after 6 hours at Rt. ^{1}H NMR ($[D_8]$THF, 300 MHz, 20 ^{o}C): δ = 3.06 (m, 6H, 6CH, La-N_3) 2.80 (m, 6H, 6CH' and 9H $3CH_3$ overlap, La-N_3); 2.60 (m, free N_3); 2.26 (m, free N_3); 0.95 (m, 8H, $2BH_4$). The signals of the 4 hydrogens relative to the allyl signal ($2CH_2$) are overlapped with the signals from coordinated N_3. The expected product $La(BH_4)_2(C_3H_5)(N_3)$ seemed to be formed.

$Nd(BH_4)_2(C_3H_5)(THF)_3$ and N_3. In a glovebox, the N_3 ligand (1.4 μL, μmol) was added to $[D_6]$benzene (0.5 ml) in an NMR tube equipped with a Young valve, followed by the addition of $Nd(BH_4)_2(C_3H_5)(THF)_3$ (3.1 mg, 7.15 μmol). This resulted in a light green solution with green precipitate. The solution was decanted and the solid was dissolved in $[D_8]$THF to form a light green solution. The solution was concentrated by evaporating off the $[D_8]$THF leaving only about quarter of the solution and it was left to stand overnight. Pentane was layered over the solution and the tube was left to stand for 3 days at RT resulting in the formation of crystals. ^{1}H NMR ($[D_8]$THF, 300 MHz, 20 ^{o}C): δ 87.69 (br s); 42.95 (br s); 18.60 (s); 15.43 (s); 12.80 (s); 12.01 (m); 10.34 (m); 7.11 (m); 5.38 (s); 2.64 (m); 2.31 (m); 0.10 (m); - 1.19 (s); -2.83 (s); -14.89 (s). Assignment of signals in detail could not be performed due to the paramagnetism of neodymium (III). The expected product $Nd(BH_4)_2(C_3H_5)(N_3)$ seemed to be formed.

$Sm(BH_4)_2(C_3H_5)(THF)_3$ and N_3. $[D_6]$benzene (0.5 ml) was added to $Sm(BH_4)_2(C_3H_5)(THF)_3$ (3 mg, 7 μmol) in an NMR tube equipped with a Young valve. The tube was the pressurized with THF vapor. The N_3 ligand (1.4 μL, 7 μmol) was then added. This resulted in a pink solution with dark brown precipitate. The solvent was then removed and $[D_8]$THF (0.5 ml) was added through distillation. The solid was partially soluble and resulted in a brown solution. ^{1}H NMR ($[D_8]$THF, 300 MHz, 20 ^{o}C): δ 16.61; 7.32; 4.35 (m, CH_2, Sm-N_3); 3.09 (m, CH'_2, Sm-N_3); 2.81; 2.63 (m, free N_3); 2.30 (m, free N_3); 1.42 (m, CH_3, Sm-N_3); -11.02 (m, BH_4). The expected product $Sm(BH_4)_2(C_3H_5)(N_3)$ seemed to be formed.

6.6 References

[1] G. R. Fulmer, A. J. M. Miller, N. H. Sherden, H. E. Gottlieb, A. Nudelman, B. M. Stoltz, J. E. Bercaw, K. I. Goldberg, *Organometallics* **2010**, *29*, 2176.

[2] P. Zinck, M. Terrier, A. Mortreux, M. Visseaux, *Polym. Test.* **2009**, *28*, 106.

[3] M. Save, M. Schappacher, A. Soum, *Macromol. Chem. Phys*. **2002**, *203*, 889.

[4] A. Kowalski, A. Duda, S. Penczek, *Macromolecules* **1998**, *31*, 2114.

[5] G. M. Sheldrick, *Acta Cryst*. **2015**, *A71*, 3.

[6] G. M. Sheldrick, *Acta Cryst*. **2015**, C*71*, 3.

[7] M. Terrier, M. Visseaux, T. Chenal, A. Mortreux, *J. Polym.Sci.: Part A: Polym. Chem.* **2007**, *45*, 2400.

[8] W. Schlenk, J. W. Schlenk, *Ber.* **1929**, *62, B*, 920.

[9] C. R. Noller, W. R. White, *Am. Chem. Soc.* **1937**, *59*, 1354.

[10] R. Kullman, *Compt. rend*. **1950**, *231*, 866.

[11] L. Palatinus, G. Chapuis, *J. Appl. Cryst.* **2007**, *40*, 786.

[12] P. W. Betteridge, J. R. Carruthers, R. I. Cooper, K. Prout, D. J. Watkin, *J. Appl. Cryst.* **2003**, *36*, 1487.

[13] T. P. A. Cao, A. Buchard, X. F. Le Goff, A. Auffrant, C. K. Williams, *Inorg. Chem.* **2012**, *51*, 2157.

[14] C. Bakewell, T. P. A. Cao, X. F. Le Goff, N. J. Long, A. Auffrant, C. K. Williams, *Organometallics* **2013**, *32*, 1475.

APPENDICES

Appendix I

^{1}H NMR in $[D_8]THF$ of the product isolated from the reaction of $Y(BH_4)_3(THF)_2$ with 1.2 eq $Mg(C_3H_5)_2(diox)_{0.06}$.

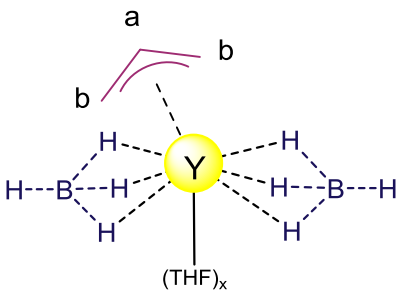

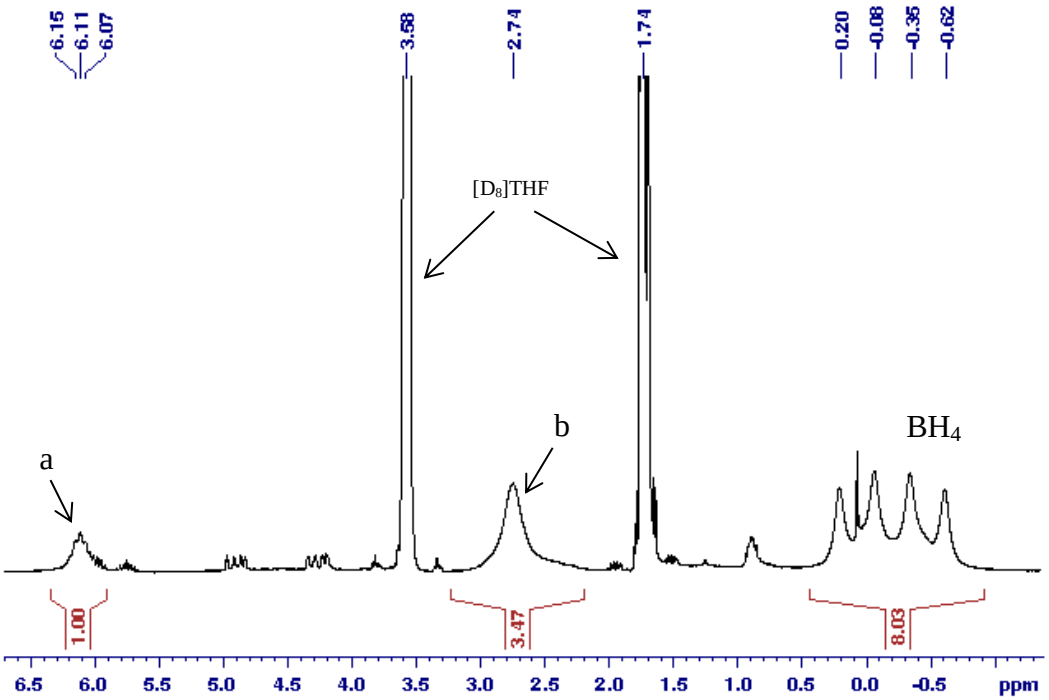

Appendix II

^{1}H NMR in [D_8]THF of the product isolated from the reaction of $Sc(BH_4)_3(THF)_2$ with 1 equiv. $(C_3H_5)MgBr$.

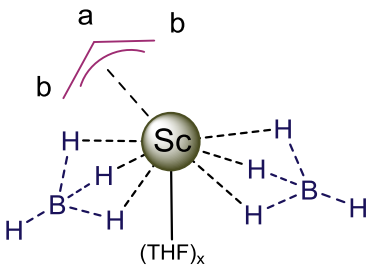

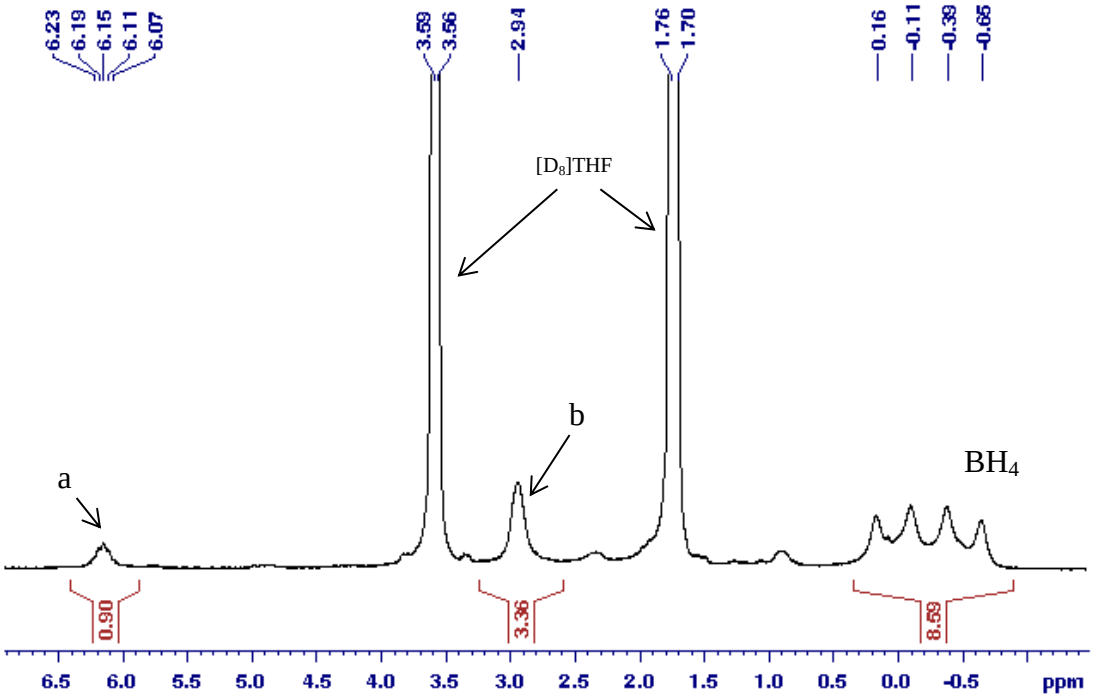

Appendix III

^{1}H NMR in [D_8]THF of the NMR-scale reaction of $Y(C_3H_5)_3$ with 1 equiv. $NaBH_4$.

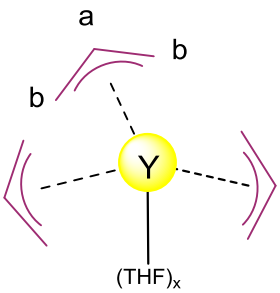

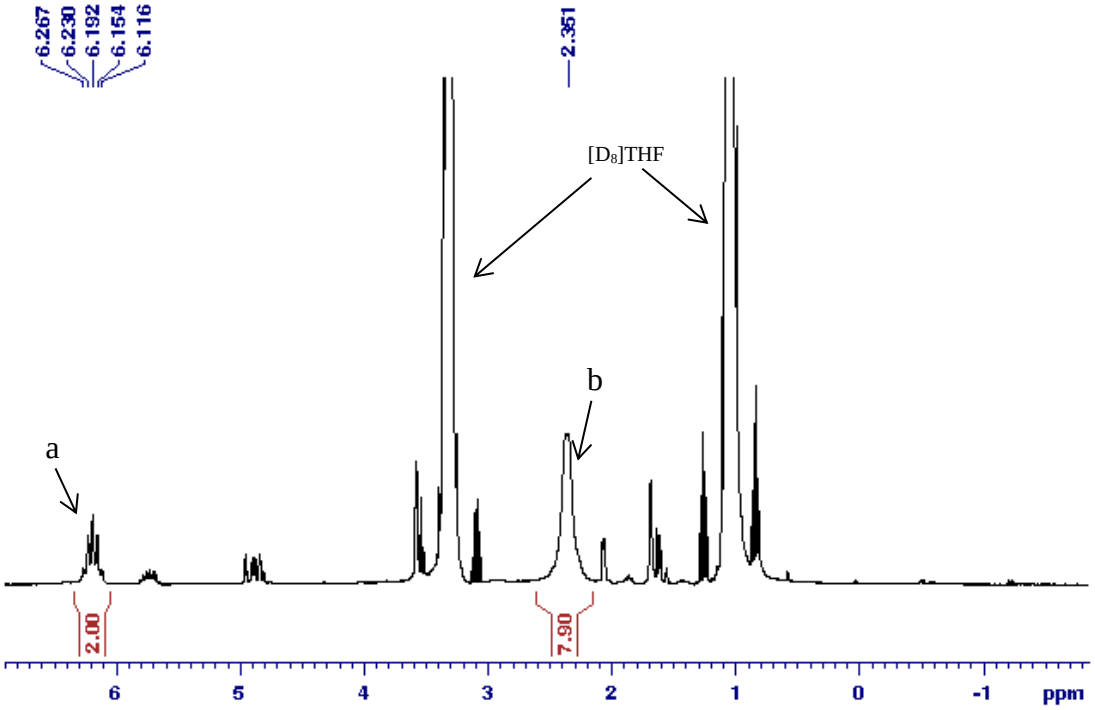

Appendix IV

^{1}H NMR in [D_8]THF of the NMR-scale reaction of $Nd(BH_4)_3(THF)_x$ with benzophenone (1 and 2 equiv.).

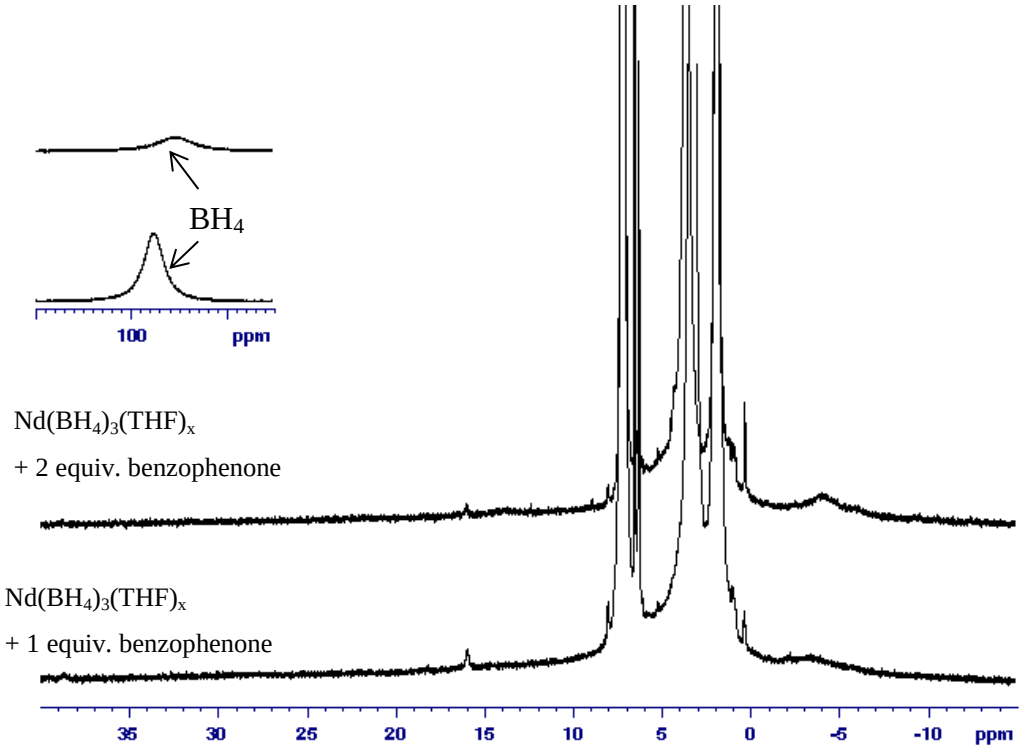

Appendix V

^{1}H NMR in [D_6]benzene of the NMR-scale reaction of $Nd(BH_4)_2(allyl)(THF)_x$ with triethylsilane.

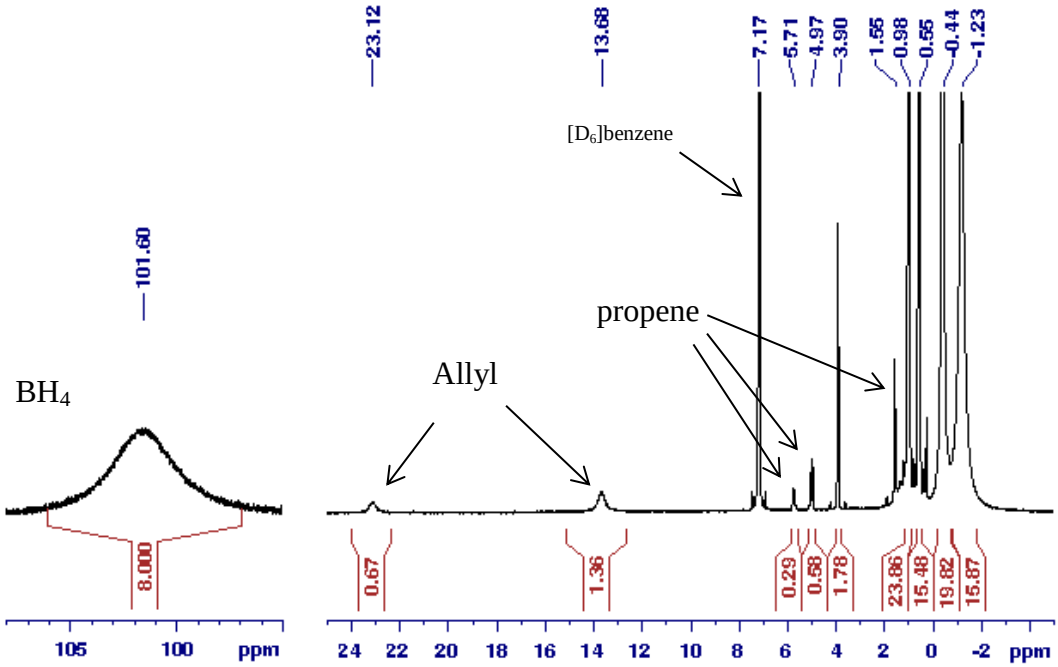

Appendix VI

*MALDI-ToF MS spectrum of polylactide obtained by using $Sc(BH_4)_2(C_3H_5)(THF)_2$ (**1**) (entry 34, Tables 3.5 and 3.6, section 3.3.3).*

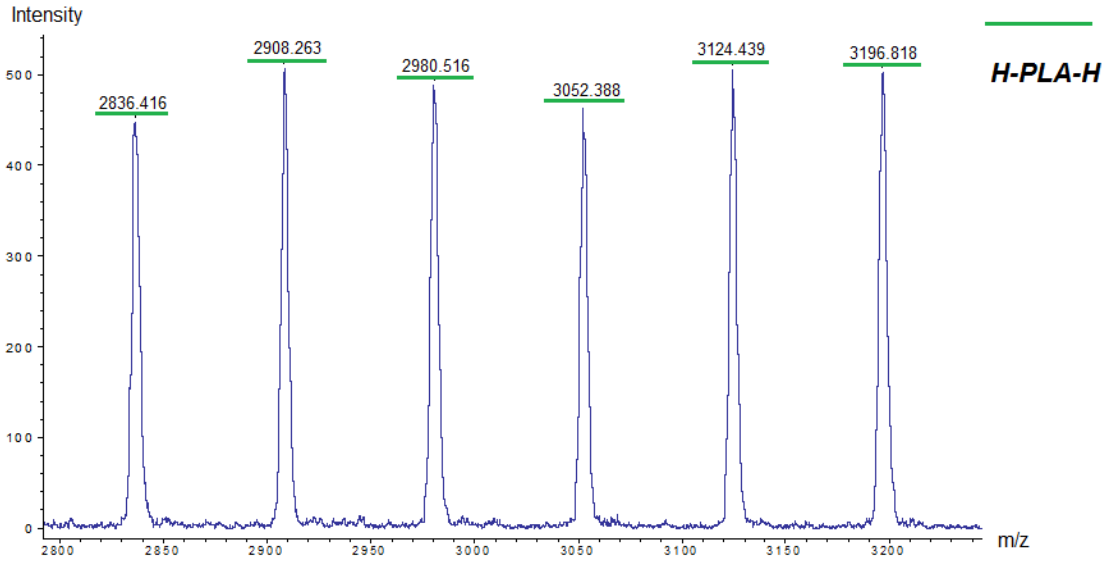

Appendix VII

*MALDI-ToF MS spectrum of polylactide obtained by using $La(BH_4)_2(C_3H_5)(THF)_3$ (**3**) (entry 36, Tables 3.5 and 3.6, section 3.3.3).*

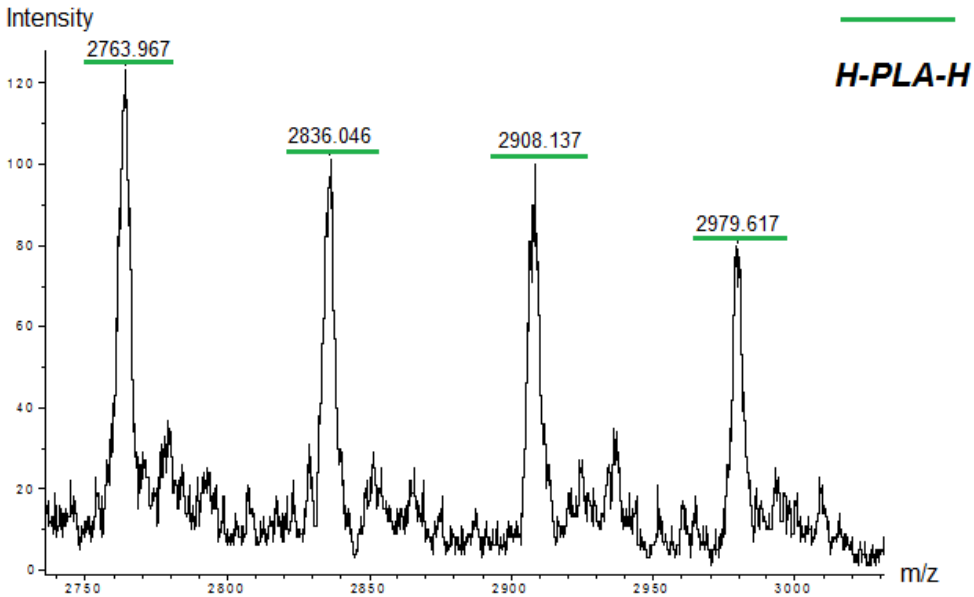

Appendix VIII

*MALDI-ToF MS spectrum of polylactide obtained by using $Sm(BH_4)_2(C_3H_5)(THF)_3$ (**5**) (entry 38, Tables 3.5 and 3.6, section 3.3.3).*

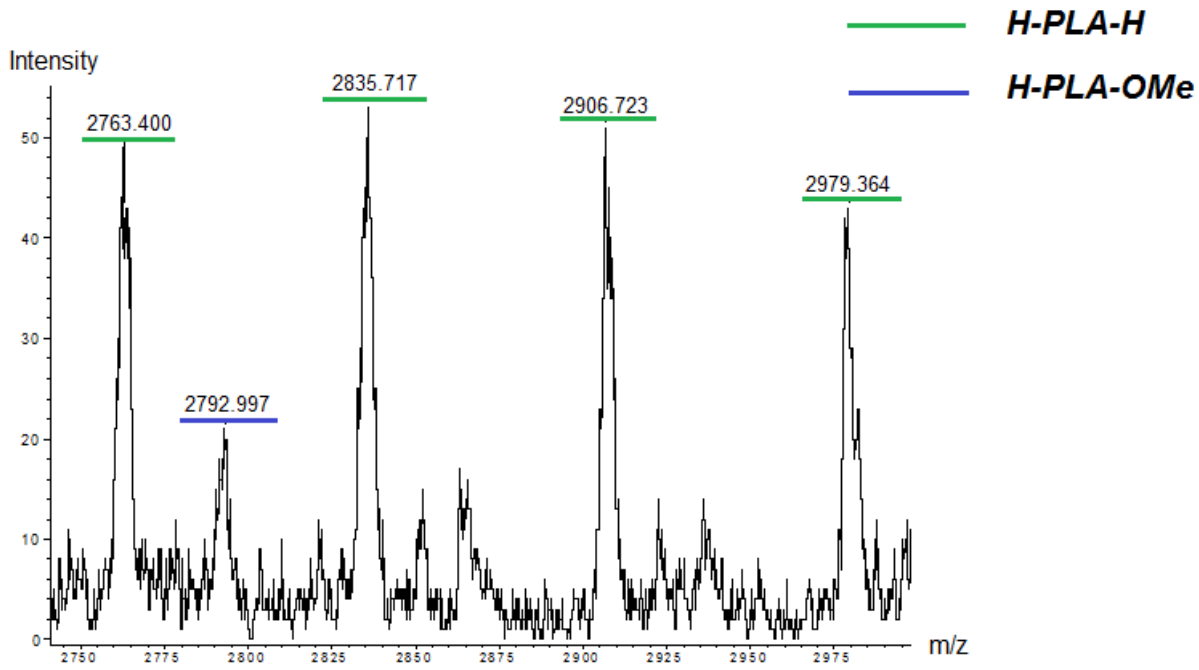

Appendix IX

^1H NMR of of L^1K_2 in $[D_8]THF$

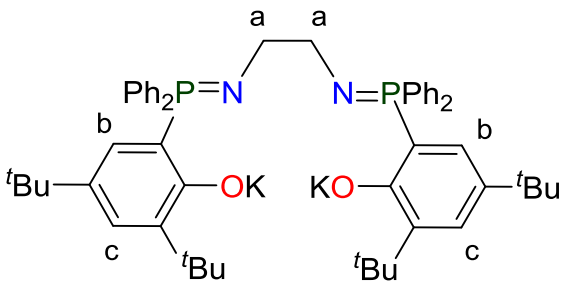

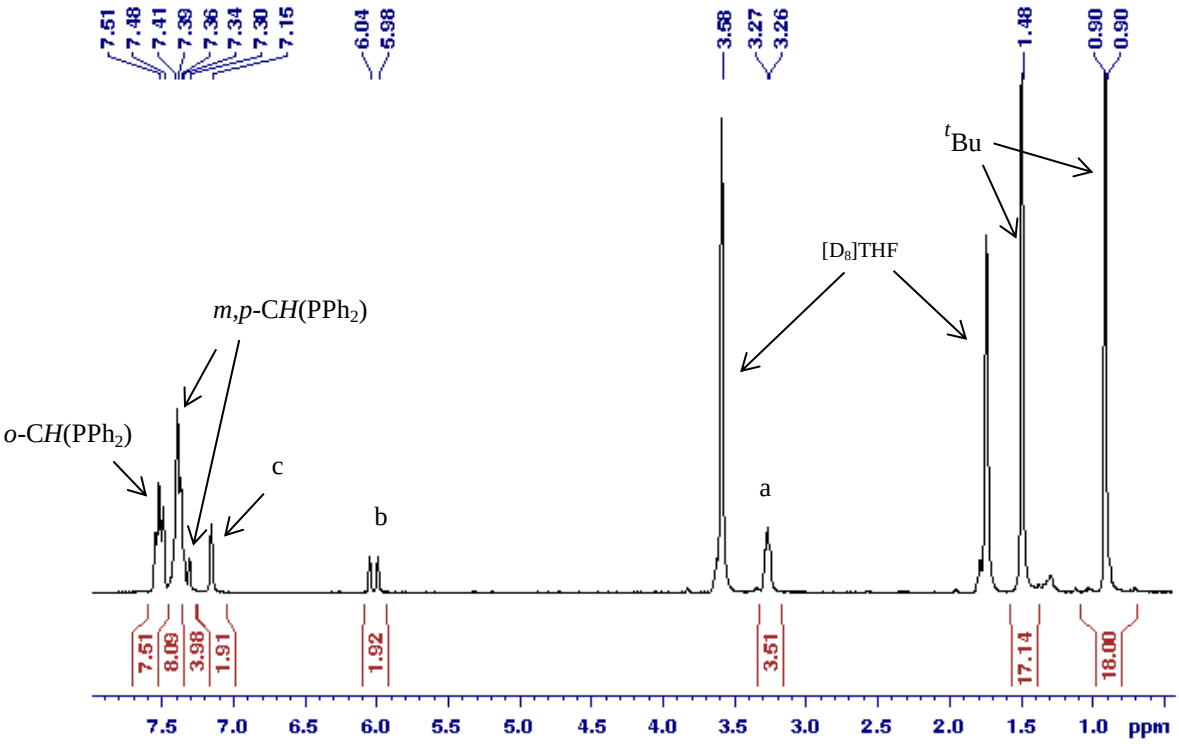

$^{31}P\{^{1}H\}$ *NMR of of* L^1K_2 *in* $[D_8]THF$

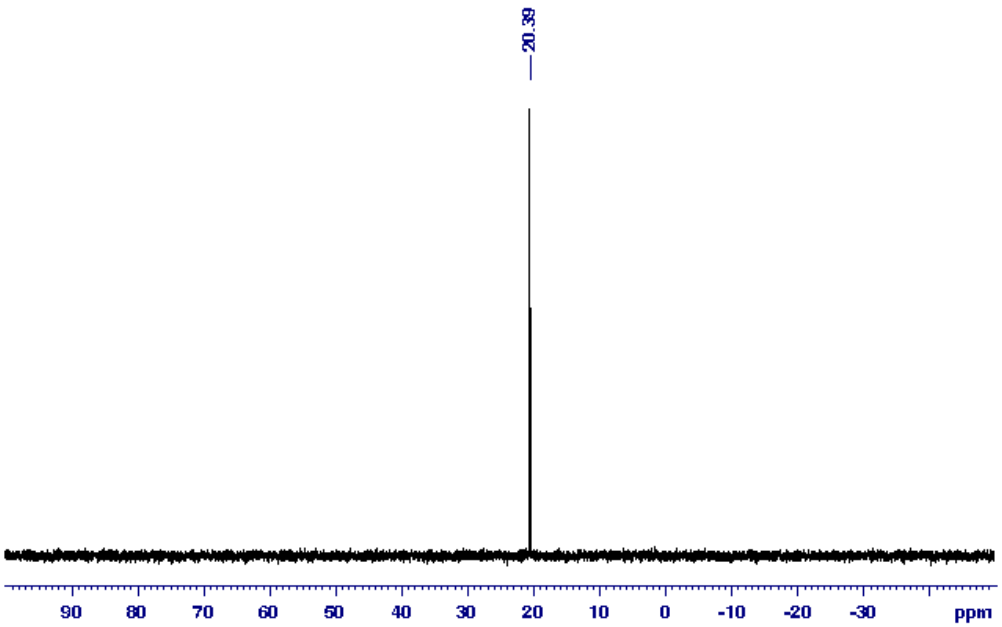

Appendix X

^1H NMR of of L^2K_2 in $[D_8]THF$

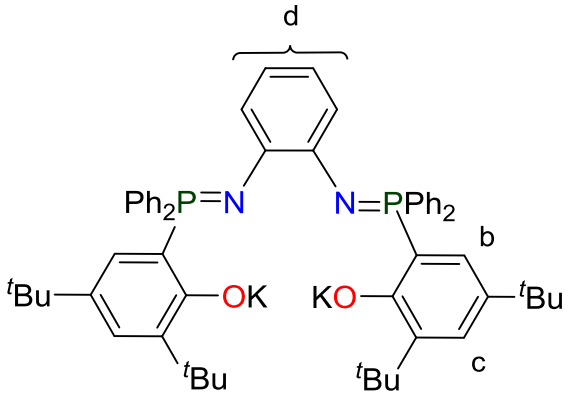

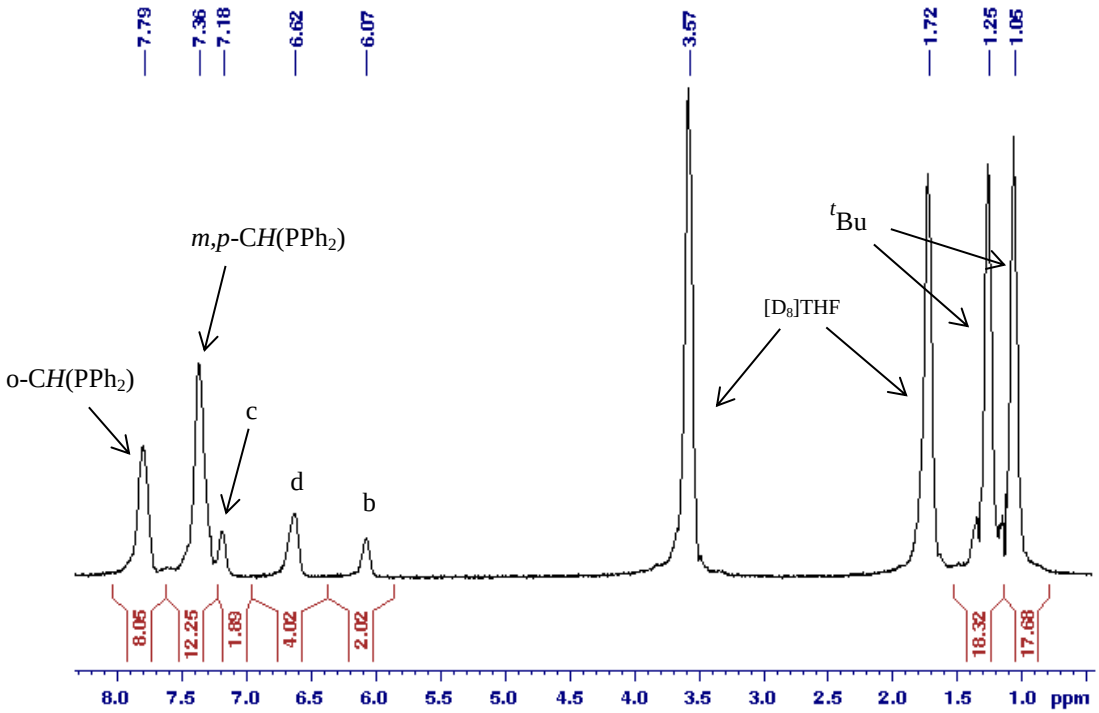

$^{31}P\{^{1}H\}$ *NMR of of* $L^{2}K_{2}$ *in* $[D_{8}]THF$

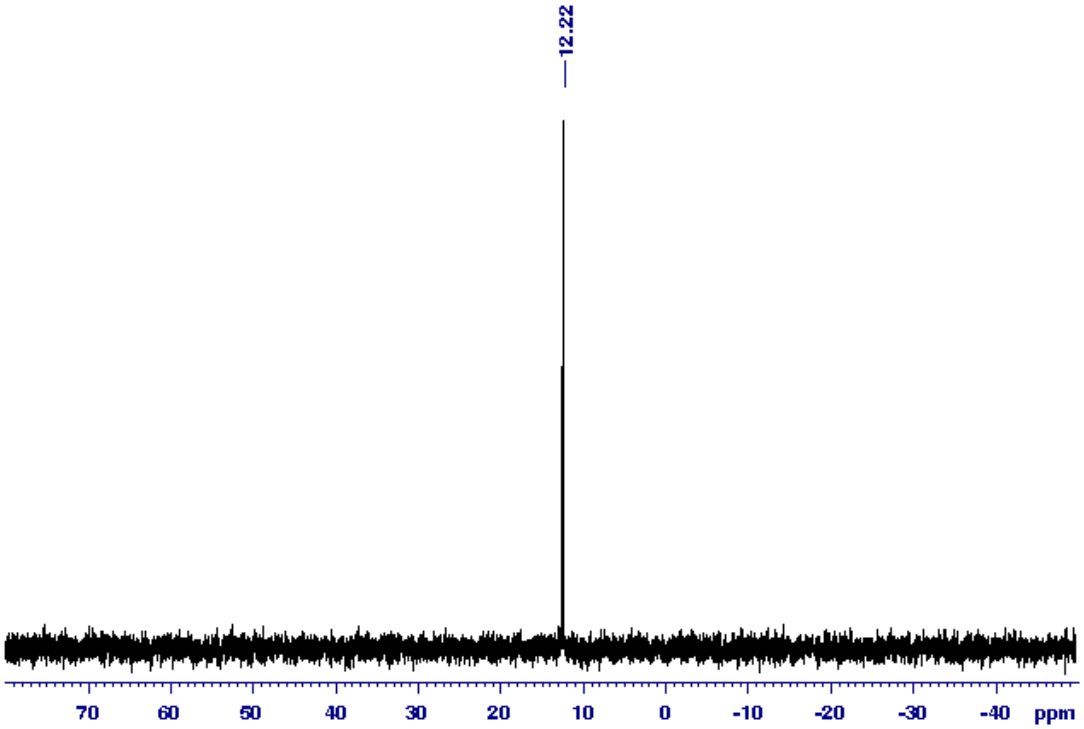

Appendix XI

*^{1}H NMR spectrum in $CDCl_3$ of the polyisoprene obtained by using $K[L^1Nd(BH_4)_2(THF)_2]$ (**13**) (section 5.3).*

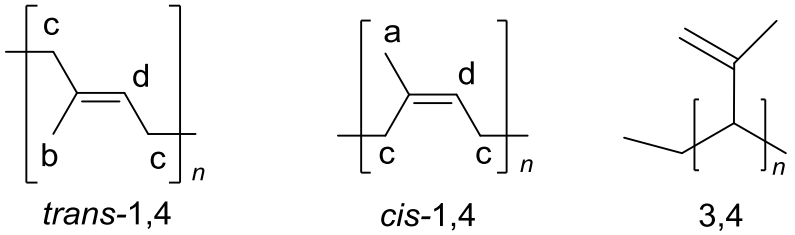

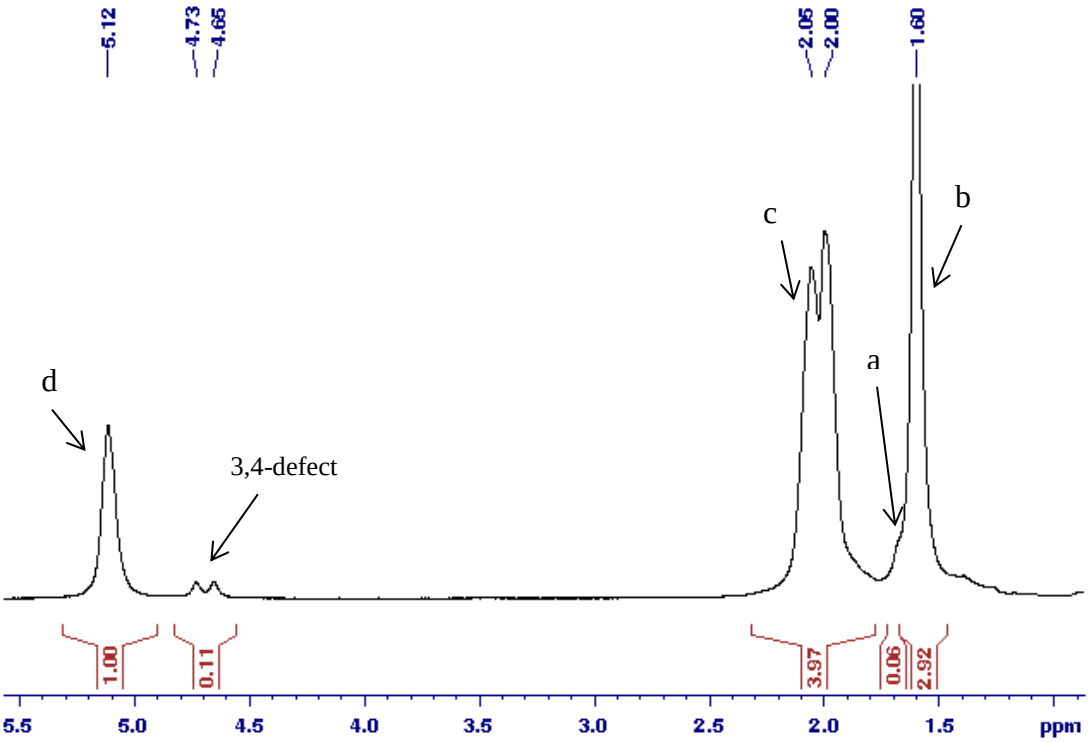

*^{13}C {^{1}H} NMR spectrum in $CDCl_3$ of the trans-polyisoprene obtained by using $K[L^1Nd(BH_4)_2(THF)_2]$ **(13)** (section 5.3).*

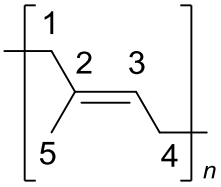

trans-1,4

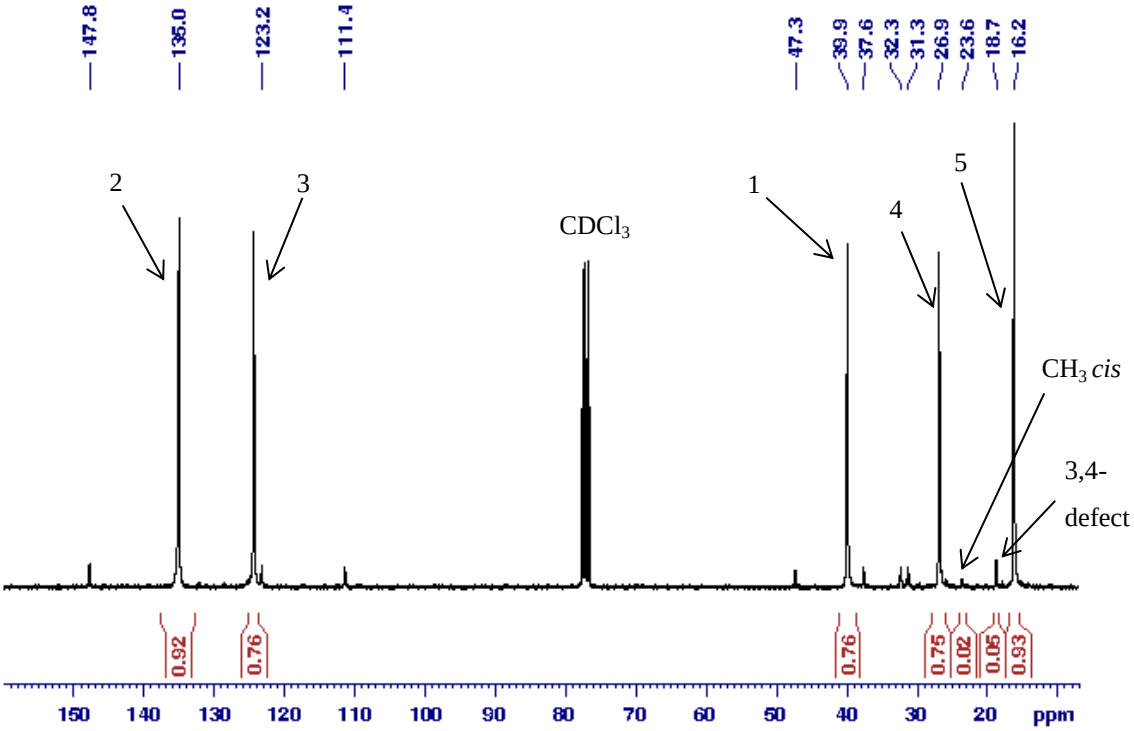

Appendix XII

DSC Analysis of P(LA/CL) copolymers.

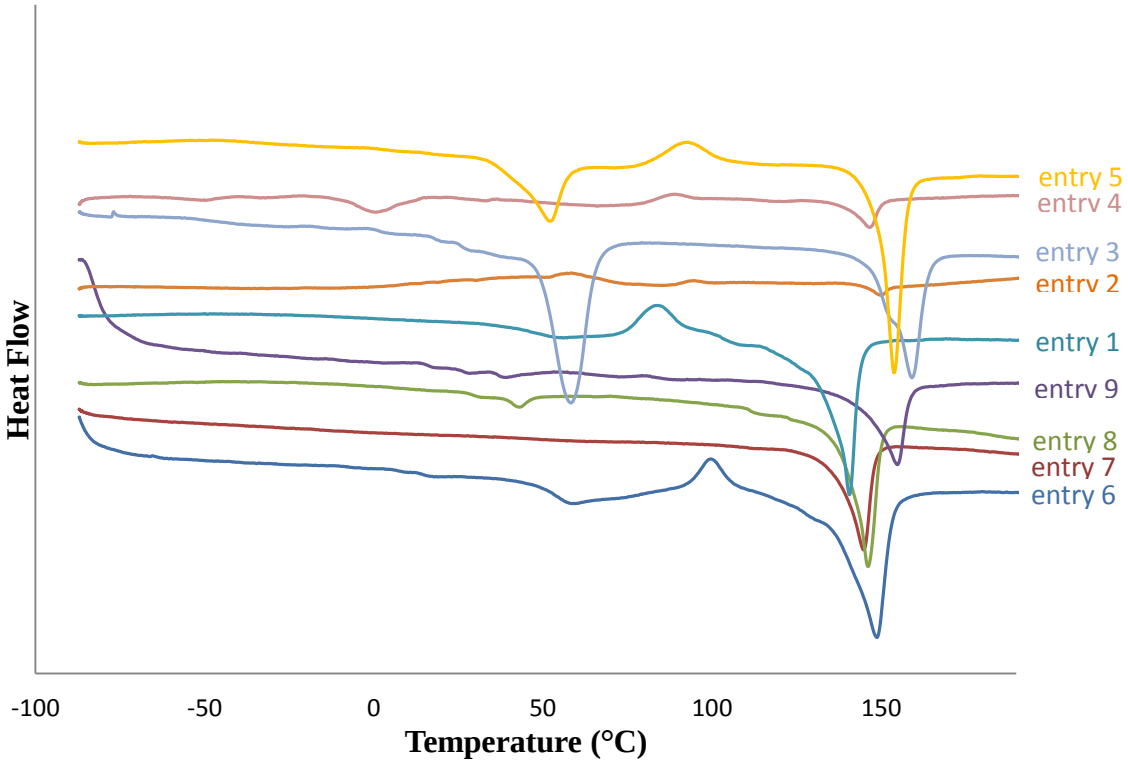

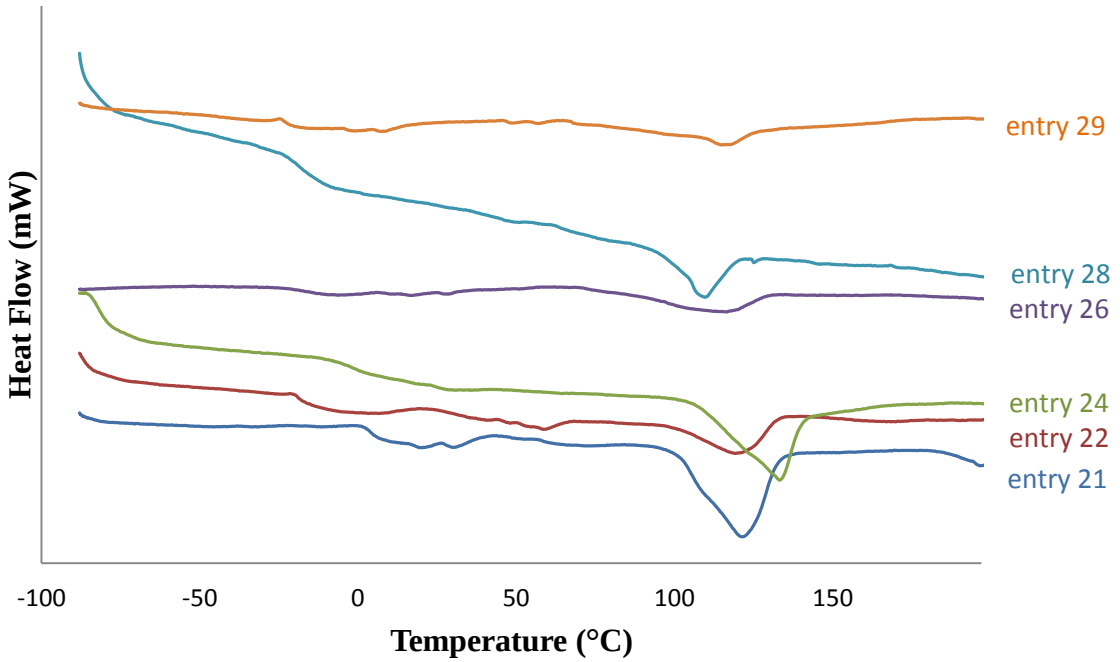

Chimie verte en polymérisation: Elaboration et développement de nouveaux complexes organométalliques à base de terres rares pour leur application en catalyse de polymérisation.

Résumé: De nouveaux complexes allyl-borohydrure de terres rares trivalents, $RE(BH_4)_2(C_3H_5)(THF)_x$ (RE = Sc, x = 2; Y, La, Nd, Sm, x = 3) ont été synthétisés. Les complexes ont été caractérisés, y compris par diffraction des rayons X, et leur réactivité vis-à-vis de l'insertion de petites molécules organiques est décrite, qui met en jeu de façon comparative les liaisons métal-borohydrure et métal-allyle. Dans ce travail de thèse, il a été montré que le complexe de néodyme est capable d'amorcer la polymérisation de l'isoprène, seul ou combiné avec un co-catalyseur de type magnésium, conduisant à du *trans*-1,4-polyisoprène avec une bonne activité. Cette famille de complexes est également très active en polymérisation par ouverture de cycle des esters cycliques tels que l'ε-caprolactone et le L-lactide, avec amorçage de la réaction via le ligand borohydrure plutôt que l'allyle. La copolymérisation statistique L-lactide/ε-caprolactone a été réalisée, conduisant à la formation de copolymères avec une large gamme de microstructures, de statistique à alternée. Une autre approche organométallique a été abordée avec la synthèse de nouveaux complexes borohydrures de terres rares (Sc, Y, Nd) à base de ligands Phosphasalen. Certains de ces complexes ont été isolés et caractérisés.

Mots Clés: Terres Rares, Catalyse Homogène, Polymerisation, Isoprène, Lactide, ε-Caprolactone, Copolymères, Borohydrure, Allyl, Ligands Phosphasalen.

Green chemistry in polymerisation: Elaboration and development of novel organometallic complexes of the rare-earth metals for the application in (Co)-polymerisation catalysis.

Abstract: A series of new trivalent rare earth allyl-borohydride complexes with the formula $RE(BH_4)_2(C_3H_5)(THF)_x$ (RE = Sc, x = 2; Y, La, Nd, Sm, x = 3) was synthesized. The complexes were fully characterized including by X-ray and their reactivity toward small organic molecules insertion is described, which involves comparatively metal-borohydride and metal-allyl bonds. In this dissertation, It was shown that the neodymium congener could initiate isoprene polymerisation, as single component or combined with a magnesium co-catalyst, to afford *trans*-1,4-polyisoprene with good activity. All the complexes were also found extremely active toward the Ring-Opening Polymerisation of ε-caprolactone and L-lactide with initiation through the borohydride rather than the allyl moiety. The statistical copolymerisation of L-lactide and ε-caprolactone was successfully performed with all complexes affording copolymers with a wide range of microstructure, from random to fairly alternating. Another organometallic approach has been studied with the synthesis of novel rare earth (Sc, Y, Nd) borohydride complexes based on Phosphasalen ligands. Some of these complexes have been isolated and characterized.

Keywords: Rare earth, Homogenous Catalysis, Polymerisation, Isoprene, Lactide, ε-Caprolactone, Copolymers, Borohydride, Allyl, Phosphasalen ligands.